TESTING AND DEVELOPMENT OF DEVICES FOR REDUCTION OF SCOUR AROUND BRIDGE PIERS

Submitted to

INDIAN NATIONAL COMMITTEE ON HYDRAULIC RESEARCH
(MINISTRY OF WATER RESOURCES)

by

Dr. U. C. KOTHYARI
(*Principal Investigator*)

Mr. B. RAMESH
(*Research Scholar*)

DEPARTMENT OF CIVIL ENGINEERING

INDIAN INSTITUTE OF TECHNOLOGY ROORKEE

ROORKEE-247667

JANUARY 2012

ABSTRACT

The main cause of concern in stability of bridges founded in river beds is the lowering of river bed level caused by scour due to flow around the bridge elements. The scour mechanism has the potential to threaten the structural integrity of bridges and hydraulic structures, ultimately causing failure when the foundation of the structures is undermined. A series of bridge failures due to pier scour, as reported in the literature, has evoked interest in furthering the understanding of the pier scour process and for developing improved ways of protecting bridges against scour. A collar device was found to be most suitable for scour reduction by many of the eariler investigations. The earlier studies on use of collar for scour reduction however, were done for clear-water scour conditions and no study was undertaken before to ascertain the effectiveness of collar in live-bed scour conditions. Hence this project focuses on testing the effectiveness of the collar device for scour reduction during the live-bed scour conditions. The effectiveness of footing (a larger diameter foundation well supporting inner dia pier) in scour reduction is also studied. Flow pattern around the pier is studied and mathematical modelling of the process of bridge scour is performed.

The laboratory experiments have shown that the collar around bridge pier is also an effective scour control device under live-bed scour condition also. With proper position and size of the collar used, the effectiveness of the collar in scour reduction is siginificant. In the present study placement of 2.5*b* size collar at bed level shows good efficacy (up to 75%) of collars in scour reduction under live-bed conditions (Here *b* is pier diameter). Based on the experimental results it can be summarised that a reduction upto 63% in scour depth is attainable on an average by use of a collar under live-bed conditions.

Oliveto and Hager (2002) have shown that most of the available models over predict the maximum scour depth and this can be attributed to the lack of understanding of flow structure causing the scour. However theoretical modeling of the scour development (for example, Kothyari, 1992 a) requires the initial erosive potential of the flow field determined as a function of some key characteristics of the stream and of the obstacle. Hence the flow around pier is quantified and the potential areas of scouring around upstream of the pier are identified in the present study. As the highest amplification of shear stress (upto fifteen time) occurs in the region of $\theta = 45^{\circ}$, the observations that scour around piers initiate in the region

is thus explained. The scour protection measures should be designed for stability, against the above reported enhancement in the shear stress (Here θ is the angle measured in the *xy* plane measured from the line of symmetry in front of the pier nose).

Bridge piers having non-uniform cross-section over their height are termed as compound bridge piers. Mostly circular piers resting on large diameter well or caissons (termed here as circular compound bridge pier) are adopted for use in the Indian sub-continent for the road and railway bridges. A vast amount of literature is available on the topic of scour around bridge piers having uniform cross-sections. However only a few studies were so far available on the topic of scour around compound piers. Another objective of the present investigation therefore, was to study the process of scour around compound piers and to develop a method for computation of temporal variation of scour around circular compound piers.

The mathematical model of Kothyari *et al.*, (1992 a) for computing temporal variation of scour depth around uniform pier has been updated in the present study by using the new data from present study as well as the literature. Two series of laboratory experiments were conducted to collect data for model application. In the first series of experiments the data on temporal variation of scour depth were collected albeit up to the transient (developing) stage of scour, respectively around the circular uniform piers and circular compound piers for clear-water scour condition. The second series of experiments was carried out to measure the size and hence the cross-sectional area of the principal vortex of the horse-shoe vortex system and to determine the bed shear stress at upstream face of the scour hole around the circular uniform pier and the circular compound piers. The mathematical model proposed here for computation of temporal variation of scour depth around circular compound pier for all possible case of footing position with respect to bed level *i.e.* footing above the bed level, footing at the bed level and footing below the bed level.

The scour prediction methods developed in the laboratories and the scour equations based on laboratory data did not always produce reasonable results for field conditions. Due to the scale effect, the scour-depth equations based predominantly on laboratory flume data may overestimate scour depth measured at bridge piers. Hence it was intended in present project to make investigations with the data obtained from field studies (proto type pier) and test the validity of the present scour predicting equations for scour due to flows having high value of pier Reynolds number as is the case in field conditions where the pier Reynolds number is larger than 10^5. In orginal project proposal it was proposed that the field studies (proto type pier) on the use of collar as a scour reduction device will be carried out by

Railway Design and Standards Organisation (RDSO), Ministry of Railways, Lucknow. However after the approval of the present project by the INCH, the investigations on proto type pier were not taken up by RDSO, Lucknow. So a facility to study the scour around bridge piers on proto type scale was also developed in IIT Roorkee, and investigations were made. The results obtained through this facility gives some idea about the scouring process around a prototype size piers, unfortunately the data obtained using the infrastructure developed were still not sufficient to make definitive conclusions.

M. Tech. Thesis Completed

1. Piyush, D. S. (2008). "Scour reduction by collar plate under live-bed conditions." M.Tech. dissertation, IIT Roorkee.

Ph. D. Thesis Completed

1. Kumar, A. (2007). "Scour around circular compound bridge piers." Ph. D. thesis, IIT Roorkee.

2. Ramesh, B. (ongoing). "Near bed particle motion over transitionally rough bed using high speed imaging", Ph. D. thesis, IIT Roorkee.

Research Papers Published

International Journals:

1. Ramesh, B., Kothyari U. C., and Murugesan, K. (2011). "Near bed particle motion over transitionally rough bed", J. of Hydraulic Res., 49(6), 757-765.

2. Kumar, A. and Kothyari, U. C. (2012). "Three-dimensional flow characteristics within the scour hole around circular uniform and compound piers." J. of Hydraulic Eng., ASCE. (in press)

3. Ramesh, B., Kothyari, U.C., Murugesan, K. "Near bed turbulent structure around a circular pier over transitionally rough bed", J. of Hydraulic Res. (Revision Submitted).

4. Kothyari, U. C., and Ashish Kumar. "Temporal Variation of Scour around Circular Uniform and Compound Bridge Piers." Journal of Hydraulic Engineering, ASCE. (Revision submitted).

5. Ashish Kumar, Kothyari, U. C., and RangaRaju, K. G. "Flow structure and scour around circular compound bridge piers – a review." Journal of Hydro-environment Research, International Association for Hydro-Environment Engineering and Research (Revision submitted).

National Journals:

1. Kothyari, U. C. and Kumar, A. (2010). "Temporal variation of scour around circular bridge piers." J. of Hydraulic Eng., ISH, 16(3), SP-1, 35–48

2. Ramesh, B., Kothyari, U.C., Murugesan, K. (2011). "Rolling motion of particles over transitionally rough beds", J. of Hydraulic eng., ISH**,** 17(SP-1), 23–31

Conferences/ Workshops:

1. Kumar, A. and Kothyari, U. C. (2011). "Flow characteristics within the scour hole around exposed circular compound bridge pier". 11th National conference HYDRO' 11, *SVNIT, Surat.*

2. Ramesh, B., Kothyari, U.C., Murugesan, K. (2010) "Rolling motion of particles over transitionally rough beds", 10th National conference HYDRO' 10, *MMEC, Mullana.*

3. Ramesh, B., Kothyari, U.C., Murugesan, K. (2010) "Rolling motion of particles over transitionally rough beds", Indo-US bilateral workshop *Sedimentation, Erosion, Flooding and Ecological Health of Rivers* (WSEHR-10), ISI, Kolkata (Poster presentation).

4. Ramesh, B., Kothyari, U.C., Murugesan, K. (2010) "Influence of Coherent Flow Structures on Near Bed Particle Motion over Transitionally Rough Bed", International conference *INDIA 2010,* EWRI of ASCE*, IIT MADRAS.*

5. Ramesh, B., Kothyari, U.C., Murugesan, K. (2009) "Preliminary investigation of near bed particle motion over partially rough bed", 9th National conference HYDRO' 09, *CWPRS, Pune.*

6. Kothyari, U. C., and Kumar, A. (2009). "Temporal variation of scour around circular bridge piers." 9th National conference HYDRO' 09*, CWPRS, Pune.*

7. Ramesh, B., Murugesan, K. and Kothyari, U.C. (2008) "Numerical simulation of flow over a backward facing step using Velocity-Vorticity formulation", 36th National conference FMFP' 08, *PES, Banglore.*

LIST OF SYMBOLS AND ABBREVIATIONS

Symbols

A_0	= cross-sectional area of primary vortex A_0
A_s	= cross-sectional area of scour hole at time *t*
A_t	= cross-sectional area of the principal vortex
b	= diameter or width of bridge pier
B	= diameter of collar
B_c	= spacing between collars
B_0	= flume width
b_*	= diameter or width of the foundation
b_e	= effective pier diameter for circular compound pier
c	= a parameter in Eq. 4.14
c_1	= a coefficient in Eq. 4.21
d	= sediment size
Ds	= scour depth below water surface
ds_c	= equilibrium scour depth due to collar
ds_p	= equilibrium scour depth due to pier
d_{50}	= median sediment grain diameter
ds_t	= depth of scour below the initial bed level at time *t*
D_v	= diameter of the principal vortex of the horseshoe vortex system
D_*	= dimensionless sediment size
F_r	= Froude number
g	= gravitational acceleration
g'	= reduced gravitational acceleration
H	= static head over weir
h	= depth of flow
I, J, K	= integer counters
k_s	= roughness size
$\hat{k}$	= normalized turbulent kinetic energy
N	= total number of velocity measurements
P	= rate at which principal vortex expands over the top of the foundation

P_{ot} = average probability of movement of the particle at time t

Q = discharge

r = distance in radial direction

rp = radius of pier

R = hydraulic radius

R_e = flow Reynolds number

R_{ep} = pier Reynolds number

s = specific gravity of sediment

S = energy slope

t = time after beginning of scour when scour depth is d_{st}

t_* = time required for single sediment particle to get scoured

u_* = bed shear velocity of approach flow

u_{*_c} = critical bed shear velocity for d_{50} size, defined by Shields' function

u_{*_t} = shear velocity at time t

U_o = velocity of approach flow

u, v, w = instantaneous velocities of flow in x, y and z directions respectively

u', v', w' = velocity fluctuation of flow in x, y and z directions respectively

$\bar{u}$, $\bar{v}$, $\bar{w}$ = time averaged velocity of flow in x, y and z directions respectively

$\hat{u}$, $\hat{v}$, $\hat{w}$ = normalized time-averaged velocity component in x, y and z directions respectively

$\sqrt{\overline{u'^2}}$, $\sqrt{\overline{v'^2}}$, $\sqrt{\overline{w'^2}}$ = turbulence intensity of flow in x, y and z directions respectively

u^+, v^+, w^+ = normalized turbulence intensity in x, y and z directions respectively

uw^+, vw^+, uv^+ =normalized Reynolds stresses

W_e = top width of scour hole on upstream nose of pier when scour depth just exceeds Y

Y = depth of the top of the foundation below the initial bed level

z = the vertical distance from the channel bed

α [°] = the angular direction of the plane

σ_g = geometric standard deviation of the sediment

ϕ = angle of repose of sediment

θ = angle measured in the x-y plane from A-Line

β = opening ratio [$(B-b)/B$]

γ_f = specific weight of fluid

γ_s = specific weight of sediment

$\Delta\gamma_s$ = $\gamma_s - \gamma_f$

ρ_f = mass density of fluid

ρ_s = mass density of sediment

ν = kinematic viscosity of fluid

τ_u = shear stress of the approach flow

τ_{pt} = shear stress at the pier nose at time *t*

τ_{*pt} = dimensionless shear stress at the pier nose at time *t*

LIST OF FIGURES

LIST OF TABLES

 # BLANK PAGE #

CONTENTS

CHAPTER 1: INTRODUCTION

1.1 GENERAL

Scour is defined as the erosion of streambed sediment around an obstruction in a flow field (Chang, 1988). The main cause of concern in stability of the bridges founded in river beds is the lowering of river bed level caused by the flow around the bridge elements. This local lowering of river bed level around the elements of a bridge such as piers, abutments and spur dikes is termed as ‘ bridge scour’ (Kothyari, 2006).The scour around piers is a result of the development of high shear stress due to three-dimensional separation of the boundary layer around the pier. Correct estimation of depth of scour at bridge sites below the streambed is very important since it influences the depth of the foundation. The underestimation of scour depth results in designing shallow foundation and thus providing a chance of exposure of the foundation to the flow which is dangerous for the safety of the bridge. However overestimation of the scour depth would results in an uneconomical design.

The scour mechanism has the potential to threaten the structural integrity of bridges and hydraulic structures, ultimately causing failure if the foundation of the structures is undermined. A series of relatively recent bridge failures due to pier scour, as reported in the literature, has rekindled interest in furthering the understanding of the pier scour process and for developing improved ways of protecting bridges against the ravages of scour. In this regard, it is interesting to note the statement by Lagasse and Richardson (2001) that, in the United States, hydraulic factors such as stream instability, long-term streambed aggradation or degradation, general scour, local scour, and lateral migration are blamed for 60% of all U.S. highway bridge failures. Hoffmans and Verheij (1997) have also noted that local scour around bridge piers and foundations, as a result of flood flows, is considered to be the major cause of bridge failure.

Scour was found to be the main cause of the 1987 Scholarie Creek Bridge failure in NewYork in which 10 people were killed (Ting *et al.*, 2001; Wardhana and Hadipriono, 2003). The 1989 catastrophic collapse of a U.S. 51 bridge over the Hatchie River in Tennessee resulted in the death of eight people (Lagasse and Richardson, 2001). In another example by Lagasse and Richardson (2001), the southbound and northbound bridges on Interstate 5 over Arroyo Pasajero (Los Gatos Creek) in California collapsed during a large

flood; four vehicles plunged into the creek, resulting in seven deaths. Chiew and Lim (2003) and Chiew (2004) reported the case of the August 2000 failure of Kaoping Bridge in Southern Taiwan. Dey and Barbhuiya (2004) made reference to the collapse due to scouring of Bulls Bridge over the Rangitikei River, New Zealand.

Besides their human toll, bridge failures cost enormous revenue each year in direct expenditure for replacement and restoration in addition to the indirect expenditure related to the disruption of transportation facilities (Lagasse and Richardson 2001). In an intensive study of bridge failure in the United States, Cheremisinoff *et al.*(1987) reported that the Federal Highways Administration in 1978 claimed that damage to bridges and highways from major regional floods in 1964 and 1972 amounted to about US $100 million per event. Citing a survey, Melville and Coleman (2000) stated that, in New Zealand, scour caused by rivers results in the expenditure of NZ$36 million per year. The failure of bridges due to scour is a common occurrence in India too and large sums of money are spent each year on the repair or reconstruction of bridges whose piers have been destroyed by scour (Dey, 1997). Few of the bridges that faced problems or failed due to scouring in India are illustrated in Figs. 1.1 to 1.4.

FIG. 1.1 Excessive scouring around footing of old bridge on river Chakki, Pathankot, Punjab

FIG. 1.2 Excessive scouring around footing of new bridge on river Chakki, Pathankot, Punjab

FIG. 1.3 Damage to Bridge on Koshi near Khagadia (Bihar) - Monsoon - 2010

FIG. 1.4 Failure of Bridge on River Gola at Haldwani, Uttrarakhand (2008)

The potential losses accruable from bridge failures and the need to guard against same have prompted for better understanding of the scour process and for better scour prediction methods and equations. Under-prediction of pier scour depth can lead to bridge failure while over-prediction leads to excess expenditure of resources in terms of construction costs (Ting *et al.* 2001). Numerous experimental and numerical studies have been carried out by researchers in an attempt to quantify the equilibrium depth of scour in various types of soil material. Moreover, while a lot of work has been done to develop equations for predicting the depth of scour, researchers have also worked extensively to understand the mechanism of scour. Raudkivi and Ettema (1983), Kothyari *et.al.* (1992 a), Ahmed and Rajaratnam (1998), Chiew and Melville (1987) and Breusers *et al.* (1977), among others, are some of the researchers that have worked on pier scour. Local scour around bridge piers was also studied by Shen and Schneider (1969) while Breusers *et al.* (1977) gave a state of the art review on local scour around circular piers. Posey (1974) provided guidance on how bridge piers in erodible material can be protected from under-scour by means of an inverted filter extending out a distance of 1.5 to 2.5 pier diameters in all directions from the face of the pier.

Current research areas include understanding the scour processes, temporal development of scour, predicting scour in cohesive soils, parametric studies of local scour, and prediction of scour depth at various types of hydraulic structures. For example, Ansari *et al.* (2002) studied the influence of cohesion on scour around bridge piers. Ahmed and Rajaratnam (1998) investigated the flow around bridge piers in their laboratory study on flow past cylindrical piers placed on smooth, rough and mobile beds. Graf and yulistiyanto (1999)

investigated the flow field around a cylinder positioned normal to the flow in an open channel for two types of flow. Jia *et al.* (2002) reported the findings of a numerical modeling study for simulating the time-dependent scour hole development around a cylindrical pier founded on a loose bed in an open channel. Lim and Chiew (2001) presented a parametric study on riprap protection and failure around a cylindrical bridge pier with uniform bed sediments. Link and Zanke (2004) studied the time-dependent scour-hole volume evolution at a circular pier in uniform coarse sand and developed a mathematical correlation between the scour volume and the maximum scour depth for water depth to pier diameter ratios between one and two.

In spite of the significant amount of research carried out on the topic of scour processes, some aspects of this topic are yet to be resolved as shown by the various contradictions reported in the literature. Raudkivi and Ettema (1983) stressed that the scientific basis for the structural design of bridges is well established whereas, in contrast, there is no unifying theory at present which would enable the designer to estimate, with confidence, the depth of scour at bridge piers. Cheremisinoff *et al.* (1987) and Hoffmans and Verheij (1997) supported the claims of Raudkivi and Ettema. This situation however is not only due to the extreme complexity of the problem but also due to the fact that stream characteristics, bridge constriction geometry and soil and water interaction are different at each bridge site as well as for each flood. Although it has been the subject of theoretical and experimental studies for many years, Federico *et al.* (2003) have also indicated that a reliable assessment of the general and local erosion of pier foundation soil cannot be safely calculated even now by means of the empirical correlations available in the technical literature.

Local scour at a bridge pier principally results from the downflow along the upstream face of the pier and the resulting horseshoe vortex which forms at the base of the pier aids the phenomenon (Kothyari *et al.*1992a, Kumar *et al.* 1999). One way of reducing pier scour is to combat the erosive action of the horseshoe vortex by armouring the riverbed using hard engineering materials such as stone riprap. Another approach is to weaken and possibly inhibit the formation of the downflow and thus the formation of the horseshoe vortex using a flow-altering device (Chiew and Lim 2003; Melville and Coleman 2000). Flow altering devices that have been used to protect piers against local scour include sacrificial piles placed upstream of the pier, Iowa vanes, a slot through the pier, and a flow deflector attached to the pier, such as a collar. The use of collars has been studied by several researchers, including Chabert and Engeldinger (1956), Laursen and Toch (1956), Thomas (1967), Tanaka and

Yano (1967), Fotherby and Jones (1993), Chiew (1992), Kumar *et al.* (1999) and Zarrati *et al.* (2006). In general, the results from collar studies have shown that they can be very effective in reducing the scour depth at a bridge pier.

Since use of a collar around bridge piers results in reduction of the scour depth around the bridge pier, the parameter of interest, therefore, is the scour depth. However the time taken to reach a particular scour depth is also very significant as scour holes take significantly less time to form. For this reason, it becomes necessary to understand the development of the local scour hole with time. In clear-water scour conditions, however, the depth of a scour hole approaches an equilibrium condition asymptotically with time (Breusser,1977). Consequently, time is also an important factor in undertaking scour studies. The temporal development of scour has been studied by many researchers (e.g. Melville and Chiew, 1999; Yanmaz and Altinbilek, 1991). Moreover, the rate of local scour around a bridge pier is a significant factor in scheduling scour mitigation measures and is also essential in understanding scour under time-varying flows (Gosselin and Sheppard, 1995). For adequate representation of the temporal development of scour and also the efficacy of using a collar as a countermeasure in a bridge pier in model studies, the definition of time to equilibrium adopted is very vital as this determines the duration of laboratory tests.

As pointed out above, the use of a collar is one strategy that has been studied as a potential mitigation strategy for pier scour. When a collar is installed on a pier, the direct impact of the downflow to the riverbed is prevented (Mashair *et al.* 2004), which serves to reduce the depth of scour that can take place. In addition to reducing the depth of maximum scour, the rate of scouring is also reduced considerably. In this regard, Mashair *et al.* (2004) observed that reducing the rate of scouring limits the risk of pier failure when short duration floods occur. On the matter of time development of maximum scour depth, Zarrati *et al.* (2004) observed that the time to reach an equilibrium condition depends on whether the pier is protected with a collar or not. This difference in the time development of local scour has significant implications for those researchers choosing to stop their tests after a fixed length of time. While the ultimate or equilibrium scour for two situations may be the same, the temporal development of the scour hole may vary. There is, therefore, the need for a critical review of some results in literature relating to excessively short testing times.

1.2 EARLIER RESEARCH ON DEVICES FOR SCOUR REDUCTION

The idea of bed protection and reduction of scour at the pier has attracted the attention of several investigators since long time. Schneible (1951) tested a number of disks of several sizes as well as a number of footing-top shapes while Chabert and Engeldinger (1956) investigated the effectiveness of an array of piles in front of a pier for scour reduction. Tanaka and Yano (1967) proposed a collar on cylindrical piers. The advantage of a collar as a scour-reducing device is its effectiveness for all orientations of approach flow. Kikkawa *et al.* (1973) found gaurds – a number of concentric plates- at different elevations on a pier to be effective in reducing scour depth around bridge pier. Chiew (1984) and Jones *et al.* (1992) tested the possibility of a cassion to act as possible scour arrester. Dargahi (1990) carried out research on the mechanisms of local scour and how a collar may influence the horseshoe vortex system and ultimately reduce the amount of scour. Chiew (1992) experimentally studied the effect of a collar, a slot and a combination of the two in reducing the local scour in the vicinity of a pier. Vittal *et al.* (1993) studied and compared the scour reduction efficacies of a circular collar on a pier group that was made up of three individual smaller piers. Similar experiment was also performed on a single solid pier. Fotherby and Jones (1993) studied the effectiveness of collars in reducing scour. They recognised the potential usage of both a collar and a footing at reducing scour. Kumar *et al.* (1999) also worked on the use of collars around a cylindrical pier to reduce the scour depth. For the experiment on collar efficacy, five different collar sizes of thickness 3 mm were used (i.e., B = 1.5b, 2.0b, 2.5b, 3.0b and 4.0b), where B= collar diameter and b= pier diameter. Most previous studies on collars have been on circular piers. Recently, however, Zarrati *et al.* (2004) worked on the application of a collar to control the scouring around rectangular bridge piers having a rounded nose. Kayaturk *et al.* (2004) studied the effect of a collar on the temporal development of scour around bridge abutments. Zarrati *et al.* (2006) studied the use of independent and continuous pier collars in combination with riprap for reducing local scour around bridge pier groups. Lauchlan (1999), Dey (1997), Whitehouse (1998), Hoffmans and Verheij (1997), and Melville and Coleman (2000) have also presented reviews on of the application of a protective collar as a countermeasure for local scour at bridge pier.

1.3 MECHANISM OF SCOUR AROUND BRIDGE PIERS

The placement of pier in the stream creates an adverse pressure gradient ahead of the pier. This results in seperation of boundary layer that develops complex three-dimensional

flow system consisting of downflow at the upstream nose of pier and a principal vortex in front of the pier. A horshoe vortex system is formed by rolling up of shear layers at the surface of the pier and on its sides. Furthermore a surface roller also forms as shown in Fig.1.5 (Melville and Coleman, 2000)

There are two schools of thought as to the main cause of scour around the piers. Shen *et al.* (1966), Baker (1980), Kothyari *et al.* (1992a) and Muzzammil *et al.* (2004) consider the horseshoe vortex to be the main cause of scour. On the other hand, Hjorth (1975), Melville (1975) and Ettema (1980) considered that scour is mainly by downflow (Garde and Ranga Raju, 2006).

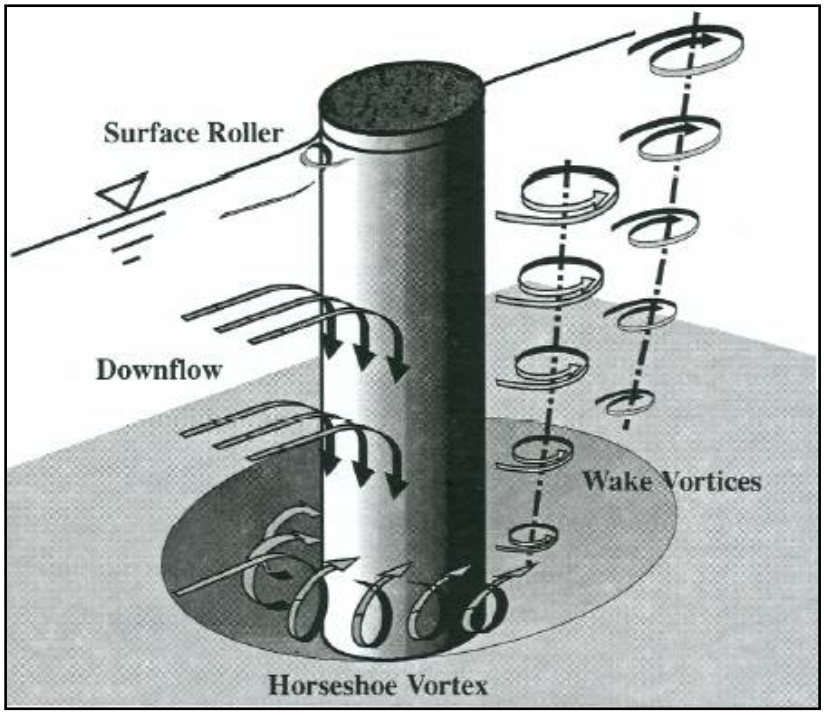

FIG.1.5. Schematic Diagram of Flow and Scour Pattern at a Circular Pier (Melville and Coleman, 2000)

In addition the bridge piers having non-uniform cross-section over their height are termed as compound bridge piers. Mostly circular piers resting on large diameter well or caissons (termed here as circular compound bridge pier) are adopted for use in the Indian sub-continent for the road and railway bridges. A vast amount of literature is available on the topic of scour around bridge piers having uniform cross-sections. However only a few studies are so far available on the topic of scour around compound piers.

1.4 SCALE EFFECTS ON LOCAL SCOUR

The scour prediction methods developed in the laboratories and the scour equations based on laboratory data did not always produce reasonable results for field conditions. Recent research indicates that laboratory investigations often oversimplify or ignore many of the complexities of the flow fields around the bridge piers. The physical scales, the fluid properties and the boundary conditions in the small-scale models (the laboratory conditions) should be derived from the large-scale prototype (the field conditions) according to the Hydraulic Similitude Laws. Geometric similarity is usually required for all models, Reynolds number similarity for models involving flow around bodies and Froude number similarity for models involving free-surface flows. In fact, it is very difficult for a physical model of local scour around a bridge pier to satisfy all these similarities.

Due to the scale effect, the scour-depth equations based predominantly on laboratory flume data may overestimate scour depth measured at bridge piers. The scour prediction methods developed based on laboratory data did not always produce reasonable results for field conditions (Melville, 1975; Dargahi, 1982; Jones, 1984). The variability and complexity of site conditions make the development of methodology for predicting local scour at bridge piers difficult. Landers *et al*. (1996) evaluated many relations developed in the laboratory by use of transformed data (to obtain a more normal distribution) and smoothing techniques to assess general trends in the data. They found only minimal agreement between the field data and laboratory-based relations. The main reason for such disagreement being that laboratory investigations often oversimplify or ignore many of the complexities that are common in the field (Mueller *et al*., 2002).

1.5 THE PROBLEM IDENTIFICATION

The bridge footings in rivers like Ganga, Yamuna and Bramaputra are required to sunk upto depth of 50 m or more below the general bed-level. This however entrails tremendous cost. Use of scour reduction devices therefore can be envisaged in design of bridge foundations. A collar device was found to be most suitable for scour reduction by most of the eariler investigations. The earlier studies on use of collar for scour reduction however, were done for clear water scour conditions and no study was undertaken before to ascertain the effectiveness of collar in live-bed scour conditions. Also only a few studies are made on the topic of scour around compound piers (however this type of foundations is commonly used in India) and furthermore, experiments with proto-scale piers are rare. Present study was undertaken to fill these gaps.

1.6 OBJECTIVES

The aim of this study entitled "Testing and Development of Devices for Reduction of Scour around Bridge Piers" is to fill up the aforementioned gaps in the literature. The following objectives were the proposed for this project.

- Assess the applicability of collars in reducing the live bed scour when there is sediment supply from the upstream as is mostly the case during flood flows.
- Quantify the flow pattern around a pier.
- To investigate the process of scour around compound piers and to develop a method for computation of temporal variation of scour around circular compound piers.
- Quantify the scale effects through a study of scour around bridge piers on proto type scale pier and validate the effectiveness of the scour reduction devices.

1.7 LIMITATIONS

The study on pier fitted with collar is limited to experimental investigation in the laboratory on live-bed scour with sediment feed and without sediment feed around circular piers. Uniform cohesionless sediments of size 0.34 mm and relative density 2.65 was used for such study with a collar of size 2.5*b*. The study is restricted to the case of steady flow.

The flow pattern around a pier is measured over a flat rigid bed whose bed roughness in approach flow falls under transitionally-rough regime.

The study on scour around compound piers is confined to clear water scour condition. Uniform circular piers having diameters of 48 mm, 88 mm and 114 mm were used during the experiments and six numbers of circular compound piers were used, having ratio of foundation diameter to pier diameter respectively as 1.84, 1.89, 2.38, 2.81, 3.46 and 4.38. Uniform cohesionless sediment of sizes 0.6 mm and 1.8 mm respectively and relative density of 2.65 were used in the laboratory experiments. The experiments are restricted to the case of steady uniform flows.

In orginal project proposal it was proposed that the field studies (proto type pier) on the use of collar as a scour reduction device will be carried out by Railway Design and Standards Organisation (RDSO) Ministry of Railways, Lucknow. An

abandoned railway bridge located in Moradabad-Ambala route on river Ganga at Balawali in U.P. was selected by the Indian Railways previously for this purpose. However after the approval of the present project by the INCH, the investigations on proto type pier by the RDSO were not taken up. So a facility to study the scour around bridge piers on proto type scale was also developed in IIT Roorkee, and investigations were made. Although the results obtained through this facility gives some idea about the scouring process around a prototype size piers, unfortunately the data obtained using the infrastructure developed were still not sufficient to make conclusions. The experiments and visual observations made in this study on scour around prototype piers are given in the Appendix-1 of this report.

 # BLANK PAGE #

CHAPTER 2: REVIEW OF LITERATURE

2.1 INTRODUCTION

A large amount of literature has been published on the local scour of cohesionless bed sediment around a bridge pier. This chapter attempts to summarise the present state of understanding of local scour in cohesionless soil, the temporal development of scour as well as mitigation strategies for minimising the local scour at a bridge pier. The chapter is included to familiarise the reader with terminologies relevant to local scour at a bridge pier as well as to facilitate the understanding of scour. The use of collars as a countermeasure for local scour is also reviewed. Besides, the scale effects on process of local scour are also discussed.

2.2 SCOUR

Breusers *et al.* (1977) defined scour as a natural phenomenon caused by the flow of water in rivers and streams. It is the consequence of the erosive action of flowing water, which removes and erodes material from the bed and banks of streams and also from the vicinity of bridge piers and abutments. Cheremisinoff *et al.* (1987) defined scour as the lowering of the level of the river bed by water erosion such that there is a tendency to expose the foundations of riverine structures such as bridges. As noted by the authors, scour can either be caused by the normal flow or flood events. Normal flow can lower the channel bed but scouring is most assisted during a peak flow in which the flow velocity is higher. In other words, scour can occur under any flow condition that makes the bed mobile within the vicinity of the obstruction but the rate of scouring is much higher with larger flow events. The amount of the reduction below an assumed natural level (generally the level of the river bed prior to the commencement of the scour) is termed the scour depth. A scour hole is defined as the void or depression left behind when sediment is washed away from a stream or river bed.

2.3 TYPES OF SCOUR

Scouring has long been acknowledged as a severe hazard to the performance of bridge piers. The total scour at a river crossing consists of three components that, in general, can be

added together (Richardson and Davies, 1995). They include general scour, contraction scour, and local scour. Cheremisinoff *et al.* (1987) on the other hand divided scour into two major types, namely general scour and localised scour. Some other sub-divisions of scour are as shown in Figure 2.1.

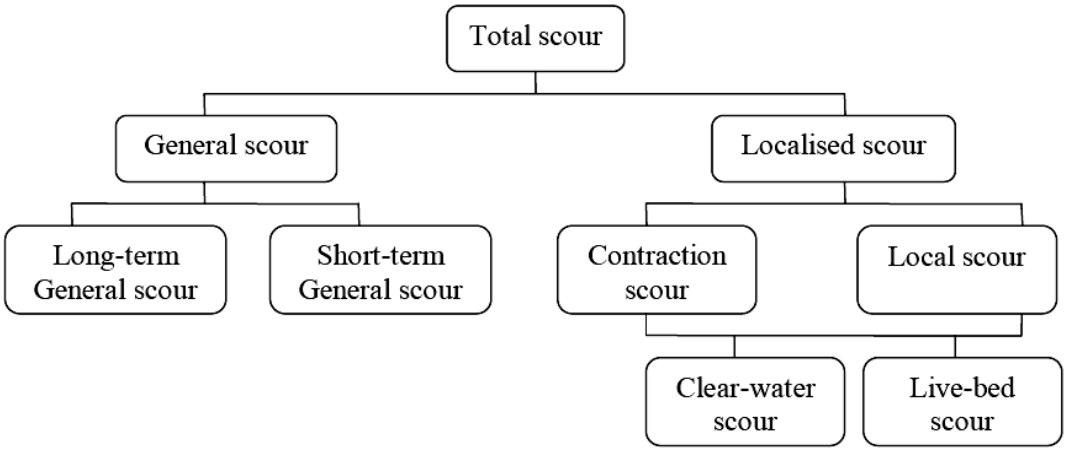

FIG 2.1 An Organogram Showing Various Types of Scour (Modified from Cheremisinoff *et al.* 1987)

2.3.1 General Scour

This type of scour deals with the changes in river bed elevation due to natural/human-induced causes with the effect of causing an overall lowering of the longitudinal profile of the river channel. It occurs through a change in the river regime resulting in general degradation of the bed level. General scour develops irrespective of the existence of a bridge. General scour can further be divided into long-term and short term scour, with the two types being differentiated by the temporal development of the scour (Cheremisinoff *et al.* 1987). Short-term general scour occurs in response to a single or several closely spaced floods whereas long-term general scour develops over a significantly longer time period, usually of the order of several years, and includes progressive degradation and lateral bank erosion.

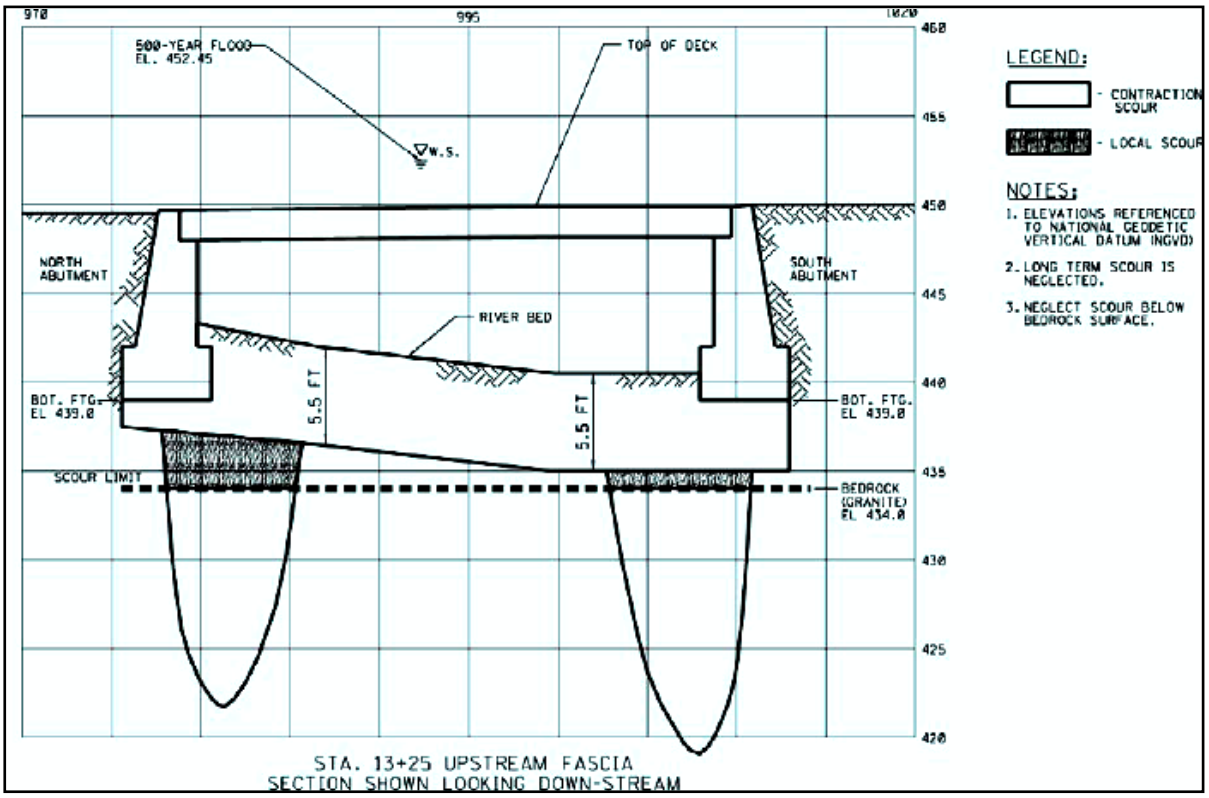

FIG 2.2 Plot of Scour Analysis Result for 500 Year Flood-Structure No.1000-041 Guinea Hollow Road over North Branch Rockaway Creek, U.S.A. (Agrawal *et al.* 2005)

2.3.2 Localised Scour

In contrast to general scour, localised scour is directly attributable to the existence of a bridge or other riverine structures. Localised scour can further be divided into contraction and local scour. Figure 2.2 shows the localised scour depicting clearly the contraction and local scour for the north branch rockaway creek, US (Agarwal *et al.* 2005). Figure 2.4 shows the failure of Kaoping Bridge, Taiwan, due to combination of general and local scour.

Contraction Scour

This type of scour occurs as a result of the constriction of a channel or waterway, either due to a natural means or human alteration of the floodplain. The effect of such a constriction is a decrease in the flow area and an increase in the average flow velocity, which consequently causes an increase in the erosive forces exerted on the channel bed. The overall effect of this phenomenon is the lowering of the channel bed. A bridge with approaches or

abutments encroaching onto the floodplain of a river is a common example of contraction scour.

Local Scour

This type of scour refers to the removal of sediment from the immediate vicinity of bridge piers or abutments. It occurs as a result of the interference with the flow by piers or abutments, which result in an acceleration of the flow, creating vortices that remove the sediment material in the surroundings of the bridge piers or abutments. Scour occurring as a result of spur dykes and other river training works is also an example of local scour. Figure 2.3 shows the typical appearance of local scour around bridge piers. As this topic is the main thrust of present study, local scour is discussed in much more detail in the following sections.

FIG 2.3 Photograph of Local Scour at Rectangular Piers (www.pepevasquez.com)

FIG 2.4 Failure of Kaoping Bridge, Taiwan, due to Combination of General and Local Scour (Chiew *et al.* 2004)

2.4 LOCAL SCOUR MECHANISMS

It has long been established that the basic mechanism causing local scour at piers is the down-flow at the upstream face of the pier and formation of vortices at the base (Heidarpour *et al.* 2003 and Muzzammil *et al.* 2004). The mechanism of vortex shredding has been well described in Fig.2.5 (Dey *et.al.*1997). The flow decelerates as it approaches the pier coming to rest at the face of the pier. The approach flow velocity, therefore, at the stagnation point on the upstream side of the pier is reduced to zero, which results in a pressure increase at the pier face. The associated stagnation pressures are highest near the surface, where the deceleration is greatest, and decrease downwards (Melville and Raudkivi, 1977). In other words, as the velocity is decreasing from the surface to the bed, the stagnation pressure on the face of the pier also decreases accordingly i.e. a downward pressure gradient. The pressure gradient arising from the decreased pressure forces the flow down the face of the pier, resembling that of a vertical jet. The resulting down-flow impinges on the streambed and creates a hole in the vicinity of the pier base. The strength of the down-flow reaches a maximum just below the bed level. The downflow impinging on the bed is the main scouring agent (Melville and Raudkivi, 1977).

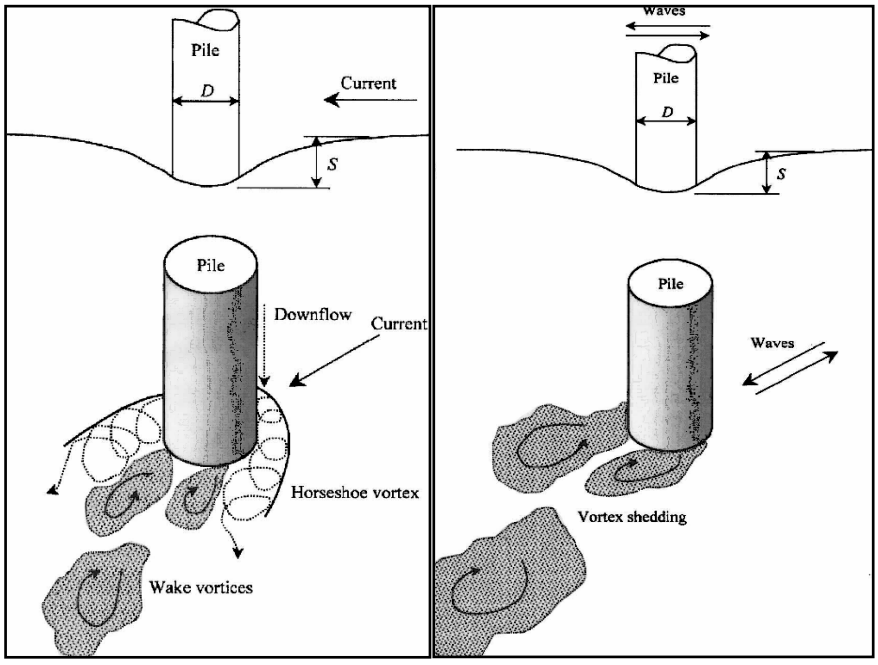

FIG 2.5 Simple Line Diagram Showing Formation and Shredding of Vortex around Pier (Dey *et al.*1997)

Figure 2.6 shows the flow and scour pattern at a circular pier. As illustrated in the figure, the strong vortex motion caused by the existence of the pier entrains bed sediments within the vicinity of the pier base (Lauchlan and Melville, 2001). The downflow rolls up as

it continues to create a hole and, through interaction with the oncoming flow, develops into a complex vortex system.

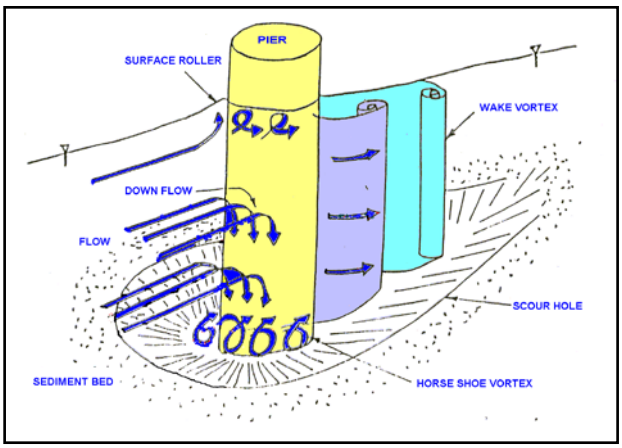

FIG 2.6 Schematic Diagram of Flow Field at a Pier (Melville and Raudkivi, 1977)

The vortex then extends downstream along the sides of the pier. This vortex is often referred to as horseshoe vortex because of its great similarity to a horseshoe (Breusers *et al.*, 1977). The formation of horseshoe vortex and the associated down flow around the bridge element results in increased shear stress and hence a local increase in transport capacity of flow (Kothyari, 2006).

As shown in Figure 2.6, besides the horseshoe vortex in the vicinity of the pier base, there are also the vertical vortices downstream of the pier referred to as wake vortices (Dargahi 1990). The separation of the flow at the sides of the pier produces the so called wake vortices. These wake vortices are not stable and shed alternately from one side of the pier and then the other.

2.5 CLASSIFICATION OF LOCAL SCOUR

Chabert and Engeldinger (1956) identified two main classifications of local scour at piers based on the mode of sediment transport by the approaching stream, namely

- Clear- water scour and
- Live bed scour.

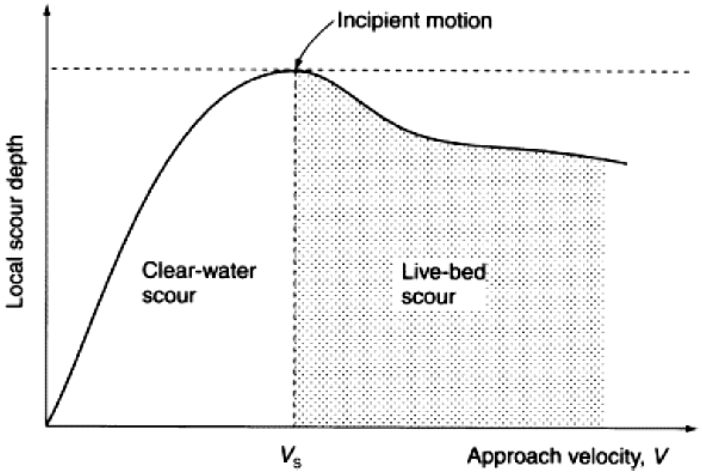

FIG. 2.7 Variation of Local Scour Depth with Approach Velocity under Clear-Water and Live-Bed Scour Conditions (Hamil *et. al*. 1999)

These classifications depend on the ability of the flow approaching the bridge to transport bed material (Chiew and Melville, 1987). Clearwater scour is defined as the case where the bed sediment is not moved by the approach flow, or rather where sediment material is removed from the scour hole but not refilled by the approach flow (Melville, 1984). Similarly, Raudkivi and Ettema (1983) defined clear-water scour as occurring when the bed material at the upstream side of the pier is not in motion. Live-bed scour, on the other hand, occurs when there is general transportation of the bed material by the flow. Live-bed scour occurs when the scour hole is continually replenished with sediment by the approach flow. Figure 2.7 shows the variation of local scour depth with approach velocity under clear-water and live-bed scour conditions

In clear-water scour, the maximum scour depth is reached when the flow can no longer remove particles from the scour hole (Breusers *et al.* 1977). In live-bed scour, an equilibrium scour depth is reached when, over a period of time, the quantity of material eroded from the scour hole by the flow equals the quantity of material supplied to the scour hole from upstream (Melville, 1984). The temporal development of the maximum scour depth under clear-water and live-bed scour conditions is illustrated in Fig. 2.8.

In coarse-grained materials (sands and gravels), an equilibrium local scour condition is rapidly attained with time in live-bed conditions (and then oscillates in response to the passage of bed forms). On the other hand, an equilibrium condition is achieved rather more slowly and asymptotically in clear-water conditions (Raudkivi and Ettema, 1983).

Clear-water scour depth reaches its maximum over a longer period of time than would occur for live-bed condition. Furthermore, local clear-water scour may not reach the maximum depth until after several floods (Richardson and Davies, 2001). According to Richardson and Davies, the maximum clear-water pier scour depth is about 10 percent greater than the equilibrium depth for live-bed pier scour. The time taken for equilibrium scour depth to develop increases rapidly with flow velocity in clear-water conditions but decreases rapidly for live-bed scour (Melville and Chiew, 1999). Since an equilibrium clear-water scour depth is reached asymptotically with time, it can take a very long time for the equilibrium scour hole to form.

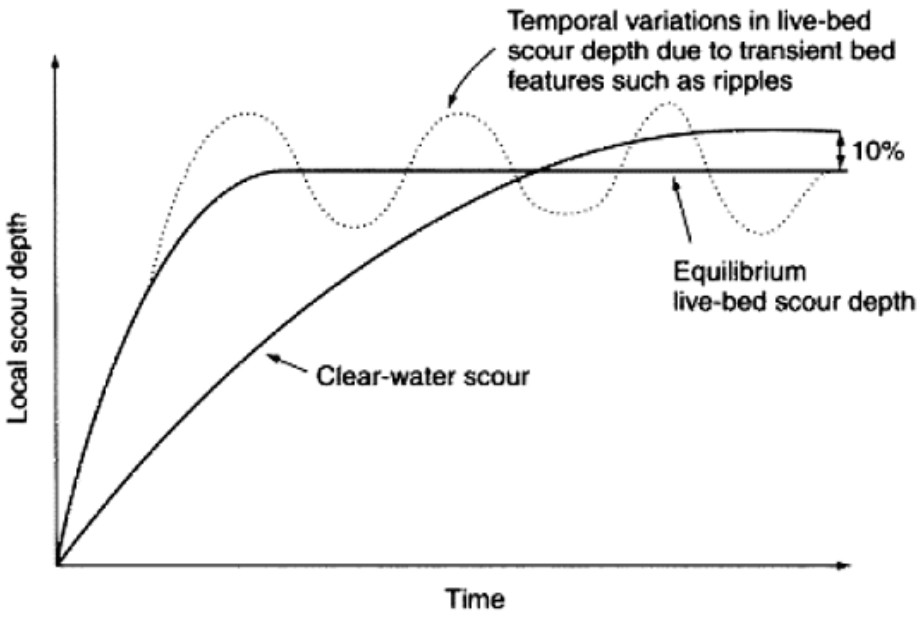

FIG 2.8 Temporal Variation of Scour Depth under Clear-Water and Live-Bed Scour Conditions (Raudkivi and Ettema, 1983)

2.6 CLASSIFICATION OF SCOUR PARAMETERS

Factors which affect the magnitude of the local scour depth at piers as given by Richardson and Davies (1995), Raudkivi and Ettema (1983) and Lagasse *et al.* (2001) are (i) approach flow velocity, (ii) flow depth, (iii) pier width, (iv) submerged weight of sediment particle, (v) pier length if skewed to the main flow direction, (vi) size and gradation of the bed material, (vii) angle of attack of the approach flow to the pier, (viii) pier shape, (ix) bed configuration, and (x) ice or debris jams.

According to Breusers *et al.* (1977) and Ansari *et al.* (2002) the parameters listed above can be grouped into four major headings, viz., Approaching stream flow parameters: Flow intensity, flow depth, shear velocity, mean velocity, velocity distribution and bed roughness, Pier parameters: Size, geometry, spacing, number and orientation of the pier with respect to the main flow direction (i.e., angle of attack), Bed sediment parameters: Grain size distribution, mass density, particle shape, angle of repose and cohesiveness of the soil and Fluid parameters: Mass density, particle submerged weight and kinematic viscosity.

Dey (1997) included the time of scouring as an additional parameter. Oliveto and Hager, (2002) and Kothyari *et al.* (2007) identified densimetric particle Froude number as the principal parameter influencing the scour process.

2.6.1 FLOW PARAMETERS

The study of flow around bluff bodies in open channels has been of interest for many decades. For example, knowledge of the flow generated around surface piercing cylinders in open channels is essential in bridge design. In spite of the considerable number of studies of flow around bridge-pier-like objects, our knowledge of flow around submerged bluff bodies remains limited (Sadeque, 2007). Piers when introduced to a flow channel result in significant changes to the flow pattern around them. A detailed description of the modified flow is essential to the understanding of the local scour which develops. The flow field around a pier is complex in detail, and the complexity is aggravated with the development of the scour hole.

Graf and Yulistiyanto (1999) investigated the flow field around a cylinder positioned normal to the flow in an open channel for two types of flow. They measured the instantaneous three dimensional velocity of the flow in different planes upstream and downstream of the cylinder using an acoustic Doppler velocity profiler. They computed the vorticity field and contours from the measurements made. Following conclusions were drawn from their study.

- In the plane of symmetry, the horseshoe-vortex system consists of a vortex, driving a counter current of negative vorticity, being suituated underneath. The strength and location of this horse-shoe vortex system depend on the approach flow velocity and it could be parametrized by the flow Reynolds number. The system is stronger and closer to the base of the cylinder for the higher flow velocity.

- The horse-shoe vortex system, created in the stagination plane, stretches while moving around the cylinder in the streamwise direction and is decaying in strength. While the vortox remains reasonably close to the cylinder, the counter-current of negative vorticity grows in size towards the outside.
- Downstream of the cylinder, seperation with flow reversal is evident, being accompanied by a considerable increase in the turbulence intensities.
- The horse-shoe vortex system, where the turbulence gets to be very strong, produces a high bed shear stress beneath it.
- This system will play an important role, if the bed of the channel is mobile. It can be imagined that the counter current does the erosion, while the vortex does the transportation of sediments.

The study of Graf and Yulistiyanto (1999) lends insight into the formation and the development of the horseshoe-vortex system as created by the flow around a cylinder.

Ali and Karim (2006) simulated the three-dimensional flow field around a circular cylinder using FLUENT CFD and obtained solutions for rigid beds and for scour holes of different sizes resulting from different time durations. They used the numerical results to obtain the variation of bed shear around the cylinder. Based on their results they concluded that the boundary shear stress alone did not account for the entrainment and transport of the sediment particles. The degree of the turbulence intensity, especially in the obstructed flow also contributed significantly in the scouring process. Moreover they could not predict the turbulence bursts which are capable of removing sediment from bed. Thus they also insisted on the need for precise turbulence flow measurements around the pier.

Graf *et al.* (2001) investigated the flow patterns in planes upstream and downstream of a cylinder and vertically in the scour hole using an acoustic-Doppler velocity-profiler (ADVP). They found that the shear stress was reduced in the scour hole as compared to the approach flow but that the turbulent kinetic energy was very strong at the foot of the cylinder on the upstream side. The turbulent kinetic energy was also very strong in the wake behind the cylinder.

2.7 DEVELOPMENT OF MAXIMUM SCOUR DEPTH WITH TIME

Chabert and Engeldinger (1956) described the behavioural pattern of scour at a cylindrical pier with respect to the variation of scour depth with time. In clear-water scour,

equilibrium scour depth is approached asymptotically with time, while in live-bed scour the scour develops rapidly and then fluctuates in response to the passage of bed forms. According to Shen *et al.* (1969), the equilibrium scour depth in live-bed scour is less than in clear-water scour by 10% (Fig. 2.8).

2.7.1 Temporal Development of Scour around Circular Piers without any Devices

A majority of scour studies have been carried out for the case of clear water flow. Most investigators have attempted to develop relationships for the maximum scour depth in steady flow, and these are used for design. However, the flow in a river during a flood is unsteady, and discharge changes are quite rapid. In natural streams at the peak discharges, the unsteadiness of flow is pronounced, and one is never certain that the maximum scour depth for a given discharge would always be reached when the discharge does not run for a long time. Therefore, hydraulic design for foundations based on computation of maximum scour depth for design discharge can be erroneous. In this context, the temporal variation of scour depth assumes importance and forms an important tool for the calculation of scour depth in case of unsteady flow. Furthermore the bed materials of the river and canals are almost always nonuniform and/or stratified. In rational approach for the determination of scour depth due to these factors of unsteadiness, non-uniformity, and stratification is taken into consideration in the study of Kothyari *et al.* (1992a).

The process of local scour in the vicinity of bridge piers is time dependent. Time development of scour is the level of maximum scour depth attained in a given time. It is often represented in graphical form by plotting the maximum scour depth against the time. Because of the complexity of the scour process, the majority of the literature is on the determination of the maximum equilibrium scour depth for a given flow and sediment condition and pier geometry. The time development of scour has attracted the attention of many researchers (e.g. Hjorth (1997), Ettema (1980), Kothayri *et al.* (1992), Melville and Chiew (1999), Oliveto and Hager (2002), Mia and Nago (2003), Chang *et al.* (2004), Dey and Barbhuiya (2004), Mashair *et al.* (2004), Kothyari *et al*. (2007)

The abovementioned investigations have mostly focused on scour around such piers which have uniform cross-section (or geometry) along their height. Most of the investigations did not pay any attention to the effects of foundation geometry on scour (Parola *et al*., 1996). But actual bridge piers are constructed in various types of geometries and many of them can

have non-uniform cross-sections along their heights (Melville and Raudkivi, 1996). Such piers are termed here as compound piers (or non-uniform piers).

Only a few investigators such as Chabert and Engeldinger, (1956); Neill, (1973); Chiew, (1984); Imamoto and Ohtoshi, (1987); Tsujimoto *et al*., (1987); Jones *et al*., (1992); Fotherby and Jones, (1993); Melville and Raudkivi, (1996); Coleman, (2005) and Ashtiani *et al.*, (2010) have studied the effect of foundation geometry on scour. Much less number of studies related to temporal variation of scour circular compound bridge piers are available so far (Melville and Raudkivi, 1996; Kumar *et al.,* 2003; and Lu *et al.,* 2011). The significance of the temporal scour evolution rather than the equilibrium scour depth has been further emphasized recently (Cardoso and Bettess, 1999; Ahmed and Rajaratnam, 2000; Melville and Coleman, 2000; Kothyari and Ranga Raju, 2001; Ballio and Orsi, 2000, Oliveto and Hager, 2002 and 2005; Mia and Nago, 2003; Chang *et al.*, 2004 and Sheppard *et al*., 2004, Ballio *et al*., 2010). Melville and Raudkivi, (1996) have presented a methodology for estimation of maximum depth of scour around the compound piers. Lu *et al.,* (2011) proposed a semiempirical model to compute the time variation of scour at circular compound pier with unexposed foundation.

The semi empirical model proposed by Mia and Nago, (2003) to compute the time variations of scour at uniform circular piers was modified to describe the scour rate ahead of the pier nose for a non uniform circular pier by using the concept of effective diameter of Melville & Raudkivi, 1996. The concept of primary vortex (Kothyari *et al*., 1992 a) and volumetric rate of sediment transport theory of Yalin, (1977) was used in the proposed model of Lu *et al.*, (2011).

2.8 MAXIMUM SCOUR DEPTH PREDICTION EQUATIONS

Several empirical and semi-analytical studies for the estimation of scour depths are available in the literature. A detailed description for the pier scour relationships can be found in Kumar (2007). Hence the same is not repeated here. Only a brief mention of some of these is made below.

Kothyari *et al.* (1992a, 1992b) have given a semi-analytical approach for the calculation of temporal variation of scour depth as well as the equilibrium scour depth around circular piers. Their method is applicable to both clear water and live-bed scour and takes into account flow unsteadiness, sediment non-uniformity and stratification of bed. Melville and

Sutherland (1998) have proposed enveloping equations for scour in which several coefficients have been introduced to take care of pier shape, pier alignment, sediment non-uniformity etc. A check on available methods by Garde and Kothyari (1998) using field data has shown the superiority of the forgoing two methods over others. As such, these two methods are recommended for the computation of scour around bridge piers in the absence of any device (Ranga Raju, 1999). Following relationships was given by Kothyari *et al.* (1992a) for the estimation of clear water scour around bridge piers.

$$\frac{d_{sc}}{b} = \alpha 0.66 \left(\frac{b}{d}\right)^{-0.25} \left(\frac{h}{d}\right)^{0.16} \left[\frac{V_0^2 - V_t^2}{\frac{\Delta\gamma_S}{\rho} d}\right]^{0.4} \quad -0.3 \tag{2.1}$$

and the expression for the V_t is given by

$$\frac{V_t^2}{\frac{\Delta\gamma_s}{\rho} d} = 1.2 \left(\frac{b}{d}\right)^{-0.11} \left(\frac{h}{d}\right)^{0.16} \tag{2.2}$$

Equation (2.1) can also be expressed as

$$\frac{d_{sc}}{d} = \alpha 0.66 \left(\frac{b}{d}\right)^{0.75} \left(\frac{h}{d}\right)^{0.16} \left[\frac{V_0^2 - V_t^2}{\frac{\Delta\gamma_S}{\rho} d}\right]^{0.4} \quad -0.3 \tag{2.3}$$

Similarly for the live-bed scour Kothyari *et al.* (1992b) state that

$$\frac{d_{se}}{d} = \alpha 0.88 \left(\frac{b}{d}\right)^{0.67} \left(\frac{h}{d}\right)^{0.4} \quad -0.3 \tag{2.4}$$

Where,

b = pier diameter,
d = size of sediment,
h = approach flow depth,
V_O = stream wise approach flow velocity,
V_t = threshold velocity of approach,
α = opening ratio $[(B_O - b)/B_O]$,
B_O = centre to centre spacing of pier or flume width,
γ_f = specific weight of fluid,
γ_s = specific weight of sediment,

ρ = fluid density,
d_{se} = equilibrium scour depth in live-bed below original bed-level
d_{sc} = equilibrium scour depth in clear water below original bed-level.

2.9 COUNTERMEASURES FOR REDUCTION OF LOCAL SCOUR AT BRIDGE SITES

The purpose of this section of the literature review is to briefly shed light on the various methods available for preventing local scour at a bridge pier. Lagasse *et al.* (2001) defined countermeasures as "measures incorporated into a highway-stream crossing system to monitor, control, inhibit, change, delay, or minimise stream instability and bridge scour problems". Mitigation measures for local scour at bridge piers can be grouped into armouring techniques and flow alteration devices (Johnson *et al.*, 2001 and Melville and Hadfield, 1999).

Armouring techniques are where piers are protected to withstand shear stresses during high flow events while the flow altering device aims to disrupt the flow field around the pier and thereby decrease the erosive strength of the down-flow and horseshoe vortex systems by way of breaking up vortices and reducing the velocity in the vicinity of the piers (Lauchlan, 1999). Armouring technique for piers and abutments include riprap, precast concrete units, grout-filled bags, foundation extensions, concrete aprons, and gabions. Armouring devices protect the river bed within the vicinity of the pier against erosive forces.

Flow altering devices at piers include the use of sheet piles and sacrificial piles placed upstream of the pier or circular shields or collars constructed around the piers. Johnson and Niezgoda (2004) identified basically two types of flow altering devices. The first category is used to break up vortices and reduce the high flow velocities, particularly upstream of a pier. Sacrificial piles, such as sill, sheet or cylindrical piles, are common examples of the first category. The second category realigns the flow to prevent local and contraction scour together with bank widening and lateral migration. The common examples of the second category of flow altering devices include vanes and guidebanks.

In the opinion of Johnson and Niezgoda (2004), feasibility of and confidence in each of the various countermeasures is a function of many variables which include effectiveness, cost, maintenance, and the ability to detect failure. Therefore, the type of protection that is applicable at a bridge pier depends on the nature of the problem.

2.10 APPLICATION OF COLLARS AS A COUNTERMEASURE FOR LOCAL SCOUR AT BRIDGE PIERS

2.10.1 Collars

Melville and Coleman (2000) defined collars as devices attached to the pier at some level usually close to the bed. A collar is in the form of a thin protective disc. A protective disc is a surface which has a negligible thickness, and which is incapable of promoting scour development (Fotherby and Jones, 1993). A collar must not be so thick that it causes an obstruction to the flow and advances scour (Whitehouse 1998). A collar extends around the outside edge of the pier with the main objective of protecting the bed from the scouring effect of the down-flow at the pier and the associated vortex action around the base of the pier. An example of a typical collar arrangement for both rectangular and circular pier is shown in Fig. 2.9. The concept behind a collar as a countermeasure is that the presence of the device will sufficiently inhibit and deflect the local scour mechanisms so that the scour is reduced.

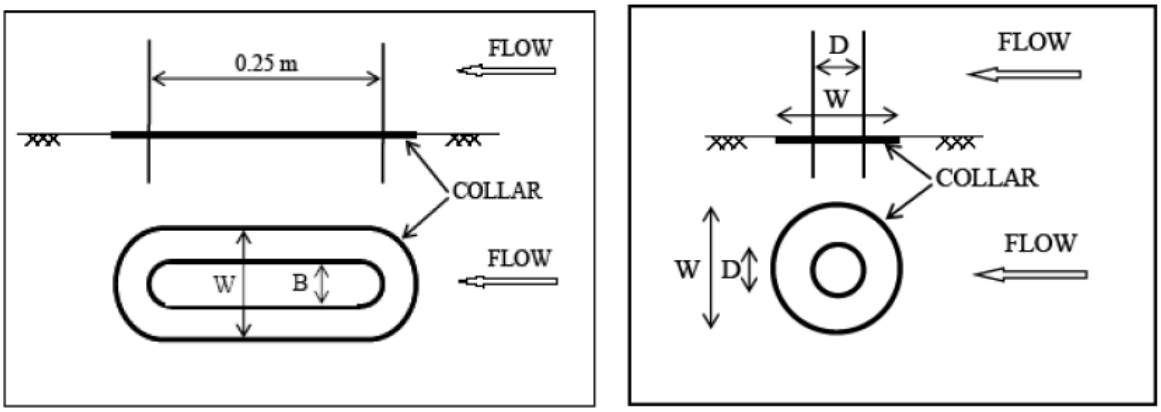

FIG. 2.9 Collars Positioned around Rectangular and Circular Pier (Mashahir *et al.*, 2004)

2.10.2 Earlier work done on the use of collars on piers

Laursen and Toch **(1956)** worked on the possibility of using a collar-like device for preventing scour at a pier. From their work, it was concluded that such devices may be useful for scour mitigation. However, there was no indication from the author as to the practicability of using collars in the field.

Chabert and Engeldinger **(1956)** found that a single circular plate placed 0.4b below the original bed elevation and having a diameter of 3*b*, where *b* is the pier diameter, could

reduce the depth of scour by 60%. No appreciable reduction in scour depth was noticed when an increased number of such plates were tested for various elevations.

***Thomas* (1967)** worked on preventing local scour at a bridge pier and observed that the depth of scour could be reduced by placing a horizontal shield on the pier. The effect of a horizontal shield, which Thomas named "anti-scour", on the depth and extent of the scour at a pier was described. Experiments were conducted using a 50 mm diameter circular pier on which had been fitted a horizontal shield. Two different sizes of shield with B= 100 mm and 150 mm were used, where B is the diameter of the collar. The relative heights of the shield above the channel bed were y_c/y_o = 0.0, 0.18, 0.317, 0.45 and 0.73. The symbol y_c is the distance above the channel bed and y_0 is the depth of the flow. The most effective diameter of the plate recommended by Thomas is three times the pier diameter positioned very close to the channel bed. This result is similar to the observation made by Chabert and Engeldinger (1956).

***Tanaka and Yano* (1967)** also studied the use of a collar to prevent scouring. In their experiment, a fine river sand of median size 0.4 mm, a flow depth of 100 mm and a circular pier of diameter 30 mm were used. A thin circular plate was fitted on the circular pier. The diameters of the plate were, B = 90 mm, 120 mm, 150 mm and 180 mm, and its position on the pier was systematically changed. It was reported that a decrease in the size of the plate led to a decrease in the effect of the plate at reducing the scour depth and vice versa. An increase in the plate elevation with respect to the bed surface also resulted in an increased scour depth. Tanaka and Yano's results are similar to the observations made by Thomas (1967).

***Ettema* (1980)** conducted a series of experiments to ascertain the possibility of using a thin collar to mitigate against local scour at a circular bridge pier. Collars were installed on a circular pier at various elevations on, above and below the channel bed. The experiments were conducted in a 0.46 m wide flume using a 45 mm diameter pier. In order for ripples not to form on the flume bed, 1.90 mm diameter coarse sand sediment was used for the experiment. The flow depth was set at 0.20 m while the ratio of u_*/u_{*c} was 0.90, where u_* is the shear velocity and u_{*c} is the critical shear velocity. A 0.4 mm thick, circular, brass collar of width two times the pier diameter was installed on the circular pier at four different locations, viz. y_c/b = 0.5, 0, -0.5 and -0.1, where y_c is the elevation of collar relative to channel bed. It was observed that, when a collar of width twice the size of the pier diameter was installed at an elevation of half the diameter (y_c/b = 0.5) above the channel bed, the

collar was not effective at reducing the scour depth. However, the effectiveness of a collar at reducing scour became noticeable when the collar was installed at the channel bed. No scour developed below the collar when the collar was installed at y_c/b = -0.1. Ettema's (1980) results compared favourably with the results obtained by Tanaka and Yano (1967) and Thomas (1967). The general conclusion was that the influence of the width of the collar on scour increased as the elevation of the collar is decreased.

***Dargahi* (1990)** carried out research on the mechanisms of local scour and how a collar may influence the horseshoe vortex system and ultimately reduce the amount of scour. The experiments were conducted using a uniformly-graded fine sand of median diameter, d_{50} = 0.36 mm. A circular pier of diameter 0.15 m was used for each test. The mean flow velocity was 0.26 m/s. The ratio of u_*/u_{*c} was 0.85 while the flow depth was maintained at 0.2 m. In order to study the effect of collar shape on performance, two separate collar shapes were tested: One shape was a thin circular collar of diameter 0.28 m (with B/b = 1.86) and the other was a collar with a Joukowski profile. The Joukowski profile has an airfoil shape that resembles the cross section of an airplane wing. The Joukowski collar was attached to the circular pier such that its blunt nose faced upstream. The collar was positioned at elevations y_c/y_o = 0.25, 0.05, -0.015, and -0.05 relative to the initial channel bed. The total test duration for each experiment was 12 hours. At the end of the test, the scour profiles were measured along the line of symmetry for each collar position.

It was observed that the collar was not effective at hindering the horseshoe vortex formation. It was reported that, irrespective of the collar position and shape, the scour mechanism was similar to the case of a circular pier unprotected with a collar. The maximum reduction in scour depth as a result of the collar occurred at a collar position of y_c/y_o = -0.015. At y_c/y_o = -0.015, it was found that the maximum reduction of scour depth was 50% and 75% at the upstream and downstream region of the pier, respectively. The collar position y_c/y_o = 0.25 did not significantly influence the amount of scour. Similar results were obtained for the two collar shapes tested. It was also reported that, when the ratio of the collar thickness to the pier diameter becomes large, an increase in the effective diameter of the pier resulted, which subsequently caused an increase in the scour depth. Dargahi, however, cautioned that further research is needed before a practical application of a collar is recommended.

***Chiew* (1992)** experimentally studied the effect of a collar, a slot and a combination of the two in reducing the local scour in the vicinity of a pier. A slot is a hole through the pier to allow the passage of flowing water. The objective of the study was to review existing mitigation approaches and to propose alternative or new devices for mitigating scour in the vicinity of bridge piers. The experiment was conducted using a 32 mm diameter pier and a median particle size of 0.33 mm. The flow intensity, (i.e., u_*/u_{*c}) was maintained at 0.9 and the depth of flow was 180 mm. The collar consisted of a 1 mm thick stainless steel plate. Experiments with 2*b* and 3*b* wide collars were tested alone and in combination with a pier slot while the positions of the collars were systematically varied. Equilibrium scour depth was defined as the depth attained when there was less than 1 mm change in scour depth in eight hours. Using this criterion, the tests were run for approximately 72 hrs.

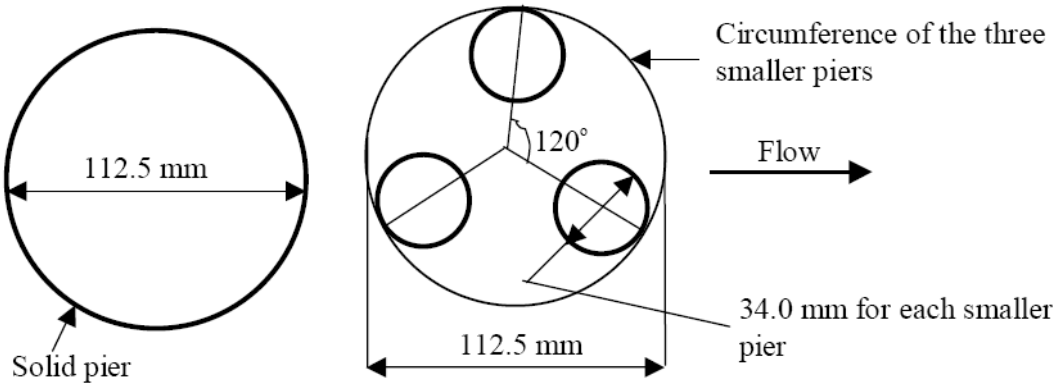

FIG. 2.10 Schematic Illustration of Vittal *et al.* Experiment (Vittal *et al.*, 1993)

The collar alone was found to reduce the scour depth by as much as 20% while no scour occurred when a *b*/4 slot was used in conjunction with a collar. Similar results were obtained for the two collar diameters tested. When designed and applied with care, Chiew concluded that a combination of collar and slot can be a suitable substitute for the use of riprap as a countermeasure for local scour at bridge piers. These results compared favourably with the results of Ettema (1980) and Tanaka and Yano (1967).

***Vittal et al.* (1993)** studied and compared the scour reduction efficacies of a circular collar on a pier group that was made up of three individual smaller piers. Similar experiment was also performed on a single solid pier. Figure 2.10 shows the schematic illustration of the pier arrangement of their experiments. In the study, a collar fitted to a group of three cylindrical piers angularly spaced at 120º was studied as a scour reduction device. The particular arrangement of the cylinders is such that any one of them can just pass through the

gap between the other two. The sediments used in their experiment were cohesionless natural riverbed sands, with a relative density of 2.65 and geometric mean sizes of 0.775 mm, 1.183 mm, 1.543 mm and 1.844 mm. The flow intensity ranged between 0.88 and 0.90. In the experiment, the diameter of the solid pier and that of the circumscribing circle of the pier group was 112.5 mm, while the width of the collar was 2*b*. The diameter of the individual three smaller piers that made up the pier group was 34 mm each. The collar was positioned at a height of 15 mm above the channel bed. The full pier group was tested at an orientation of θ = 0º, 15º, 30º, 45º and 60º with respect to the approach flow direction. The duration of each test was six hours. The scour due to the pier group was compared with that of a solid circular pier.

Regarding scour reduction, the full pier group alone without the collar was found to be more effective than a solid cylinder having a full slot of width equal to half the cylinder diameter and as effective as a solid cylinder fitted with a collar of width 3.5 times its diameter. They observed that a collar of 2.0*b* on a full pier group is equivalent to a collar of more than 6.0*b* on solid pier. Vittal *et al.* (1993) concluded that a collar fitted to a pier group is much more effective than the one fitted on a solid pier as far as scour mitigation is concerned.

Fotherby and Jones **(1993)** studied how effective collars are at reducing scour. The authors recognised the potential usage of both a collar and a footing at reducing scour. According to Fotherby and Jones, the parameters influencing the scour mechanism for footings and collars are their height above the channel bed, the width and the thickness. It was concluded that the larger the collar the more its effectiveness at reducing scour and that collar effectiveness reduces when the collar is placed at a greater elevation above the channel bed. Fotherby and Jones pointed out that a collar has been recognised as a conceptual scour countermeasure technique but has not been used in practice.

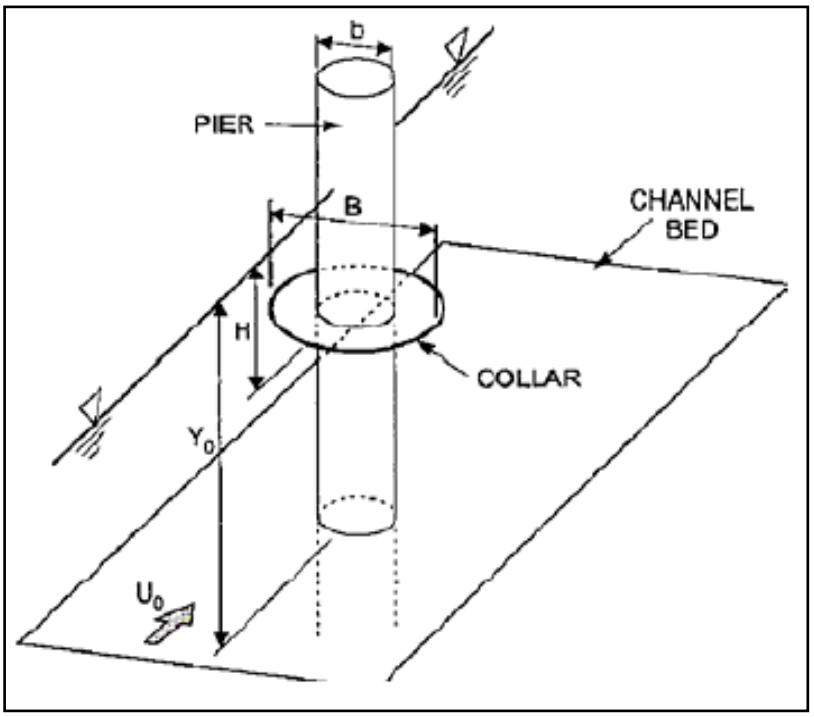

FIG. 2.11 Collar Installation on the Pier above the Channel Bed (Kumar *et al.*, 1999)

***Kumar et al.* (1999)** also worked on the use of collars around a cylindrical pier to reduce the scour depth. For the experiment on collar efficacy, five different collar sizes of thickness 3 mm were used (i.e., B = 1.5b, 2.0b, 2.5b, 3.0b and 4.0b). Figure 2.11 shows the collar-pier arrangement used by Kumar *et al*. (1999) in their experiment. It was observed that the width of the collars as well as the relative position of the collars to the bed affected both the depth and location of the maximum scour location. It was also observed that small collars resulted in large scour holes at the upstream pier face, while scour depth was greatest in the wake regions for the larger collars. Generally, Kumar *et al.* (1999) concluded that a large collar placed at a low elevation relative to the bed was most effective at reducing scour. Kumar *et al.* also worked on the possible combination of collars and slot and found the combination to be very effective at reducing scour. They cautioned, however, that a slot is practically ineffective if the approach flow has a high angle of attack with respect to the slot.

***Singh et al.* (2001)** worked on a collar as a scour protection device around a circular pier. The authors believed that the growth of a vortex can be arrested by retaining the vortex on a rigid surface such as a collar plate. Experiments were conducted in a flume containing fine sediment, d_{50} = 0.285 mm and σ_g = 2.51 where σ_g is relative density and d_{50} is geometric mean size of the sediment. The piers tested were of diameters 25 mm and 62 mm and the

duration of the test was kept at 300 minutes. It was observed that the efficacy of a collar in preventing scour is a function of its width and its vertical location with respect to the channel bed. It was observed that, as the size of a collar plate increases, the scour decreases. Collar plates of sizes B = 1.5b, 2.0b and 2.5b placed on the channel bed resulted in a reduction of scour by 50%, 68% and 100%, respectively, of an unprotected pier. Collar plates of size B = 2.0b when placed at 0.1b below the bed gave a maximum reduction in scour depth of 91%. However, when the same collar plate was located at 0.5b above the bed, a 25% reduction in scour depth resulted.

Most previous studies on collars have been on circular piers. Recently, however, ***Zarrati et al.*** **(2004)** worked on the application of a collar to control the scouring around rectangular bridge piers having a rounded nose. It was found that collar effectiveness improves as the collar becomes wider and as the level at which it is positioned on the pier becomes lower. They also found that the effectiveness of a collar is reduced as the pier skewness with respect to the flow is increased. On the time of development of the maximum scour depth, Mashahir and Zarrati (2002) and Zarrati *et al.* (2004) concluded that the time to reach an equilibrium condition is different depending on whether or not the pier is protected with a collar. According to them, it took 20 hrs to reach an equilibrium condition when the pier was unprotected with a collar as compared to 50 hours that was required to reach an equilibrium condition for the pier protected with a collar. Mashahir *et al.* (2004) also studied the temporal development of scour depth at a bridge pier. In their experiment, a collar size of three times the pier diameter was used. The sediment material had a median size of 0.95 mm and a geometric standard deviation which was less than 1.2 (i.e., very uniform). While the diameter of the circular pier used in the study was 400 mm, the ratio of the shear velocity to the critical shear velocity was calculated to be 0.92 based on the Shield's criterion. Using a definition of time to equilibrium scour depth for which the change in scour depth was less than 2% of the pier diameter in eight hours, the duration of each experiment was limited to 44 hours. FigureS 2.12 and 2.13 show the flow pattern and collar geometry given by Zarrati *et.al.* (2006)

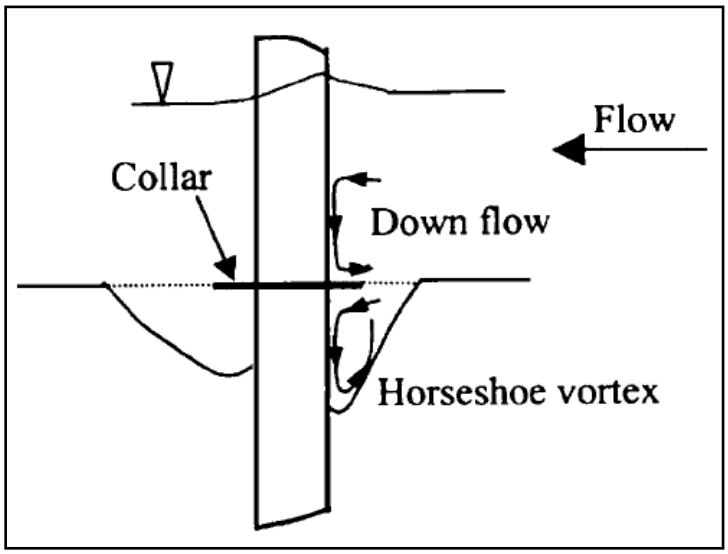

FIG.2.12. Scouring and Flow Pattern around a Pier (Zarrati *et.al.* 2006)

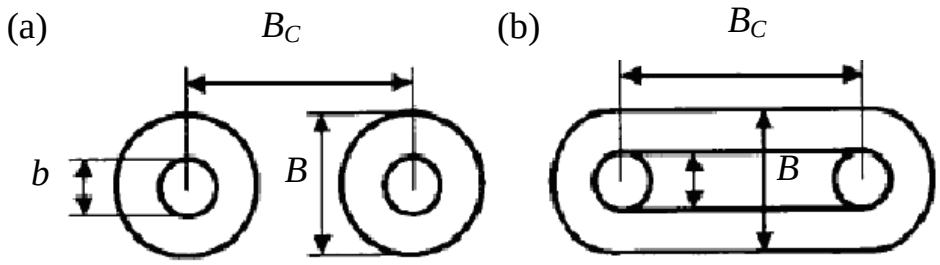

FIG.2.13 Type of Collars: (a) Independent (b) Continuous (Zarrati *et. al.*, 2006)

As concluded in the study by Mashahir *et al.* (2004), placing the collar below the channel bed level did not lead to an appreciable increase in the efficacy of the collar. This was so because the depth of sediments above the collar will itself become part of the scour hole as this is swept away very fast by the erosive action of the flow. Comparison of the results for rectangular piers aligned with the flow and the previous experiments on circular piers by Zarrati *et al.* (2004) and Mashahir *et al*. showed that a collar of B/b = 3 is more effective at reducing the depth of the scour hole for rectangular piers than for circular piers.

For a possible application of two collars at the same time, it was reported by Zarrati *et al.* (2004) that installation of a second collar at an elevation above the channel bed increases the effectiveness of collars. Mashahir *et al.* (2004) reported that collars not only reduce scour depth but also reduce the scouring rate considerably.

***Mashahir et al.* (2004)** observed that a collar has a better efficiency at reducing the rate of scour than a pier foundation of the same width installed on the same level. When a

collar is installed on the pier, the direct impact of the downflow to the riverbed is prevented. In addition to a reduction of the maximum scour depth, the rate of scouring is also reduced considerably. Reduction in the rate of scouring can reduce the risk of pier failure when the duration of floods is short (Melville and Raudkivi, 1996; Melville and Chiew, 1999).

***Kayaturk et al.* (2004)** studied the effect of a collar on the temporal development of scour around bridge abutments. The experiments were conducted in a 1.5 m wide flume having a bottom slope of 0.0001. With a flow intensity of 0.90, all of the tests were run under clear-water scour conditions. Operating at a flow depth of 100 mm and a discharge of 0.05m^3/s, each experiment was limited to duration of six hours. The soil material had a d_{50} = 1.48 mm and geometric standard deviation, σ_g = 1.28. In this study, the time development of the local scour around the abutment fitted with and without collar plates was studied. The effects of various sizes of collars fitted at different elevations on the temporal development of scour depth at the abutment were also studied.

Four different collar widths, B = 0.025 m, 0.050 m, 0.075 m and 0.10 m, were tested. Since the effectiveness of the collar on the development of the scour hole is also a function of its vertical location on the abutment, all collar types were tested at various elevations, including at the bed level, 0.025 m and 0.050 m above the bed level, and 0.025 m and 0.050 m below the bed level. According to Kayaturk *et al.* (2004), a 67% reduction in the scour depth was achieved when the collar was positioned at an elevation of 50 mm below the channel bed.

The results of Kayaturk *et al.* (2004) are in agreement with the other researchers that, as the collar width increases, the scour depth decreases for a given time. They concluded that application of collars at abutments is very effective at reducing the development of scour depth.

***Zarrati et al.* (2006)** studied the use of independent and continuous pier collars in combination with riprap for reducing local scour around bridge pier groups. Their results showed that with two piers in line, a combination of continuous collars and riprap led to a scour reduction of about 50% and 60% for the front and rear piers, respectively. In another experiment with two piers in line, independent collars showed better efficiency than a continuous collar around both the pier. It was also observed that the efficiency of collars is more on a rectangular pier aligned to the flow than two piers in line.

Lauchlan (1999), Dey (1997), Whitehouse (1998), Hoffmans and Verheij (1997), and Melville and Coleman (2000) also gave a brief review of the application of a protective collar as a countermeasure for local scour at bridge pier. The general agreement is that a collar can be used to reduce scour depth as well as to reduce the scouring rate.

In summary, based on a variety of experimental studies that have been undertaken using collar techniques, the general agreement appears to be that a reasonably large collar placed at or slightly below the bed level can provide significant protection against scour. It should be noted, however, that all of the above studies on collars have been done for clear-water conditions.

2.11 SCALE EFFECTS ON LOCAL SCOUR

The scale effect become evident when one considers the similitude requirements for hydraulic modeling of pier scour. The requirements are difficult to meet because the equations do not include key parameters needed for pier-scour similitude. Therefore the scour prediction methods developed in the laboratories and the scour equations based on laboratory data did not always produce reasonable results for field conditions.

The variability and complexity of site conditions make the development of methodology for predicting scour at bridge piers difficult. The early investigations concentrated mostly on local scour estimation and those were based on dimensional analysis and data correlation of small-scale laboratory experiments. The current equations and methods for estimating local scour at bridges are based primarily on laboratory research. A literature review (McIntosh, 1989) found that more than 35 equations had been proposed till then for predicting the scour depth at a bridge pier. Most local-scour equations are based on research in laboratory flumes with non-cohesive, uniform bed material and limited verification of results with field data. The existing bridge scour equation from HEC-18 (Richardson et al., 2001) was developed from laboratory experiments in relatively small scale based on Froude similarity, in which effects of Reynolds number or turbulence effects were ignored due to the difficulties in meeting both Froude number and Reynolds number similarities. Although Froude number similarity generally plays a more significant role in free surface water flow, effects of turbulence may not be negligible for flows near a bridge pier. Very little field data has been collected to verify the applicability and accuracy of the

various design procedures for the range of soil conditions, stream flow conditions and bridge designs encountered throughout the country.

Mueller *et al*., (2002) compared 22 number of scour equations using field data collected by the USGS. He concluded that the HEC-18 equation was good for design because it rarely under predicted measured scour depth. However, it frequently over-predicted the observed scour.

Gao *et al*. (1993) presented an equation that has been used in China for more than 20 years by highway and railway engineers. The equation was developed from Chinese data of local scour at bridge piers, including 212 data points representing live-bed scour data and 40 data points representing clear-water scour data. The equations have been tested using field data given by Froehlich (1989) and 184 number of filed data points from U.S.S.R.

Ansari and Qadar (1994) fitted envelop equations to more than 100 field measurements of pier scour depth, derived from 12 different sources and several countries, including 40 measurements from India. They also presented a comparison of the field data they used with estimates of scour depth obtained by Neil (1973), Melville and Sutherland (1988).

Landers *et al*. (1996) presented a detailed analysis of a subset of the local pier scour data, only one measurement being included for each bridge. They compare the field data with trends derived from laboratory studies and those developed in New Zealand and concluded that the laboratory-based relations provide a reasonable description of the field data.

Unfortunately, most of the field observations of bridge pier scour were of poor quality, often lacking in important details. The parameters that influence local scour are difficult to include explicitly in an equation based primarily on field data because of the difficulties to control flow and channel conditions in field situations.

Physical model test has been one of the most effective ways to understand local scour process so far. However, it is subject to some drawbacks. Apart from being expensive and time consuming, small-scale laboratory tests do suffer from scale effects because most of the scale down models cannot satisfy the similarity laws. There are several scale effects such as the Reynolds number, Froude number, and so on. The scale effects need to be considered when the experimental results are extrapolated to prototype situations.

Unfortunately, it is very difficult for a model and a prototype to satisfy the requirements of both Reynolds number and Froude number similarities. Hence, most of the physical models for local scour search are distorted models. The big errors may be existent if the results of distorted models are used to predict the behaviors of the prototypes.

The local scour depth equation was derived from small-scale laboratory experiments based on Froude similarity, in which effects of Reynolds number were ignored due to the difficulties in meeting both Froude number and Reynolds number similarities. Therefore, the physical models are distorted models. Although Froude similarity generally plays a more important role in gravity surface water flow, effects of turbulence may not be negligible for flows near bridge pier, i.e., Reynolds number similarity should therefore be considered too in the physical model.

Yang (2005) performed numerical investigations of scale effects on local scour around a bridge piers using CFD software. The differences between the results of large-sized simulation model and the physical model derived results from the small-sized simulation model following Froude law are shown in Fig. 2.14 (where *rp* is radius of pier). Large differences exist in the results because the physical model is affected by scale effects.

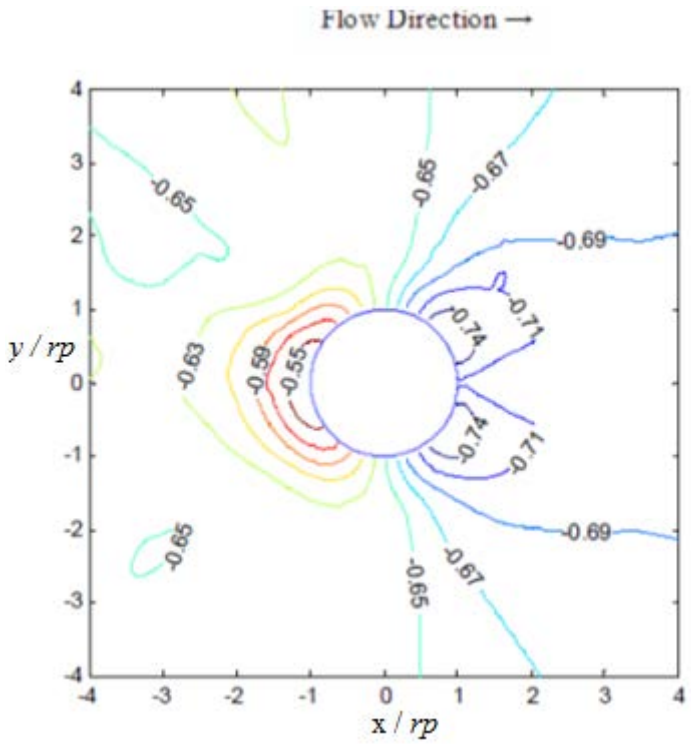

FIG. 2.14 Contours of Relative Scour (D_s / *rp*) Differences between the Large-Sized Simulation Model and the Physical Model Derived From the Small-Sized Simulation according To Froude Law (Yang, 2005).

Ignoring Reynolds similarity in physical modeling approach may result in errors while computing scour in large bridge piers. The degree of the turbulence intensity, especially in an obstructed flow field, also contributes significantly in the scouring process. In a physical model, not all relevant quantities could be furnished. Some physical quantities in a turbulence flow are difficult to measure. One of these quantities is the vortex, which is known to be the major factor responsible for base scouring.

Sheppard *et al.* (2004) performed local clear-water scour tests with three different diameter circular piles (0.114, 0.305, and 0.914 m), three different uniform cohesionless sediment diameters (0.22, 0.80, and 2.90 mm) and a range of water depths and flow velocities. The tests were performed in large size flume which was the 6.1 m wide, 6.4 m deep, and 38.4 m long flume at the United States Geological Survey Conte Research Center in Turners Falls, Mass. Their tests extend local scour data obtained in controlled experiments to prototype size piles and ratios of pile diameter to sediment diameter varied from 4 to 155. Water for flow through flume in their experiments was supplied by a hydroelectric power plant reservoir wherein the concentration of suspended fine sediment (wash load) could not be controlled. Equilibrium scour depths were found to also depend on the wash load concentration. Time history plots of scour depth along with the curve fits used to estimate equilibrium depth presented by them is illustrated in Fig. 2.15. Fig. 2.16 shows three time history plots for the 0.914 m diameter pile in the 0.22 mm sediment.

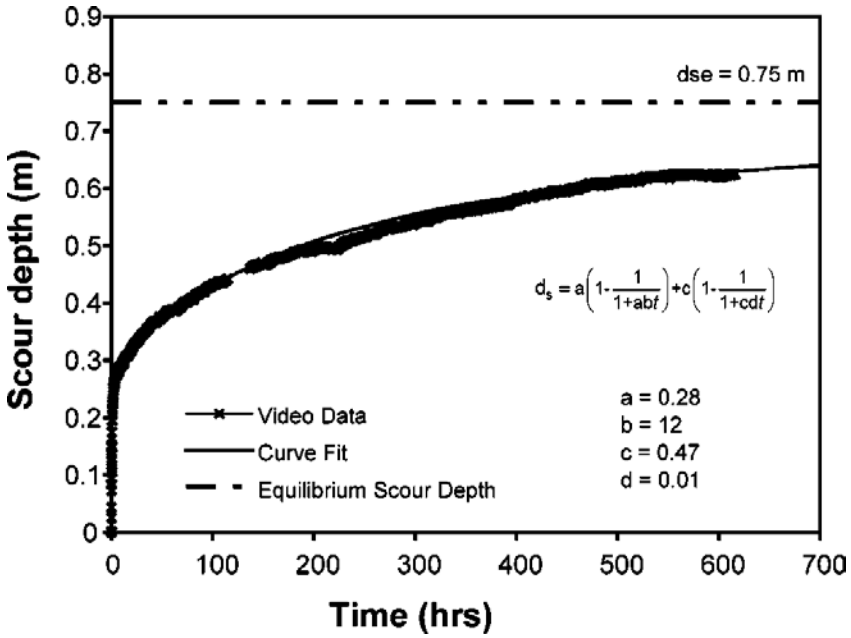

FIG. 2.15 Time History of Scour Depth (Sheppard *et al.*, 2004)

The experiments of Sheppard *et al.* (2004) have extended local structure-induced sediment scour data to the lower ranges of prototype values of b/d_{50}. They also verified the functional dependence of normalized equilibrium scour depth d_{se} /b on b/d_{50} in the clear-water scour range reported earlier by Sheppard *et al.* (1995) and Sheppard (private communication, 2004). This relationship has major implications in scour depth prediction for prototype structures in relatively fine sands as well as the interpretation of physical model test results. The discovery of the sensitivity of clear-water equilibrium scour depth and scour rate on suspended sediment concentration is also significant. This might help explain some of the scatter in published data and the differences in data obtained by different researchers. It might also help explain why laboratory data results often over predict clear-water scour values observed in the field.

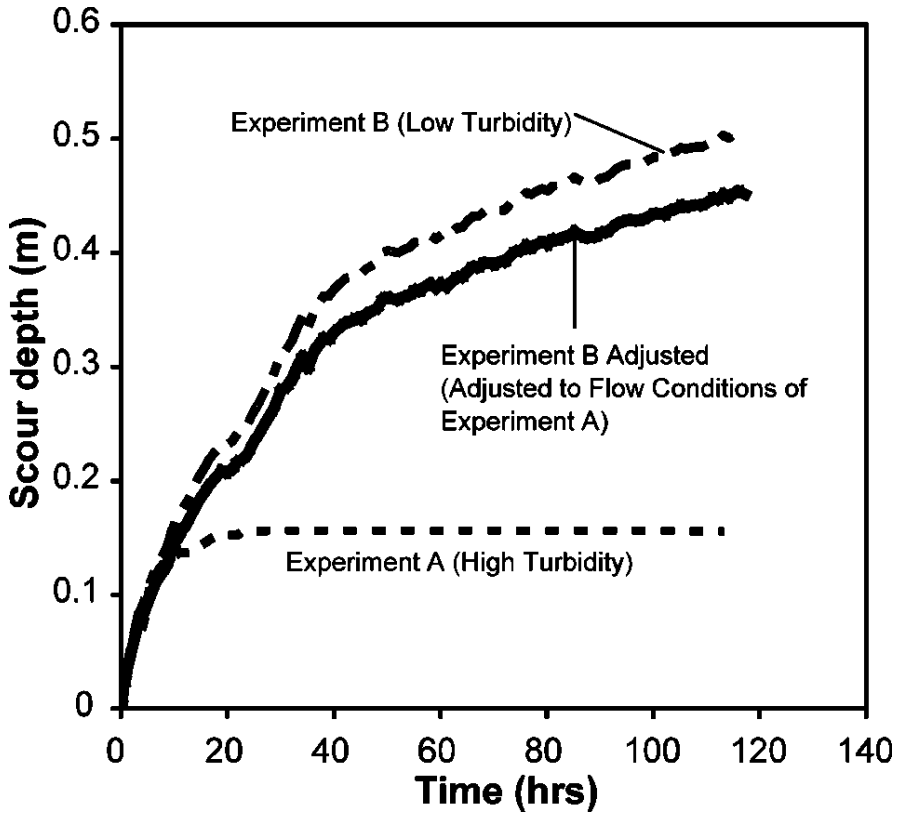

FIG. 2.16 Scour Time Rate Plot Demonstrating Wash Load Effects on Scour Depths (Sheppard *et al.*, 2004)

2.12 CONCLUDING REMARKS

As a precursor to this research study, an extensive literature review has been undertaken. The outcome of the review revealed that further work is needed on various

aspects of scour in the presence of collars, especially in the area of temporal development of scour around collars under live bed conditions and below the collar at pier nose and sideways in both clear water and live-bed conditions. The evaluation of the efficacy of a collar as a countermeasure for local scour at a bridge pier needs additional work before a practical application of a collar can be confirmed. The philosophy upon which devices such as collars is based on the premise that their existence will sufficiently prevent and deflect the downflow and rotating vortex causing scour with the overall effect of reducing the scour depth. Based on the findings reported herein, the use of collars is an effective method for reducing local scour at a bridge pier.

Model studies revealed that collars are not only very effective at reducing scour but are also much more economical when compared to countermeasure techniques like riprap. It has been concluded that the larger is the extent of collar around the pier the greater is the scour reduction level, and for maximum performance the collar should be placed at or below the channel bed level. All previous studies on the use of a collar as a countermeasure for local scour at a bridge pier are based on experiments carried out using a physical hydraulic model and as such the practicality of using a collar on the field through a prototype study was not done yet.

In most of the cases circular compound bridge pier are adopted for use in the Indian sub-continent for the road and railway bridges. A vast amount of literature is available on the topic of scour around bridge piers having uniform cross-sections. However the studies on scour around compound piers are very less. So another objective of the present investigation therefore, is to study the process of scour around compound piers and to develop a method for computation of temporal variation of scour around circular compound piers. Note that top surface of the footingof compound piers always acts as a collar plate around the pier. The studies on compound pier scour therefore are related to those on scour reduction due to collar plate.

The scour prediction methods developed in the laboratories and the scour equations based on laboratory data did not always produce reasonable results for field conditions. However most of the laboratory data reported in the literature has been for relatively small piers, up to about 0.15 m in diameter. Scale effect also becomes evident when one considers the similitude requirements for hydraulic modeling of pier scour. Therefore a detailed experimentation on prototype should be made, which thereby would enhance the potential in

identifying a new set of controlling parameters which influences the scouring around pier and thereby an effective pier scour model could be developed. The flow structure around the bridge pier therefore needs to be investigated to decipher the turbulence structure and vortex characteristics in the flow around bridge piers.

CHAPTER 3: EXPERIMENTAL SETUP AND PROCEDURE

3.1 INTRODUCTION

In view of the objectives of the present study extensive experimental work was planned and carried out to monitor the deepest scour for its location with and without a collar plate. Moreover the flow around pier during live-bed condition is quantified. The experiments were conducted in the Hydraulics Laboratory of Department of Civil Engineering, Indian Institute of Technology Roorkee, Roorkee, India. In this chapter, the experimental arrangements, hydraulic models, data acquisition system and variables measured in the model study are described.

3.2 EXPERIMENTAL SET-UP

3.2.1 Flume

Experiments were conducted in a fixed bed masonry flume of length = 30.0 m, width = 1.0 m and depth = 0.6 m. The flume receives water supply from a constant head overhead tank. The supply of flow to the flume was regulated with the help of a valve provided at the inlet of the flume. Honeycomb masonry grid wall built of small size bricks were provided at the upstream end of the flume to minimize the disturbance in the flow entering the flume. Flow straighteners were provided just downstream of the grid wall at the upstream end of the flume to make the flow perfectly parallel to the flume walls. Boulders were placed on flume bed, from flume entrance to 2.0 m length towards downstream to dissipate the excess energy in the flow entering the flume. An adjustable wooden tail gate was provided at the downstream end of the flume to enable adjustment of the depth of flow in the flume. A glass-walled working section 3.0 m long, 1.0 m wide and 0.6 m deep was located at 12.0 m downstream of the flume entrance for conducting the experiments. The mean flow in the working section was thus in a fully developed state (Kirkgoz and Ardiclioglu, 1997). In order to simulate the same roughness as in the work sections, sediment particles were glued uniformly on the bed in the portion of the flume upstream and downstream of the working section. Figure 3.1 illustrates the general layout of the flume used in experimentation, Fig. 3.2 shows the photographic view of the flume and Fig. 3.3 illustrates the photographic view of the flume after live bed scour measurement.

3.2.2 Flow Measuring Instruments

(I) Discharge measurements

An ultra sonic flow-meter was fixed over the inlet water supply pipe to measure the discharge entering into the channel. The ultrasonic flow meter measures the velocity of any liquid or gas passing through a pipe using ultrasonic transducers. Ultrasonic sound is transmitted into a pipe with flowing liquids, and the discontinuities (such as tiny solid particles in flow) reflect the ultrasonic wave with a slightly different frequency that is directly proportional to the rate of flow of the liquid. In addition, a sharp crested weir provided at the downstream end of the channel was also used for reconfirming the measurement of channel discharge. The water level over the sharp crested weir was measured by a Vernier point gauge with an accuracy of ± 0.1 mm. The calibration curve for this weir (Fig. 3.4) was established by Kumar (1996). The same was verified and used for the determination of discharge during the present experiments. The discharge Q is expressed as a function of head of water H over the still level of sharp crested weir as $Q = 1.79H^{1.5}$.

(II) Water surface levels and bed slope

The water surface level was measured by a Vernier point gauge with an accuracy of ± 0.1 mm. The point gauge was attached to an instrument carriage which could move streamwise as well as transverse direction. Theodolite was used to measure the slope of the channel bed.

(III) Velocity and flow field

The instantaneous three-dimensional velocity components were measured using a 16 MHz 3D "Acoustic Doppler Velocimeter" (ADV) developed by SonTek/YSI. Acoustic Doppler velocimeters are capable of reporting accurate instantaneous values of flow velocity in three directions (Kraus *et al..*, 1994; Lohrmann *et al..*, 1994; Voulgaris and Trowbridge, 1998; Lopez and Garcia, 2001). The Micro-ADV uses acoustic Doppler technology to measure 3D flow in a small sampling volume (0.09 cm^3) located at 5 cm from the probe. The sampling volume almost resembles a cylinder with a diameter of 4.5 mm ± 0.3 mm. The height of the sampling volume is defined by the "convolution of the transmitted acoustic pulse with the receive window over which the return signal is sampled". In the standard configuration it can be estimated that the sample volume height is between 4.5 mm and 5.6 mm. A single estimate of velocity is referred to as a ping. Depending on the velocity setting of the instrument, the ADV pings at a rate of 150-250 times per second. Pings are averaged together for each

sample specified by the user frequency setting. Data can be acquired at sampling rates up to 50 Hz and it can measure flow velocities from less than 1 mm/s to over 2.5 m/s. The micro-ADV consists of three basic elements: the probe, the signal conditioning module and the processor. The measuring probe consists of a sound emitter transducer and three sound receiver transducers. The sound emitter generates an acoustic signal that is reflected back by sound scattering particles present in the water, which are assumed to move with the same velocity as of water. The scattered sound signal is detected by the receivers and the flow velocity in the three directions is calculated. The probe is attached to the conditioning module, which contains low-noise receiver electronic enclosed in a submersible housing. The conditioning module and probe are connected to the processing module using a custom shielded cable. The micro-ADV processor is a set of three printed circuit cards that operates from external DC power and outputs data using serial communication or a set of analog voltages. The micro-ADV can be operated from any PC-compactable computer running the data acquisition program. A real-time display of the data in graphical and tabular forms was provided by the data acquisition software.

The ADV used for measuring the velocity profile was operated with a sampling rate of 30Hz for duration of 4 min. A sampling time of 4 minutes was determined so that mean velocity measurements in the stream-wise direction were time independent (keeping consistency with the previous investigations using ADV). The coordinate system for data collection and analysis was set with the x-direction (u) positive in the stream-wise direction, the z-direction (w) positive in the vertical, and the y-direction (v) followed the right-hand rule and was positive to the left when facing downstream. Although every attempt was made to align the instrument to the direction of flow, a slight misalignment was unavoidable during the experiments (Stone *et al*., 2007). The tilt correction algorithms, proposed by Wilczak, (2001) were used to realign the data to the actual streamline coordinate system.

Data Filtering

The instrument noise and measurement strength were quantified using two parameters. The "signal-to-noise ratio" (SNR) is an indication of the amount of scattering material in the sampling volume. The "correlation" (COR) is a function of how dissimilar successive pulse echoes are from each other (Martin *et al*., 2002). Filtering the raw ADV data usually involves choosing a cut-off value (CR) for the signal-to-noise ratio (SNR_{CR}) and correlation (COR_{CR}). Data outside the cut-off values are filtered from the data set. Sontek^{TM} recommends using SNR_{CR} = 15 and COR_{CR} = 70, but these values, especially COR_{CR}, have come under scrutiny

recently since they filter out much of the data in turbulent flows near the bed (Strom and Papanicolaou, 2007, Cea *et al*., 2007). Low correlation scores can be caused by turbulent flows, air bubbles, low SNR values, large velocity gradients in the sampling volume, large individual particles near the sampling volume, and/or interference from the boundary (Martin *et al*., 2002). Strom and Papanicolaou, (2007) suggested a method to find the critical correlation score.

Most of the flow depth other than the points very close to the flume bed had a signal to noise ratio higher than 20 dB. The data possessing a signal to noise ratio lesser than 15 dB and a correlation score less than 70% were filtered using WINADV software, thus conforming to the criteria by Wahl, (2000). Along with the SNR and COR filters, the phase space threshold despiking algorithm developed by Goring and Nikora, (2002) and modified by Wahl, (2000) was also used to clean the data. This data cleaning process filtered about 2 to 3% data at most of the measurement points, but nearly 16% of data was filtered out especially at the measurement points very close to the flume bed (4.64 mm above the flume bed). Velocity was measured even closer up-to 3.5 mm above the flume bed, but more than 30% of the data from this were required to be removed during the filtration process (using Wahl, 2000 filtration criteria). But when the filtration criteria for correlation score and SNR were reduced to 50% and 12 dB respectively, more than 70% of the data could be retained. Strom and Papanicolaou, (2007) adopted a correlation score = 50% and SNR = 10 for filtering their data. Whereas Martin *et al*.., (2002) adopted a correlation score of 40 %. The velocity profile data measured in the approach flow of the flume (Chapter 4) was filtered using Wahl, (2000) filtration criteria; thereby the data measured herein at height smaller than 4.64 mm above the flume bed have not been used in computations (to have a uniform filtration criteria throughout the flow depth). But whereas the velocity profile measurements (Chapter 5) made around the circular pier, in its upstream, near the flume bed (3.5 mm above the flume bed) were filtered with a revised filtration criteria (correlation score = 50% and SNR = 12 dB along with the phase space threshold despiking algorithm), which is in agreement with the previous investigators (Strom and Papanicolaou , 2007 and Martin *et al*. , 2002).

However, there was no requirement of seeding to the flow during the experiments, as the signal-noise ratio (SNR) was around 20 in general. Comparison of data obtained using the micro-ADV probe and a laser Doppler velocimeter are found to show good agreement in shape and peak of the signals from the two instruments (Kraus *et al*., 1994). Figure 3.5 shows the various components of the micro-ADV used.

3.2.3 Instrument Carriage

An instrument carriage was used for fixing the instruments over the flume. Adjustable rails and trolleys mounted on the two walls of the flume constitutes the instrument carriage and was used to carry the pointer gauge and other equipment used for measurement of flow pattern, water surface and bed levels.

3.2.4 Sediment

River sand retained and passed between two successive sieves was used in all the experiments as the sediment. Non-cohesive sand of median size (d_{50}) 0.34mm and a relative density of 2.65 were used in present study. Only one type of sediment, having uniform size distribution was used. The sediment used for feeding was the same as used for bed material in test section. Figure.3.6 shows the photographic view of the sediment.

Two such uniform size non-cohesive river bed sediment having median size (d_{50}) = 0.4 mm, geometric standard deviation σ_g = 1.2 and d_{50} = 1.8 mm, σ_g = 1.17 were used in the experiments as the sediment during the investigations on circular compound piers.

3.2.5 Sediment Feeding

After conducting the reference run for the required flow conditions, a predetermined amount of sediment was added carefully to the flow at 1m upstream of pier. The duration of sediment addition was as such the sediment leaving the test section and sediment entering the test section remains constant. Engelund-Hansen method (Garde and RangaRaju, 2006) was adopted for calculating the sediment for feed. Figure.3.7 shows the photographic view of process of feeding of the sediment across the width of channel.

3.2.6 Pier

Circular cylindrical G.I. pipe as shown in Fig. 3.8, having diameter 112.5mm was used as pier model. The surface of the model was painted to give it a smooth finish. The pier model always protruded well above the water surface and is placed in the middle of the working section. Fig. 3.8 shows the photographic view of pier.

The investigations on circular compound piers were made with three circular cylinders of uniform section having diameters of 48 mm, 88 mm and 114 mm. The same circular uniform piers were also used as the pier of the compound footing. Six set of circular compound piers having ratio of footing diameter to pier diameter as 1.84 (b = 114 mm), 1.89 (b = 88 mm), 2.38 (b= 48 mm), 2.81 (b = 114 mm), 3.46 (b = 48 mm) and 4.38 (b = 48 mm)

were used as models of the bridge foundation.

3.2.7 Collar

Collar was cut out of M.S. plate of 3mm thickness. Only one collar of size 2.5*b* is used on pier of size 114 mm as shown in Fig. 3.9. The collar-pier junction was made watertight.

3.3 EXPERIMENTAL PROCEDURE

In view of the objectives of the present study, following four groups of experiments were performed. First group of experiments were conducted in a turbulent open channel flow to quantify the turbulence charateristics of flow around the upstream of a circular pier model and in the approach flow. Second group of experiments were conducted around the circular pier model with and without a collor to quantify the reduction in scour due to the presence of collor. Third group of experiments were performed to collect the data regarding temporal variation of scour depth around compound pier models and to measure the size and hence cross-sectional area of principal vortex and bed shear stress in the scour hole at the upstream nose of pier after time *t* from the start of the scour process. Fourth group of experiments (Appendix A) were performed in a proto type scale pier to investigate the scale effects on scour prediction.

3.3.1 Turbulence charateristics of flow

The first group of experiments is conducted in the working section of the flume which is located at 12.5 m downstream of the flume entrance. The bed in the working section is made flat and rigid to facilitate the flow measurement around the pier. Experiments were conducted under steady and sub-critical flow conditions. The near-bed flow characteristics were quantified for a flow with depth, h = 150 mm. The flow parameters maintained in the approach flow during the experiments are shown in Table 3.1.

I) Turbulence flow charateristics in approach flow

Vertical distributions of the instantaneous flow velocities were measured using the micro-ADV at twenty five points across the flow depth at a distance of 2m upstream the pier. The location for approach flow measurement is so selected, that they are not influenced by the presence of pier. The characteristics of the near bed turbulence were obtained by analyzing the velocity records closer to the bed. The velocity time series were statically averaged to get the turbulence properties, including time averaged velocities, turbulence intensity, turbulent kinetic energy and bed shear stress.

TABLE 3.1 Hydraulic Parameters Maintained in the Approach Flow

Details	**run: h_{15}**
Flow depth, h (mm)	150
Aspect ratio, B_0/h	6.667
Water surface slope, S	0.0009
Flow rate, Q (m^3/s)	0.088
Mean flow velocity, U_0 (m/s)	0.592
Reynolds number, R_e ($\times 10^5$)	0.888
Froude number, F_r	0.488
Shear velocity, u_* (m/s)	0.0307
Roughness size, k_s (mm)	0.84
$k_s^+ = \frac{k_s}{\nu/u_*}$	25.86

$R_e = U_0 h/\nu$, ν denotes kinematic viscosity of water and $F_r = U/(gh)^{1/2}$, g is acceleration due to gravity

II) Turbulence flow charateristics around upstream of the pier model

The near bed turbulence characteristics in the upstream around a circular pier model mounted over a flat rigid bed is also studied. A schematic diagram of the experimental set-up illustrating the Cartesian coordinate system used for describing the flow around the pier model is shown in the Fig. 3.10. The origin of the Cartesian coordinate system is set at the intersection of the bed, centerline of the flume and the upstream nose of the pier. The velocity components in the Cartesian coordinate system (x, y, z) are represented by (u, v, w). Flow velocities closer to the bed (3.5 mm above the flume bed surface) around the pier model were sampled at 869 (Fig. 3.11) locations on the x-y plane. Measurements obtained using an acoustic Doppler velocimeter (ADV) were used to investigate the time averaged velocity components, turbulence intensity components, Reynolds stresses and bed shear stress near the bed.

3.2.2 Scour measurements around the pier with and withour collar

For this group of experiments the working section is filled with sediments (same sediment is used for feeding) to the level of the flume bed and made level before the start of the run for the temporal variation of scour depth under the required flow conditions (Figs. 3.12 and 3.13). The area around the pier and collar was levelled and the covered with a 3mm thick Perspex sheet (Fig. 3.14). When the desired flow conditions were achieved by operating the tailgate and inlet valve, the Perspex sheet was removed carefully so that no scour occurs during this process. All experiments were conducted for the desired flow conditions as

mentioned in Table 3.2.

Scour measurements around the pier were taken under the following conditions

(i) Scour under clear-water conditions without collar (CWSNC)

(ii) Scour under live-bed degradation without collar (LBSNCNFS)

(iii) Scour under live-bed condition without collar (LBSNCWFS)

(iv) Scour under clear-water conditions with collar (CWSWC)

(v) Scour under live-bed degradation with collar (LBSWCNFS)

(vi) Scour under live-bed with collar (LBSWCWFS)

If the flow conditions in approach flow correspond to the live-bed condition but no sediment is transported by upstream flow *i.e.* no feeding of sediment is done in the experiments, general bed degradation will occur in this condition particularly in the approach flow. Experimental runs conducted with collar under such conditions are called herein as scour under live-bed degradation with collar.

The methodology adopted is to simulate the run for all the possible cases as shown above for the live-bed conditions for a particular u_*/u_{*c}.

The scour depth was measures temporally over some fixed points A, B, C around collar as shown in Figs. 3.15 & 3.16, and the corresponding scour depths were measured. Since for low values of u_*/u_{*c} maximum scour was observed to occur in wake region, therefore maximum scour depth was measured for such cases irrespective of condition whether it occurred at either of points A, B, C. The point gauge with flat bottom was used to measure the scour depth and the observation period was kept low for live-bed conditions since the scour process is very dynamic for live-bed condition.

TABLE 3.2 Values of Hydraulic Parameters in the Study of Scour around Circular Pier with and withour Collar

Run Type	Run No.	h (cm)	Q (m^3/s)	B (cm) $2.5b$	b (cm)	d (mm)	u_*/u_{*c}
CWSNC	1	10.5	0.0243		11.4	0.34	0.87
	2	10.0	0.025		11.4	0.34	0.89
	3	5.0	0.011065		11.4	0.34	1.089
	4	7.0	0.0174		11.4	0.34	1.1
	5	8.0	0.02184		11.4	0.34	1.266
	6	7.0	0.02436		11.4	0.34	1.335
	7	6.0	0.01765		11.4	0.34	1.42
	8	9.0	0.0263		11.4	0.34	1.488
	9	6.5	0.0244		11.4	0.34	1.88
	10	6.0	0.016		11.4	0.34	2.05
LBSNCWFS	11	5.0	0.011065		11.4	0.34	1.089
	12	7.0	0.0174		11.4	0.34	1.1
	13	8.0	0.02184		11.4	0.34	1.266
	14	7.0	0.02436			0.34	1.335
	15	6.0	0.01765		11.4	0.34	1.42
	16	9.0	0.0263		11.4	0.34	1.488
CWSWC	17	10.5	0.0243	28.5	11.4	0.34	0.87
	18	10.0	0.025	28.5	11.4	0.34	0.89
LBSWCNFS	19	5.0	0.011065	28.5	11.4	0.34	1.089
	20	7.0	0.0174	28.5	11.4	0.34	1.1
	21	8.0	0.02184	28.5	11.4	0.34	1.266
	22	7.0	0.02436	28.5	11.4	0.34	1.335
	23	6.0	0.01765	28.5	11.4	0.34	1.42
	24	9.0	0.0263	28.5	11.4	0.34	1.488
	25	6.5	0.0244	28.5	11.4	0.34	1.88
	26	6.0	0.016	28.5	11.4	0.34	2.05
LBSWCWFS	27	5.0	0.011065	28.5	11.4	0.34	1.089
	28	7.0	0.0174	28.5	11.4	0.34	1.1
	29	8.0	0.02184	28.5	11.4	0.34	1.266
	30	7.0	0.02436	28.5	11.4	0.34	1.335
	31	6.0	0.01765	28.5	11.4	0.34	1.42
	32	9.0	0.0263	28.5	11.4	0.34	1.488

Theoretically, scour depth varies asymptotically with time. However, it was difficult

to conduct experiments for long time especially with sediment feed as we were conducting the experiments with manual feed. All experiments were conducted to reach an equilibrium state however it is very difficult to achieve equilibrium state for live-bed condition. The experiments without sediment fed were generally conducted for around 8 hours time duration and with sediment feed for almost 5 hours such that the scour depth did not change by more than 1mm over a period of one hour. The scour depth was measured temporally for each run. The maximum depth of scour was measured with and without collar at the end of each run. Range of the data used for the present study is given in Table 3.3 and all the experiments were conducted as per the conditions listed in Table 3.4.

TABLE 3.3 Ranges of Experimental Data Collected in the Study of Scour around Circular Pier with Collar

Variables	**Range**
d (mm)	0.34
h (cm)	5.0 to 10.5
b (m)	0.114
B (m)	0.285
h (m)	0
u_*/u_{*c}	0.87 to 2.05

TABLE 3.4 Values of Hydraulic Parameters of Experimental Data Collected in the Study on Scour around Circular Pier with and withour Collar

Sl. No.	Set No.	Experiment	u_*/u_{*c}	Flow conditions	Pier Diameter b(cm)	Mean Particle Size d_{50} (mm)	Maximum scour(cm)	
							With Collar	Without Collar
1	1	CWSNC1	0.87	Clear-water	11.4	0.34		8
2		CWSNC2	0.89					10.3
3	2	LBSNCNFS1	1.089	Live-bed degradation	11.4	0.34		7.7
4		LBSNCNFS2	1.1					9.1
5		LBSNCNFS3	1.266					7.8
6		LBSNCNFS4	1.33					8.2
7		LBSNCNFS5	1.42					9.4
8		LBSNCNFS6	1.488					11.3
9		LBSNCNFS7	1.8					11.5
10		LBSNCNFS8	2.05					14.2
11	3	LBSNCWFS1	1.089	Live-bed	11.4	0.34		7.2
12		LBSNCWFS2	1.1					8.7
13		LBSNCWFS3	1.266					6.7
14		LBSNCWFS4	1.33					7.5
15		LBSNCWFS5	1.42					8.3
16		LBSNCWFS6	1.488					10.0
17	4	CWSWC1	0.87	Clear-water + collar	11.4	0.34	3.6	
18		CWSWC2	0.89				3.9	
19	5	LBSWCNFS1	1.089	Live-bed degradation+ collar	11.4	0.34	4.4	
20		LBSWCNFS2	1.1				4.9	
21		LBSWCNFS3	1.266				2.9	
22		LBSWCNFS4	1.33				3.3	
23		LBSWCNFS5	1.42				5.2	
24		LBSWCNFS6	1.48				3.0	
25		LBSWCNFS7	1.87				5.8	
26		LBSWCNFS8	2.05				6.2	
27	6	LBSWCWFS1	1.089	Live-bed + collar	11.4	0.34	2.2	
28		LBSWCWFS2	1.1				3.2	
29		LBSWCWFS3	1.266				4.8	
30		LBSWCWFS4	1.33				2	
31		LBSWCWFS5	1.42				2	
32		LBSWCWFS6	1.488				3.2	

3.2.3 Experiments on circular compound piers

Each pier model was first founded in sediment bed having d_{50} = 0.4 mm with discharge Q of 0.045m^3/s and flow depth h of 0.16 m and next in sediment of d_{50} = 1.8 mm with discharge = 0.071m^3/s and flow depth = 0.165 m. In all 6 number of experiments on circular uniform pier and 36 experiments on circular compound bridge piers models have been conducted.

Before the start of each run on the temporal variation of scour, the working section was filled with desired sediment and the pier or footing was inserted in it vertically and centrally. The area around the model was leveled, and then covered with 3 mm thick perspex sheet. The predetermined discharge was allowed into the flume slowly so that it did not disturb the bed. Firstly the required flow depth for the experiment was maintained using the tail gate operation and then perspex sheet was removed carefully so that no scouring occurred around the pier/footing model due to this operation. Now the desired flow conditions were established using pre-calibrated tailgate and the inlet valve.

TABLE 3.5: Specifications of Circular Uniform Pier and Circular Compound Pier Models Used in Laboratory Experiments

S. No.	Diameter of pier b (mm)	Diameter of foundation b_* (mm)	b_* / b	Y
1	114	210	1.84	$b_*/10, 0, -b_*/10$
2	88	166	1.89	$b_*/10, 0, -b_*/10$
3	48	114	2.38	$b_*/10, 0, -b_*/10$
4	114	320	2.81	$b_*/10, 0, -b_*/10$
5	48	166	3.46	$b_*/10, 0, -b_*/10$
6	48	210	4.38	$b_*/10, 0, -b_*/10$
7	114	-	-	-
8	88	-	-	-
9	48	-	-	-

Y = level of top surface of footing with respect to channel bed

The temporal variation of scour depth at the nose of the pier was measured using an electronic bed profile indicator *MKV* manufactured by the Deltares, Delft, The Netherlands. This profile indicator automatically measures continuously the mobile bed levels. The bed level was measured at intervals varying from one minute in the beginning of the run to half

an hour at the end of the run. The initial and final bed levels were also measured with the help of a pointer gauge.

Theoretically, scour depth develops asymptotically with time. It is well known that scour development is rapid initially and becomes slow after a few hours. All experiments were therefore, conducted for a duration of seven hours. Thus temporal variation of scour depth in transient (developing) stage only has been measured here.

The experiments on flow pattern was carried out to get basic idea of flow structure and to measure the size and hence to the cross-sectional area of the principal vortex of the horse-shoe vortex system. Cross-sectional area of the principal vortex was used to determine the bed shear stress at upstream face of the scour hole around the circular uniform pier and the circular compound piers. A total of four experiments on flow pattern around the circular uniform and compound piers were conducted under clear-water condition. One experiment was conducted on the circular uniform pier model named as *UPSH* (b=114 mm). The rest three experiments were conducted on circular compound pier models (b= 114 mm, b_*=210 mm) in which top of the footing was placed at three different elevations with respect to general bed level *i.e.* above the bed level ($Y = -b_*/10$) for run *NUPSH* 2, at the bed level (Y = 0) for run *NUPSH* 1 and below the bed level ($Y = b_*/10$) for run *NUPSH* 3. In these experiments too, the scour hole was allowed to develop in a similar way as it was done for the previous series of experiments. For the scour experiments pier was founded in uniform size non-cohesive river bed sediment having d_{50} = 0.4 mm and σ_g = 1.2. The discharge Q of 0.045 m^3/s and flow depth h of 160 mm was maintained during the experiments. The scour hole was developed for seven hours and this stage is treated as transient (developing) stage. As the basic purpose of the these experiments was to get idea of observed cross-sectional area of the principal vortex of the horse-shoe vortex system and bed shear stress at upstream face of the scour hole around the circular uniform pier and the circular compound piers at any time t of scour activity. So duration of the scour activity does not affect the basic purpose of the experiments on flow pattern.

The observations for velocity field within the developing (transient) scour hole along the central line of the flow on the upstream face of the pier models were made using Sontek acoustic Doppler velocimeter (A*DV*). Before taking measurements on velocity field, the geometry of developed scour hole was stabilized by spraying light solution of cement over its surface after the water was completely drained from it at the end of the scour activity.

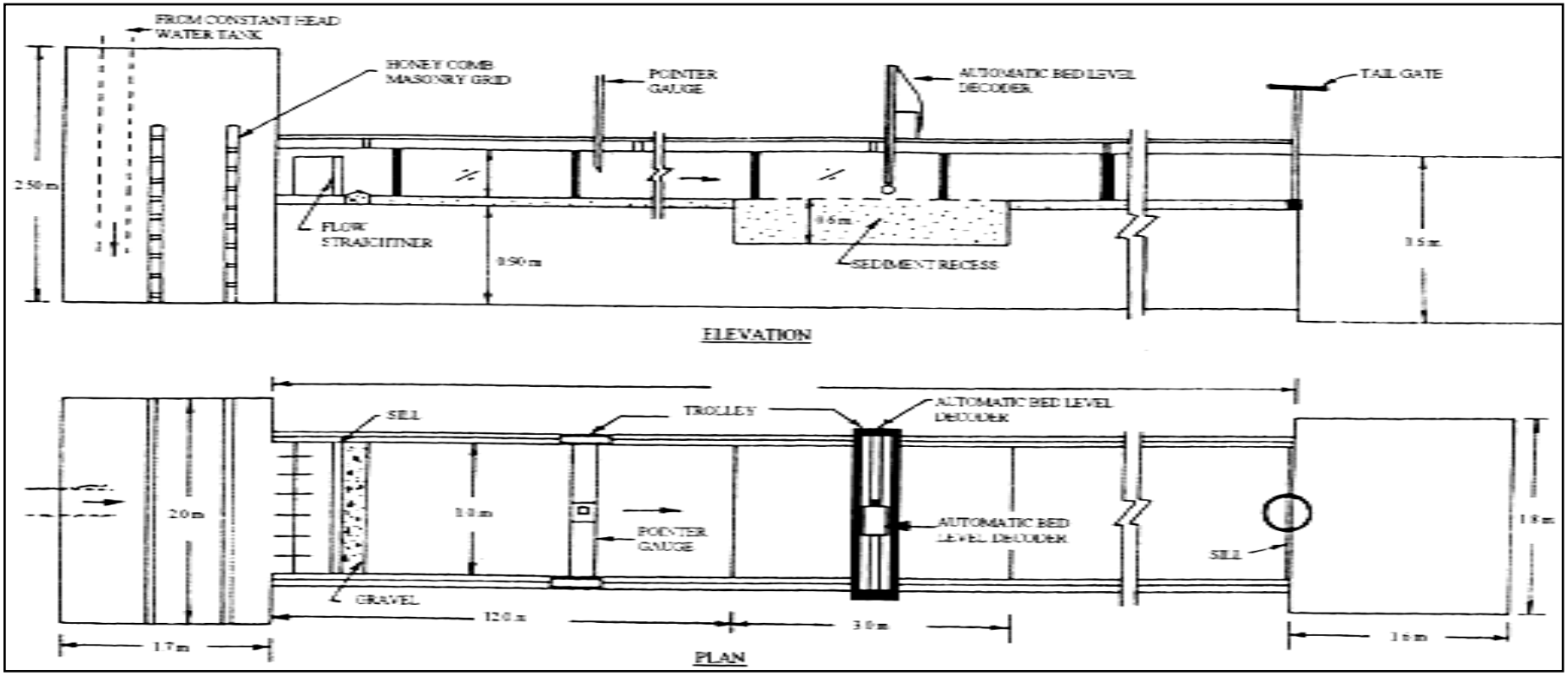

FIG. 3.1 General Layout of the Flume

FIG.3.2 Photographic View of the Experimental Flume

FIG.3.3 Photographic View of the Experimental Flume after Live-bed Scour Run

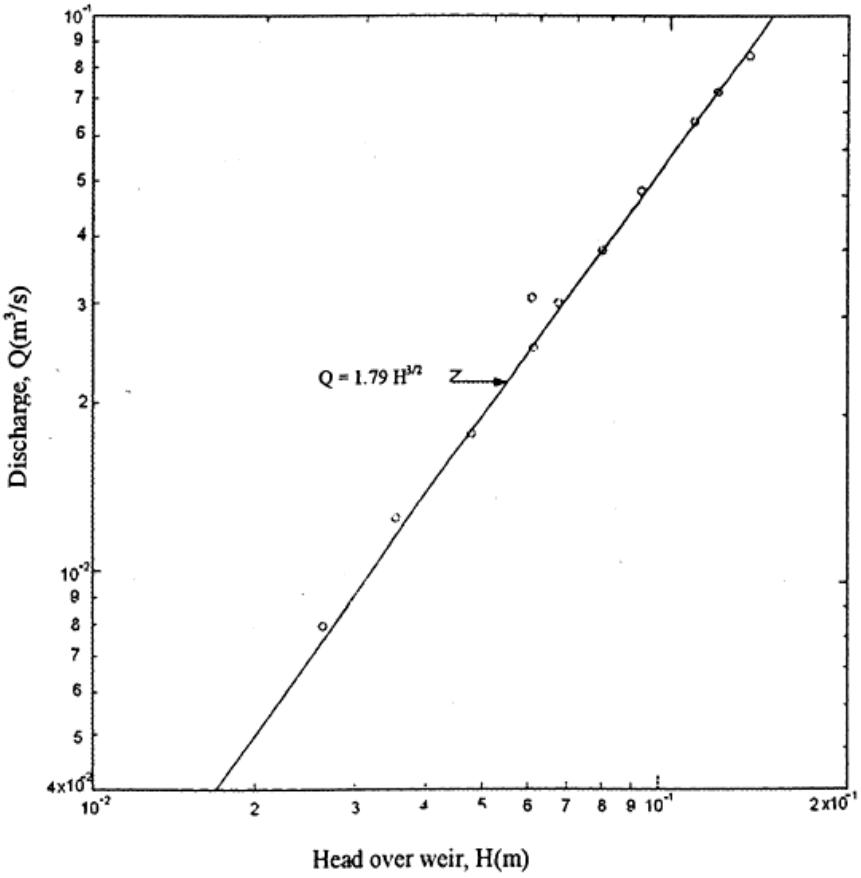

FIG.3.4 Calibration Curve of Sharp Crested Weir (Kumar *et.al.*, 1996)

FIG. 3.5 Various Components of the Micro ADV

FIG.3.6 Photographic View of the Sediment

FIG.3.7 Photographic View of Feeding of Sediment

FIG.3.8 Photographic View of Pier

FIG.3.9 Photographic View of Collar Size 2.5*b* for 0.114 m Pier

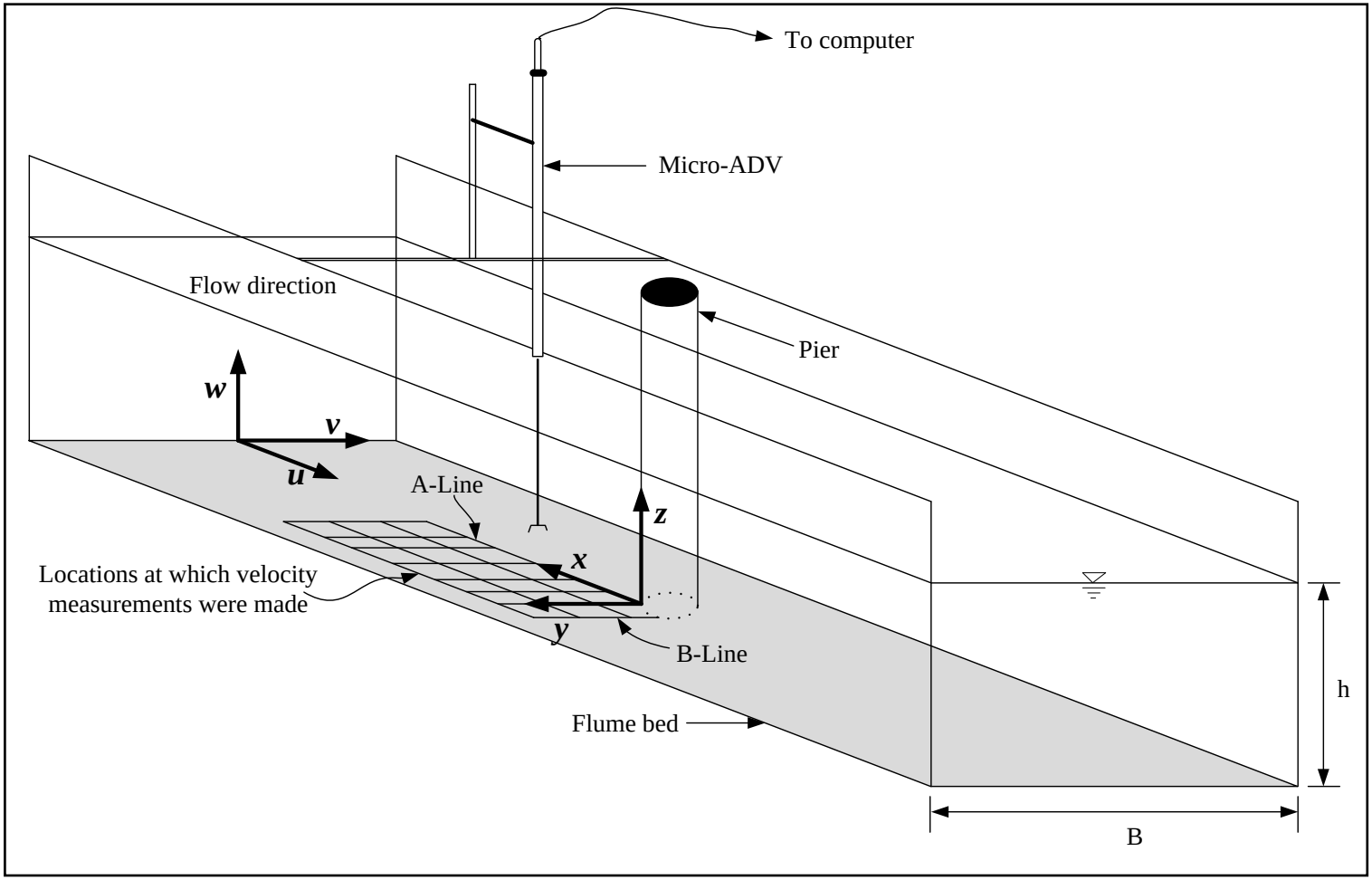

FIG. 3.10 Schematic Diagram of the Experimental Setup. Origin of *xyz* Coordinates is at the Pier Nose

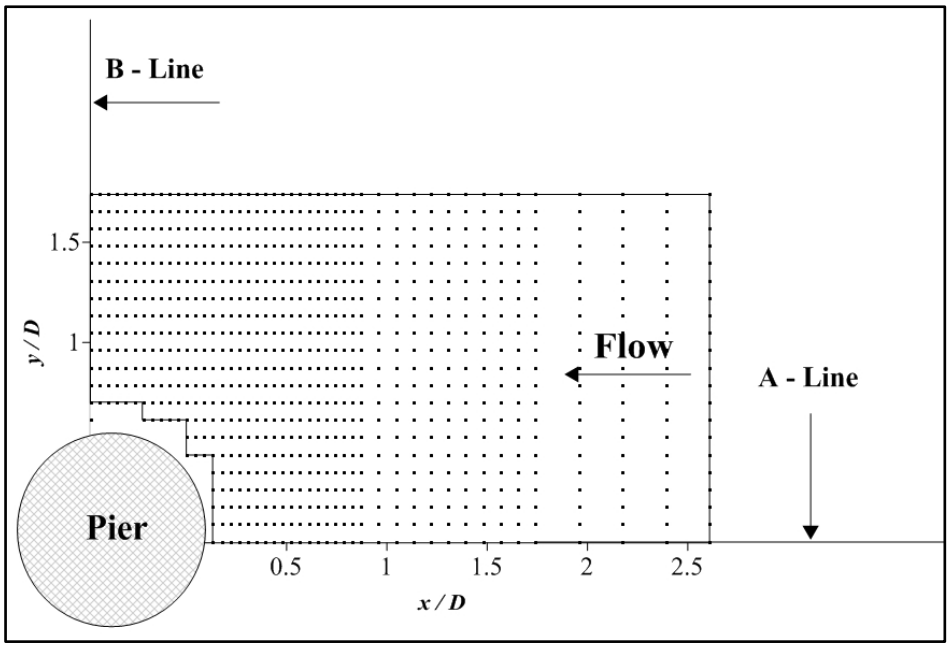

FIG. 3.11 Relative Position of the Circular Pier and the Locations in Horizontal Plane in which Velocity Measurements were Made with ADV

FIG.3.12 Photographic View of Collar Arrangement for the Present Study

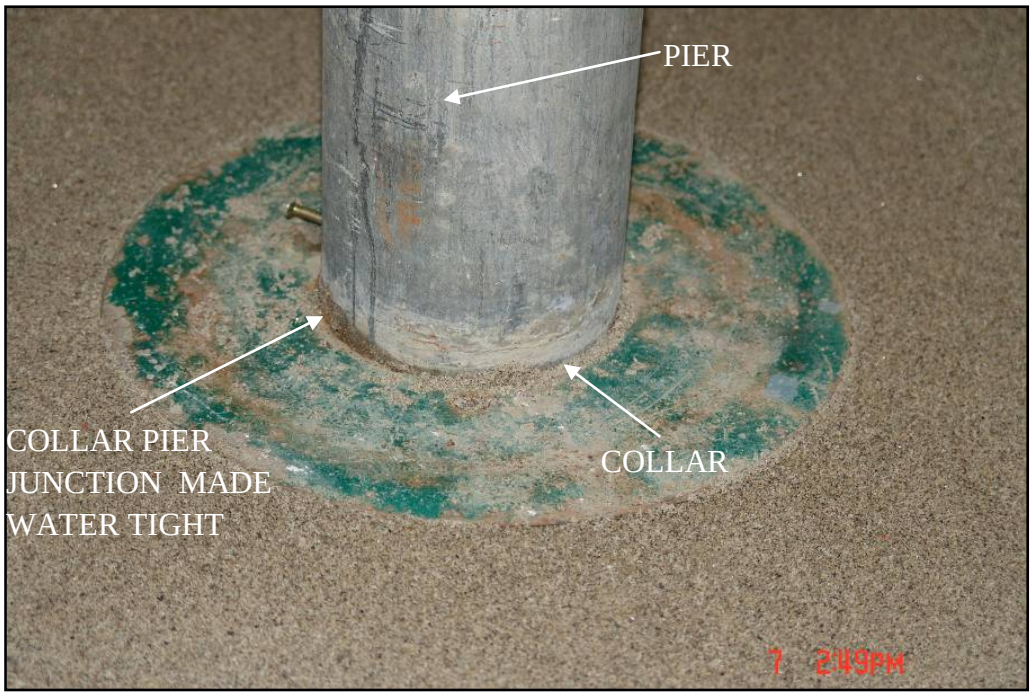

FIG.3.13 Photographic View of Placement of Collar at Bed Level

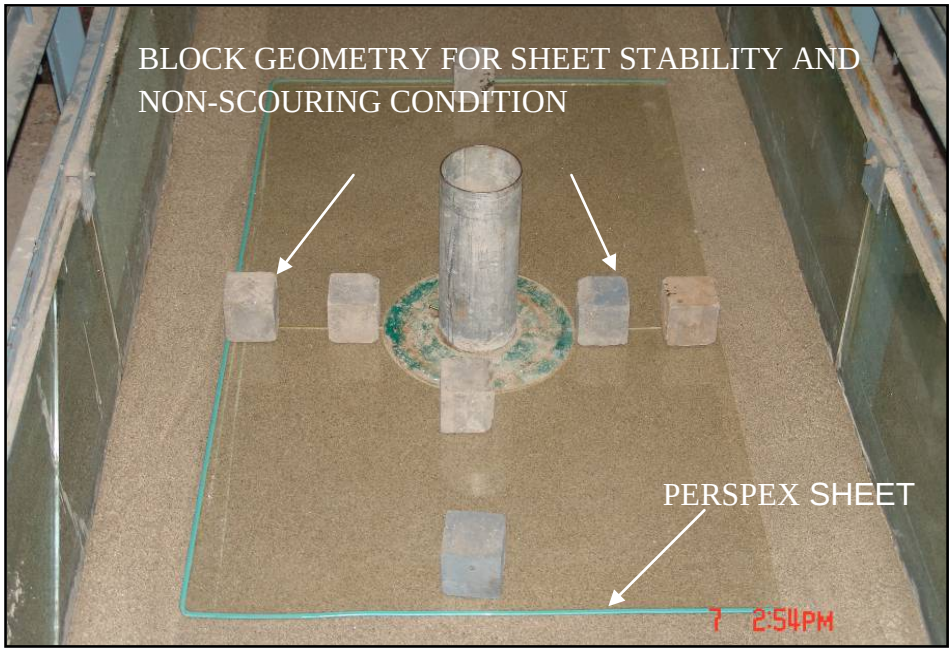

FIG.3.14 Photographic View of Experimental Setup

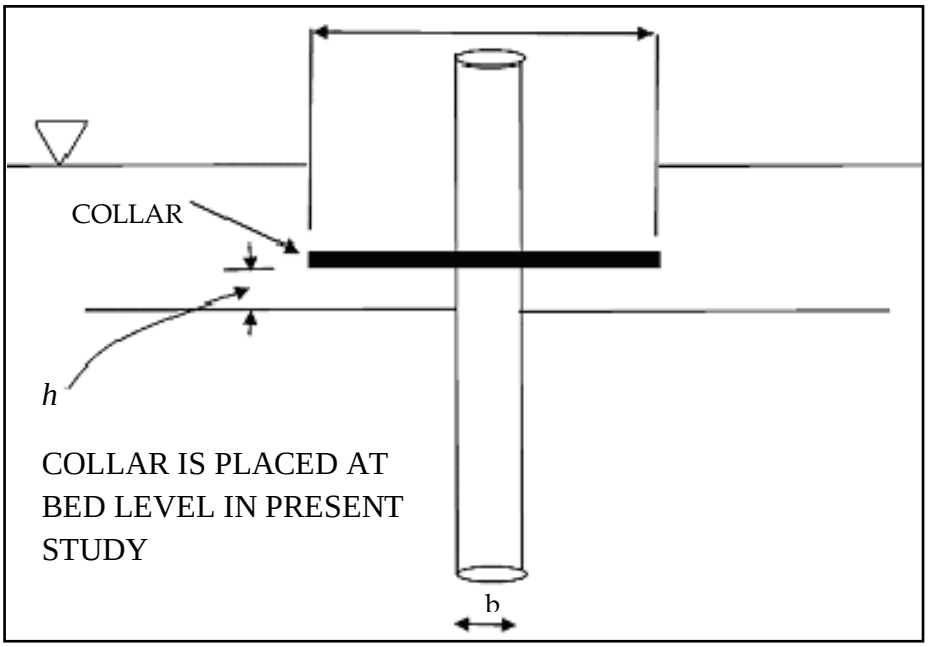

FIG.3.15 Schematic Illustration of the Pier-Collar Setup Used Under the Present Study

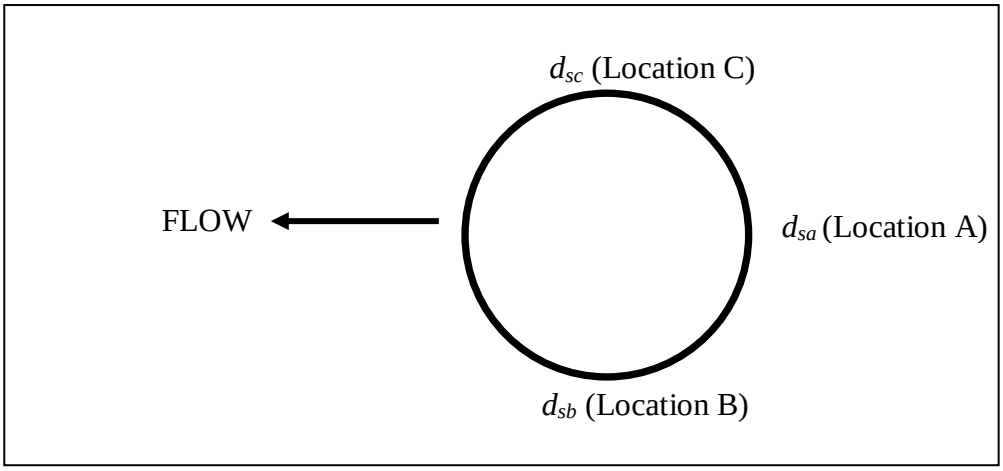

FIG.3.16 Observation Points for Scour Depth (d_s), around the Collar

 # BLANK PAGE #

CHAPTER 4: ANALYSIS OF DATA AND DISCUSSION OF RESULTS

4.1 GENERAL

The data collected in the present study are analysed and the results obtained are discussed in this chapter. The flow around pier during live-bed condition is quantified and the potential areas of scouring around the pier are notified. The process of scour around circular bridge pier without collar was studied under both live-bed and clear-water conditions. After this, data collected for combination of collar and pier for varying flow conditions were studied. Experiments on bridge pier scour in the absence of collar were conducted for sediment of size 0.34 mm under the clear-water condition, live-bed degradation condition and live-bed condition. Then the same experiments were repeated by attaching a collar to the pier. The results obtained from the experiments are used to evaluate the effectiveness of collar in reducing the scour. In addition, the results obtained in circular compound piers are also discussed in this chapter. However flow structure in the approach flow and around the pier is discussed first in the present chapter.

4.2 TURBULENCE CHARATERISTICS OF FLOW AROUND PIER DURING LIVE-BED CONDITION

Turbulence characteristics of the flow in the approach flow and the variations in its characteristics due to the presence of the pier are quantified using measurements of an acoustic Doppler velocimeter. The velocity time series were statically averaged to get the turbulence properties, including time averaged velocities, turbulence intensity, turbulent kinetic energy and bed shear stress.

4.2.1 Mean velocity distributions

The time averaged velocities are defined as

$$\overline{u} = \frac{1}{N}\sum_{i=1}^{N} u_i \qquad (4.1)$$

$$\bar{v} = \frac{1}{N}\sum_{i=1}^{N} v_i \tag{4.2}$$

$$\bar{w} = \frac{1}{N}\sum_{i=1}^{N} w_i \tag{4.3}$$

where N is the total number of velocity observations at a given point. The instantaneous velocity fluctuations in longitudinal, lateral and vertical directions (u', v', w') of the respective recorded velocities (u, v and w) were calculated from the time averaged velocities ($\bar{u}$, $\bar{v}$, $\bar{w}$) as $u' = \bar{u} - u$, $v' = \bar{v} - v$ and $w' = \bar{w} - w$. Figure 4.1 compares the vertical distributions of the non-dimensionalized time averaged stream-wise flow velocity [($\bar{u} / u_*$) versus z^+ (= zu_*/ν, where z is the vertical distance from the flume bed). The procedure used for computation of u_* is explained in section 4.2.5 for the present observations as well as for the distributions predicted using the equations available in the literature for smooth (log-law developed by Prandtl, 1932 and von Karman, 1930), transitional (Le Roux, 2004) and rough surfaces (law of the wall).

Log law for hydraulically smooth boundaries,

$$\frac{\bar{u}}{u_*} = \left(\frac{1}{k}\right) \ln\left(u_* z/\nu\right) + B_p \tag{4.4}$$

where, k is Von Karman constant and parameter B_p = 5.3 (Le Roux, 2003).

Law of wall for transitionally rough boundaries,

$$\frac{\bar{u}}{u_*} = 2.5 \ln\left(\mathrm{R}_{e^*} z/k_s\right) + 5.3 - 0.1206(\mathrm{R}_{e^*} - 5) \tag{4.5}$$

Log-law for hydraulically rough boundaries,

$$\frac{\bar{u}}{u_*} = \left(\frac{1}{k}\right) \ln\left(z/k_s\right) + B_p \tag{4.6}$$

where, parameter B = 8.5 (Le Roux, 2003).

It is seen from Fig. 4.1 that the measured velocity profile is in close agreement with the profile predicted by the law of wall for transitionally rough boundaries (Le Roux, 2004). As expected, slight deviations from the law of wall is observed near the flume bed and near the water surface. Further, it can be observed from the above figure that the experimental data obtained from the present study lie between the plots of flows over hydrodynamically smooth

and rough beds and are therefore considered to represent the transitionally rough bed. For the present experimental data, the value of shift in log law, Δu^+ due to roughness is computed on the basis of roughness Reynolds number and found to be equal to 2.9. For the purpose of comparison, using the values of Δu^+ reported in the literature, a graph is drawn between $k_s{}^+$and Δu^+ as shown in Fig. 4.2. From this figure one can easily note that the value of Δu^+ computed using the present experimental data lies in the region closer to the values reported in the literature for transitionally-rough bed (Schlichting, 1979, Bergstrom *et al.*, 2001, Schultz and Flack, 2003, Bigillon *et al.*, 2006) and rough boundaries (Schlichting, 1979 and Balachander and Patel, 2002).

The normalized profiles of mean flow velocities in three directions are illustrated in Fig. 4.3. The mean flow velocities in directions *y* and *z* ($\overline{v}$, $\overline{w}$) were almost zero. The flow characteristics were normalized using the shear velocity, u_* = 0.0306 m/s. The reductions of $\overline{u}$ values near the water surface (for h_{20}) are due to the velocity dip phenomenon, which commonly occurs in the rectangular channels whose aspect ratio $B_0 / h \leq 5$ (Nezu and Rodi, 1986).

The contour plots of the normalized time-averaged velocity components $\hat{u}$ ($=\overline{u} / \overline{u}_0$), $\hat{v}$ ($=\overline{v} / \overline{u}_0$) and $\hat{w}$ ($=\overline{w} / \overline{u}_0$) in the plane (of measurements) nearest to the bed (3.5 mm above the bed) in the upstream of the pier is shown in Fig. 4.4. These figures quantify the flow pattern around the pier. The quantity $\hat{u}$ in the approach flow progressively decelerates as its magnitude decreases with the distance towards the pier nose. The deflected flow results in an increase in flow velocity along the side of the pier and a maximum magnitude of $\overline{u}$ =1.88 $\overline{u}_0$ is observed at $\hat{x} = -0.48$ and $\hat{y} = 0.61$. The component of transverse velocity ($\hat{v}$) was very weak in the approach flow, but it becomes prominent near the pier due to the flow separation. Maximum amplification in $\hat{v}$ was observed to occur at $\hat{x} = 0$ and $\hat{y} = 0.44$ (Fig. 4.4). However measurements could not be made at points that were more close to the pier due to limited accessibility for the ADV. Away from the pier the vertical velocity, $\hat{w}$ is positive albeit small in magnitude which thereby indicates the existence of a weak flow in the upward direction. Nearer to the pier, however, the $\hat{w}$ component is stronger and it reverses in direction .The amplification of the negative values of $\hat{w}$ thus quantify the strong downward flow which exist in front of the pier (Ahmed and Rajaratnam, 1998, Barbhuiya and Dey, 2004).

Figure 4.5 shows the vector fields of time averaged velocity superimposed over the contour plot of the normalized resultant velocity [$(\hat{u}_r = \hat{u}^2 + \hat{v}^2 + \hat{w}^2)^{0.5}$] in the plane of measurement taken in the close proximity of the bed on the upstream of the pier. The magnitude and direction of the arrows representing the resultant velocity are computed using the expressions $(\bar{u}^2 + \bar{v}^2)^{0.5}$ and arctan $(\bar{v} / \bar{u})$ respectively. It can be seen from Fig. 4.5 that the approaching flow is deflected on the upstream of the pier and thereby a skewed flow occurs along the bottom of the flume bed. The vector fields of time averaged velocities with magnitudes $(\bar{u}^2 + \bar{v}^2)^{0.5}$ and $(\bar{u}^2 + \bar{w}^2)^{0.5}$ and their respective directions viz. arctan $(\bar{v} / \bar{u})$ and arctan $(\bar{w} / \bar{u})$ along the line of symmetry (termed as A-line, see; Fig. 3.11) are shown in Fig.4.6. Here u^+, v^+, w^+ represent the normalized turbulence intensity in the *x*, *y*, *z* directions respectively and Φ_{xy} and Φ_{xz} represent the directions of streamwise and vertical velocity vectors respectively. The point along the A-line at which the velocity vector changes its direction was considered to be the point of flow separation. Figure 4.6 thus indicates that flow separation occurs nearly at $\hat{x}$=0.351 upstream of the pier nose, which is a measure of the size of primary vortex forming in front of the pier (Kothyari *et al*., 1992). Roulund *et al*., (2005) reported a value of $\hat{x}$ = 0.46 as the point of flow separation based on their experiments on smooth bed. The separation point at the line of symmetry computed using the semi empirical formula given by Kothyari *et al*., (1992) for flat alluvial beds was found to be $\hat{x}$ = 0.29. Ahmed and Rajaratnam, (1998) also showed that the shear vector turned less in the case of rough bed when compared to the smooth bed and it was due to the larger resistance offered by rough beds on the limiting streamlines as they turn outward under the influence of lateral pressure gradient.

4.2.2 Turbulence intensity

The turbulence intensity components in the *x*, *y* and *z* directions can be represented as follows:

$$\sqrt{\overline{u'^2}} = \left[\frac{1}{N} \sum_{i=1}^{N} (u_i - \bar{u})^2 \right]^{0.5} \tag{4.7}$$

$$\sqrt{\overline{v'^2}} = \left[\frac{1}{N} \sum_{i=1}^{N} (v_i - \bar{v})^2 \right]^{0.5} \tag{4.8}$$

$$\sqrt{\overline{w'^2}} = \left[\frac{1}{N} \sum_{i=1}^{N} (w_i - \bar{w})^2 \right]^{0.5} \tag{4.9}$$

The vertical normalized profiles of the mean turbulence intensities measured in the streamwise, transverse, and vertical directions (u_a^+, v_a^+, w_a^+) of the approach flow are illustrated in Fig. 4.7. Near the bed, the roughness elements have a direct impact on the turbulence, and the turbulence intensity increases with z up to a peak value (Carollo *et al*., 2005). Nezu and Nakagawa (1993) attributed this observation to the presence of bed roughness elements penetrating the flow forcing the decomposition of large-scale vortices into smaller vortices. Present study also witnessed similar observations with the peak value measured at a distance of $z/h \approx 0.1$. The turbulence intensity then steadily decreases in the region far from the bed and becomes independent from the bed roughness (Carollo *et al*., 2005).

The turbulence intensity components around upstream of the pier are normalized by using the value of the turbulence intensity measured in the approach flow in the plane 3.5 mm above the flume bed ($u^+ = \sqrt{\overline{u'^2}} / \sqrt{\overline{u_0'^2}}$, $v^+ = \sqrt{\overline{v'^2}} / \sqrt{\overline{u_0'^2}}$, $w^+ = \sqrt{\overline{w'^2}} / \sqrt{\overline{u_0'^2}}$) and the contour plots of the same are shown in Figs. 4.8(a) to 4.8(c). The turbulence intensity along the plane of symmetry in the upstream of the pier increases due to the deceleration of the approaching flow and attains a maximum value within the flow separation region. The maximum value of turbulence intensity (u^+) is approximately three times higher than its value in the approach (undisturbed) flow as reported in the literature (Ahmed and Rajaratnam, 1998, Schappman, 1975, Graf and Istiarto, 2002). Although w^+ is relatively less dominant in the approach flow, its amplification in the region of flow separation is more when compared to other intensities observed in x and y directions. The distribution characteristics of v^+ and u^+ are mostly similar as noted in Figs. 8(a) and 8(b)

4.2.3 Turbulent Kinetic energy

The vertical distribution of turbulent kinetic energy in the approach flow is illustrated in Fig. 4.9. As can be seen from this figure, the maximum value of k^+ is noticed closer to the bed. This can be attributed to the reason that near the bed, the roughness elements have a direct impact on the turbulence. In general, the value of k^+ decreases when moved away from the bed. However, the rate of decrease is seen to be smaller near the bed surface as compared to that above the mid depth.

The contour plot of the normalized turbulent kinetic energy [$k^+ = 0.5(u^{+2}+v^{+2}+w^{+2})$] illustrated in Fig. 4.8(d) depicts the cumulative effect of u^+, v^+ and w^+ near the bed. The

general distribution of turbulent kinetic energy is similar to those of u^+ and v^+. Maximum value of k^+ is noticed to occur along the A-line.

Distributions of turbulent kinetic energy at different flows synchronize to the distributions of turbulence intensities and Reynolds stresses (discussed subsequently). If sediment transport and scour are initiated from high turbulence activities, the high turbulent kinetic energy zone indicates potential sediment entrainment and consequent erosion. In this regard, the turbulent kinetic energy distribution is a better representation of turbulence activities in a distributed flow field and provides a better indicator of potential erosion and sedimentation.

4.2.4 Reynolds stresses

The vertical distribution of the normalized Reynolds stress in the approach flow is illustrated in Fig 4.10. In the wall region Reynolds stress attains a maximum and decreases towards the bed. Similar results have been reported in other studies with smooth (Antonia, and Krogstad, 2001) and rough beds (Nikora and Goring, 2000). Viscous effect is the reason for such behavior in smooth beds, whereas in rough beds it can be explicated by the existence of a roughness sub-layer where additional mechanisms for momentum extraction emerge (Nikora and Goring, 2000). The fluctuations of the longitudinal velocity and vertical velocity were distributed according to the Gaussian function. But the turbulence shear stress fluctuations near the bed surface were skewed and followed log normal distribution. The skewness of the turbulence shear stress fluctuations decreases and tends to attain symmetry when moved towards the main flow from the bed (Fig. 4.11). These observations were similar to those of the previous investigators over rough beds (Cheng and Law, 2003)

The contour plot of the normalized Reynolds stresses uw^+ ($=\overline{u'w'}/\overline{u'w'_0}$) and uv^+ ($=\overline{u'v'}/\overline{u'v'_0}$) around the upstream of the pier near the flume bed are shown in Fig. 4.12. The Reynolds stresses get amplified closer to the zone of flow separation and reaches its maximum (approximately $16\,\overline{u'w'_0}$) at $\theta = 60^\circ$ (θ is the angle measured in the *x-y* plane from A-Line), which is in close agreement with the value reported by Roulund *el al*. (2005) who predicted the largest amplification of bed shear stress to occur between $\theta = 60^\circ$ and 70°. The close proximity of the contour lines of Reynolds stresses near the pier as shown in Fig. 4.12 also confirms significant variations of Reynolds stresses within this region.

4.2.5 Bed shear stress

The shear velocity (u_*) is an important parameter in sediment transport studies, therefore it requires accurate evaluation. Le Roux and Brodalkab (2004) compared different methods for determination of u_* and concluded that the shear velocity computed by using the adjusted velocity profile method (Middleton and Southard, 1984 and Perry and Joubert, 1963) gives the best performance in predicting the initiation of bed load transport. Hence in the present work, the bed shear stress ($\tau_o = \rho u_*^2$) of the approaching flow is estimated with the shear velocity obtained using the adjusted velocity profile method. Bed shear stress around the pier is estimated by two different methods based on stream-wise flow velocity and Reynolds stress distributions.

The method proposed by Wu and Rajaratnam, (2000) has been used to compute the bed shear stress based on the stream-wise velocity components measured in the plane nearest to the flume bed. The shear stress thus estimated is normalized using the bed shear stress of the approach flow. Figure 4.13(a) shows the contour plot of the normalized bed shear stress around the upstream of the pier. The maximum amplification of bed shear stress in the separated region reported in the literature is of the order of 1.25 to 1.5 for a smooth bed (Dargahi, 1989, Ahmed and Rajaratnam, 1998) and 2.75 to 3.25 for a rough bed (Ahmed and Rajaratnam, 1998). However, not many literatures report the bed shear stress for transition regime. In the present case, the maximum shear stress amplification along the line of flow separation is found to be of the order of 2.54 and it occurs at $\hat{x} = -0.45$ and $\hat{y} = 0.85$. The present value lies between the values reported for smooth and rough beds and thus it confirms the validity of our experimental data according to the expected physics underlying the problem. Figure 4.14 shows the variation of bed shear stress along the B-line which is perpendicular to the line of symmetry. Bed shear stress at the pier sides is about five times greater than the approach flow bed shear stress. The variations of bed shear stress obtained around the upstream of the pier in the transition bed compares well with the results reported by Sadeque *et al*. (2007) on smooth beds as seen from the above figure.

The method used by Barbhuiya and Dey (2004) is adopted to compute the bed shear stress based on the Reynolds stresses measured in the horizontal plane nearest to the flume bed. The shear stress thus estimated is normalized using the bed shear stress of the approach flow determined using the Reynolds stresses measured at a point of 3.5 cm above the flume bed in the approach flow. Figure 4.13(b) shows the contour plot of the normalized bed shear stress around the pier upstream. The variations of bed shear stress around the pier upstream showed amplification of higher magnitude (τ_r / $\tau_{r0} \approx 16$, where τ_r is the bed shear stress

around upstream of the pier determined using the Reynolds stresses and τ_{r0} is the approach flow bed shear stress determined using the Reynolds stresses) in the region of $\theta = 45^{\circ}$ and this is the region where the scouring is expected to initiate. Thus our results confirm the Reynolds shear stress estimated by Graf and Yulistiyanto (1998) who also reported a similar amplification in the region of $\theta = 45^{\circ}$. As the highest amplification of shear stress occurs in the region of $\theta = 45^{\circ}$, the observations that scour around piers initiate in the region is thus explained. The scour protection measures like rip-rap should be designed for stability, against the above reported enhancement in the shear stress.

4.3 SCOURING AROUND PIER WITH AND WITHOUT COLLAR

Experiments were conducted around the circular pier model with and without a collor to quantify the reduction in scour due to the presence of collor.

4.3.1 Visual Analysis

Scouring process in the case of pier with collar started from the sides of the collar and approached towards the nose of pier and collar. Maximum scour depth is observed to occur in front of the pier nose in the absence of the collar and on the sideways when the collar was in position. The position of scour mainly depends upon the position and size of the collar and the prevailing flow conditions.

I) Clear-water Scour without Collar

In each run without collar, it was noted that in all cases the initiation of scour process starts in the upstream half of the pier at an angle of about 40^0 to 60^0 from the central axis of flow. The scour extent then rapidly extended and reached up to the upstream nose of the pier in a short span of time. Beyond such a stage the scour occurred in the upstream half of the pier and the geometry of the scour hole resembled to an inverted frustum of a cone. These observations were in good confirmation with the studies of the previous investigators.

II) Live-bed Degradation without Collar

As already mentioned the flow conditions in approach flow correspond to the live-bed situation but no sediment is transported by upstream flow (no feeding of sediment is done in the experiment). General bed degradation will occur in this condition particularly in the approach flow. The basic observation under the live-bed degradation condition was that the scour hole formation was very rapid initially and the scour hole shows non-uniform behaviour temporally. The variation of scour depth with time was noticed to be periodic,

which was not seen in case of clear-water. Significant deposition however, was noticed to occur on the downstream of the pier under this condition.

III) Live-bed Condition without Collar

The basic observations under the live-bed were same as in the case of the live-bed degradation runs. However, in live-bed condition the dune movement on the upstream of pier was noticeable and periodic nature in the temporal variation was more pronounced.

IV) Clear-water Condition with Collar

When a collar of size 2.5*b* was placed at bed level under clear-water condition, no scour was observed at the upstream nose of the collar. The scour initiates from the side of the collar and it tried to propagate to the pier front but since the horse-shoe vortex was supported on collar no well defined scour pattern was developed at pier nose. Bed forms of significant sizes were noticed to occur on the downstream of the pier (Fig. 4.15).

V) Live-bed Degradation Run with Collar

When a collar of size 2.5*b* was placed at bed level under live-bed degradation condition, scour was observed at the nose of the collar after a long period of scour activity. The scour generated from the side of the collar and it tried to propagate in front, hence the scour starts at the sideways and after 2 or 3 hours scour can be noticed in front also. Since no feed of sediment was done and the ratio of u_*/u_{*c} was greater than unity, the scour depth varies periodically and significant undulations were developed on the downstream. It was observed under degradation runs that the bed forms on the upstream side were developed and these bed forms extended upto the downstream end of the pier (Fig. 4.16 and 4.17).

VI) Live-bed Condition with Collar

When a collar of size 2.5*b* was placed at bed level under live-bed condition, minimum scour was observed at the nose of the collar. Since there was continuous feeding of sediment hence sediment front was observed on the upstream of the pier and this front moves ahead over the time. The periodic variation of the scour depth can be very clearly seen under conditions of sediment feeding as against the lesser periodicness under the live-bed degradation run condition (Fig 4.18 to 4.22).

From the visual analysis of the present study we deciphered that different scour pattern for different flow conditions with collar were developed. The line diagrams illustrated in Fig.

4.23 to 4.26 shows these scour patterns and thus the effect of collar on general scour development for different flow conditions i.e. clear-water condition with collar, live- bed degradation condition with collar and live-bed condition with collar.

Pattern in Clear-water Condition with Collar

When collar was placed under clear-water condition scour was first observed at the side of the collar which further propagated along the sides over the time. Literally no scour was observed at the nose of the pier and a mound was formed at the collar nose (Fig.4.23).

Pattern in Live-bed Degradation Run with Collar

When collar was placed under live-bed degradation condition, scour was first observed at the side of the collar which developed very rapid initially and further propagated along its sides towards the collar nose. Apart from the upstream and downstream sides, large undulations were seen to develop below and around the collar as well. It was very difficult to observe the scour depth in this condition as the flow was always muddy (Fig.4.24).

Pattern in Live-bed Condition with Collar

When collar was placed under live-bed condition scour was again first observed at the side of the collar which developed very rapidly initially and further propagated along its sides towards the collar nose. But the scour development became very slow after a short period of time (about 45 min later). The feeding of the sediment from the upstream led to the formation of sediment fronts which collapsed under gravity and led to the decrease in scour depth and increase in scour hole area over the long period of time. There was considerable amount of scour reduction when a collar is placed around the pier during live-bed condition as well (Fig. 4.25).

4.3.2 Temporal Variation of Scour Depth for Different Flow Conditions

The observed temporal variation of scour depth for all the runs is shown in Fig. 4.27 to 4.58. The comparisons shown in Figs. 4.27 to 4.42 are for experiments conducted without any protective devices. The Figs. 4.43 to 4.58 show the temporal variation of scour with placement of collar. For all the runs single size pier of diameter 114mm is used for a sand size of 0.34mm and rest of the respective flow conditions are listed in the corresponding figures.

4.4 TEMPORAL VARIATION OF SCOUR AROUND PIER WITH AND WITHOUT COLLAR

4.4.1 Effect of Live- Bed condition on Scour

The temporal variation of scour under the live-bed is highly periodic nature in time. The fluctuations in scour depth can be well observed provided the interval of observations is small. When there is constant feeding of sediment from the upstream, sediment fronts are formed on the upstream and these fronts move up to pier front and collapse under their self weight at a certain distance near the pier or collar nose, hereby increasing the diameter of scour hole and providing periodicity to temporal variation of scour depth by decreasing the depth of scour. This phenomenon is repeated in time. In case of live-bed degradation condition however significant movement of bed features could not be seen on pier upstream.

For the live-bed conditions repeatability of the bed forms is difficult to achieve due to the less control on movement of the bed forms during the experimentation. Hence for similar flow conditions and pier size, different patterns in scour depth variation are noticed. Also the feeding of the sediment must be well controlled as the scour pattern is highly influenced by this activity. Hence, live-bed condition requires due care and precision during flume study.

4.4.2 Effect of Collar on Clear-water Scour

When collar is placed under clear-water condition considerable amount of reduction in scour depth could be seen. A collar of size 2.5*b* gives maximum protection when placed at bed level (Kumar *et. al*. 1996). When the collar is placed at bed level, scour in the wake region starts right from the beginning of the wake zone. In all cases scour in the sides and front develops later. The instantaneous deepest wake scour occurs under the collar on both sides.. The deepest scour initially moves upstream and eventually to the downstream. This movement is due to the temporal variation of scour depth at the front and the sides vis-à-vis the wake scour. The variation of scour depth in front for clear-water also shows slight periodic nature.

4.4.3 Effect of Collar on Live-bed Scour

The effect of collar on live-bed is not as significant as in case of clear-water condition. Even after reaching the equilibrium scour the scour process continues but the rate of scour is very low. The rate of scour thus never becomes zero and equilibrium scour is not attained. With time, the scour depth shows periodicity. Inspite of high periodic nature of

scour depth variation the collar proves to be an effective scour reduction device for live-bed scour condition as well.

4.4.4 Reduction of Scour

Considerable reduction of scour around pier after the placement of collar was noticed. Figure 4.59 shows the comparison of ratio of maximum scour depth to global maximum scour depth with different flow conditions. It can be seen from this figure that maximum reduction in scour occurs by collar under live-bed conditions. The scour depth is reduced by 75% under this condition. Figure 4.60 shows the comparison of ratio of maximum scour depth to global maximum scour with ratio of shear velocity to critical shear velocity. It can be seen from this figure that reduction in scour due to collar is more in live-bed condition as compared to that in degrading bed condition.

Figure 4.61 shows time variation of scour depth in a circular pier with and without collar under clear-water conditions (u_*/u_{*c}=0.89). Similarly variation of scour depth under live-bed condition with and without collar is presented in Fig. 4.62 to 4.63. These figures indicate considerable success is achieved in reduction in the scour rate by the use of collars. Comparison of rate of scour and time variation of scour depth with results of earlier investigators is also made. Figure 4.64 shows a good conformity of the present results with the results of Mashahir *et.al.*(2004) for clear-water scour. The variation of scour depth for live-bed under collar for circular pier alone is shown in Fig. 4.65 with comparison to Mashahir *et al.* (2004) and Melville & Raudkivi (1996). The conformity of the results from the two investigators may be noted.

Figure 4.66 shows the comparison in the difference of the maximum scour depth occurred during the experiments conducted for varying u_*/u_{*c}, with and without collar. It was observed that there is considerable reduction (upto 75%) in maximum scour depth after collar was provided in live-bed condition (Fig. 4.66 to 4.73). For the clear-water condition 2.5*b* collar gives no scour in front of pier but scour was observed in sideways of collar. In live-bed condition the maximum scour was observed below the collar at a certain distance in front of the pier nose.

Table 4.1 shows the percentage reduction in the values of scour depth for different ratios of u_*/u_{*c} under varying flow conditions. It was observed that there is a reduction of more than 70% in the maximum scour depth with live-bed conditions.

TABLE 4.1 Percentage Reductions in Maximum Scour Depth Due to Placement of Collar

Sl. No.	Set No.	Experiment	u_*/u_{*c}	Flow conditions	Pier Diameter b(cm)	Mean Particle Size d_{50} (mm)	Maximum scour(cm)		Percentage reduction in scour depth
							With Collar	Without Collar	
1	1	CWSNC1	0.87	Clear water	11.4	0.34		8	
2		CWSNC2	0.89					10.3	
3	2	LBSNCNFS1	1.089	Live bed degradation	11.4	0.34		7.7	
4		LBSNCNFS2	1.1					9.1	
5		LBSNCNFS3	1.266					7.8	
6		LBSNCNFS4	1.33					8.2	
7		LBSNCNFS5	1.42					9.4	
8		LBSNCNFS6	1.488					11.3	
9		LBSNCNFS7	1.8					11.5	
10		LBSNCNFS8	2.05					14.2	
11	3	LBSNCWFS1	1.089	Live bed	11.4	0.34		7.2	
12		LBSNCWFS2	1.1					8.7	
13		LBSNCWFS3	1.266					6.7	
14		LBSNCWFS4	1.33					7.5	
15		LBSNCWFS5	1.42					8.3	
16		LBSNCWFS6	1.488					10.0	
17	4	CWSWC1	0.87	Clear water + collar	11.4	0.34	3.6		55%
18		CWSWC2	0.89				3.9		62%
19	5	LBSWCNFS1	1.089	Live bed degradation + collar	11.4	0.34	4.4		43%
20		LBSWCNFS2	1.1				4.9		46%
21		LBSWCNFS3	1.266				2.9		63%
22		LBSWCNFS4	1.33				3.3		60%
23		LBSWCNFS5	1.42				5.2		45%
24		LBSWCNFS6	1.48				3.0		73%
25		LBSWCNFS7	1.87				5.8		50%
26		LBSWCNFS8	2.05				6.2		56%
27	6	LBSWCWFS1	1.089	Live bed + collar	11.4	0.34	2.2		69%
28		LBSWCWFS2	1.1				3.2		63%
29		LBSWCWFS3	1.266				4.8		29%
30		LBSWCWFS4	1.33				2		73%
31		LBSWCWFS5	1.42				2		76%
32		LBSWCWFS6	1.488				3.2		68%

4.5 SCOURING AROUND COMPOUND PIERS

4.5.1 Process of Scour around Circular Compound Piers

The defination diagram of compound pier is shown in Fig. 4.74. It has been observed previously as well as in the present study that, for the case of circular uniform pier, under clear-water approach flow condition, the deepest scour hole occurred in the pier upstream front and side while wake scour was much smaller in depth.

The temporal variation of scour depth around the circular compound piers was measured for $\frac{b_*}{b}$ ratio ranging from 1.84 to 4.37. The position of top surface of the footing was systematically varied and the same was placed respectively above the channel bed level, at the bed level and below the channel bed level. The followings features of the scour process were noticed.

(a) In comparison to the scour depth around the circular uniform pier, for same flow and sediment conditions, the depth of scour is more around the compound pier when top of the footing is placed above general bed level of the channel. The extent of scoured area is also larger in this condition due to the exposure of the larger height of footing to the flow. The deepest scour in this case occurs at the upstream nose of the pier/footing.

(b) When top of the footing is placed at the level of channel bed, the depth and extent of scour is dependent on the value of b_* / b. For $b_* / b < 2.8$ the scour is generally deeper than that at a uniform pier of size b. However, for $b_* / b > 2.8$, the scour is generally smaller than that at a uniform pier of size b while top surface of footing is at the level of channel bed.

When top surface of the footing is placed below the level of channel bed, the scour depth around the compound pier is considerably smaller compared to that around the circular uniform pier having same diameter as pier of the circular compound pier. It was noticed that scour process in this condition initiates from the pier sides and /or the downstream. However the position of deepest scour was either at upstream nose of the pier or in the wake region. The deepest scour occurred in the wake region while $\frac{b_*}{b} > 2.8$. The reduction of maximum depth of scour is attributed to the reason that in this condition the principal vortex rests on the

projected top surface of the footing which is rigid. This characteristics has been termed as the vortex supporting ability of the footing (Kumar and Kothyari, 2012).

4.5.2 Modelling for Temporal Variation of Scour Depth around Circular Uniform and Compound Piers

Kothyari *et al*., (1992 a) proposed a semi-analytical model for computation of temporal variation of scour depth that is applicable to coarse as well fine sediments and steady as well as unsteady flows. Investigators like Mia and Nago, (2003), Lu *et al*., (2011) *etc*., made the model of Kothyari *et al*., (1992 a) as basis for their studies. Therefore, the model of Kothyari *et al*., (1992 a) is updated herein based on the new data collected in the present study and from literature. The updated model is used for computation of temporal variation of scour depth around circular uniform and compound piers.

Effective Diameter of the Circular Compound Pier

In case of circular compound pier, the estimation of scour depth on the basis of either pier diameter or footing diameter shall give inaccurate results. So the effect of the foundation geometry is taken into account while computing the scour depth around the circular compound bridge pier.

Therefore the effective diameter of the circular compound pier is defined for scour computations as that diameter of the uniform circular pier which shall produce same temporal variation of scour depth as the circular compound pier. The effective diameter of a circular compound pier is computed as below (Melville and Raudkivi, 1996):

$$b_e = b\left(\frac{h+Y}{h+d_s}\right) + b_*\left(\frac{d_s - Y}{d_s + h}\right) \tag{4.10}$$

Here b_e is the effective diameter of the circular compound pier and d_s is the depth of scour below the initial bed level at time t, $b_*$is footing diameter and Y denotes position of top surface of footing with respect to general bed level of channel.

In the above equation the effective diameter is determined by considering the weighted average of pier diameter and footing diameter. Here weighting factors respectively are the height of pier and height of footing exposed to the flow. The scour depth increases with the time and simultaneously footing height exposed to the flow increases with scour development. This aspect has been accounted in the Eq. (4.10) for computation of temporal variation of the scour depth.

Assumptions Regarding the Horseshoe Vortex

The horseshoe vortex is considered to be the prime agent causing scour around the bridge piers and thus diameter of the principal vortex of the horseshoe vortex system, D_v is calculated from the equation given below (Kothyari *et al*., 1992 a)

$$\frac{D_v}{h} = 0.28\left(\frac{b}{h}\right)^{0.85} \tag{4.11}$$

Throughout the process of scour, the upstream half of the scour geometry can be approximated as an inverted frustum of a right circular cone having an angle of frustum equal to the value of ϕ. As the scour hole develops at the pier nose, the horseshoe vortex expands and sinks into it (Melville, 1975). The cross-sectional area of principal vortex of horseshoe vortex system at any time *t* is equal to initial cross-sectional area of primary vortex (A_0) plus cross-sectional area of the scour hole (A_s) at time *t* (Kothyari *et al*., 1992 a):

$$A_t = A_0 + A_s \tag{4.12}$$

or $A_t = \frac{\pi}{4} D_v^2 \varphi + \frac{d_s^2}{2} cot$

The value of angle of repose ϕ can be assumed to be 30° for the purpose of computations. Before scour begins at the pier, the average shear stress at the nose of the pier is increased on an average by four times the shear stress in the approach flow (Hjorth, 1975; Ettema, 1980; Kothyari *et al*., 1992 a).

It may be mentioned that Eqs. (4.11) and (4.12) proposed by Kothyari *et al*., (1992 a) were also used by Mia and Nago, (2003) and Lu *et al.*, (2011). The suitability of these equations is verified herein for uniform circular piers by using the experimental data on flow pattern collected from literature and that in the present study. For circular compound pier, the data of present study are used for this purpose.

The cross-sectional area of principal vortex A_t around the compound pier is computed by using Eqs. (4.11) and (4.12) by substituting the known value of scour depth and using for value of b_e in place of *b*.

The observed size of principal vortex was determined by using experimentally observed velocity vector fields for the compound pier model and uniform pier model as depicted in Fig. 4.75 (Kumar and Kothyari, 2012). In Fig. 4.756, *r* (mm) is the radial

distance (r = 0 is the center of the pier), α [°] is the angular direction of the plane and z [mm] is the vertical direction. For this, the velocity vectors bending downwards and clockwise from the horizontal and having inclination more than 10° with the horizontal were included inside the upper periphery of the vortex. The A_t value for principal vortex is considered to be equal to the area of thus formed vortex structure. The A_t values were also determined in similar manner by using the experimental data on flow pattern of Melville, (1975); Graf and Istiarto, (2002) and Dey and Raikar, (2007 a) for uniform circular piers. The A_t values thus determined are termed here as the observed A_t.

Figure 4.76 shows the comparison between computed A_t and observed A_t. It can be seen that Eqs. (4.11) and (4.12) have well estimated the values of A_t. Therefore, Eqs. (4.11) and (4.12) are considered to be suitable for the computation of area of primary vortex at time t of scour development in compound pier also and the same are therefore used in the present modelling.

The bed shear stress τ_{pt} within the scour hole at the pier nose after time t from the start of the scour process is computed by the following equation Kothyari *et al*., (1992 a).

$$\tau_{pt} = 4.0\tau_0 \left(\frac{A_0}{A_t} \right)^{0.57} \tag{4.13}$$

Here τ_0 is the shear stress of the approach flow. As the scour process proceeds there is consequent decrease in the shear stress value.

The measurements on bed shear stress have been used to validate the Eq. (4.13). The bed shear stress within the scour hole at the nose of pier at time t was calculated from the Eq. (4.13) for the experimental data of uniform pier model of present study, and for similar data of Melville, (1975); Ahmed and Rajaratnam, (1998); Graf and Istiarto, (2002), and Dey and Raikar, (2007 a). Here value of A_t was calculated using Eq. (4.12) by utilizing the observed value of scour depth corresponding to the condition for which the τ_{pt} was calculated. Thus determined values of shear stress are termed as the computed bed shear stress. The observed (experimental) shear stress value of Melville, (1975); Ahmed and Rajaratnam, (1998); Graf and Istiarto, (2002), and Dey and Raikar, (2007 a) was extracted from their papers. The observed bed shear stress for the data of present study was determined by using the method of Wu and Rajaratnam, (2000) which is based on velocity measurements. For this purpose the ADV measurements on velocity field (see Fig. 4.75) within the scoured area were utilized.

Based on the forward velocity *u* and vertical velocity *w* measured at a vertical distance $z \approx 4$ mm above the scoured bed level, the velocities parallel to the bed slope of the scour hole were determined. These velocities were utilized according to Wu and Rajratnam, (2000) to estimate the shear stress along the bed of the scour hole. Thus determined values of shear stress are termed as the observed bed shear stress.

Figure 4.76 shows the plot between observed and computed value of τ_{pt}. It can be seen that Eq. (4.13) has well estimated the bed shear stress within the scour hole at upstream nose of the pier at time *t* after start of the scour process except for one data point. One of the possible reasons for this anomalous point is that, data is extracted from the figure of the paper of Graf & Istiarto and there may be some discrepancies while extracting the data from the figure. Therefore Eq. (4.13) is used in the present model for scour computations.

Estimation of Time Required for Removal of a Single Sediment Particle

If the bed shear stress τ_{pt}, acting at the upstream nose of pier nose at any time *t* can be obtained from the relationship mentioned above, then the time t_* required for a sediment particle to get scoured due to τ_{pt} can be estimated using the equation having the following form (Paintal, 1971; Kothyari *et al*., 1992 a)

$$t_* = \frac{c\ d_{50}}{P_{ot}\ u_{*t}} \tag{4.14}$$

and

$$u_{*t} = \sqrt{\frac{\tau_{pt}}{\rho_f}} \tag{4.14}$$

In the above, c is a parameter, u_{*t} is the shear velocity at time *t*, ρ_f is mass density of fluid and P_{ot} = average probability of movement of the particle at time *t* (Paintal, 1971). Ettema, (1980) and Oliveto and Hager, (2002, 2005) illustrated the process of scour to be different in fine and coarse sediments. However the method of Kothyari *et al.*, (1992 a & b) used the same value of parameters *c* for computing rate of scour in coarse and fine sediments. The present work overcomes this limitation.

The data collected in present study on temporal variation of scour depth around circular uniform piers, and these data of Chabert and Engeldinger, (1956); Ettema, (1980); Kothyari, (1989); Yanmaz and Altinbilek, (1991); Melville and Chiew, (1999); Oliveto and Hager, (2002); Mia and Nago, (2003) and Sheppard *et al*., (2004) were used for computation

the value of parameter *c* of Eq. 4.14 a. The range of experimental data on scour around circular uniform pier compiled herein is given in Tables 4.2. In Table 4.2, β is the opening ratio which is equal to $(B_0 - b)/B_0$.

Table 4.2 Range of experimental data on circular uniform pier scour

S. No.	Variables	Range
1	Velocity of approach flow ,U_0 (m/sec)	0.17 - 1.14
2	Depth of flow, h (m)	0.042 - 1.9
3	Width of pier, b (m)	0.022 - 0.91
4	Median sediment grain diameter, d_{50} (m)	0.0004 - 0.0078
5	Width of flume, B_o (m)	0.6 - 1.52
6	Opening ratio, β	0.81 - 0.98

Detailed data analysis revealed that the value of parameter *c* is mainly a function of the variables $b,\ d_{50}, h, g, \rho_s, \rho_f,\ u_{*t}$ and the kinematic viscosity of fluid ν, i.e.

$$c = f(b,\ d_{50},\ h, g, \rho_s,\ \rho_f, u_{*t},\ \nu) \tag{4.15}$$

Here, g is gravitational acceleration and ρ_s is the mass density of sediment. The variables in Eq. (6) are arranged into the following non-dimensional form

$$c = f(D_*, \frac{b}{h}, \frac{u_{*t} d_{50}}{\nu}) \tag{4.16}$$

Here D_* is the dimensionless sediment size (sedimentological variable) and is given by

$$D_* = d_{50}\left(g'/\nu^2\right)^{1/3} \tag{4.17}$$

In the above $g' = g(s\text{-}1)$ is reduced gravitational acceleration. Here s is the specific gravity of sediment.

The open channel flow characteristics are dependent upon channel bed roughness and viscous effects. The channel roughness is appropriately represented by the dimensionless sediment size D_*. Following Oliveto and Hager (2002, 2005) the channel bed surface is defined as hydraulically smooth while $D_* \le 25$, hydraulically rough for $D_* > 80$ and in the transition state with $25 < D_* \le 80$.

In the hydraulically smooth regime, viscous effect is dominant and it was also evident from the number of trials made for derivation of the relationship for *c* for scour in fine sediments. Thus while $D_* \le 25$, parameter *c* is found to be dependent on $\frac{u_{*t} d_{50}}{\nu}$ and $\frac{b}{h}$ as

$$c = 2.2 \times 10^{-4} \left(\frac{u_{*t} d_{50}}{\nu} \right)^{1.3} \left(\frac{b}{h} \right)^{1.4} \quad ; \quad D_* \le 25 \qquad (4.18)$$

In the transition regime ($25 < D_* \le 80$) both the roughness of the bed surface and viscous effects play role in defining the parameter *c*. After a number of trials the following relationship is proposed for *c*

$$c = 2.5 \times 10^{-10} \left(D_* \right)^{3.0} \left(\frac{u_{*t} d_{50}}{\nu} \right)^{1.2} \left(\frac{b}{h} \right)^{0.1} \quad ; \quad 25 < D_* \le 80 \qquad (4.18)$$

Similarly the following relationships is found suitable for *c* while channel bed and behaves as hydraulically rough bed

$$c = 9.6 \times 10^{-12} \left(D_* \right)^{4.4} \left(\frac{b}{h} \right)^{0.3} \quad ; \quad D_* > 80 \qquad (4.18)$$

Following Paintal, (1971) the relations given below are also proposed for estimation of P_{ot}

$$P_{ot} = 0.8 \left(\tau_{*pt} \right)^{4.2} \quad ; \quad \text{for } \tau_{*pt} \le 0.5 \qquad (4.19)$$

$$P_{ot} = 0.18 \ln \left(\tau_{*pt} \right) + 0.17 \quad ; \quad \text{for } \tau_{*pt} > 0.5 \qquad (4.19)$$

Here τ_{*pt} is the non-dimensional shear stress which is equal to $\left(\frac{\tau_{pt}}{\Delta \gamma_S d} \right)$, $\Delta \gamma_s$ = $\gamma_s - \gamma_f = \gamma_f (s-1)$, γ_f is the specific weight of fluid and γ_s is the specific weight of sediment.

To find out the temporal variation of scour depth around the pier following procedure is adopted. For known flow conditions in approach flow, pier diameter, sediment size, the value of τ_u , initial diameter of the principal vortex of the horseshoe vortex system is computed using Eq. (4.11) and the bed shear stress at pier upstream nose is computed using Eq. (4.13), with the condition that at $t = 0$, $d_s = 0$. The value of time t_* required for a single sediment particle to get scoured is computed using Eq. (4.14). So the scour depth d_s

after time t_* is equal to d_{50}. Now the Eqs (4.12-4.14) and (4.18-4.19) are to be used in a recursive way to find out the time variation of scour around the pier.

The computations should be stopped when the value of shear velocity in the scour hole is equal to or smaller than the critical shear velocity (u_{*c}) for incipient motion of sediment particle within the scour hole. Such a shear velocity is expected to be smaller than that computed by using Shields criteria (u_{*c}) due to the steep slope of the scoured area and the three-dimensional flow. The temporal evolution of scour has been considered herein to stop when $\frac{u_{*t}}{u_{*c}} \leq 0.5$.

4.5.3 Methodology for Computation of Temporal Variation of Scour Depth around Circular Compound Piers

The methodology for computation of temporal variation of scour depth around the circular compound pier is presented herein for three cases of footing placement, which covers all the situations of placement of footing. The three cases which have been dealt here are as (i) top level of the footing above the non-scoured bed level (Y = -ve) (ii) top level of the footing placed at the non-scoured bed level (Y =0) and (iii) top level of the footing below the non-scoured bed level (Y = +ve).

The methodology for computation of scour depth for all three cases is explained in this section.

Top surface of footing is above general level of the channel bed (negative Y values)

When top of the footing level is above the general level of bed, the non- uniformity of the compound pier along their height influences the scour process. Hence estimation of scour depth only on the basis of pier diameter will produce wrong results. So in order to take consideration of size of footing, diameter of the pier will be replaced by effective diameter of the circular compound pier as depicted by the Eq. (4.10). The temporal variation of the scour depth around circular compound piers can be then computed using Eqs. (4.12 - 4.14) and (4.18 - 4.19) as explained in previous section.

Top of footing is below general bed level of the channel (positive Y values)

When the top surface of the footing is placed below the level of channel bed *i.e.* the Y values were positive, three conditions arise while computing the scour depth in such cases.

Case (a) When $d_s < Y$; the circular compound pier in this case acts as a circular pier having diameter b and there is no effect of the footing on scour until scoured bed reaches up to top surface of footing. This case is also valid for uniform circular pier.

Case (b) When $d_s \approx Y$; The condition $Y = 0$ *i.e.* when top of the footing is kept at the bed level, is also covered under this scenario. In such case, the principal vortex rests on the top surface of footing at upstream nose of the pier. No scour can develop at the upstream nose during this condition. However, the vortex continues to expand laterally due to scouring activity on the sides and downstream of the pier. During such a time period the expansion of principal vortex over top rigid surface of the footing is considered to occur in the similar manner as in case of a scouring around uniform circular pier.

The lateral extent of scour hole $W_{e,}$ at the condition when the principal vortex of the horseshoe vortex system would have expanded up to the outer edge of the footing at pier upstream is computed as per Fig. 4.78 and is given by

$$W_e = \left(\frac{b_* - b}{2}\right) + \frac{Y}{\tan\phi} \tag{4.20}$$

Initially at $Y = 0$, when principal vortex touches to the top surface of the footing, the soild surface of the footing stops the scouring activity. At this stage lateral extent of scour hole is $\frac{Y}{\tan\phi}$ with an shape of inverted frustum of a right circular cone having an angle ϕ. Now it is considered that principal vortex will continue to expand in lateral direction up to a value of W_e by an amount $\frac{c_1 J d_{50}}{\tan\phi}$ in a similar way as scour depth increases from scour depth d_s to $d_s + d_{50}$ in new time t_*.

Here J is an integer counter, the value of which is considered as unity while the expansion of principal vortex just initiates on the top surface of the footing and c_1 is a coefficient depending on the hydraulic characteristics of the stream bed.

Hence the time rate for expansion of the principal vortex on the top surface of the footing at upstream nose of the pier is computed by the following equation

$$P = \left(\frac{Y + c_1 J d_{50}}{\tan\phi}\right) \tag{4.21}$$

During the process of expansion of vortex over the footing it is assumed that scour depth will continue to increase in a similar manner as in case of uniform pier for calculation purpose. The time taken by the principal vortex to expand up to the outer edge of the foundation is computed by simultaneously utilizing Eqs. (4.12-4.14) to (4.18-4.21). The scour depth at the pier nose is considered to remain constant and equal to Y up to such time as the vortex expands horizontally over the top rigid surface of footing at the upstream nose of the pier.

For circular compound piers the data of Melville and Raudkivi, (1996) and Lu *et al*., (2011) were also compiled for analysis. Table 4.3 shows the range of experimental data on circular compound pier scour.

Table 4.3 Range of experimental data on circular compound pier scour

S. No.	Variables	Range
1	Diameter of pier, b (m)	0.03 - 0.05
2	Diameter of foundation, b_* (m)	0.050 - 0.081
3	Depth of flow, h (m)	0.179 - 0.204
4	Depth of the top of the foundation below the initial bed level, Y (m)	(-) 0.045 - 0.064
5	Median sediment grain diameter, d_{50} (m)	0.0008 and 0.00052
6	Width of flume, B_0 (m)	0.44 and 0.6

The data on temporal variation of scour depth around bridge pier of the present study and data of Melville and Raudkivi, (1996) was used to find out the value of coefficient c_1.

In case of smooth boundaries *i.e.* when $D_* \leq 25$, the rate of expansion of principal vortex is slower. After making a number of trials it was noticed that for hydraulically smooth boundaries, the value of coefficient c_1 was equal to 0.8 whereas for the rough surfaces and the surfaces in transition *i.e.* when $D_* > 25$ the value of coefficient c_1 is equal to 1.0.

Case (c) As long as the principal vortex reaches to the outer edge of the top of the footing, the part of length of footing will exposed to the flow. So in this case $d_s > Y$. In such scenario methodology for computation of temporal variation of scour depth proposed is the same as for the case while Y was negative.

The cross-sectional area of principal vortex is computed based on effective diameter of the pier using Eq. (4.10). The initial diameter of principal vortex is re-computed in this

case by substituting b_e in place of b in Eq. (4.11) and similarly A_t is computed by using Eq. (4.12). The scour depth corresponding to previous computational step is used while computing b_e as per Eq. (4.10). The computation for temporal variation of scour depth was carried out as per the flow chart given in Fig. 4.79. The temporal evolution of scour was considered to stop when $\frac{u_{*t}}{u_{*c}} \leq 0.5$ due to the reasons already mentioned.

Figure 4.80 shows comparison of observed and computed temporal variation of scour depth around circular uniform pier for some data of Ettema, (1980); Melville and Chiew, (1999); Mia and Nago, (2003); Sheppard *et al.*, (2004) as illustration. The runs included in Fig. 4.80 also correspond to long duration experiments. In many cases the agreement between observed and computed values was near perfect, for example; runs MN3 and many other runs plots for which are not shown here due to space limitation. However maximum difference of $\pm$20% in other runs as also can be seen as illustration in runs MC1 and E5. In general these plots and other such plots (not shown here, given in Kumar, 2007) showed a good agreement between observed and computed temporal variation of scour depth around uniform circular piers. Only in a few cases the poor comparison (not shown here) was noticed between observed and computed scour depths. Thus the proposed algorithm for computation of temporal variation of scour depth is considered to have been well supported by a wide range of data collected by different investigators.

Computed temporal variation of scour depth was graphically compared with the corresponding observed values for all the data of present study, Melville and Raudkivi, (1996) and Lu *et al.*, (2011). Reasonably good agreement between the corresponding observed and computed values was mostly noticed. However some discrepancies between observed value and computed values are observed. Figure 4.81 shows such comparison for the data collected in the present study as illustration for some typical runs, while Fig. 4.82 shows it for the data of Melville and Raudkivi, (1996). It is seen from these figures that a near perfect agreement is obtained between the computed and observed scour values in some cases; for example runs 3 and run 22 of present study (Fig. 4.81). In a few runs the maximum difference between the computed and observed values is found to be about $\pm$30% (see; Figs. 4.81 and 4.82) for example run 14 and 26 of present study. Figure 4.83 shows the variation of scour depth with time for data compiled from Lu *et al.*, (2011). It may be noted that data of Lu *et al.* were not included in the development of the algorithm for scour computations. It is clear from the Fig. 4.83 that the proposed algorithm well predicts the temporal variation of

scour for unexposed as well as exposed footings of *Lu et al*. except for two of the runs. In general good agreement was noticed between predicted and observed values of scour depth (Figs. 4.81 to 4.83).

4.6 CONCLUDING REMARKS

The flow around pier during live-bed condition is quantified and the potential areas of scouring around upstream of the pier are identified. As the highest amplification of shear stress occurs in the region of $\theta = 45^{\circ}$, the observations that scour around piers initiate in the region is thus explained. The scour protection measures should be designed for stability, against the above reported enhancement in the shear stress.

Through laboratory experiments the collar around bridge pier has proved to be an effective scour control device under live-bed scour condition as well. With proper position and size of the collar used, the effectiveness of the collar in scour reduction is increased considerably. In the present study placement of 2.5*b* collar at bed level shows good efficacy (up to 75%) of collars in scour reduction under live-bed conditions. Based on the results summarised in Table 4.1, however it can be stated that a reduction of 63% in scour depth is attainable on an average by collar under live-bed conditions.

The temporal variation of scour around circular compound piers was not studied in detail so far. The algorithm proposed herein for computing temporal variation of scour depth around circular compound piers is noticed to reasonably well estimate the scour depth and therefore it can be used to compute the design scour depth around the circular bridge piers resting over large circular caisson or footing while top of the footing positioned either at bed level or above the bed level (footing exposed) and also below the bed level.

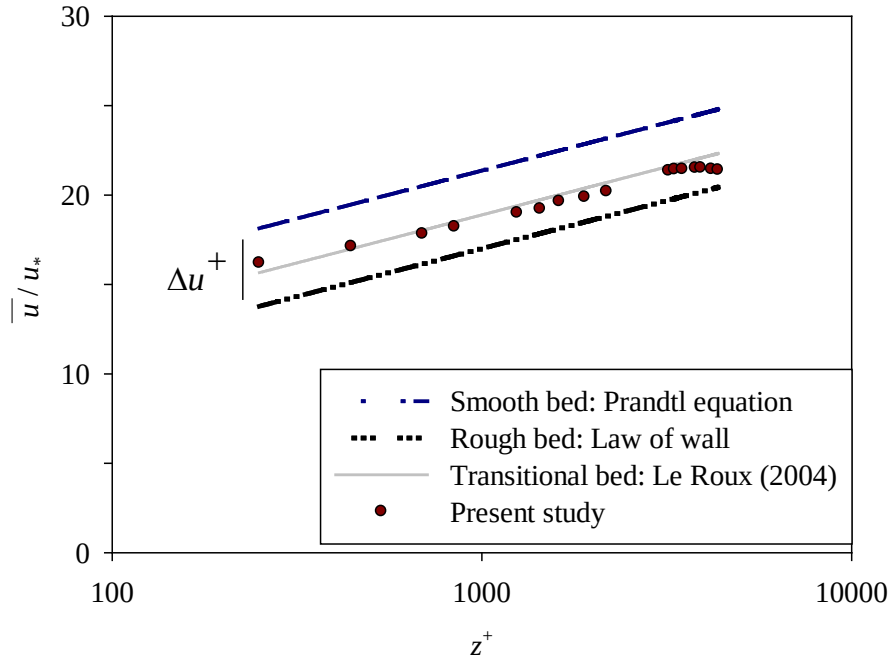

FIG. 4.1 Distribution of the Dimensionless Time Averaged Approach Flow Velocity

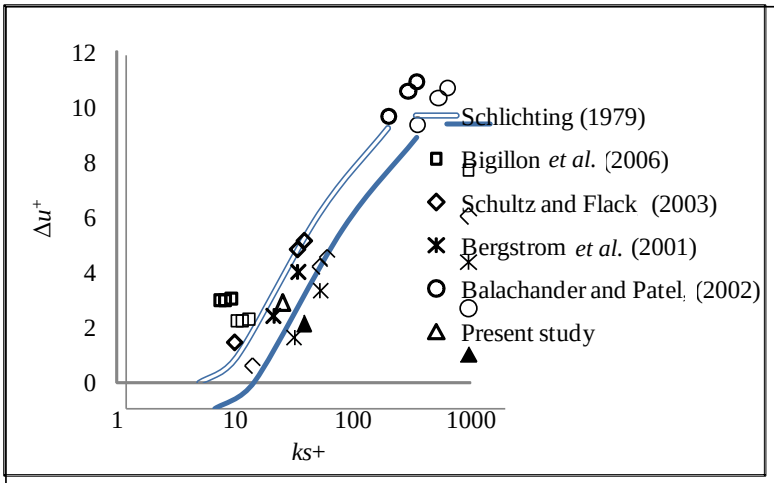

FIG. 4.2 Mean Velocity Shift ΔU^+ as a Function of the Roughness Reynolds Number k_s^+

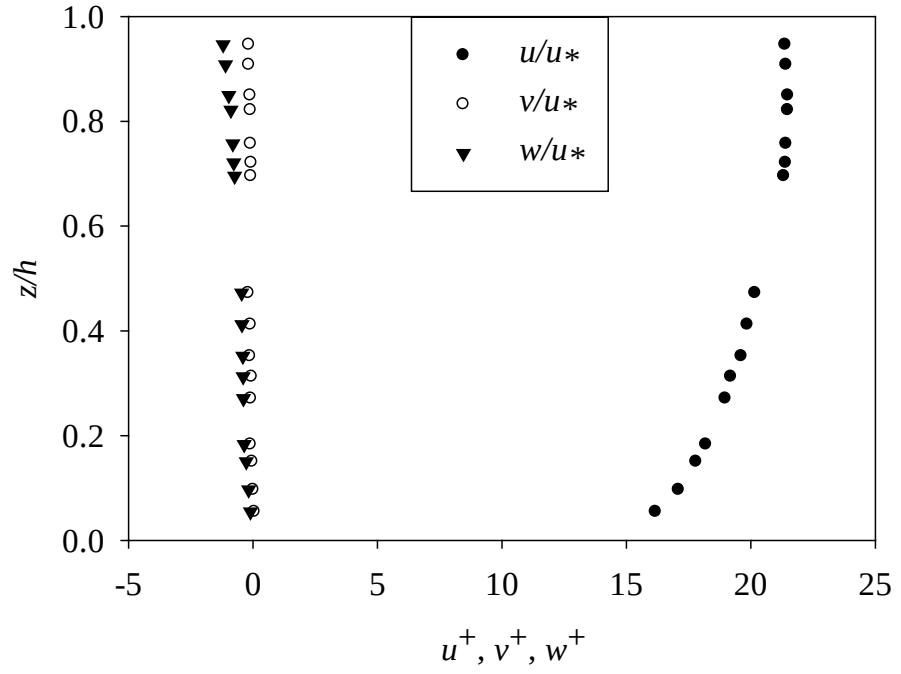

FIG. 4.3 Normalized Profiles of Mean Flow Velocities in Three Directions

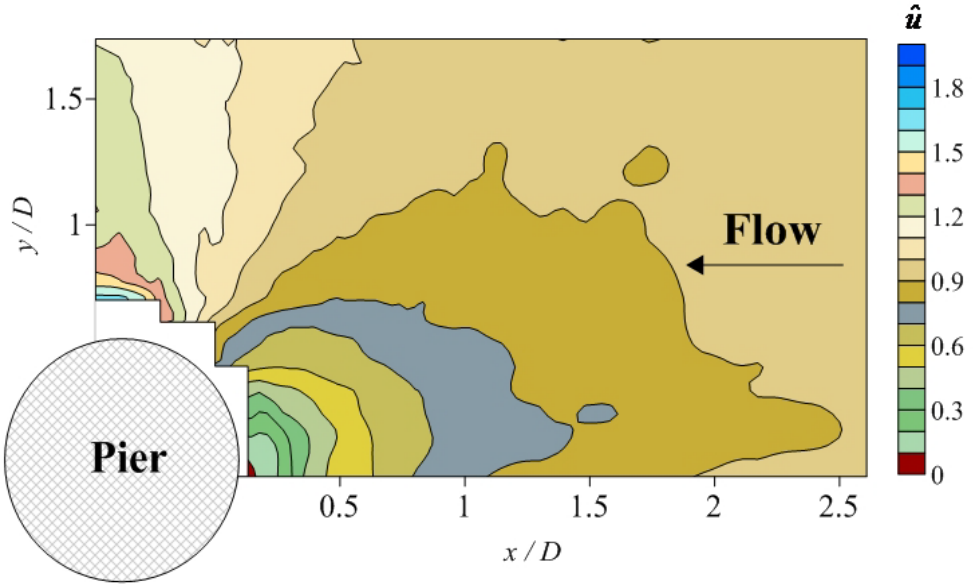

FIG. 4.4(a) Contours of Normalized Longitudinal Velocity, $\hat{u}$ in the Measurement Plane Nearest to the Flume Bed

(A)

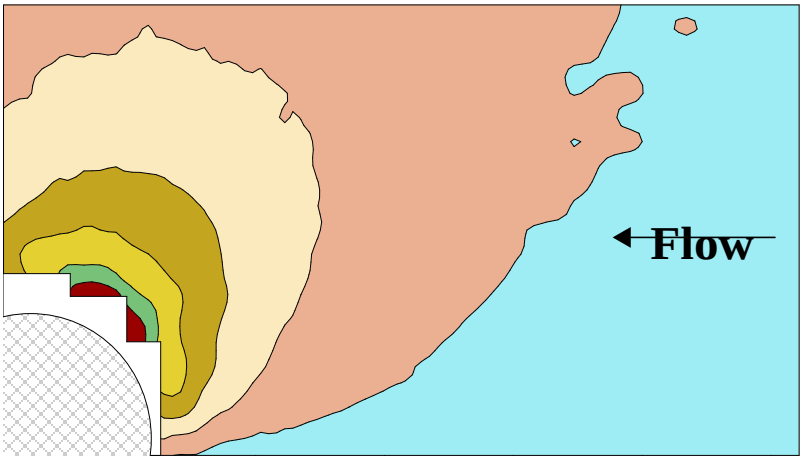

(B)

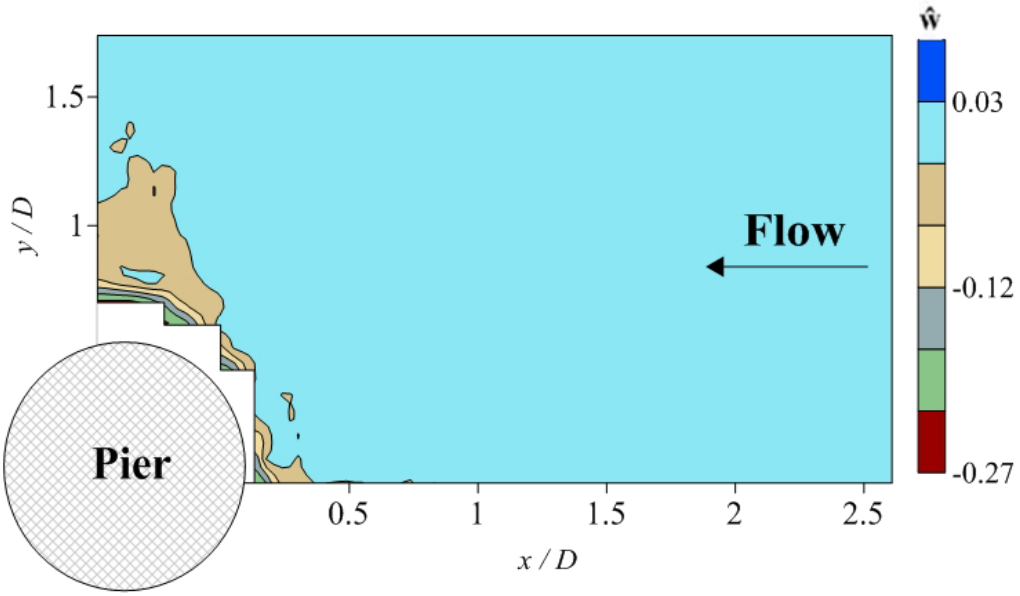

FIG. 4.4(b) Contours of Velocity Components in the Measurement Plane Nearest to the Flume Bed (A) Normalized Transverse Velocity, $\hat{v}$ (B) Normalized Vertical Velocity, $\hat{w}$

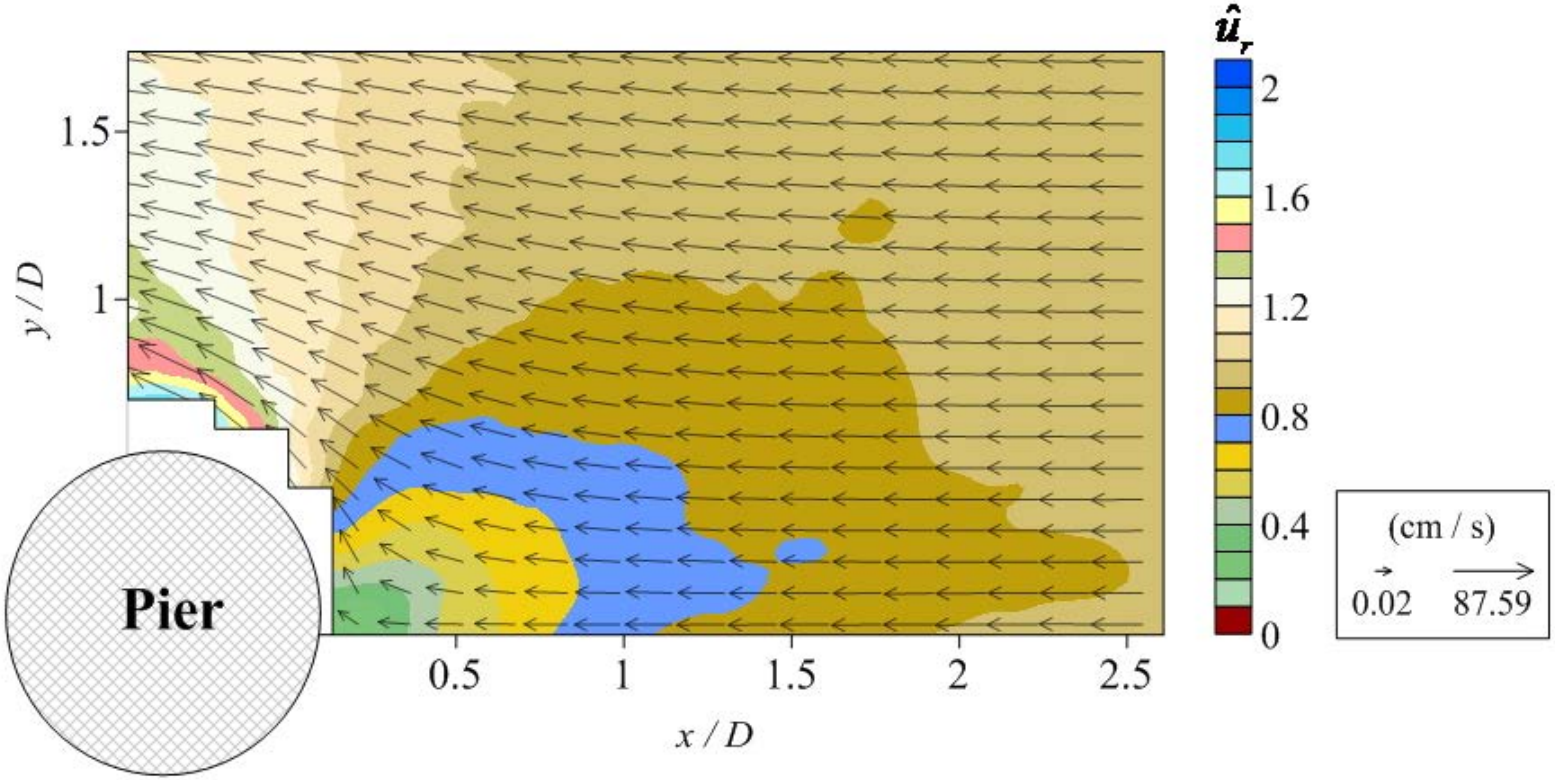

FIG. 4.5 Velocity Vectors Superimposed over the Contour Plot Illustrating the Distribution of the Normalized Resultant Velocity in the Horizontal Plane 3.5 mm above the Flume Bed

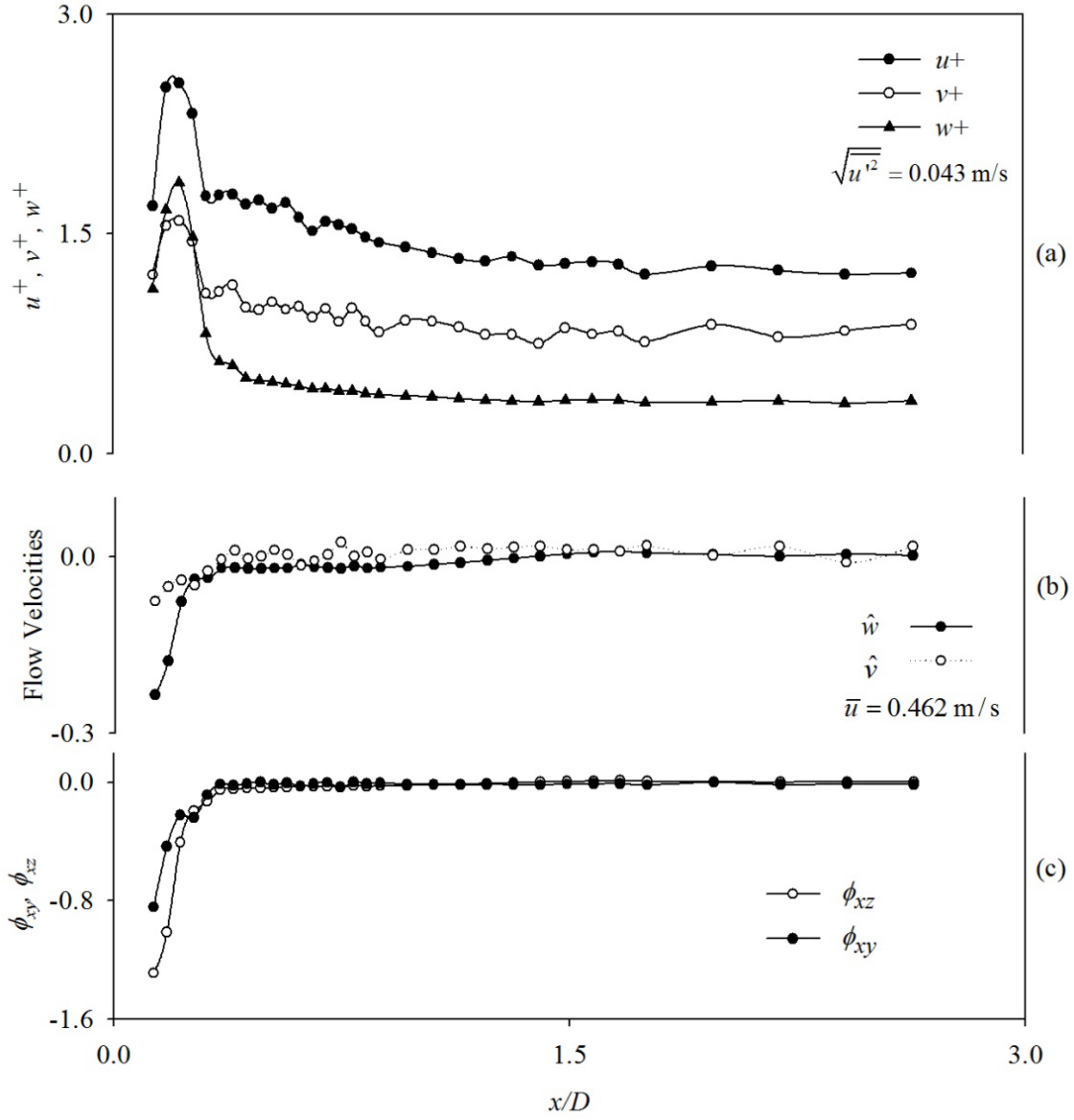

FIG.4.6 Variations along the Line of Symmetry (A-Line) with respect to *X/D* (A) Normalized Turbulence Intensities, U^+, V^+, W^+ (B) Normalized Lateral Velocity ($\hat{v}$) and Vertical Velocity ($\hat{w}$) (C) Directions of Both Stream-Wise and Vertical Velocity Vectors

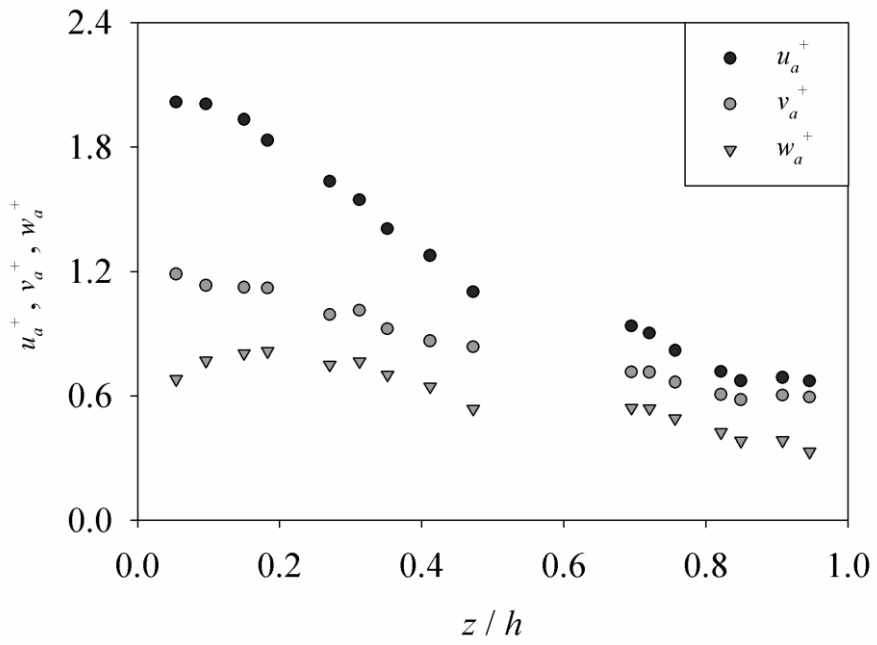

FIG. 4.7 Vertical Normalized Profiles of the Mean Turbulence Intensities Measured in the Streamwise, Transverse, and Vertical Directions (U_a^+, V_a^+, W_a^+) of the Approach Flow

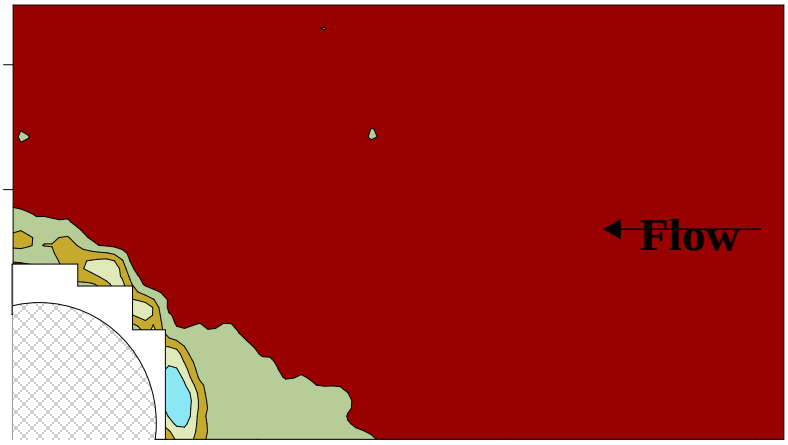

FIG.4.8(a) Contours of Normalized Longitudinal Turbulence Intensity, u^+, at First Measuring Horizontal Plane above Flume Bed

(A)

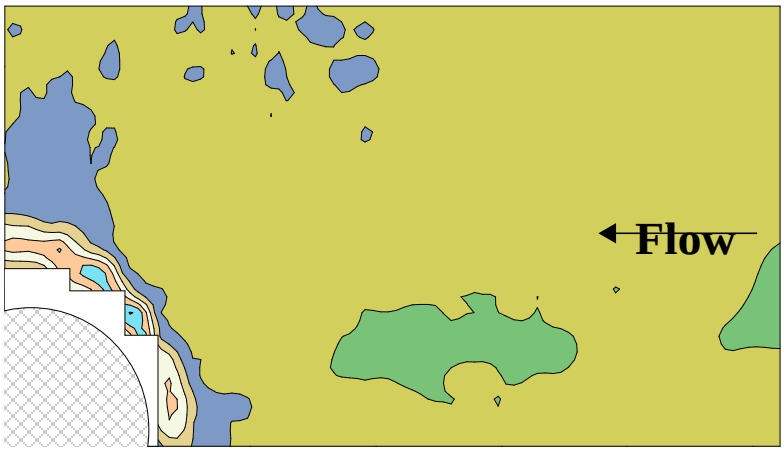

(B)

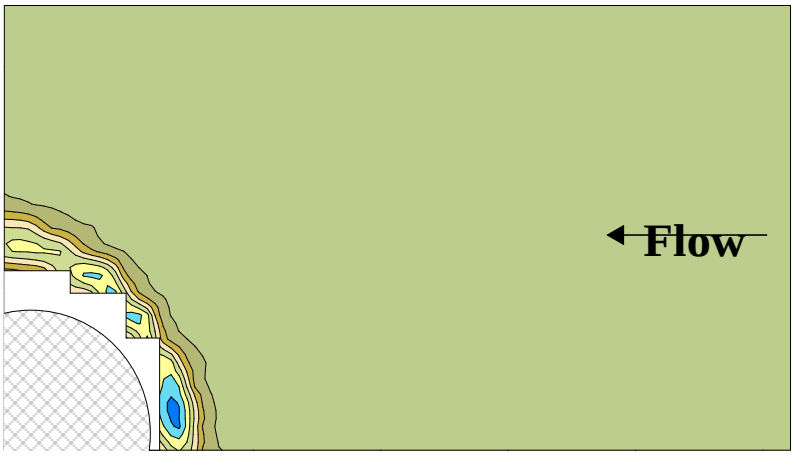

FIG.4.8(b) Contours of Normalized Turbulence Intensity Components at First Measuring Horizontal Plane above Flume Bed (A) Transverse Turbulence Intensity, V^+ (B) Vertical Turbulence Intensity, W^+

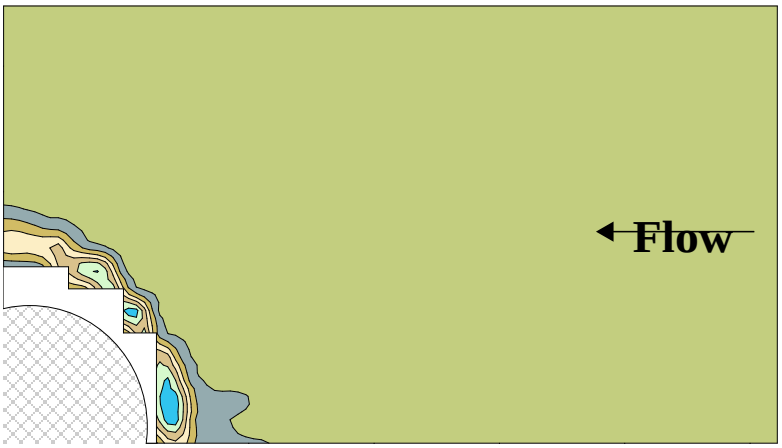

FIG.4.8(c) Contours of Normalized Turbulent Kinetic Energy, K^+, at First Measuring Horizontal Plane above Flume Bed

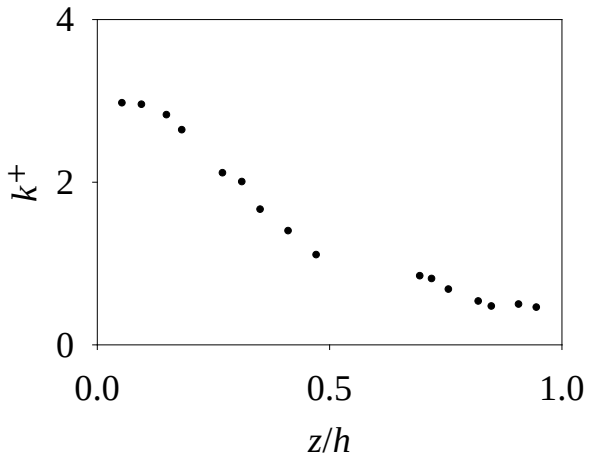

FIG. 4.9 Vertical Distribution of Turbulent Kinetic Energy in the Approach Flow

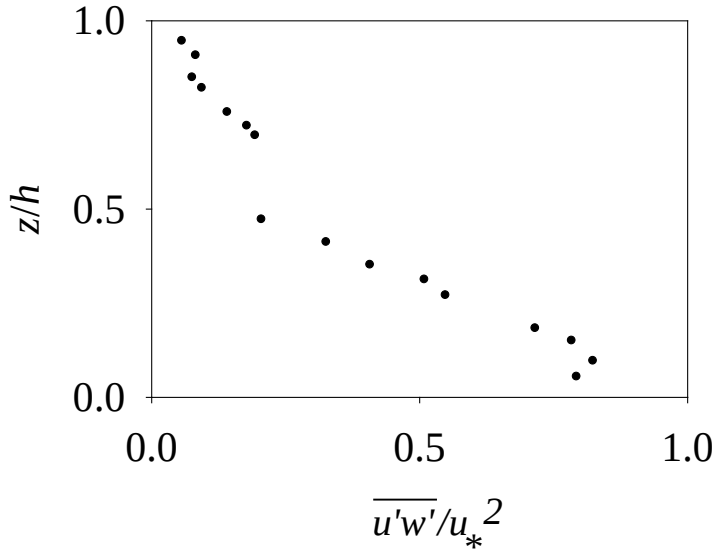

FIG. 4.10 Vertical Distribution of Reynolds Stresses in the Approach Flow

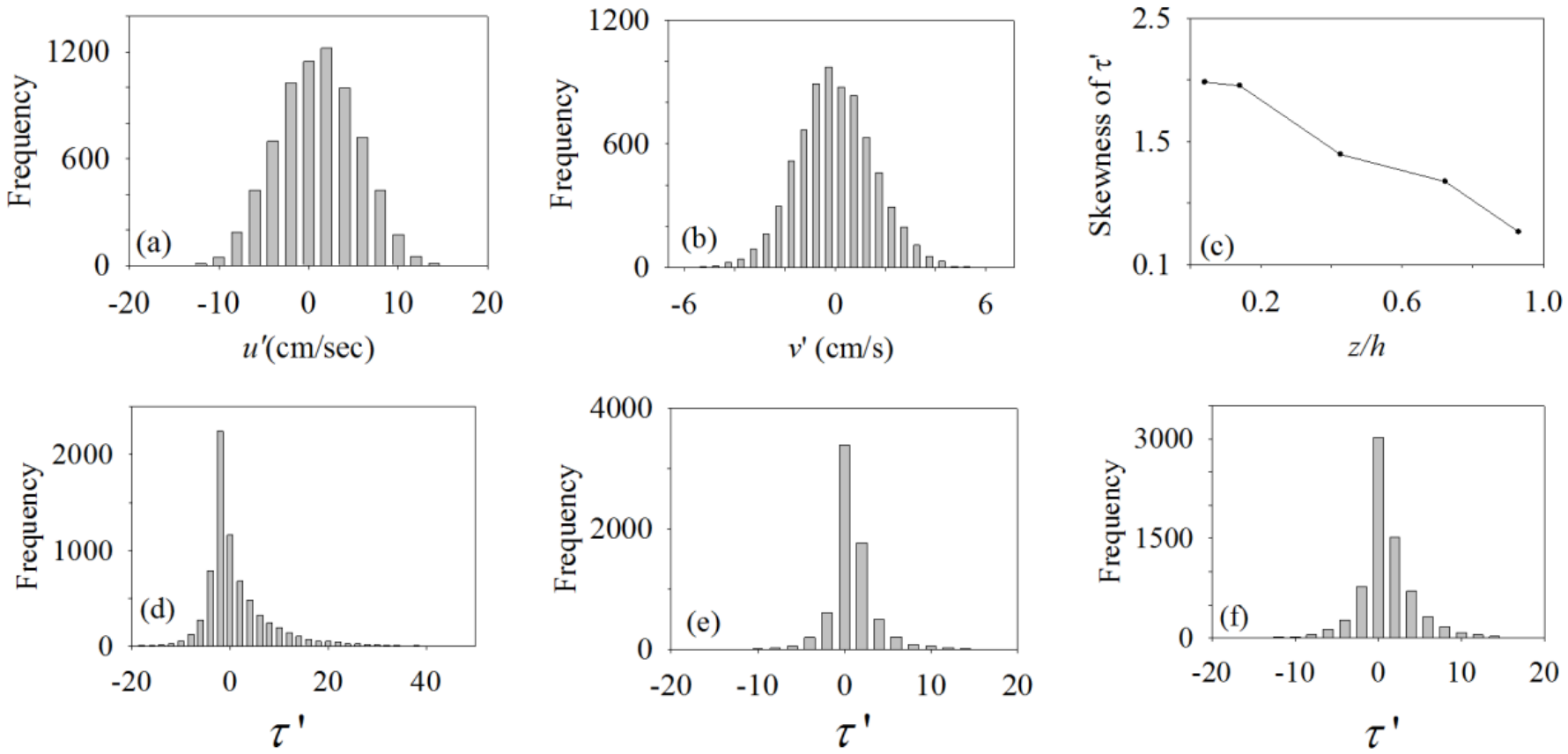

FIG. 4.11 (A) Fluctuations of Longitudinal Velocity (u') at $z / h = 0.02$, (B) Fluctuations of Vertical Velocity (v') at $z / h = 0.02$ (C) Skewness of Turbulent Momentum Flux across Flow Depth (D)Fluctuations of Turbulent Momentum Flux at $z / h = 0.02$, (E) at $z / h = 0.425$ and (F) at $z / h = 0.93$

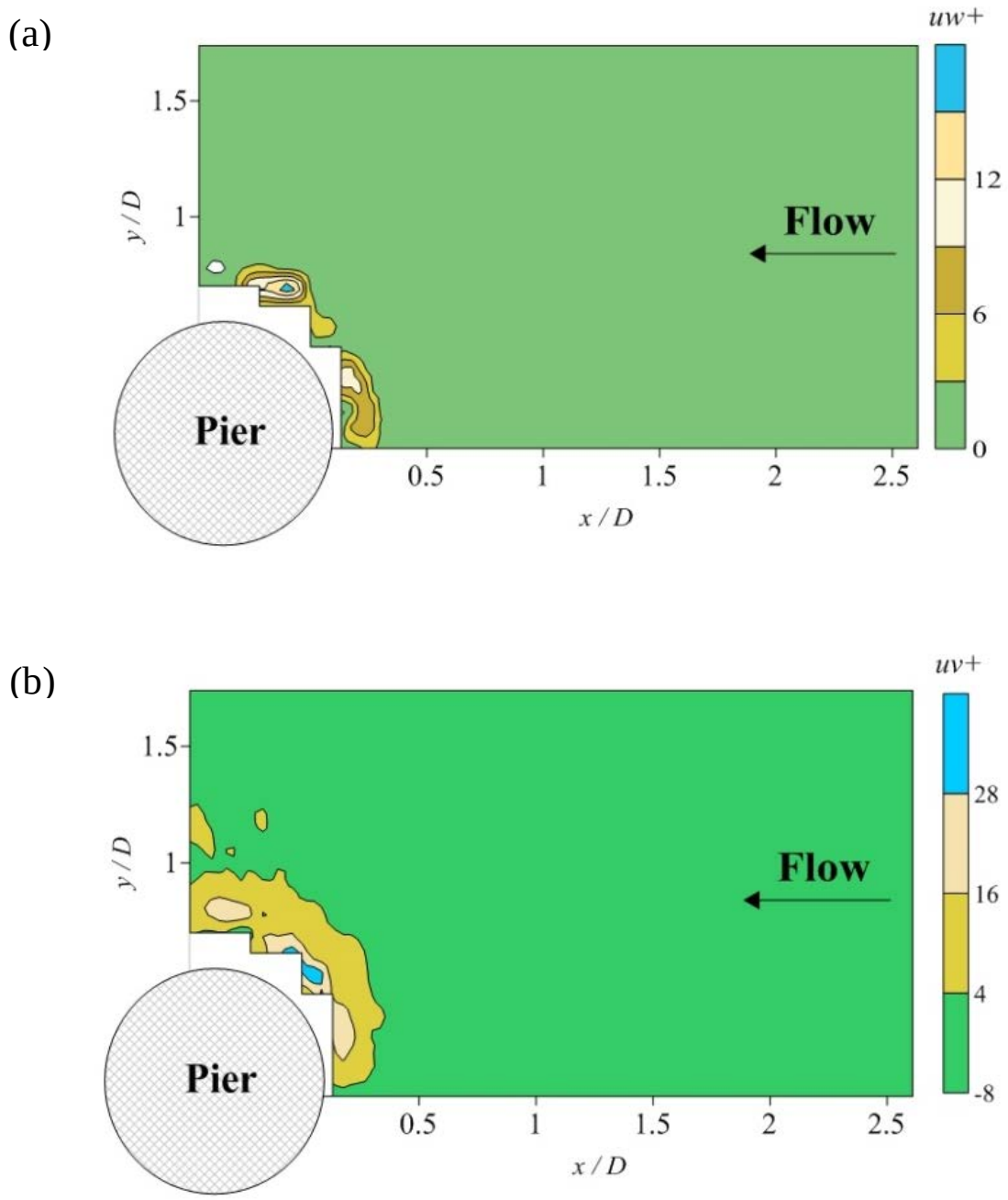

FIG. 4.12 Normalized Reynolds Stresses at First Measuring Horizontal Plane above Flume Bed (A) uw^+ (B) uv^+

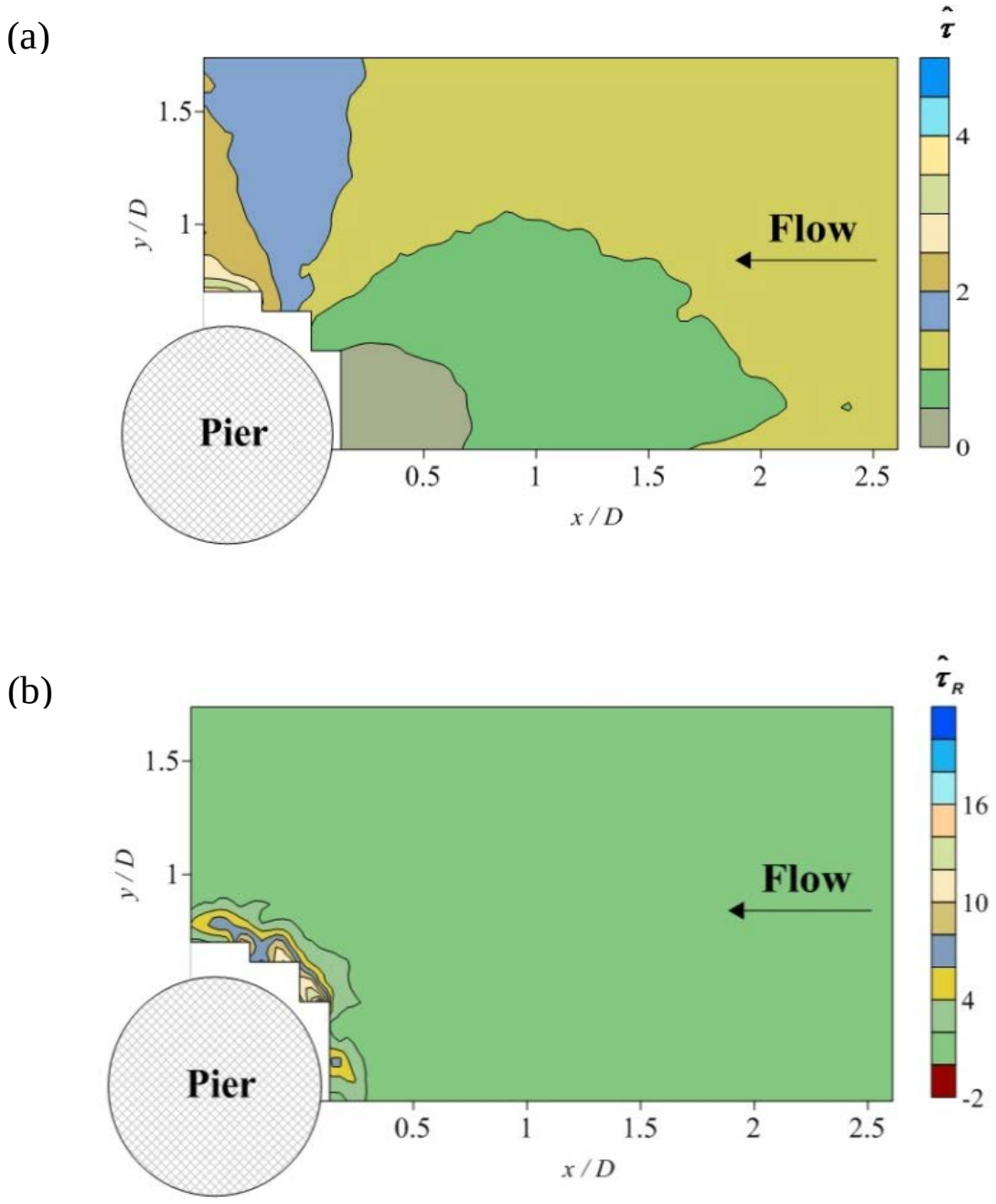

FIG.4.13 Normalized Bed Shear Stress around Upstream of a Circular Pier over a Transitionally Rough Bed (A) Estimated using Stream-Wise Flow Velocity Component (B) Estimated using Reynolds Stresses

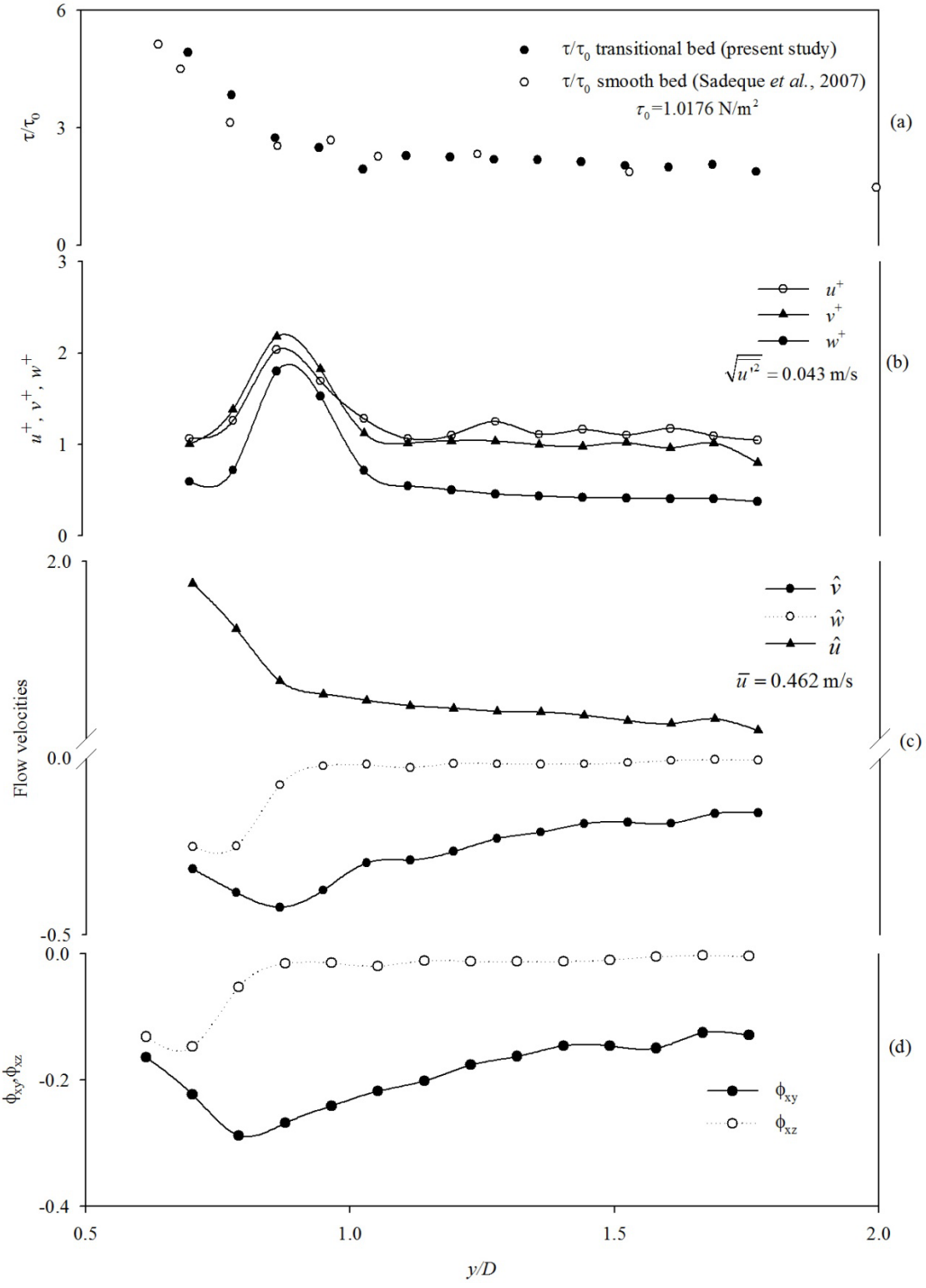

FIG.4.14 Variations at the Line Perpendicular to the Symmetry Line in the Side of the Pier with respect to *Y/D* (B-Line) (A) Normalized Bed Shear Stress (B) Normalized Turbulence Intensities, U^+, V^+, W^+(C) Normalized Lateral Velocity ($\hat{v}$) and Vertical Velocity ($\hat{w}$) (D) Directions of Both Stream-Wise and Vertical Velocity Vectors

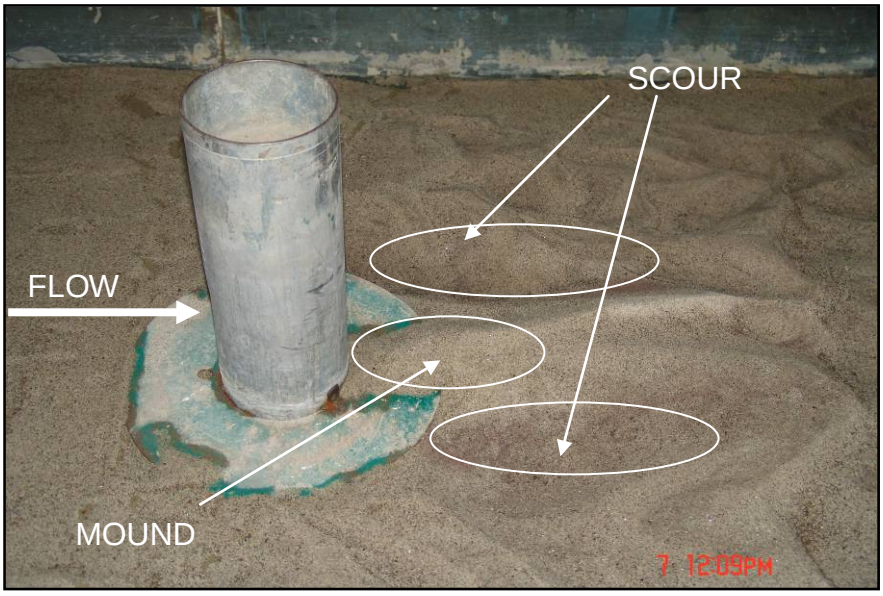

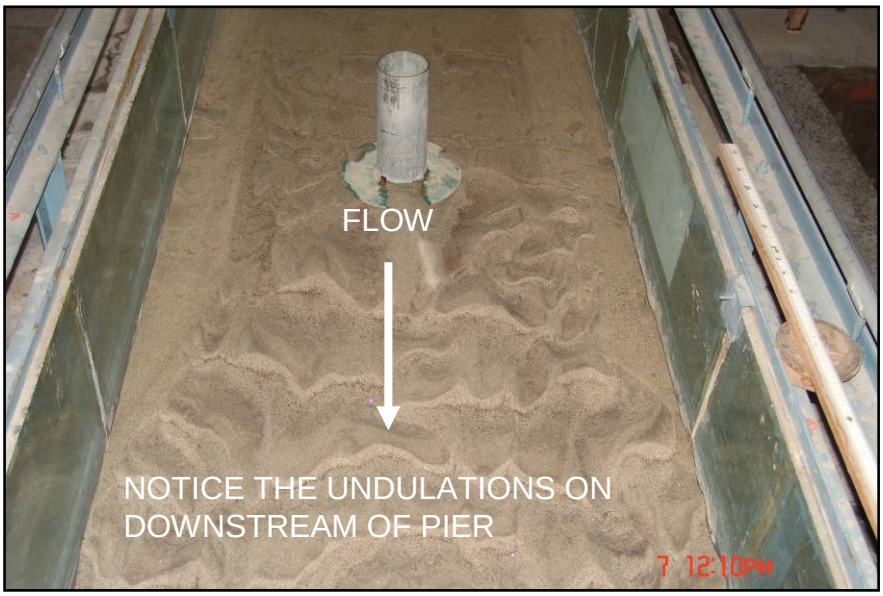

FIG.4.15 Photographic View Showing Geometrical Configuration of Scour Hole for Clear-Water Condition for a Depth of 10.0 cm and $u_*/u_{*c} = 0.89$

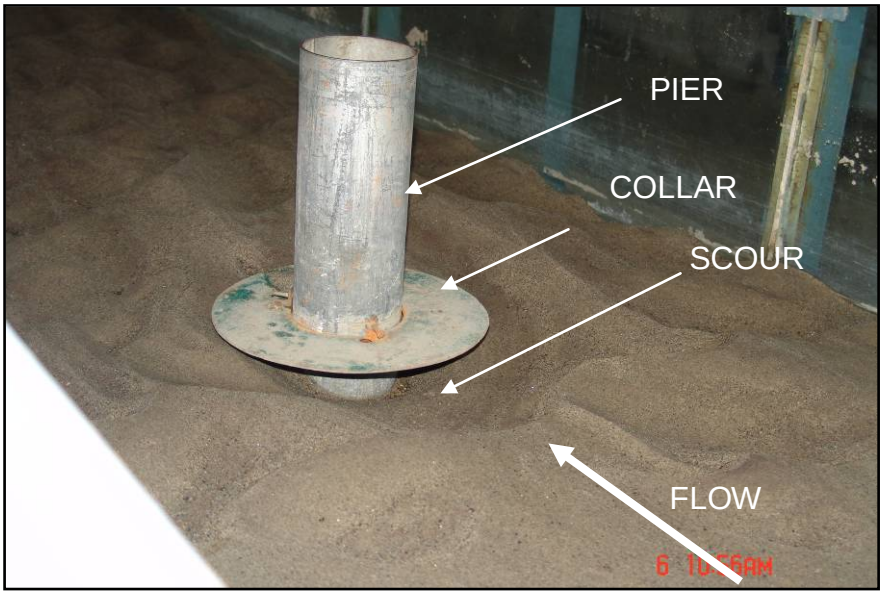

FIG.4.16 Photographic View Showing Geometrical Configuration of Scour Hole for Live-Bed Degradation with Collar Condition for a Depth of 6.5 cm and u_*/u_{*c}=1.87

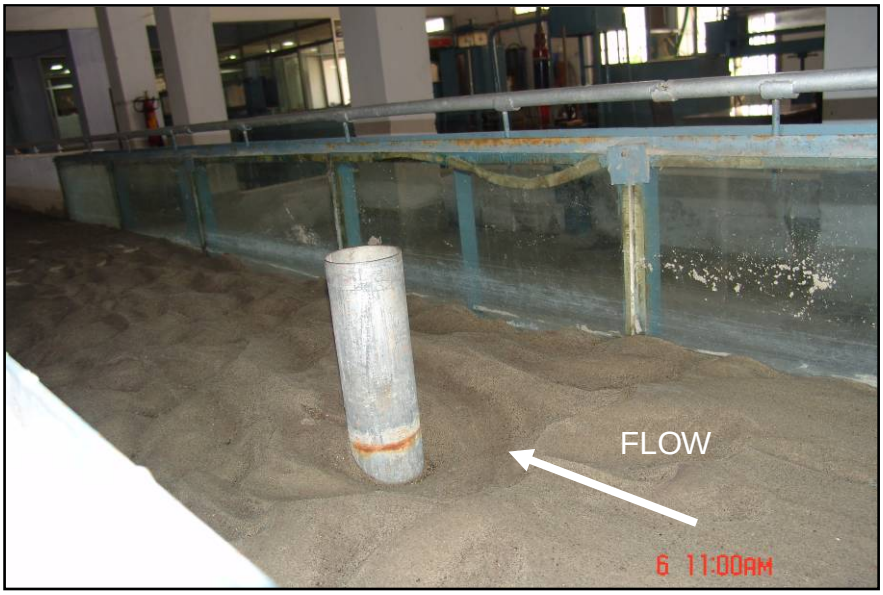

FIG.4.17 Photographic View Showing Geometrical Configuration of Scour Hole without Collar for Live-Bed Degradation Condition for a Depth of 6.5 cm and u_*/u_{*c}=1.87

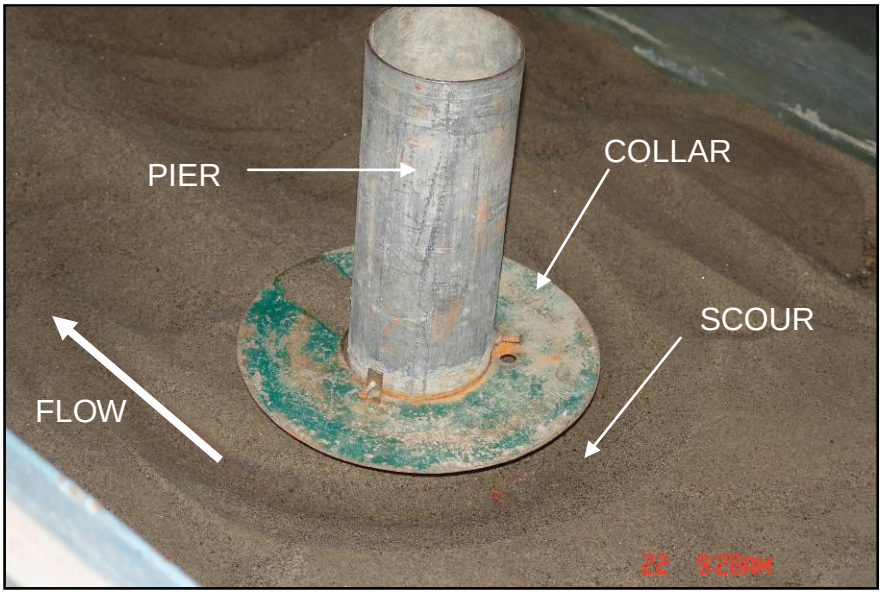

FIG.4.18 Photographic View Showing Geometrical Configuration of Scour Hole for Live-Bed Condition with Sediemnt Feed for a Depth Of 9.0 cm and u_*/u_{*c}=1.49

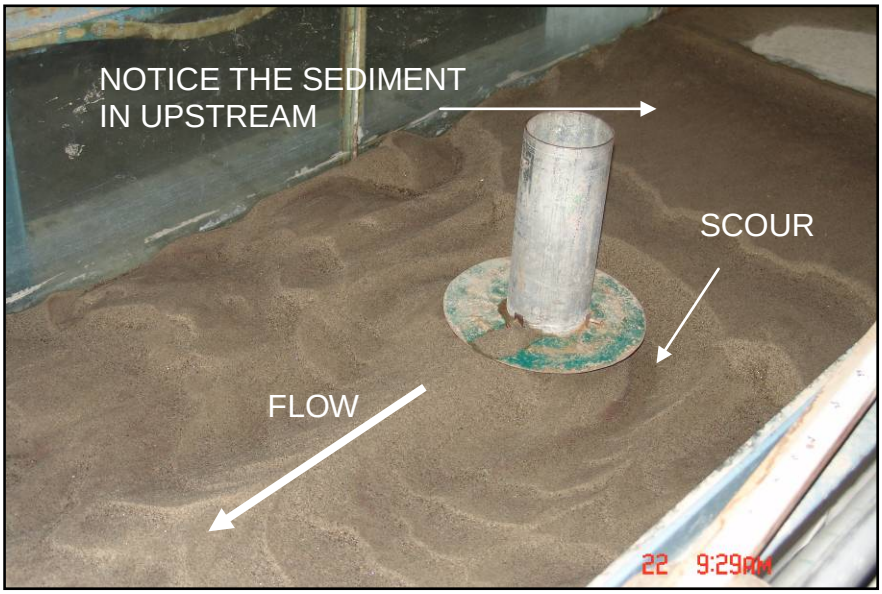

FIG.4.19 Photographic View Showing Geometrical Configuration of Scour Hole for Live-Bed Condition with Sediment Feed for a Depth of 9.0 cm and u_*/u_{*c}=1.49

FIG.4.20 Photographic View Showing Geometrical Configuration of Scour Hole without Collar for Live-Bed Condition with Sediment Feed for a Depth of 9.0 cm and u_*/u_{*c}=1.49

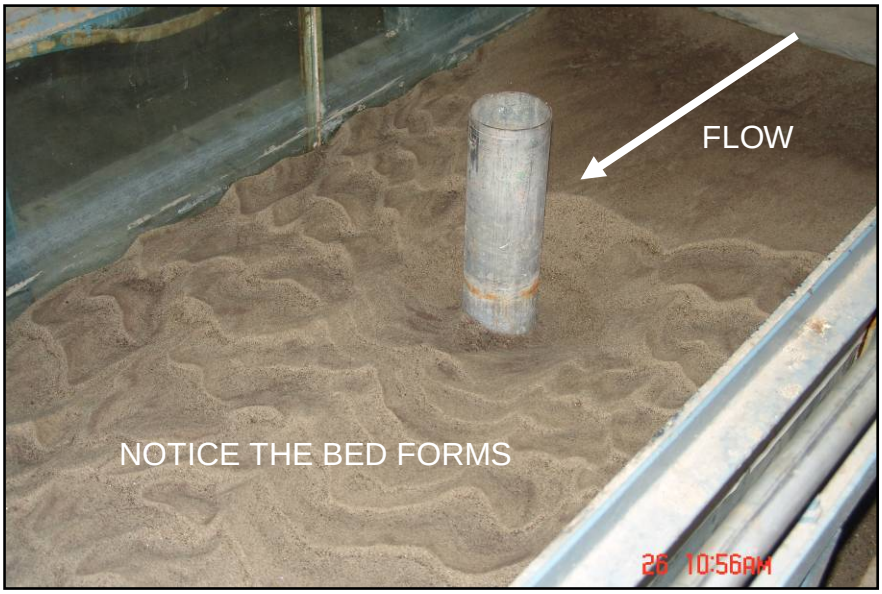

FIG.4.21 Photographic View Showing Geometrical Configuration of Scour Hole without Collar for Live-Bed Condition with Sediment Feed for a Depth of 7.0 cm and u_*/u_{*c}=1.335

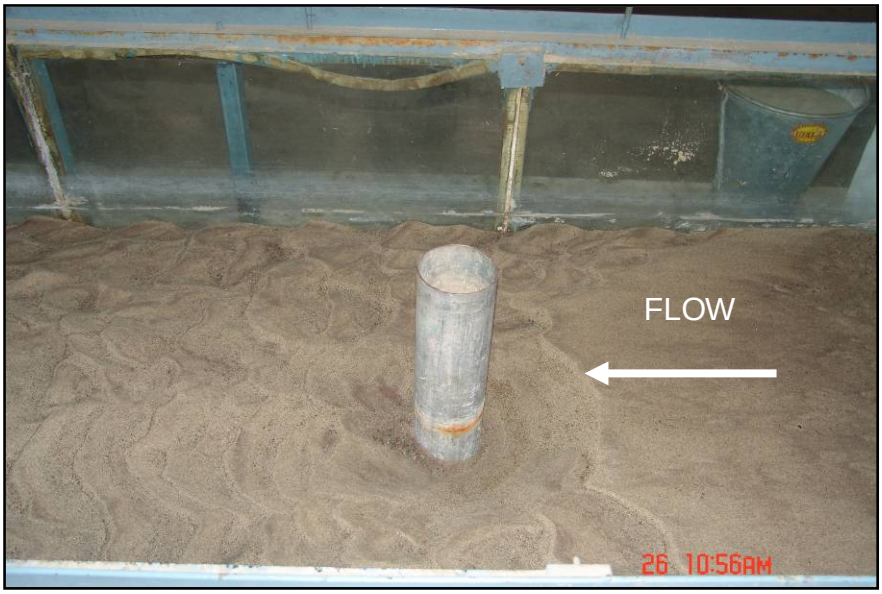

FIG.4.22 Photographic View Showing Geometrical Configuration of Scour Hole for Live-Bed Condition for a Depth of 7.0 cm and u_*/u_{*c}=1.335

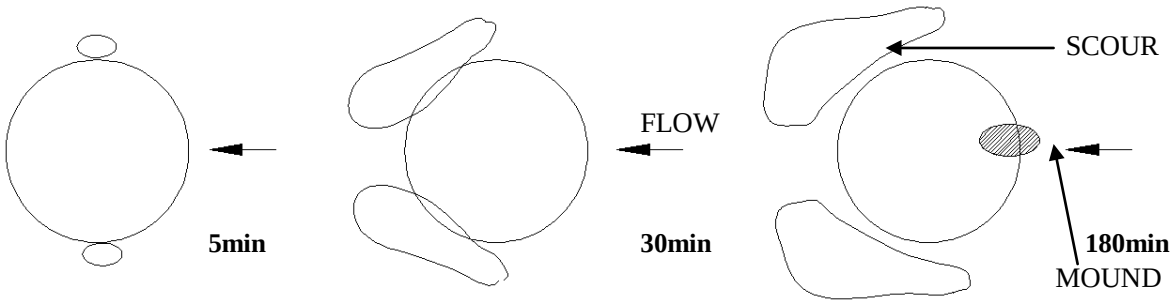

FIG.4.23 Schematic Illustration of the Scour Development for a Circular Pier under Clear-Water Condition in the Present Study

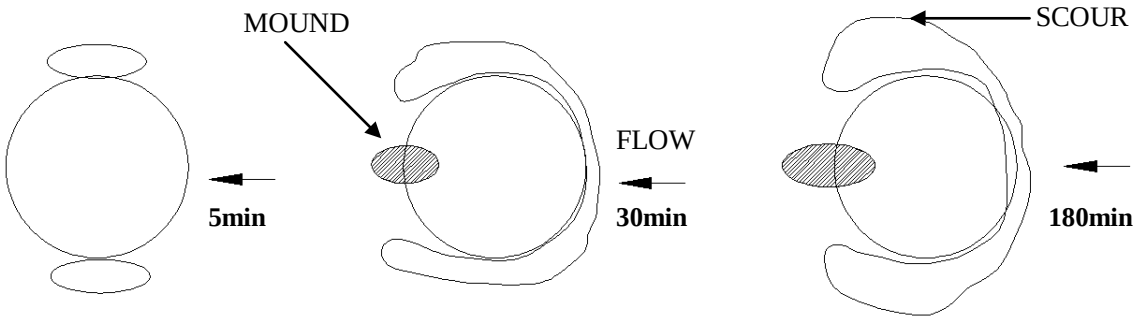

FIG.4.24 Schematic Illustration of the Scour Development for a Circular Pier under Live-Bed Degradation Condition in the Present Study

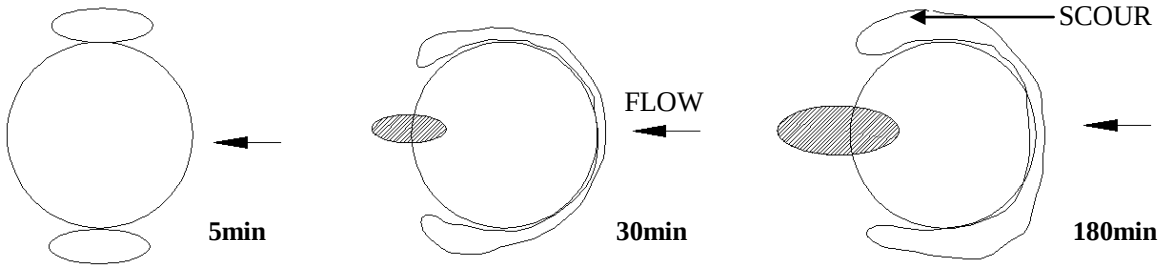

FIG.4.25 Schematic Illustration of the Scour Development for a Circular Pier under Live-Bed Condition in the Present Study

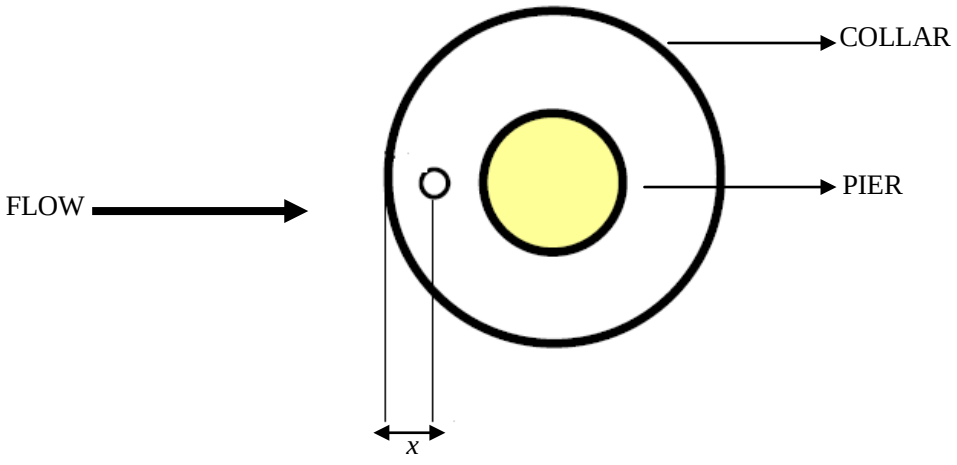

FIG.4.26 Location of Point of Maximum Scour Depth beneath the Collar in the Present Study

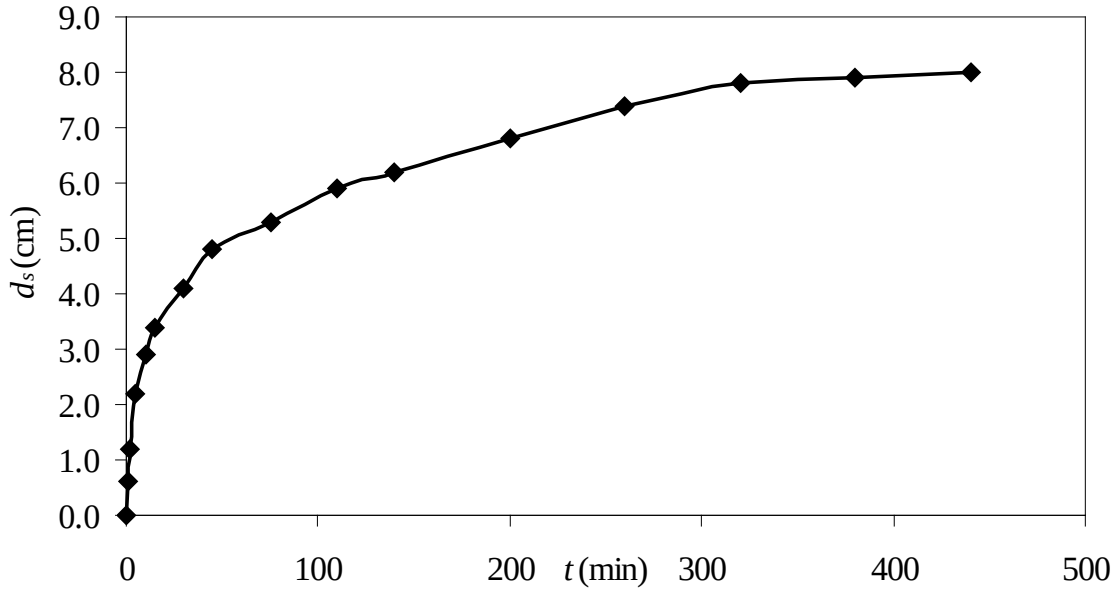

FIG.4.27 Temporal Variation of Maximum Scour Depth for a Depth of 10.5cm and u_*/u_{*c}=0.87 (Clear-Water Condition, Run No.1)

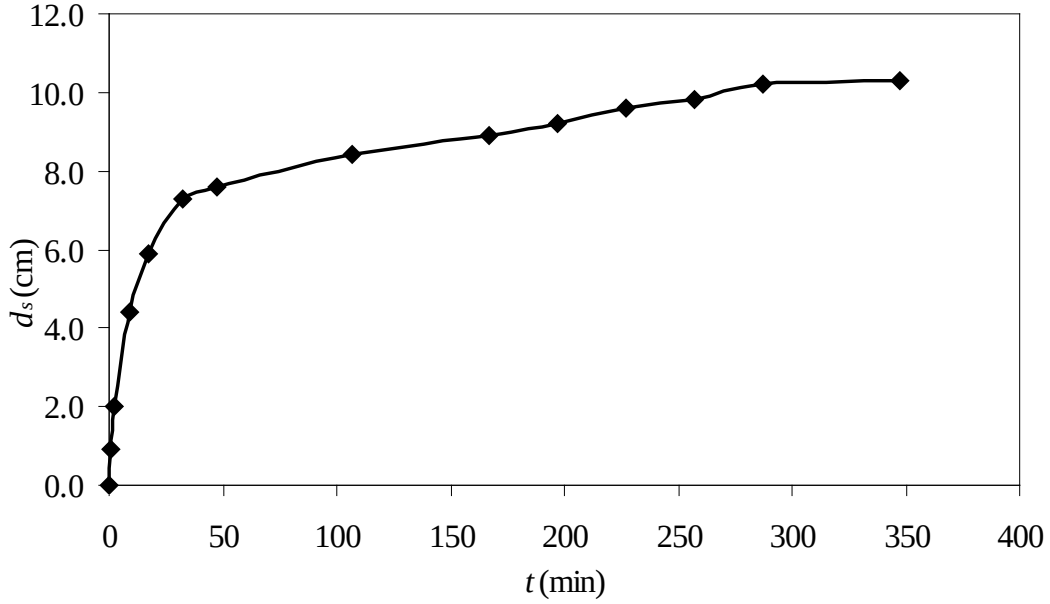

FIG.4.28 Temporal Variation of Maximum Scour Depth for a Depth of 10.0cm and u_*/u_{*c}=0.89 (Clear-Water Condition, Run No.2)

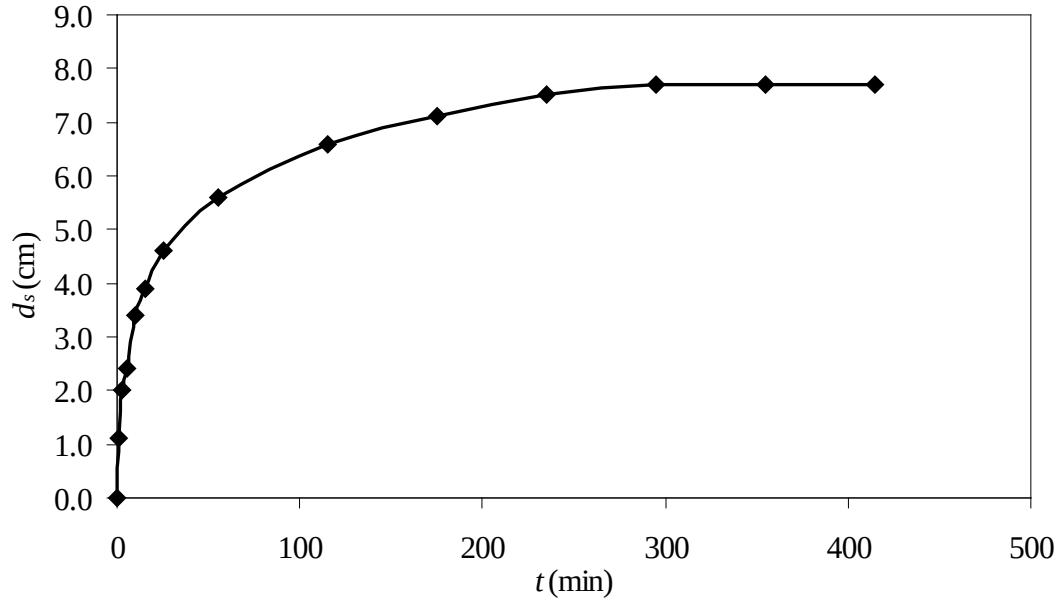

FIG.4.29 Temporal Variation of Maximum Scour Depth for a Depth of 5.0cm and u_*/u_{*c}=1.089 (Live-Bed Degradation Condition, Run No.3)

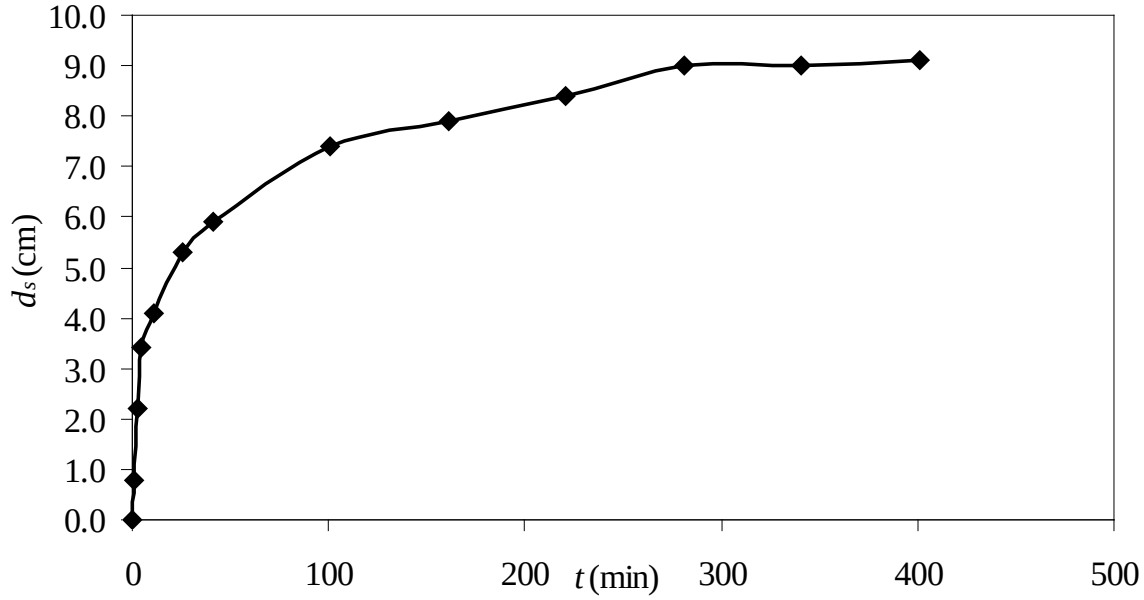

FIG.4.30 Temporal Variation of Maximum Scour Depth for a Depth of 7.0cm and u_*/u_{*c}=1.1 (Live-Bed Degradation Condition, Run No.4)

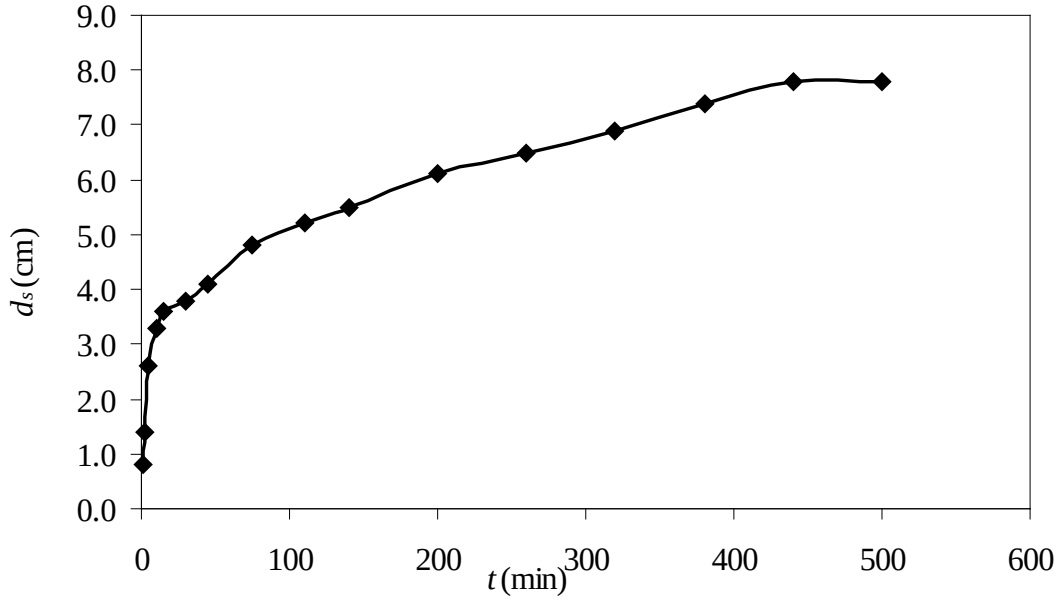

FIG.4.31 Temporal Variation of Maximum Scour Depth for a Depth of 8.0cm and u_*/u_{*c}=1.266 (Live-Bed Degradation Condition, Run No.5)

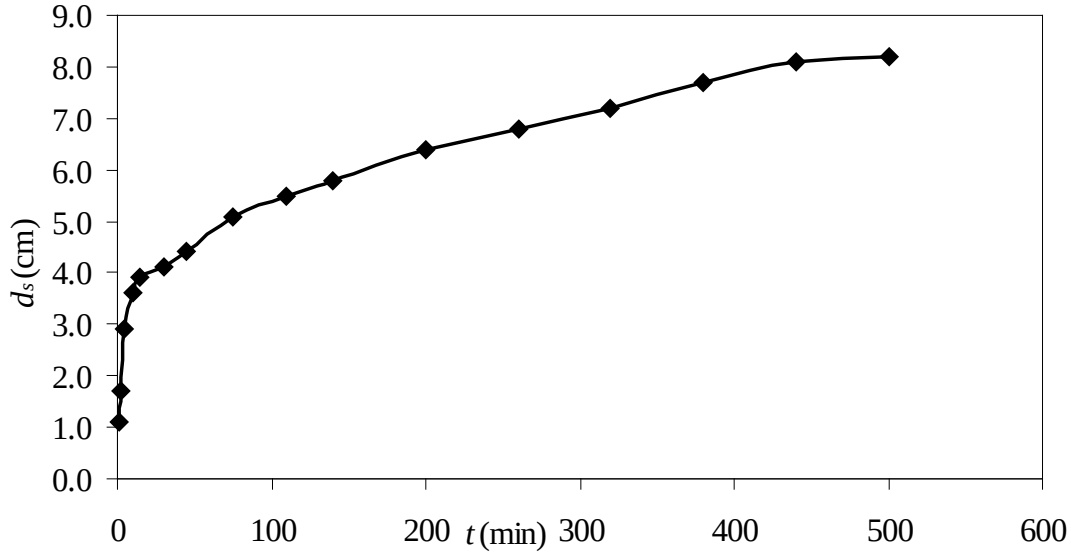

FIG.4.32 Temporal Variation of Maximum Scour Depth for a Depth of 7.0cm and u_*/u_{*c}=1.335 (Live-Bed Degradation Condition, Run No.6)

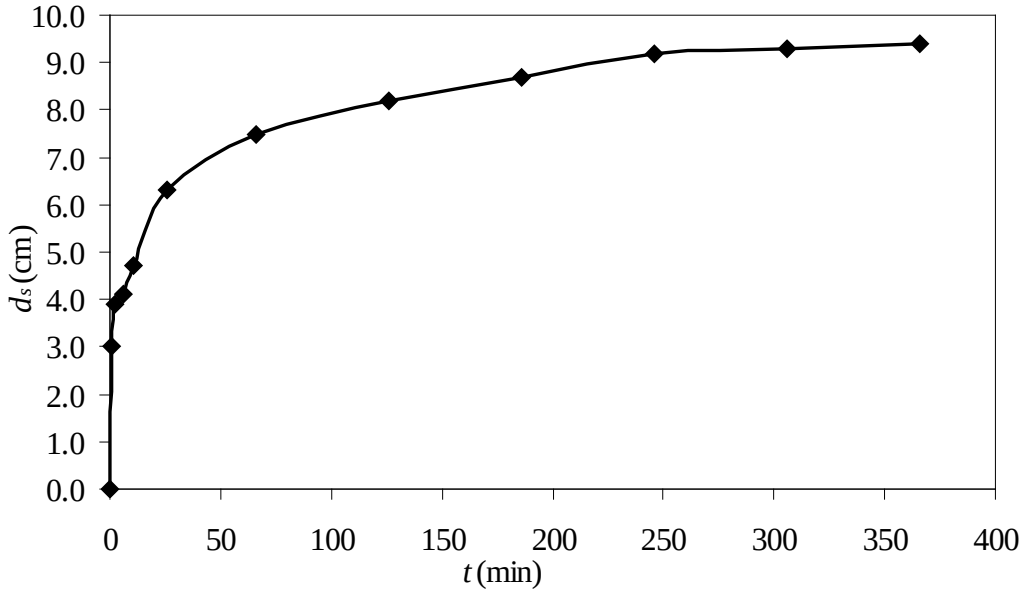

FIG.4.33 Temporal Variation of Maximum Scour Depth for a Depth of 6.0cm and U_*/U_{*C} =1.42 (Live-Bed Degradation Condition, Run No.7)

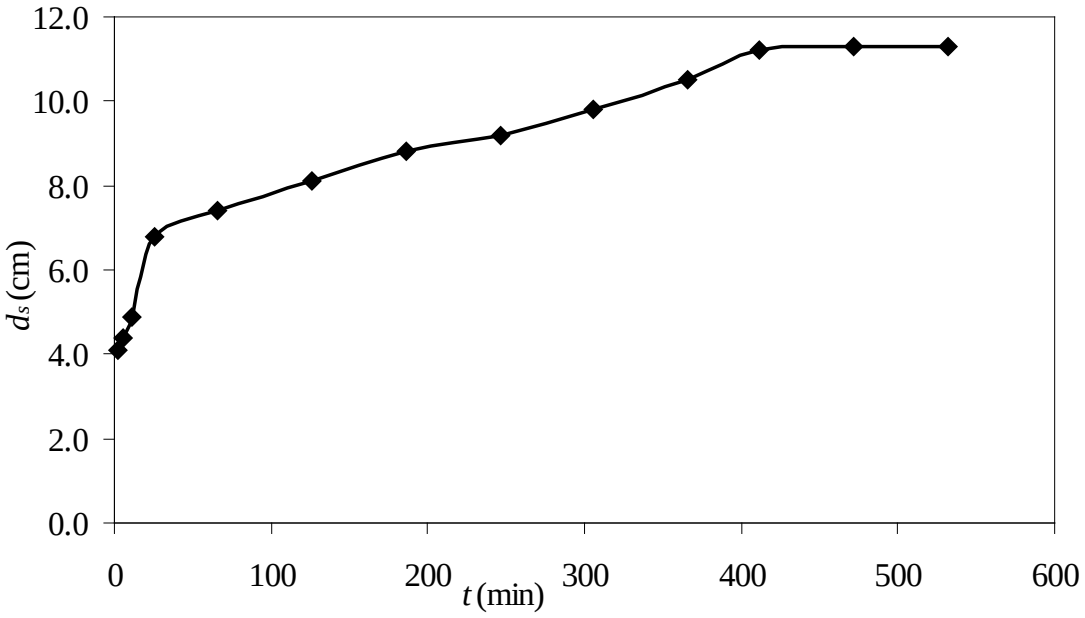

FIG.4.34 Temporal Variation of Maximum Scour Depth for a Depth of 9.0cm and u_*/u_{*c} =1.488 (Live-Bed Degradation Condition, Run No.8)

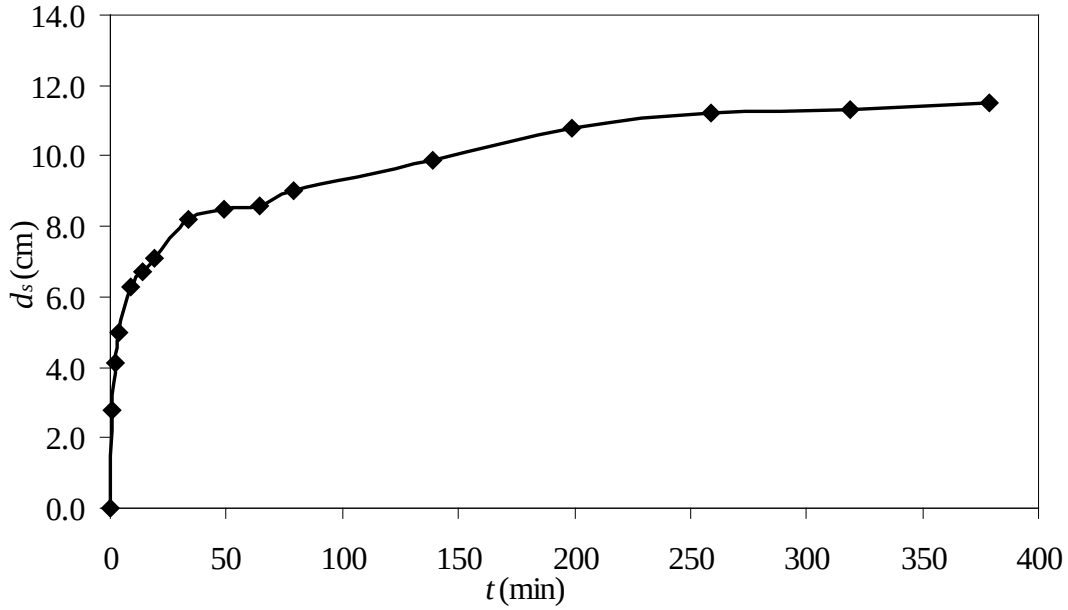

FIG.4.35 Temporal Variation of Maximum Scour Depth for a Depth of 6.5cm and u_*/u_{*c}=1.88 (Live-Bed Degradation Condition, Run No.9)

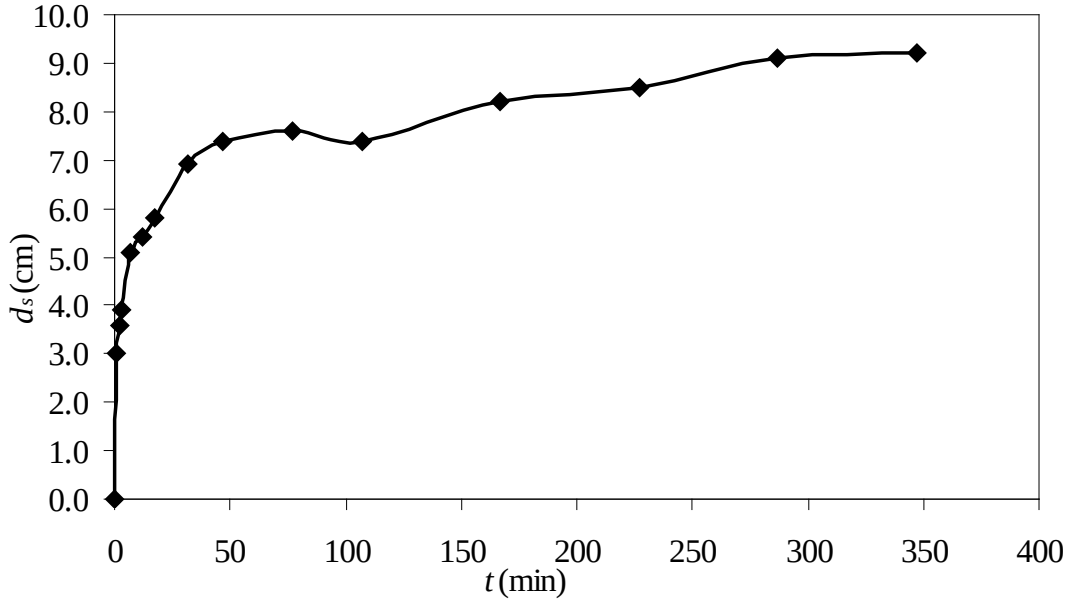

FIG.4.36 Temporal Variation of Maximum Scour Depth for a Depth of 6.0cm and u_*/u_{*c}=2.05 (Live-Bed Degradation Condition, Run No.10)

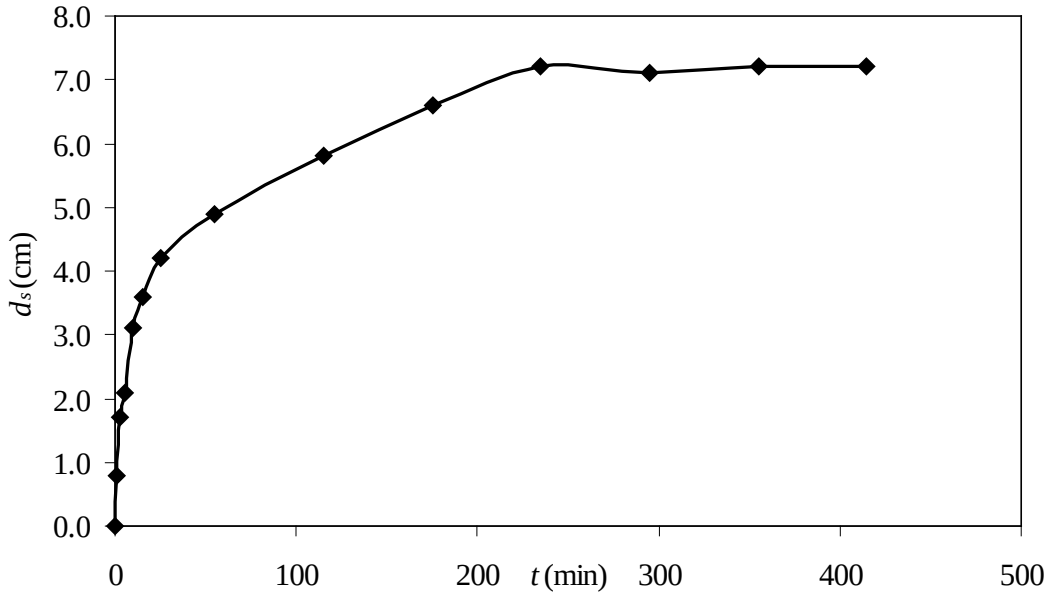

FIG.4.37 Temporal Variation of Maximum Scour Depth for a Depth of 5.0cm and u_*/u_{*c}=1.089 (Live-Bed Condition Run No.11)

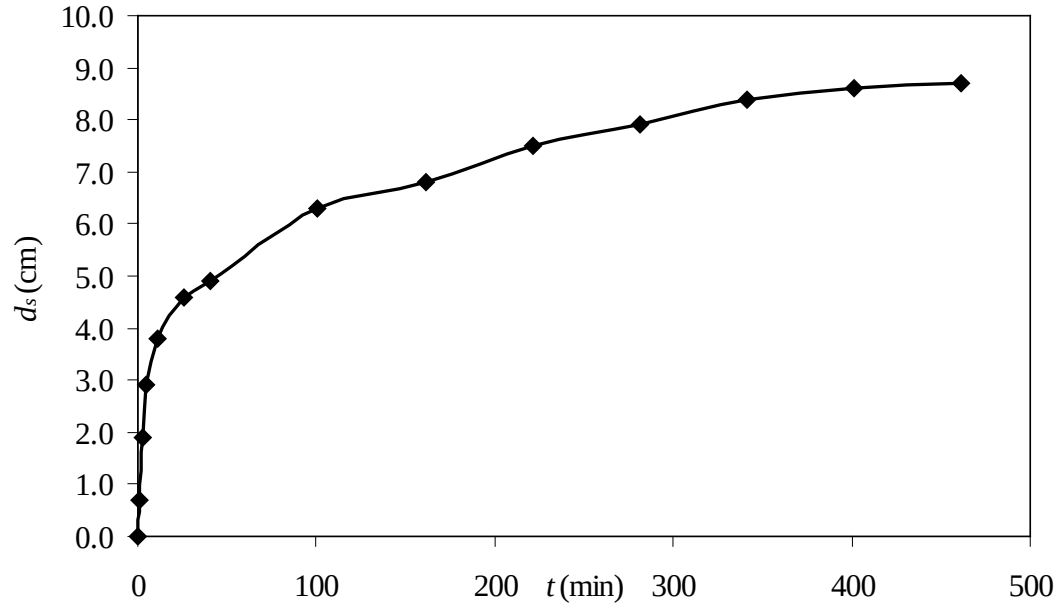

FIG.4.38 Temporal Variation of Maximum Scour Depth for a Depth of 7.0cm and u_*/u_{*c}=1.1 (Live-Bed Condition, Run No.12)

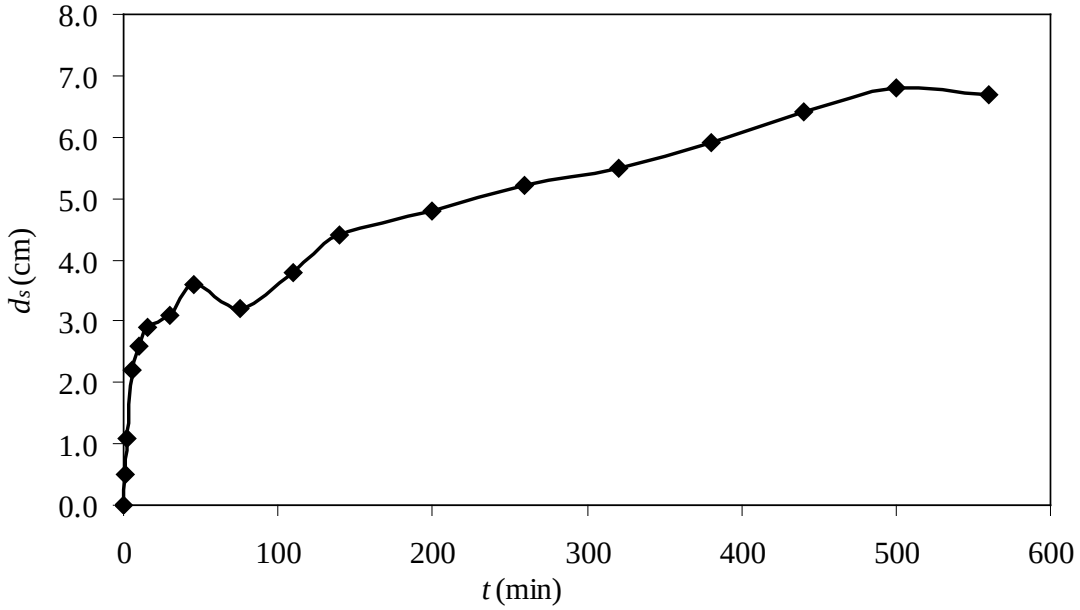

FIG.4.39 Temporal Variation of Maximum Scour Depth for a Depth of 8.0cm and u_*/u_{*c}=1.266 (Live-Bed Condition, Run No.13)

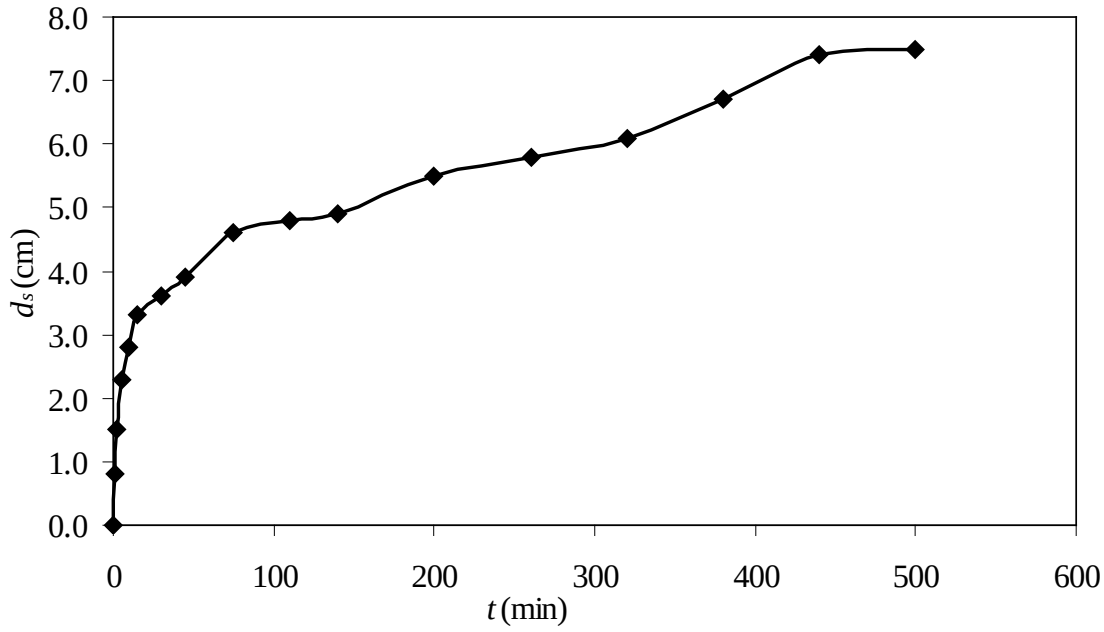

FIG.4.40 Temporal Variation of Maximum Scour Depth for a Depth of 7.0cm and u_*/u_{*c}=1.335 (Live-Bed Condition, Run No.14)

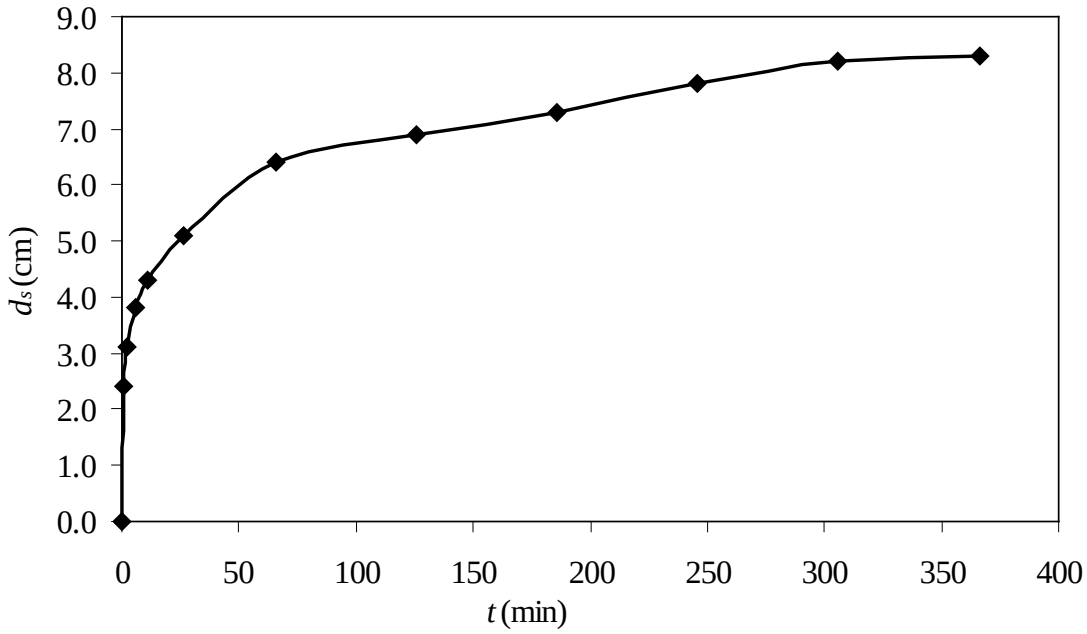

FIG.4.41 Temporal Variation of Maximum Scour Depth for a Depth of 6.0cm and U_*/U_{*C}=1.42 (Live-Bed Condition, Run No.15)

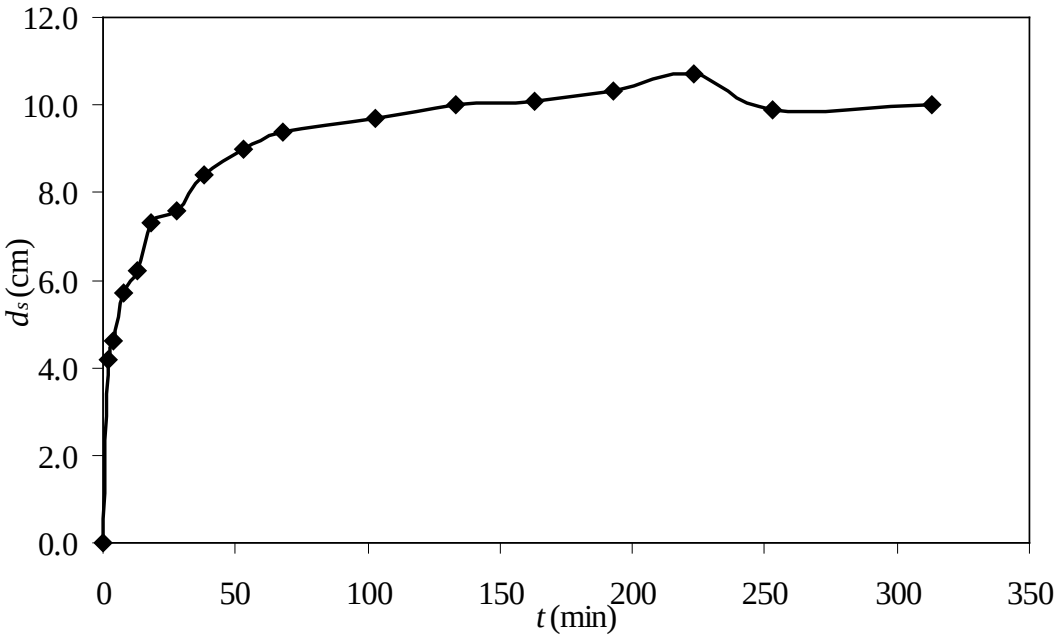

FIG.4.42 Temporal Variation of Maximum Scour Depth for a Depth of 9.0cm and u_*/u_{*c}=1.488 (live-bed condition, run no.16)

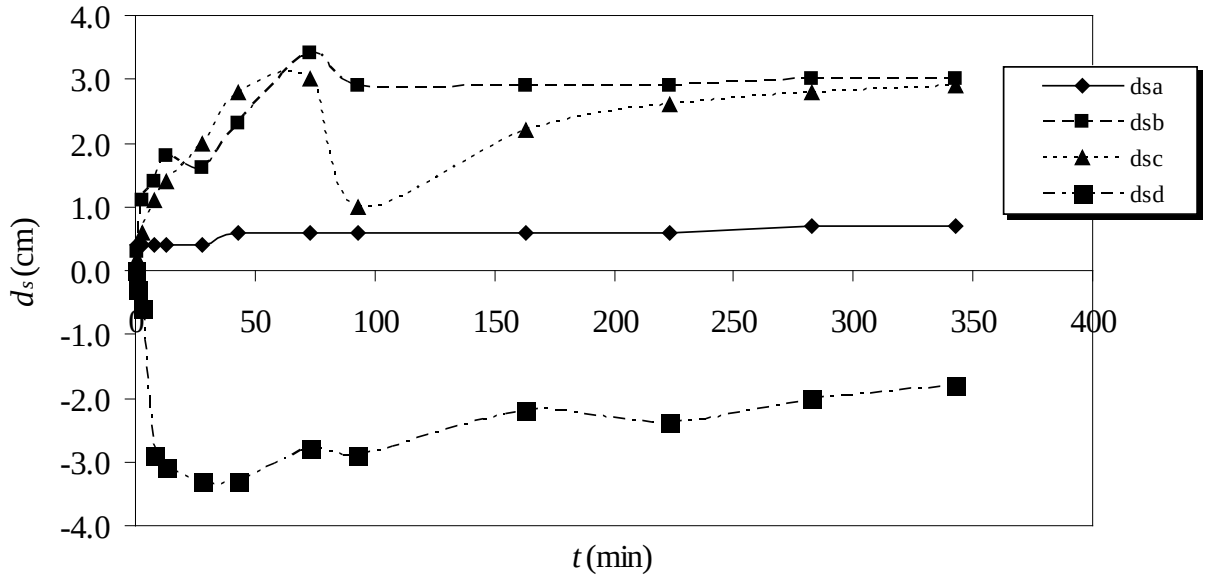

FIG.4.43 Temporal Variation of Scour Depth for a Depth of 10.5cm and u_*/u_{*c}=0.87 (Clear-Water Condition with Collar, Run No.17)

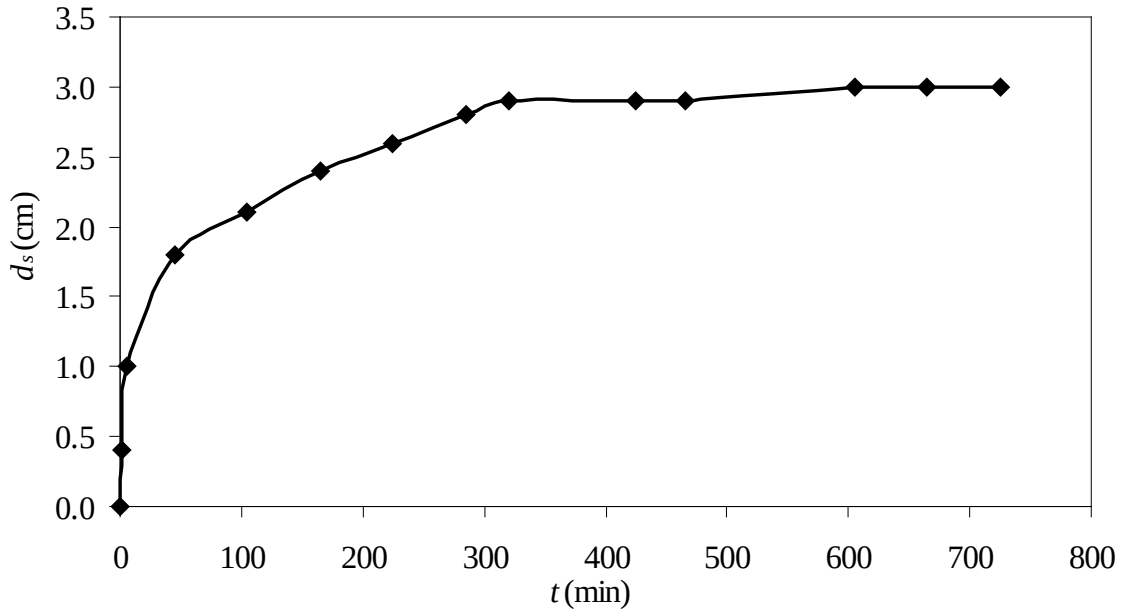

FIG.4.44 Temporal Variation of Maximum Scour Depth for a Depth of 10.0cm and u_*/u_{*c}=0.89 (clear-water condition with collar, run no.18)

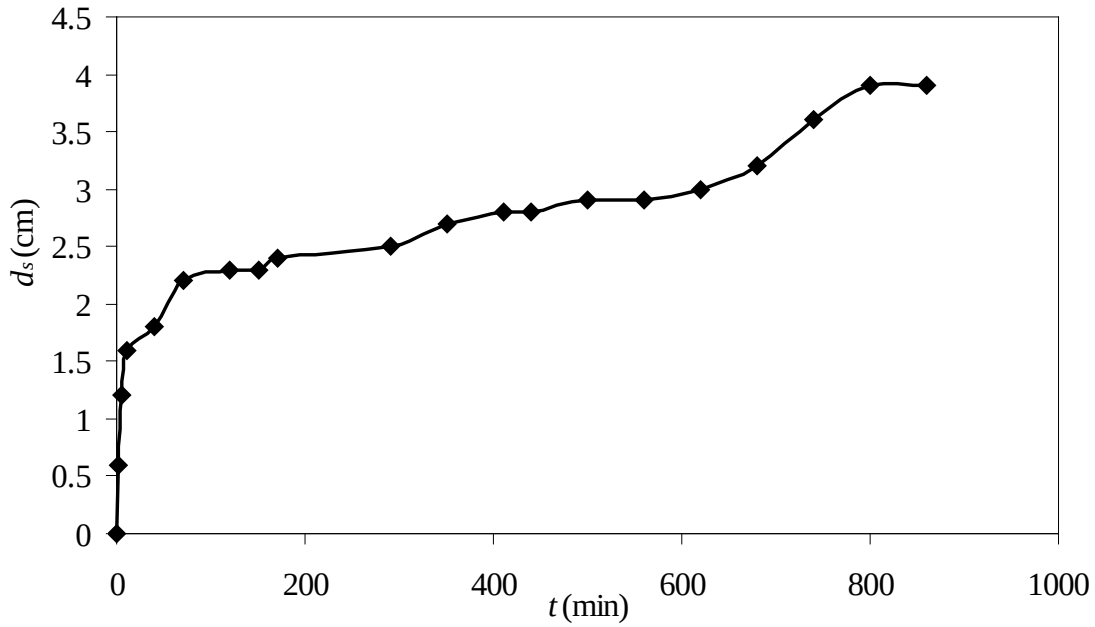

FIG.4.45 Temporal Variation of Maximum Scour Depth for a Depth of 5.0cm and u_*/u_{*c}=1.089 (Live-Bed Degaradation Condition With Collar, Run No.19)

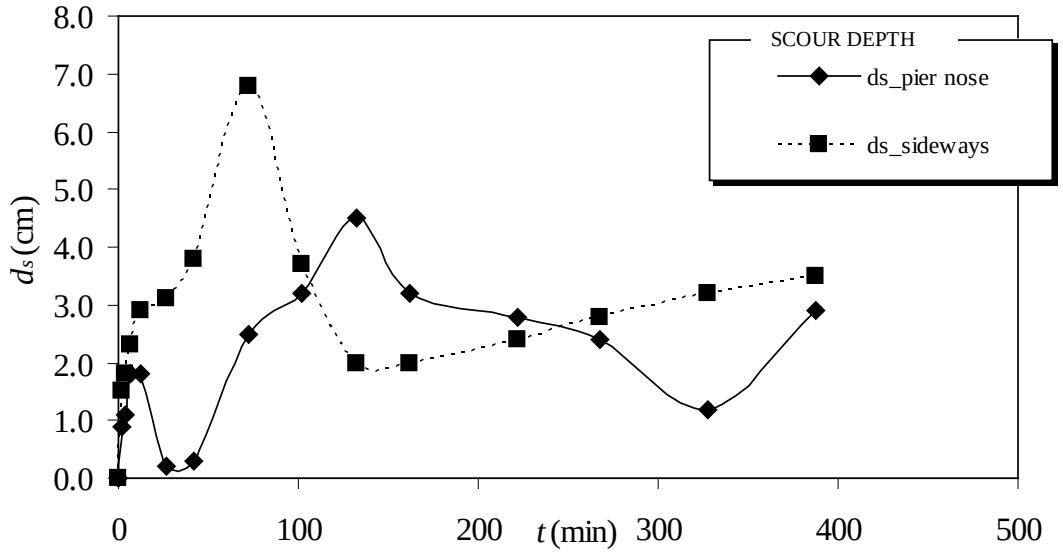

FIG.4.46 Temporal Variation of Scour Depth for A Depth of 7.0cm and u_*/u_{*c}=1.1 (Live-Bed Degaradation Condition with Collar, Run No.20)

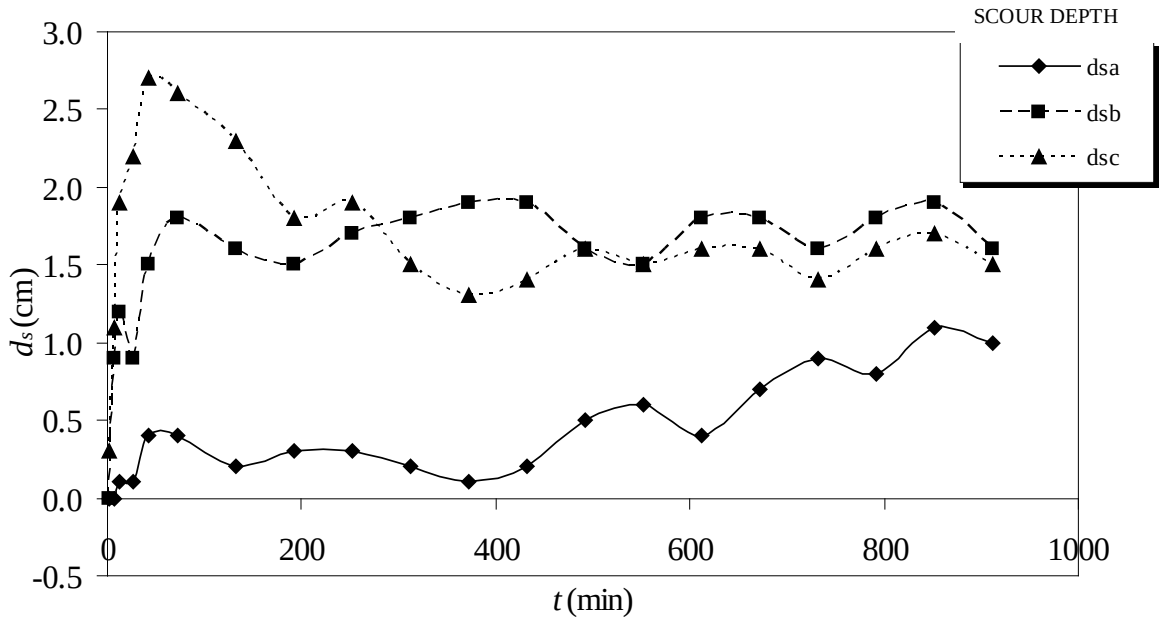

FIG.4.47 Temporal Variation of Scour Depth for A Depth of 8.0cm and u_*/u_{*c}=1.266 (Live-Bed Degaradation Condition with Collar, Run No.21)

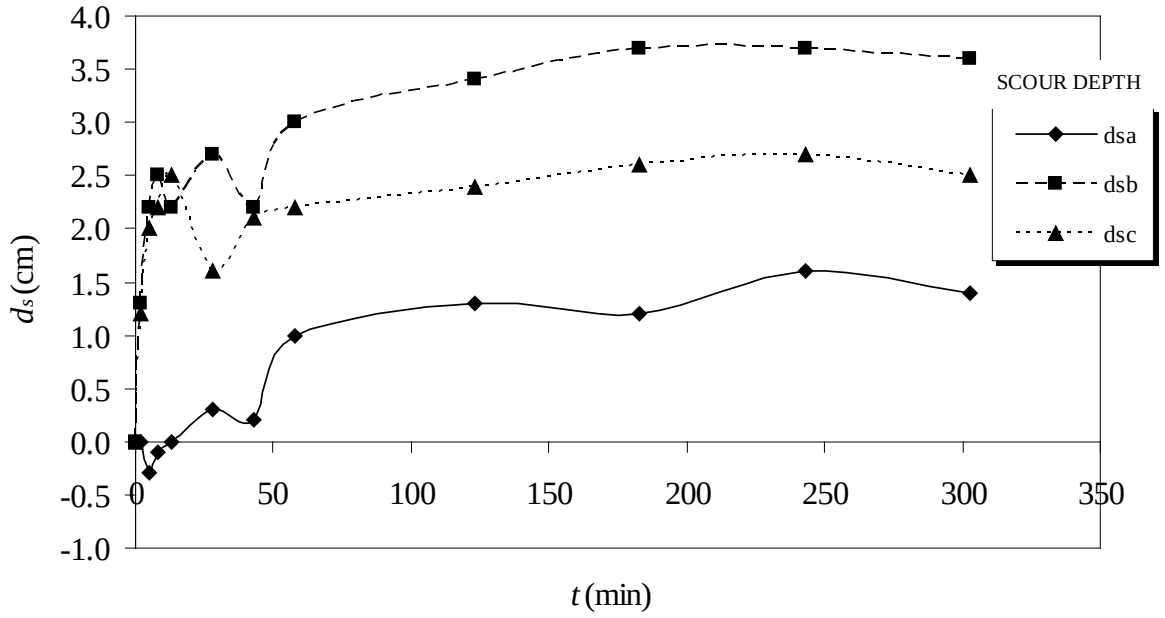

FIG.4.48 Temporal Variation of Scour Depth for A Depth of 7.0cm and u_*/u_{*c}=1.335 (Live-Bed Degaradation Condition with Collar, Run No.22)

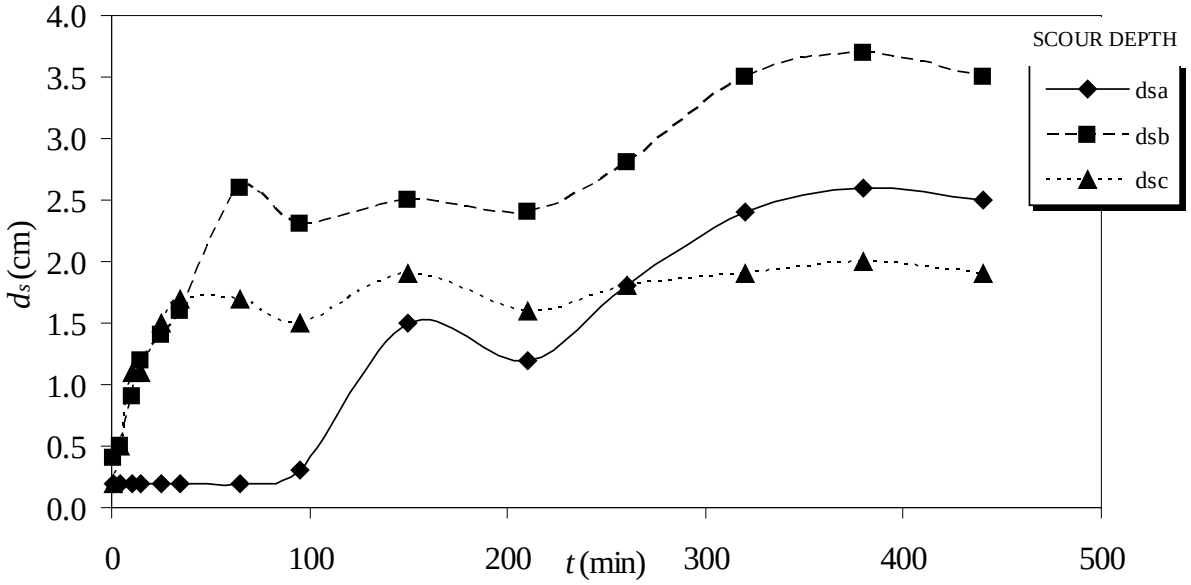

FIG.4.49 Temporal Variation of Scour Depth for a Depth of 6.0cm and u_*/u_{*c}=1.42 (Live-Bed Degaradation Condition with Collar, Run No.23)

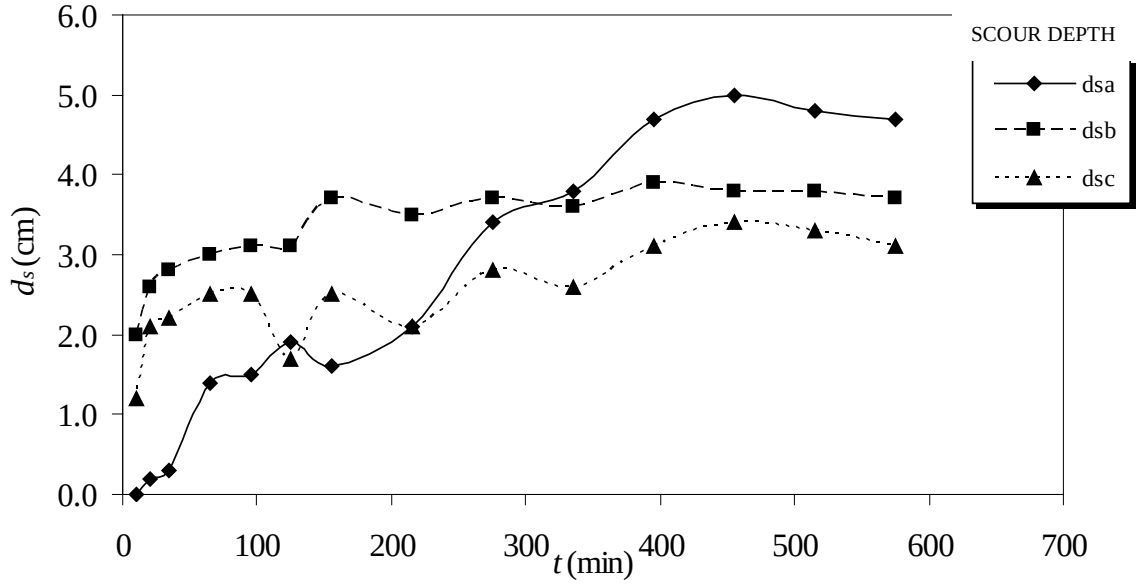

FIG.4.50 Temporal Variation of Scour Depth for A Depth of 9.0cm and u_*/u_{*c}=1.488 (Live-Bed Degaradation Condition with Collar, Run No.24)

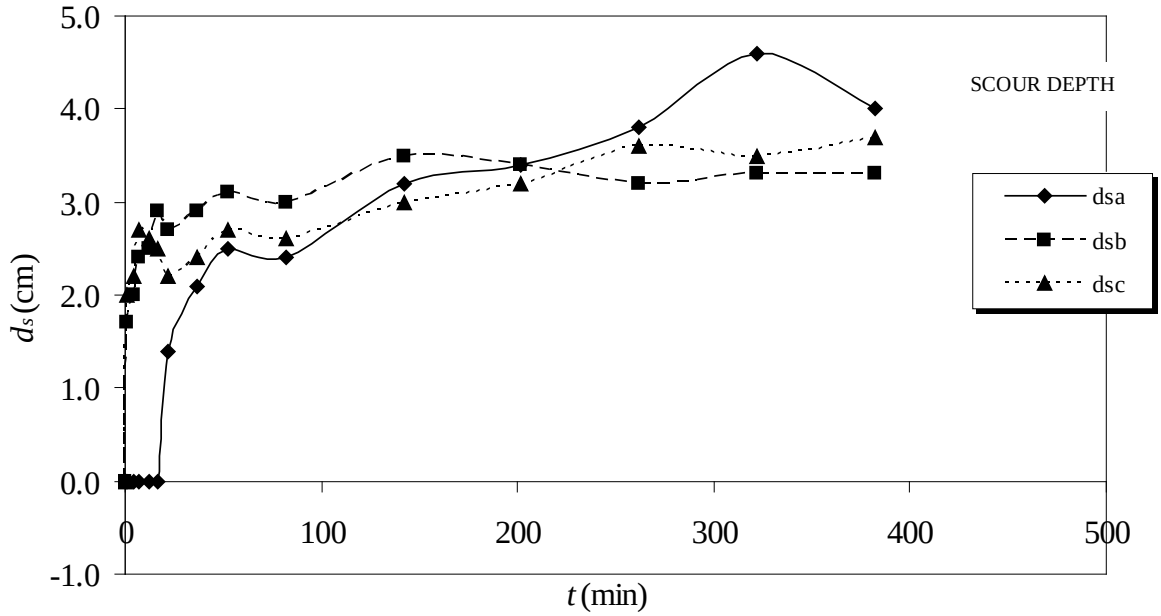

FIG.4.51 Temporal Variation of Scour Depth for a Depth of 6.5cm and u_*/u_{*c}=1.88 (Live-Bed Degaradation Condition with Collar, Run No.25)

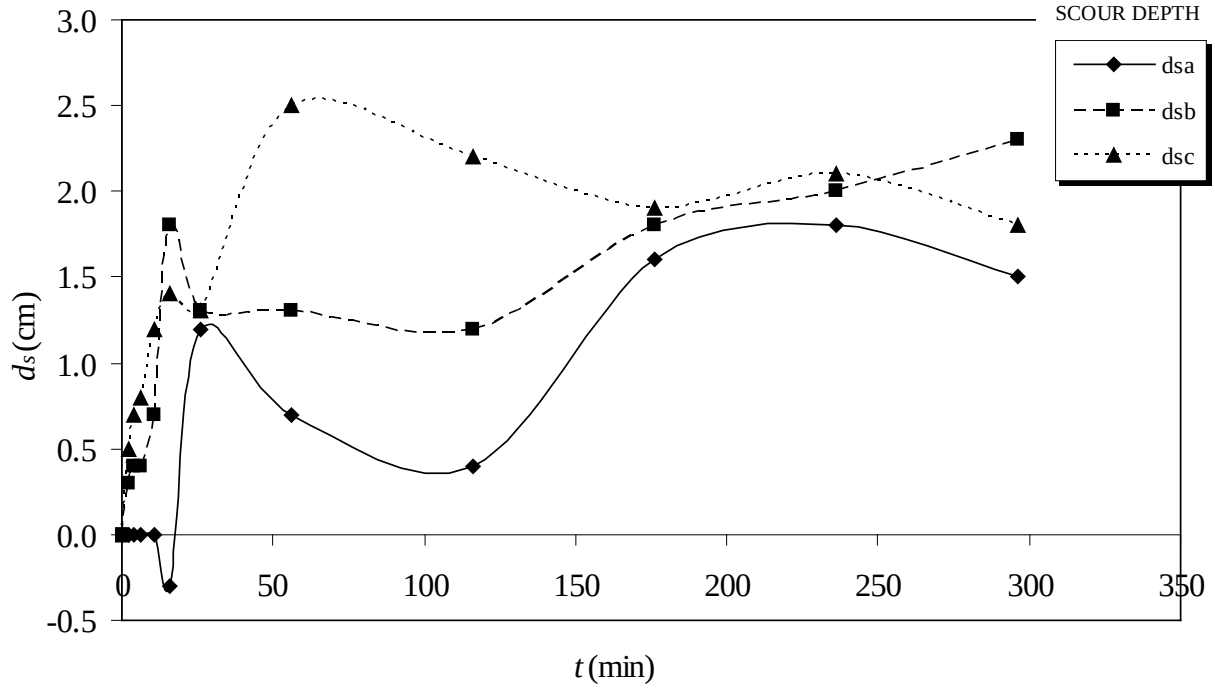

FIG.4.52 Temporal Variation of Scour Depth for a Depth of 6.0cm and u_*/u_{*c}=2.05 (Live-Bed Degaradation Condition with Collar, Run No.26)

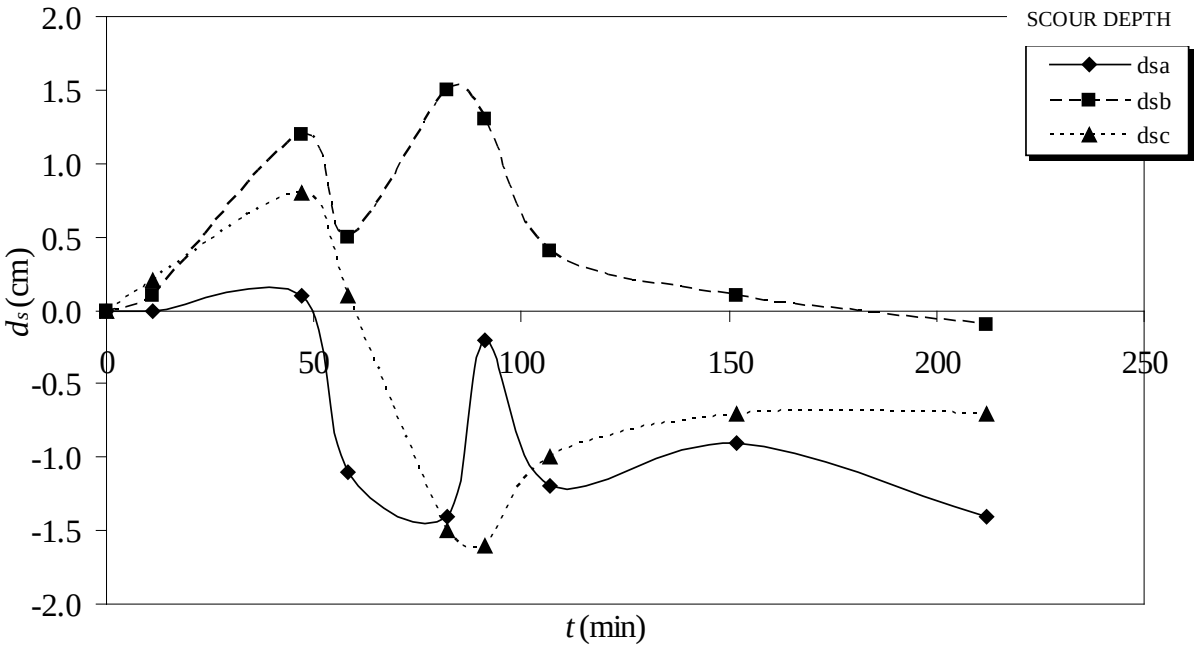

FIG.4.53 Temporal Variation of Scour Depth for A Depth of 5.0cm and u_*/u_{*c}=1.089 (Live-Bed Condition with Collar, Run No.27)

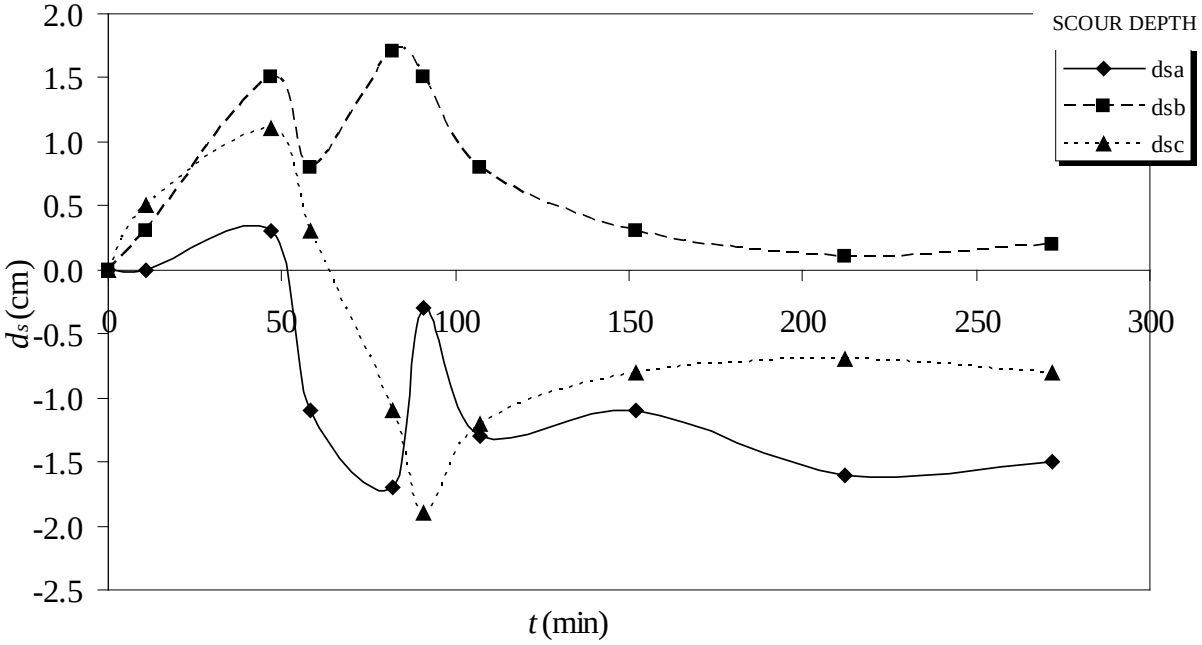

FIG.4.54 Temporal Variation of Scour Depth for A Depth of 7.0cm and u_*/u_{*c}=1.1 (live-bed condition with collar, run no.28)

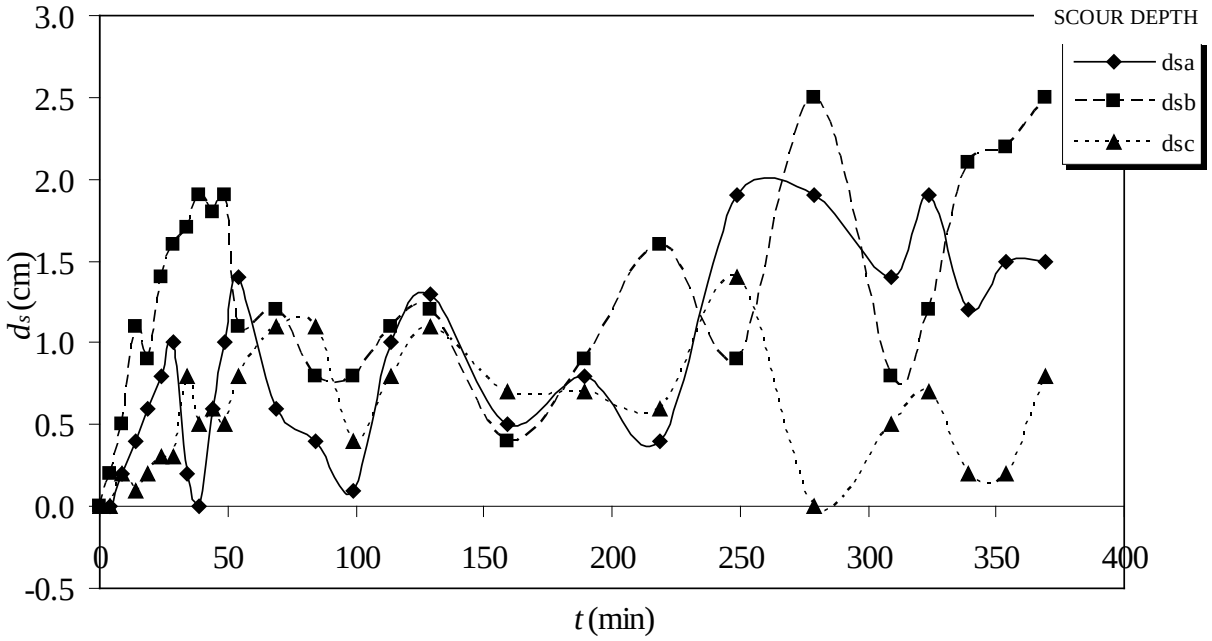

FIG.4.55 Temporal Variation of Scour Depth for A Depth of 8.0cm and u_*/u_{*c}=1.266 (Live-Bed Condition with Collar, Run No.29)

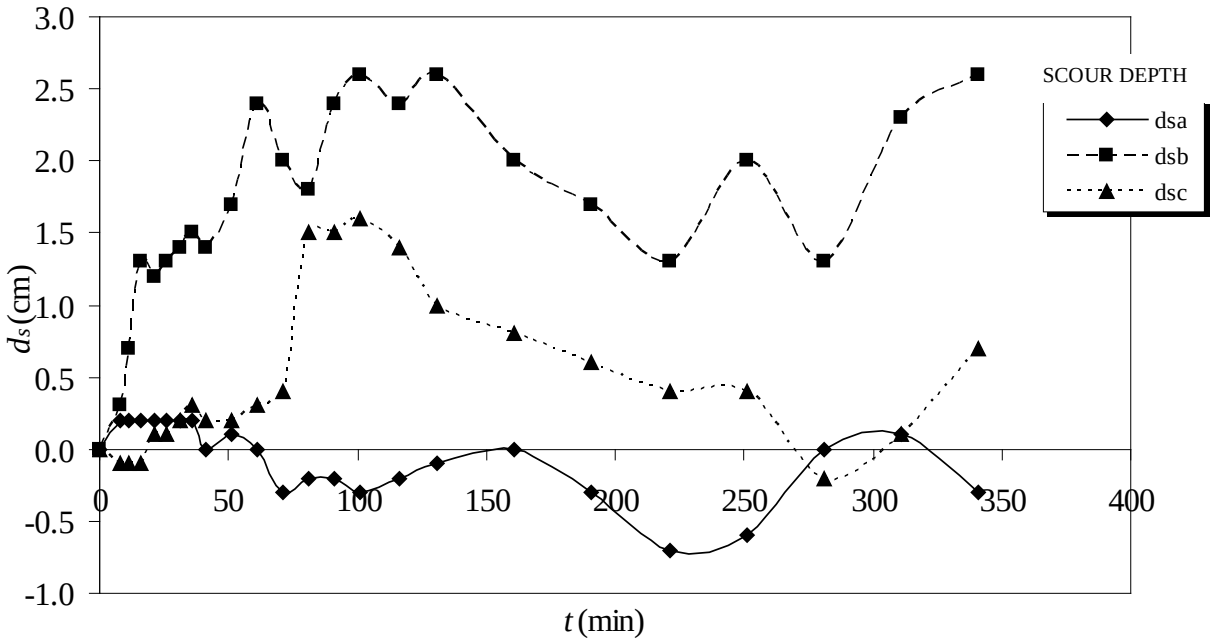

FIG.4.56 Temporal Variation of Scour Depth for A Depth of 7.0cm and u_*/u_{*c}=1.335 (Live-Bed Condition with Collar, Run No.30)

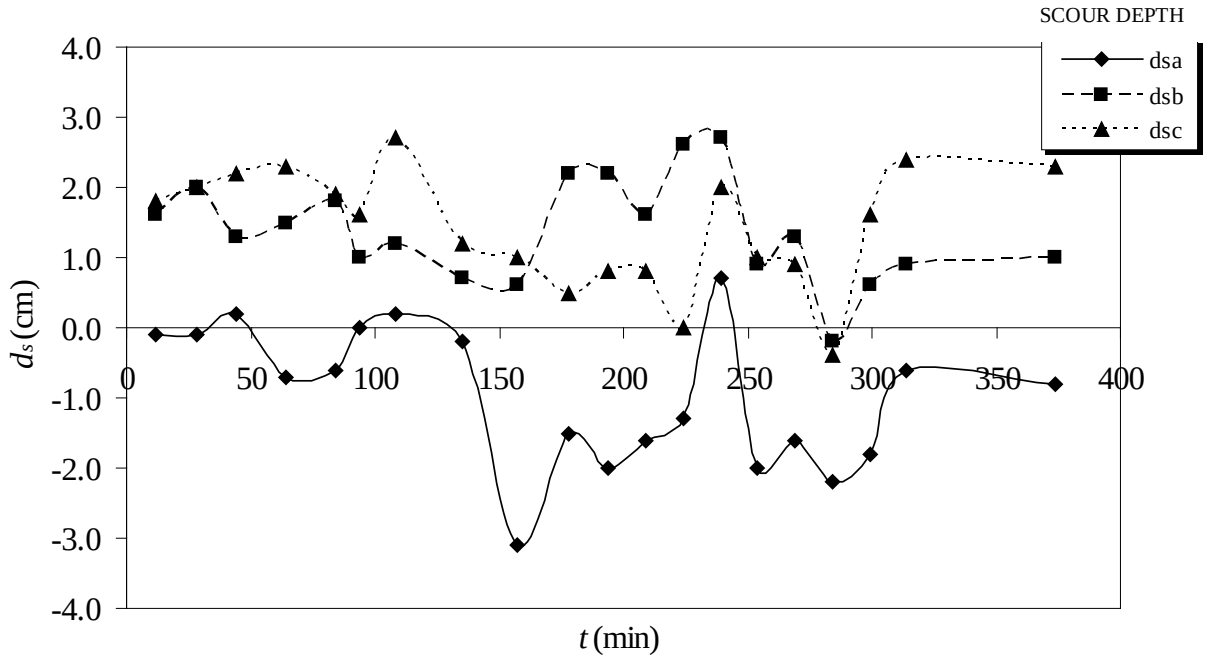

FIG.4.57 Temporal Variation of Scour Depth for a Depth of 6.0cm and u_*/u_{*c}=1.42 (Live-Bed Condition with Collar, Run No.31)

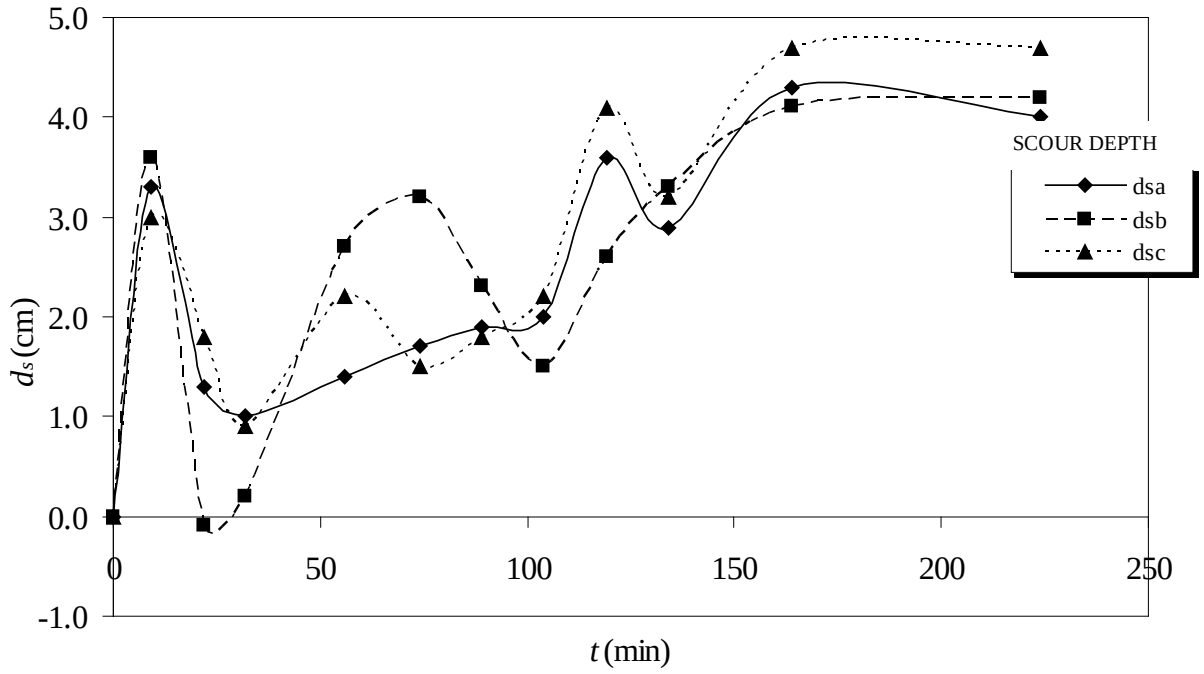

FIG.4.58 Temporal Variation of Scour Depth for A Depth of 9.0cm and u_*/u_{*c}=1.488 (Live-Bed Condition with Collar, Run No.32)

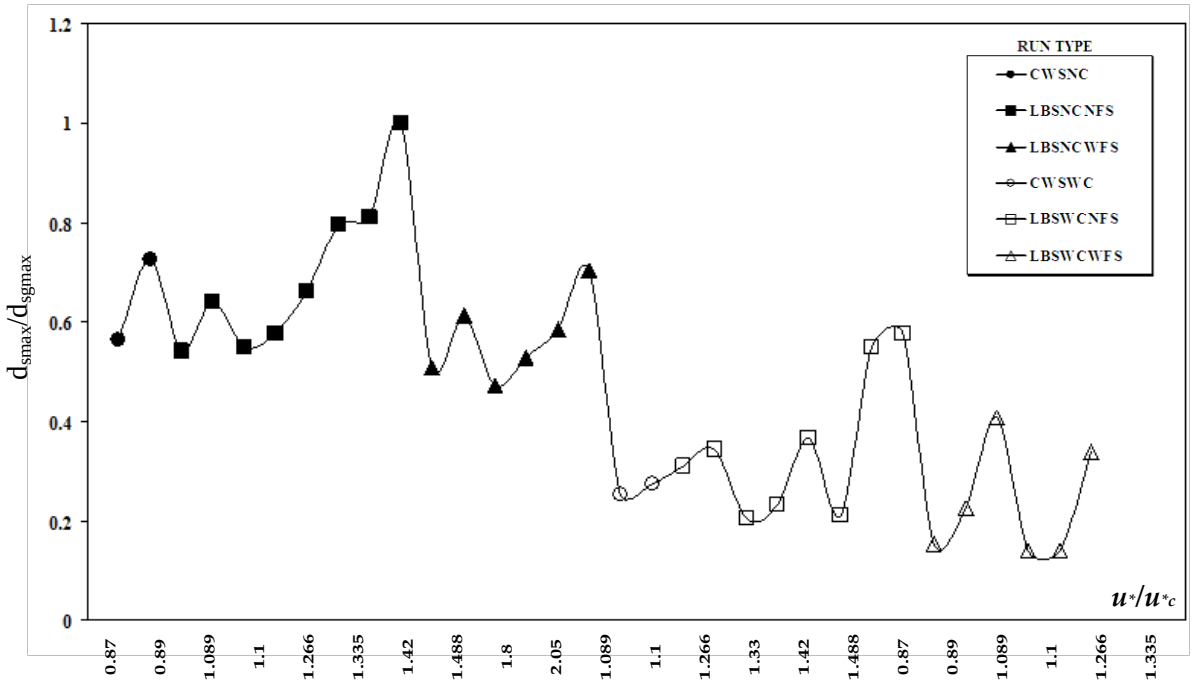

FIG.4.59 Comparision of Reductions in Maximum Scour Depth under Different Flow Conditions

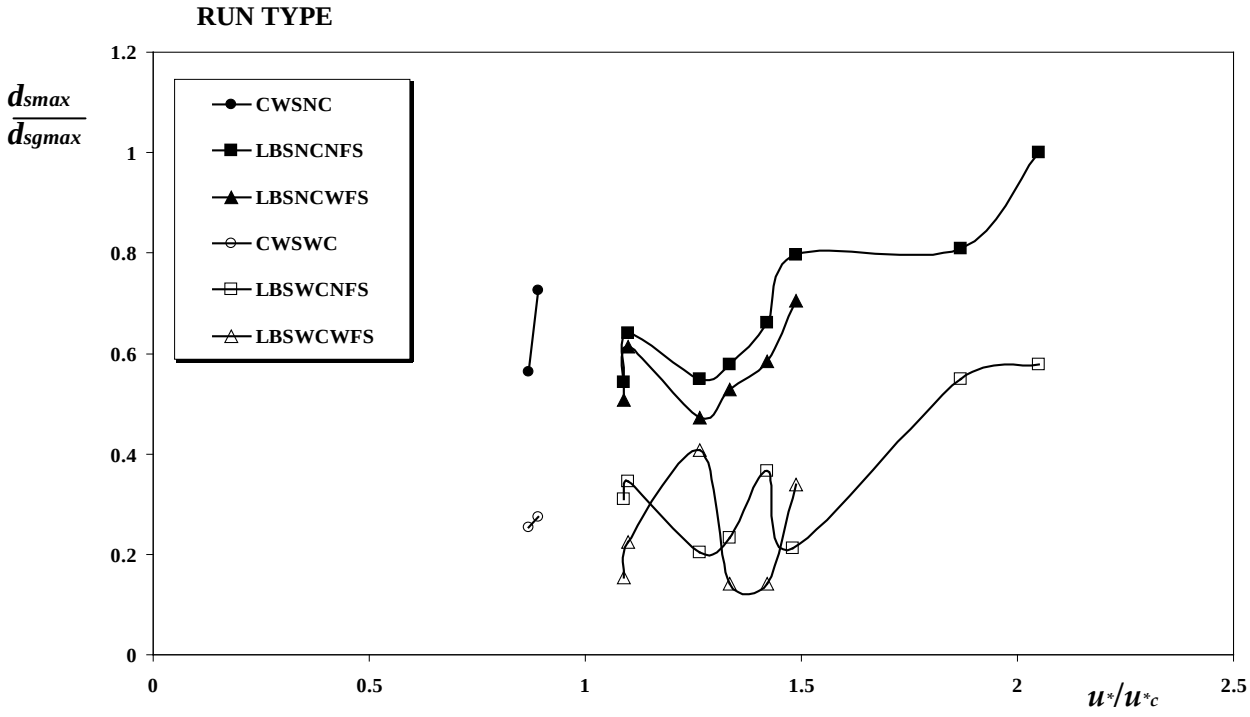

FIG.4.60 Comparision of Reduction of Maximum Scour Depth by Collar under Varying Flow Conditions

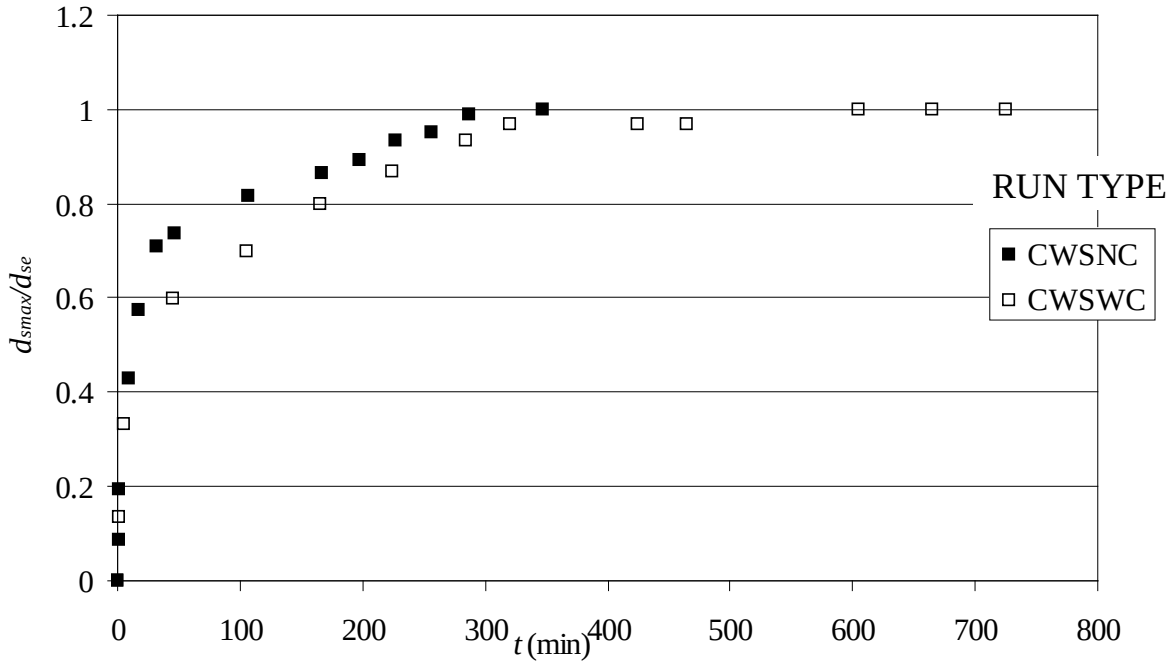

FIG.4.61 Time Variation of Scour Depth in a Circular Pier with and Without Collar under Clear-Water Conditions (u_*/u_{*c}=0.89)

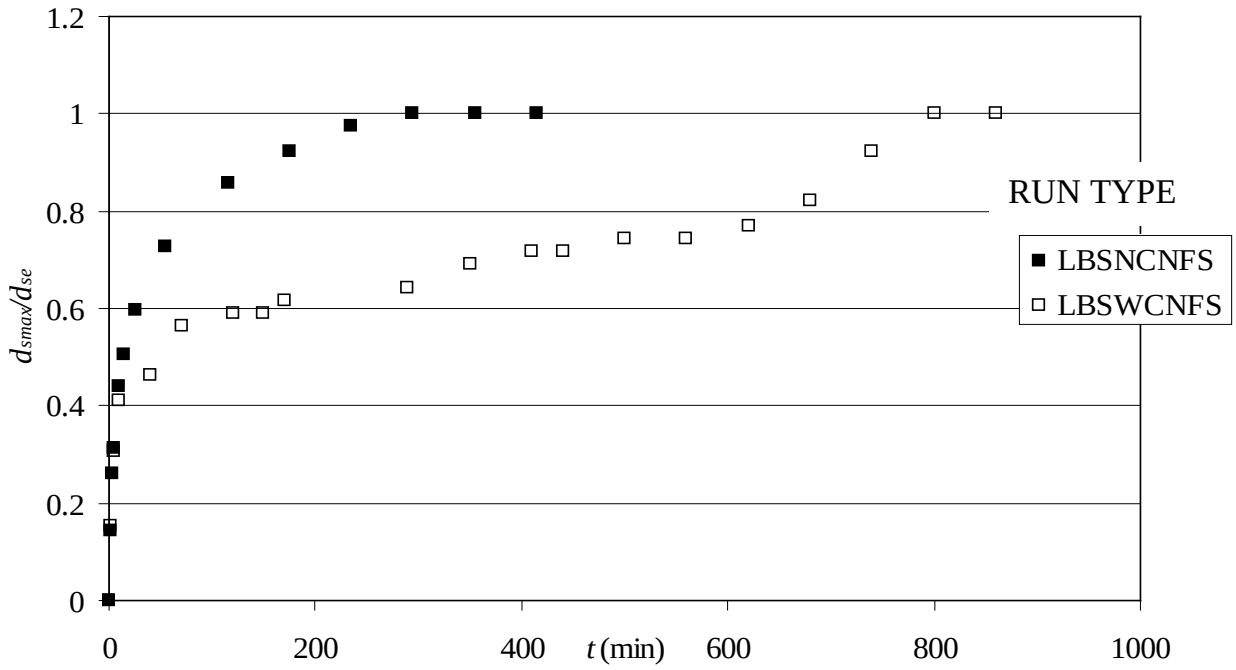

FIG.4.62 Time Variation of Scour Depth in A Circular Pier with and Without Collar under Live-Bed Conditions (u_*/u_{*c}=1.08)

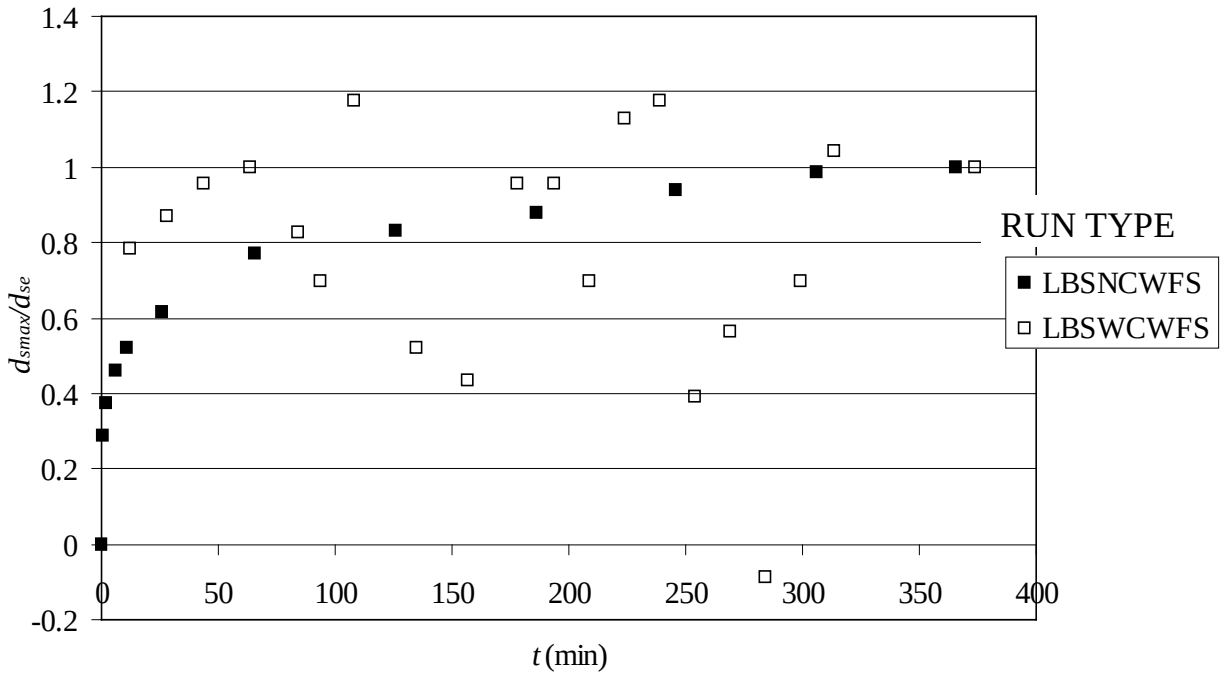

FIG.4.63 Time Variation of Scour Depth in a Circular Pier with and Without Collar under Live-Bed Conditions (u_*/u_{*c}=1.42)

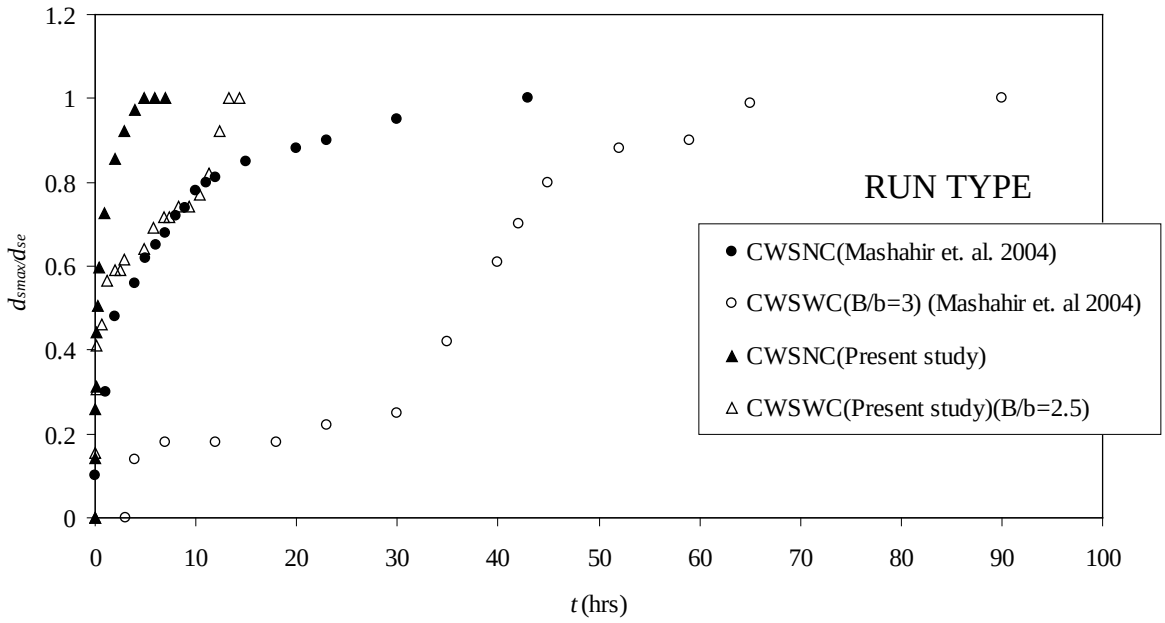

FIG.4.64 Comparison of Patterns of Time Variation of Scour Depth in a Circular Pier with and without Collar under Clear-Water Conditons Observed By Different Investigators

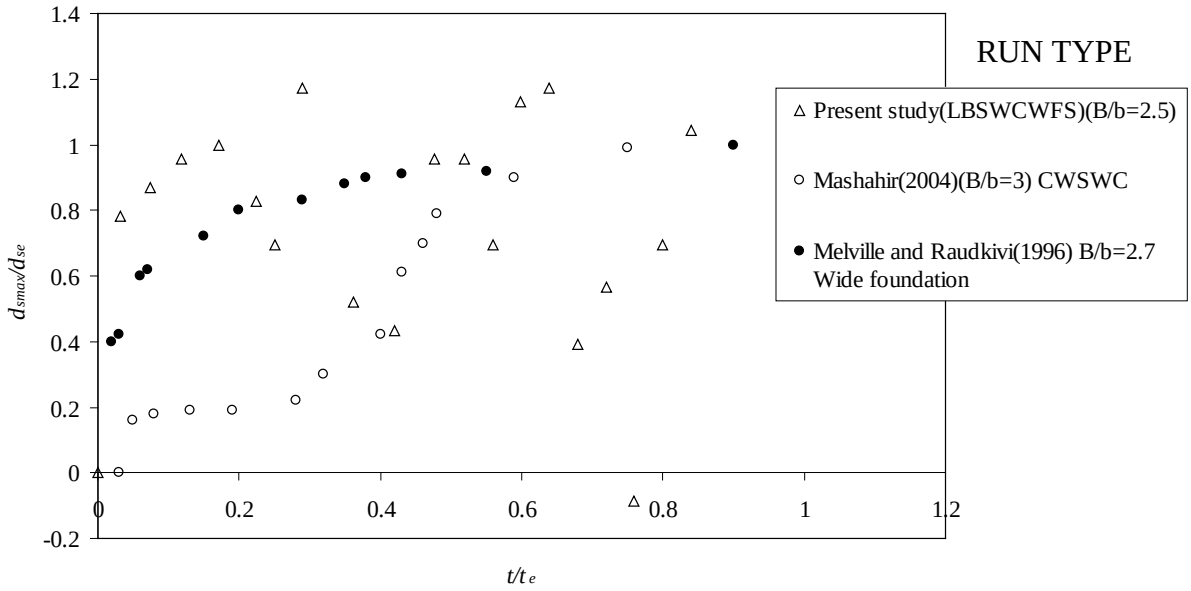

FIG.4.65 Comparision of Reduction of Scour in a Pier Protected With Collar under Live-Bed Conditions and Under Clear-Water Conditions with Scour Reduction by Wide Foundation

.

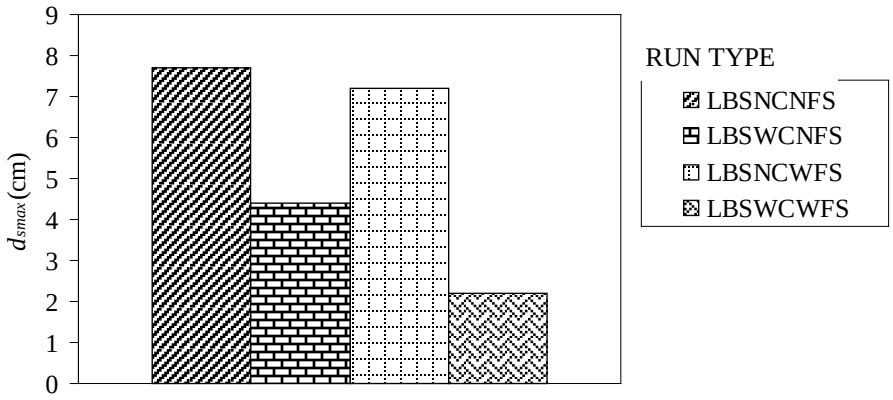

FIG.4.66 Comparision of Maximum Scour Depth with and Without Collar for u_*/u_{*c}=1.089

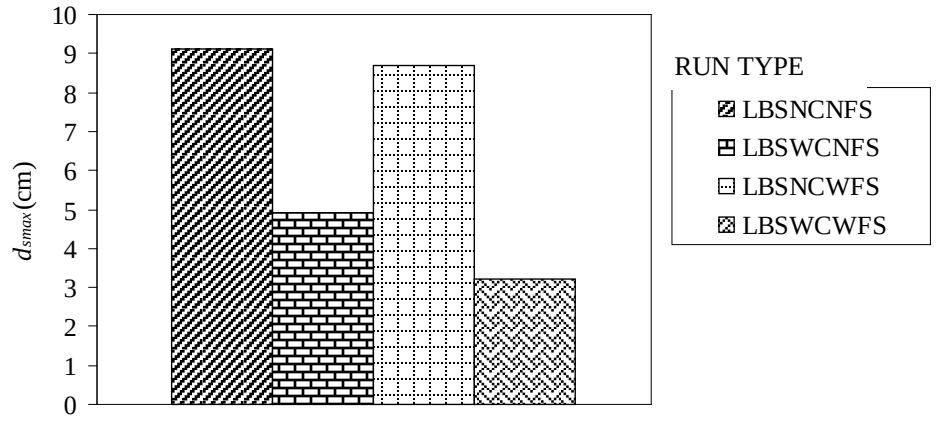

FIG.4.67 Comparision of Maximum Scour Depth with and Without Collar for u_*/u_{*c}=1.1

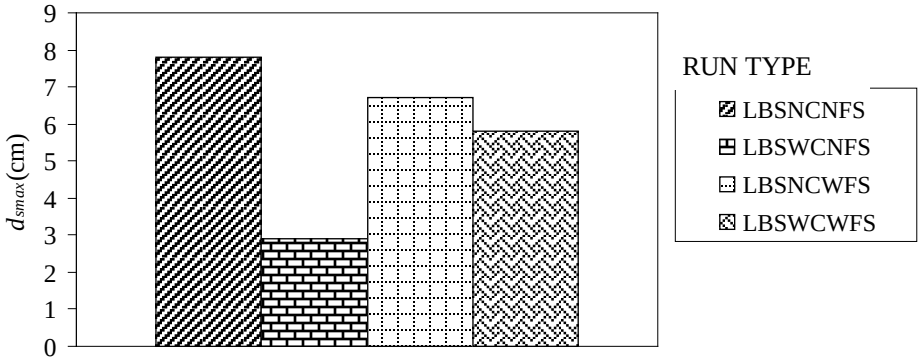

FIG.4.68 Comparision of Maximum Scour Depth with and Without Collar for u_*/u_{*c}=1.266

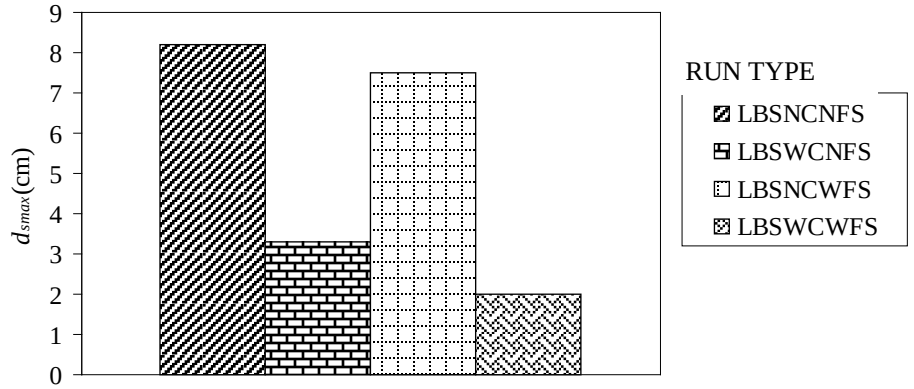

FIG.4.69 Comparision of Maximum Scour Depth with and Without Collar for u_*/u_{*c}=1.33

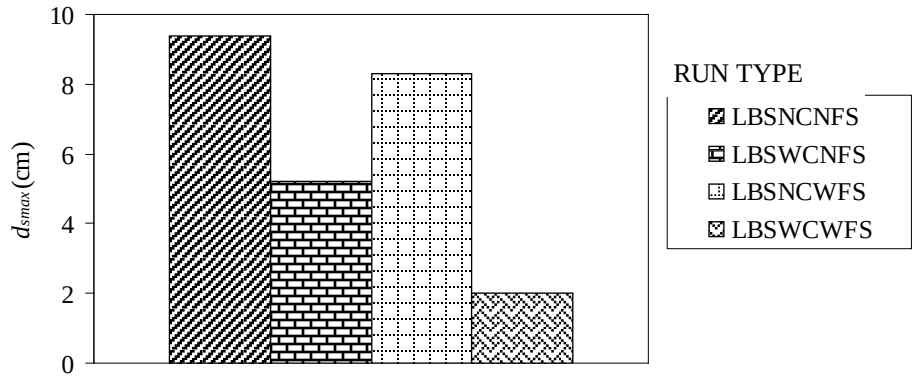

FIG.4.70 Comparision of Maximum Scour Depth with and Without Collar for u_*/u_{*c}=1.42

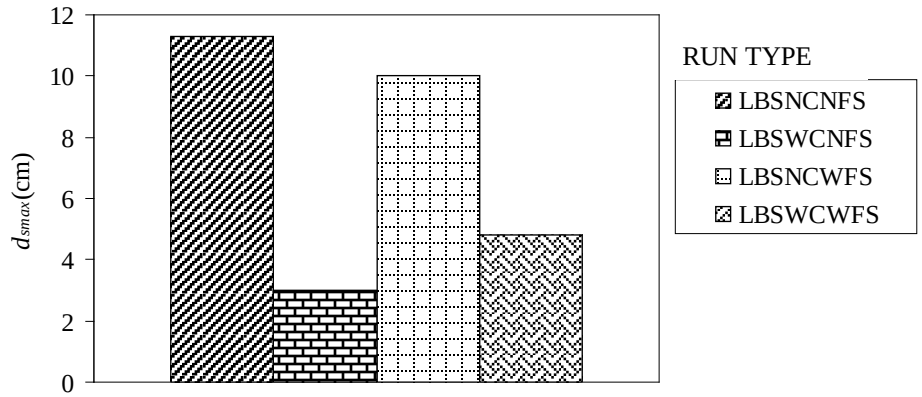

FIG.4.71 Comparision of Maximum Scour Depth with and Without Collar for u_*/u_{*c}=1.488

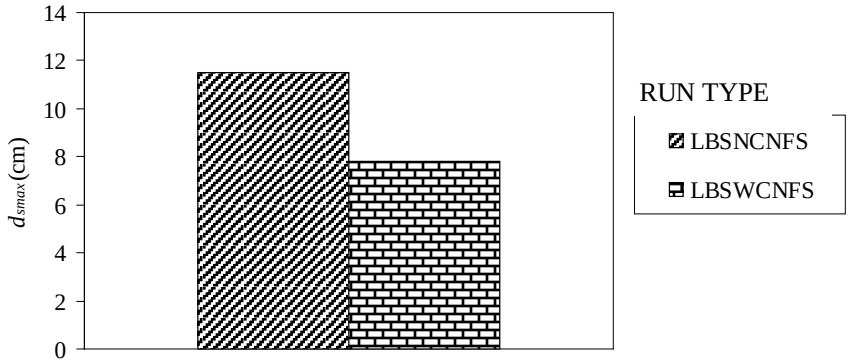

FIG.4.72 Comparision of Maximum Scour Depth with and Without Collar for u_*/u_{*c}=1.88

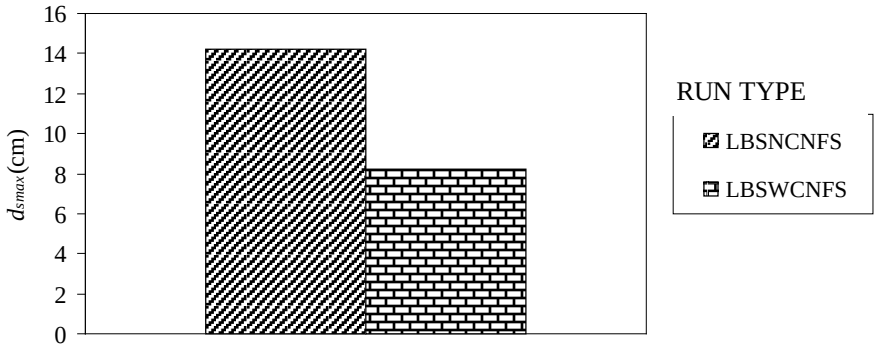

FIG.4.73 Comparision of Maximum Scour Depth with and Without Collar for u_*/u_{*_c}=2.05

TABLE 4.1 Percentage Reductions in Maximum Scour Depth Due To Placement of Collar

Sl. No.	Set No.	Experiment	u_*/u_{*c}	Flow conditions	Pier Diameter b(cm)	Mean Particle Size d_{50} (mm)	Maximum scour(cm)		Percentage reduction in scour depth
							With Collar	Without Collar	
1	1	CWSNC1	0.87	CLEAR-WATER	11.4	0.34		8	
2		CWSNC2	0.89					10.3	
3	2	LBSNCNFS1	1.089	LIVE-BED degradation	11.4	0.34		7.7	
4		LBSNCNFS2	1.1					9.1	
5		LBSNCNFS3	1.266					7.8	
6		LBSNCNFS4	1.33					8.2	
7		LBSNCNFS5	1.42					9.4	
8		LBSNCNFS6	1.488					11.3	
9		LBSNCNFS7	1.8					11.5	
10		LBSNCNFS8	2.05					14.2	
11	3	LBSNCWFS1	1.089	LIVE-BED	11.4	0.34		7.2	
12		LBSNCWFS2	1.1					8.7	
13		LBSNCWFS3	1.266					6.7	
14		LBSNCWFS4	1.33					7.5	
15		LBSNCWFS5	1.42					8.3	
16		LBSNCWFS6	1.488					10.0	
17	4	CWSWC1	0.87	CLEAR-WATER + collar	11.4	0.34	3.6		55%
18		CWSWC2	0.89				3.9		62%
19	5	LBSWCNFS1	1.089	LIVE-BED degradation+ collar	11.4	0.34	4.4		43%
20		LBSWCNFS2	1.1				4.9		46%
21		LBSWCNFS3	1.266				2.9		63%
22		LBSWCNFS4	1.33				3.3		60%
23		LBSWCNFS5	1.42				5.2		45%
24		LBSWCNFS6	1.48				3.0		73%
25		LBSWCNFS7	1.87				5.8		50%
26		LBSWCNFS8	2.05				6.2		56%
27	6	LBSWCWFS1	1.089	LIVE-BED + collar	11.4	0.34	2.2		69%
28		LBSWCWFS2	1.1				3.2		63%
29		LBSWCWFS3	1.266				4.8		29%
30		LBSWCWFS4	1.33				2		73%
31		LBSWCWFS5	1.42				2		76%
32		LBSWCWFS6	1.488				3.2		68%

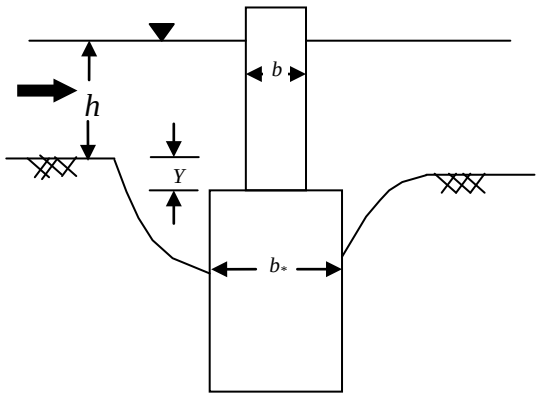

FIG. 4.74 Definition Diagram of Circular Compound Bridge Pier

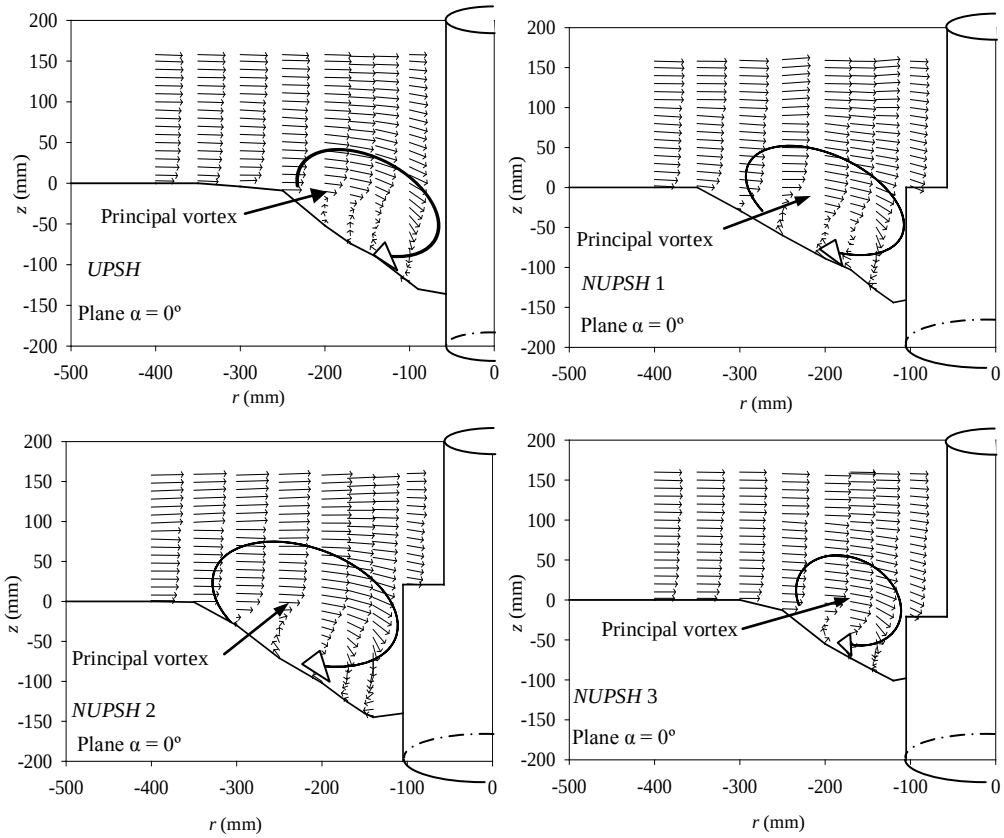

FIG. 4.75 Measured Velocity Vector Field at the Central Line of the Flow on the Upstream Face of the Circular Uniform Pier and Circular Compound Pier Models.

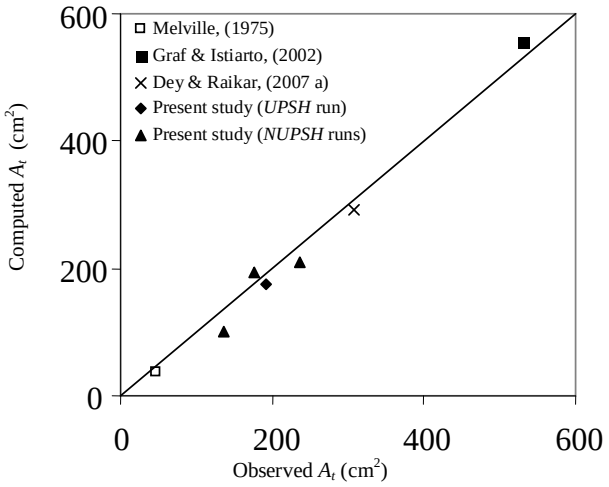

FIG. 4.76 Comparison between Computed and Observed Cross-Sectional Area of Principal Vortex for Compound Circular Pier

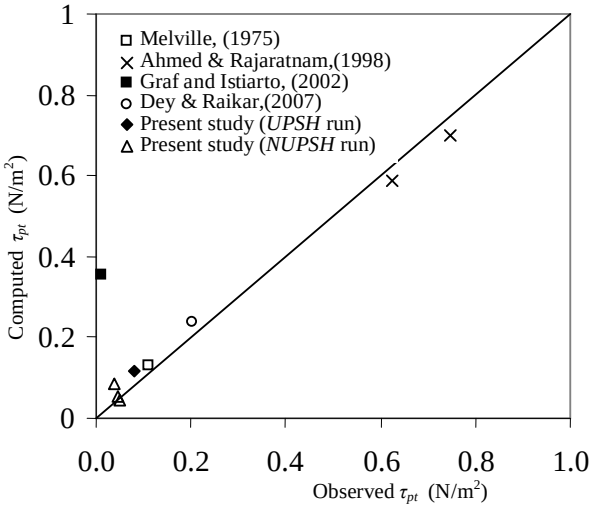

FIG. 4.77 Comparison between Computed and Observed Bed Shear Stress at Pier Upstream Nose in Scoured Area for Uniform Circular Pier and Compound Circular Pier

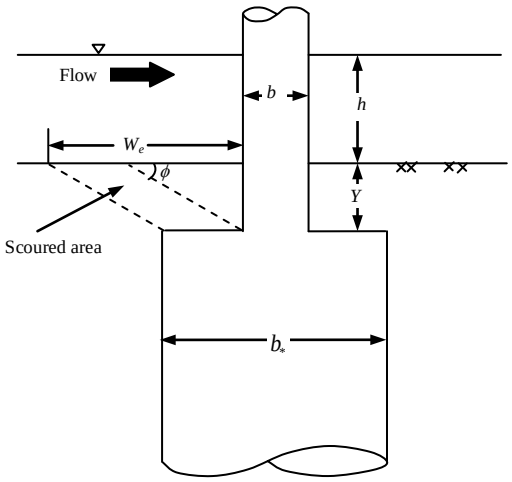

FIG. 4.78 Schematic Diagram for Illustration of the Modelling of Scour Process around Circular Compound Pier

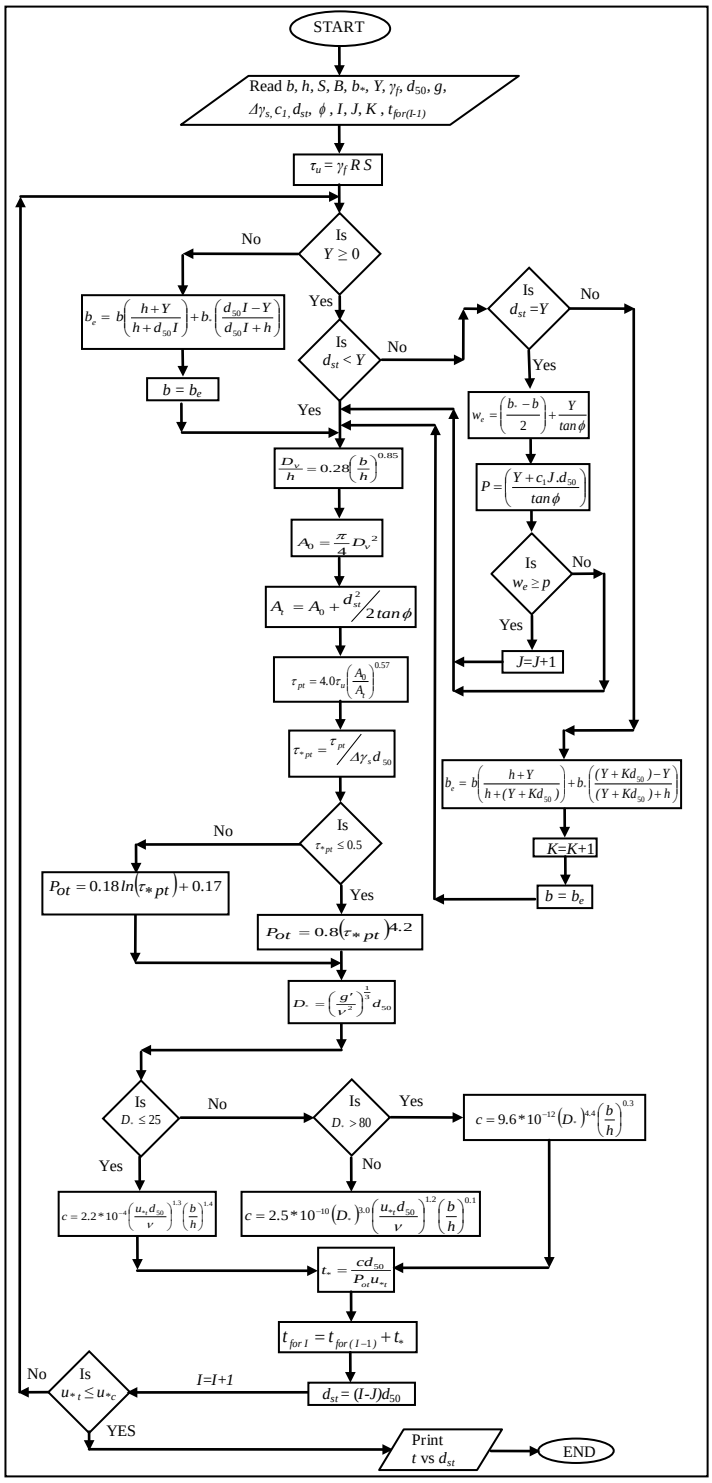

FIG. 4.79 Algorithm for Computation of the Temporal Variation of Scour Depth around Circular Compound Pier

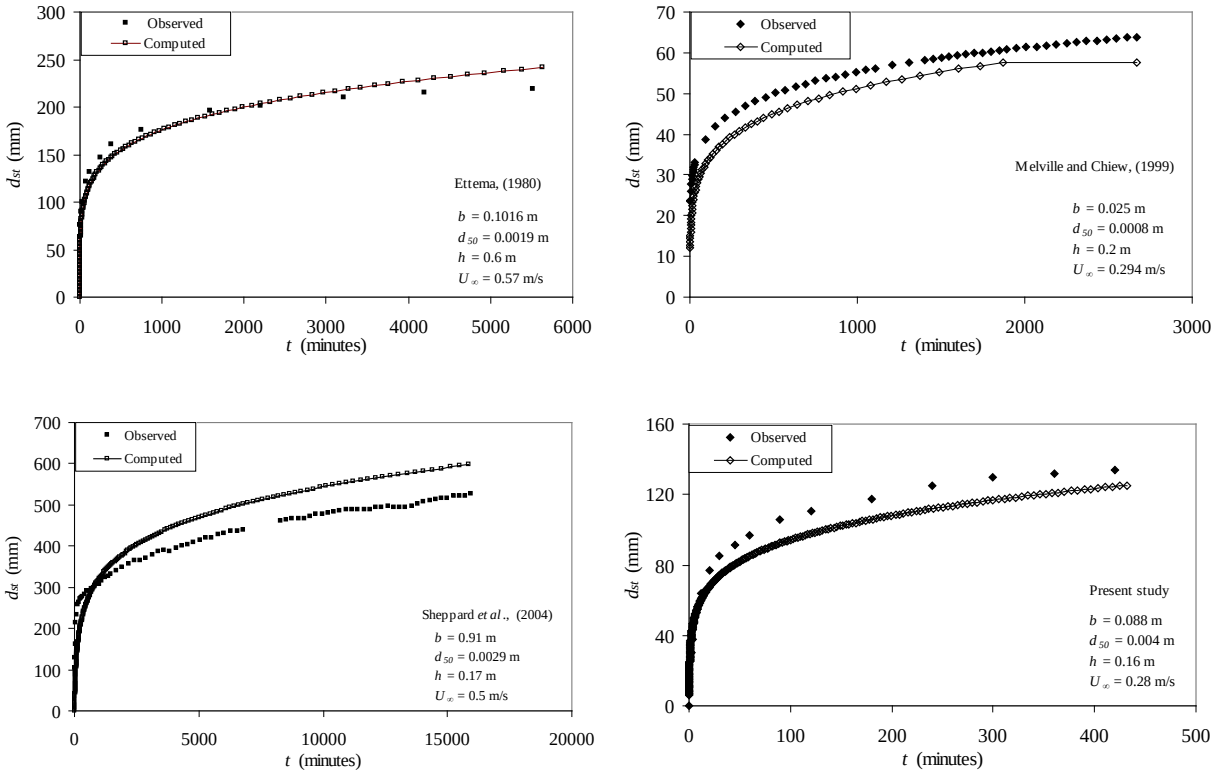

FIG. 4.80 Comparison of Observed and Computed Temporal Variation of Scour Depth around Circular Uniform Pier

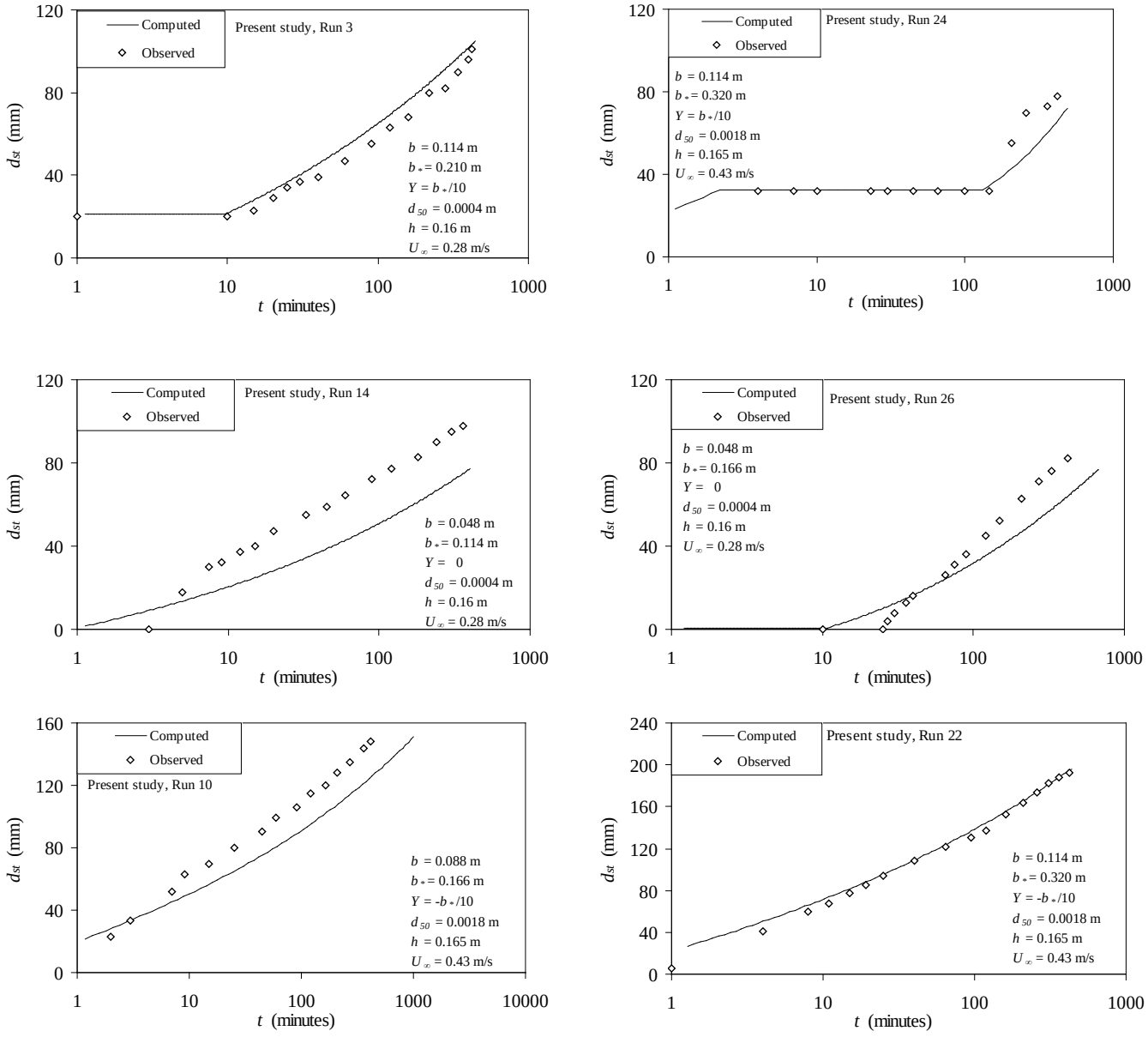

FIG. 4.81 Comparison of Observed and Computed Temporal Variation of Scour Depth around Circular Compound Pier for the data of Present Study

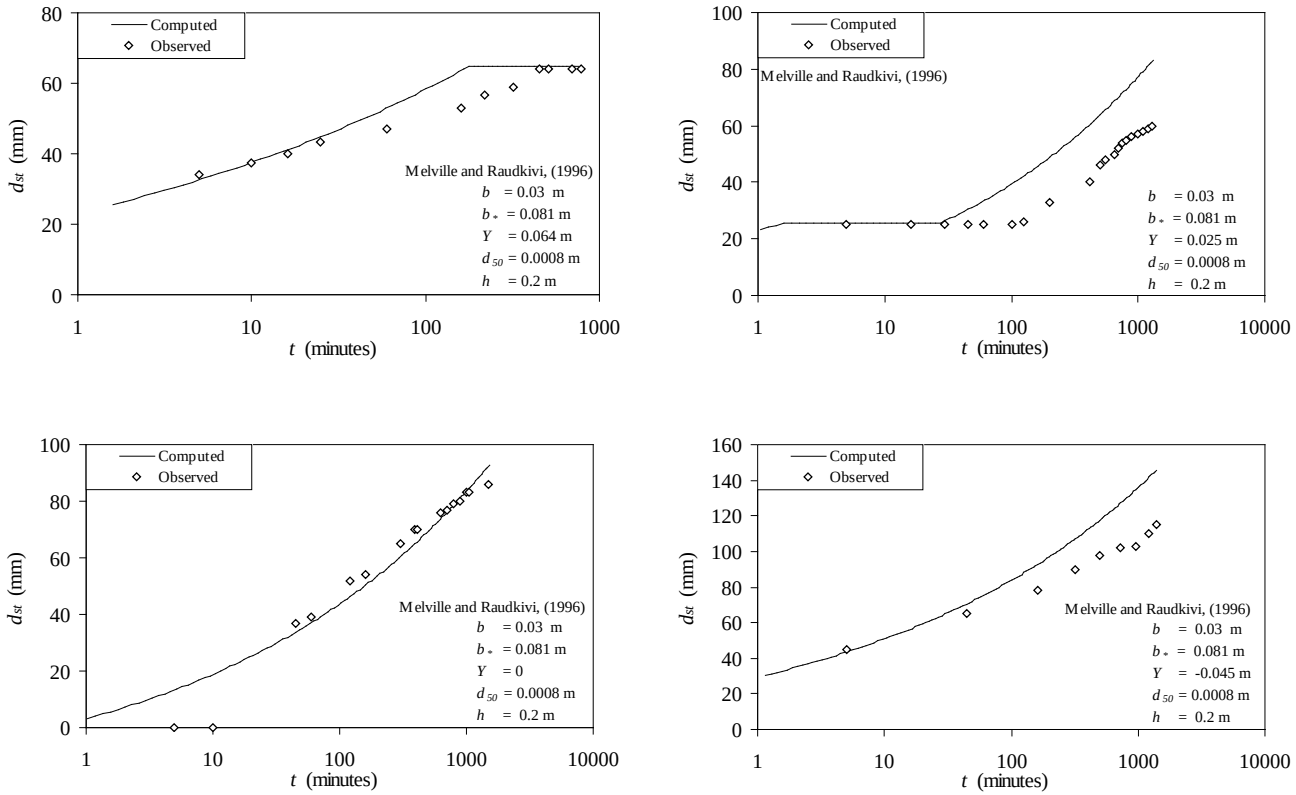

FIG. 4.82 Comparison of Observed and Computed Temporal Variation of Scour Depth around Circular Compound Pier for Data of Melville And Raudkivi, (1996)

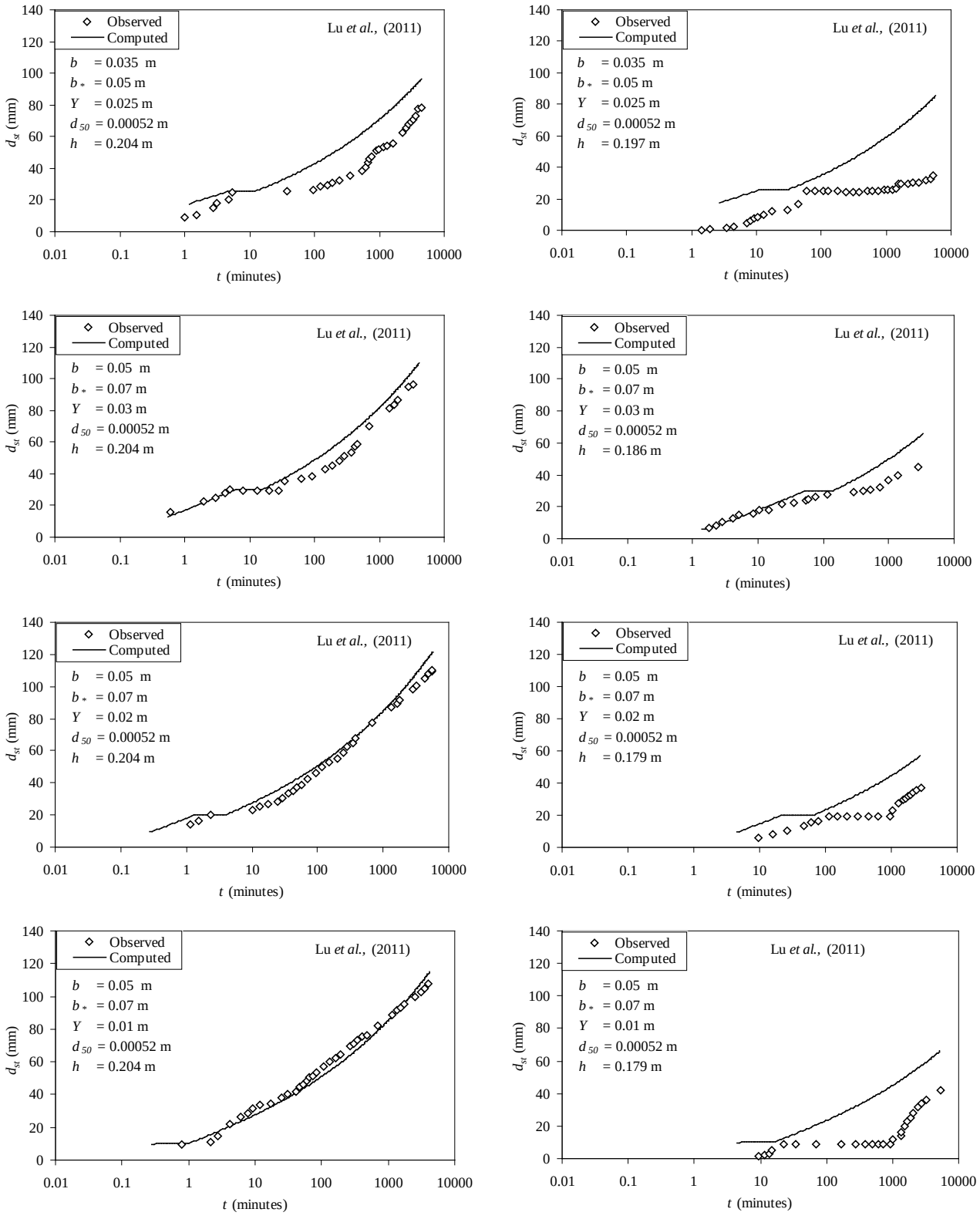

FIG. 4.83 Comparison of Observed and Computed Temporal Variation of Scour Depth around Circular Compound Pier for Data of Lu *et al*., (2011)

CHAPTER 5: CONCLUSIONS AND SCOPE FOR FUTURE STUDY

5.1 CONCLUSIONS

The main objective of the present study was to understand the effectiveness of collar for scour reduction under live-bed conditions. Initially we planned to also investigate the effectiveness of collar as scour reduction device bytaking observations under prototype conditions. But this objective could not be persued as the RDSO, Lucknow did not take up this task which albeit was agreed upon with this. The study was made by conducting experiments for live-bed conditions. The flow around pier during live-bed condition is quantified and the potential areas of scouring around upstream of the pier are identified. Experiments for scouring around piers with collor were conducted to quantify the effectiveness of collar for scour reduction under live-bed conditions which match more closely with the field conditions. The experiments for live-bed degradation condition and clear-water were also made to make a comparative study. The design of collar was not studied in the present work as it is already known that a collar of 2.5*b* is most effective in scour reduction when placed at or below the channel bed level (Kumar *et al.*, 1996). The process of scour around compound piers was also investigated and a mathematical model for computation of temporal variation of scour around circular compound piers is developed. The flow structure around uniform and compound piers was also quantified.

Following are the specific conclusions of the present study:

Turbulence charateristics of flow around pier during live-bed condition

1. Aspects of turbulence in the near field immediately upstream of a pier on a flat bed are examined through the 3D velocity measurements around a pier. Systematic analyses of statistics for the flow field are extensively presented.
2. Vector plot of near bed velocity is used for quantification of the size of primary vortex, on the upstream of the cylinder.
3. The amplification of maximum bed shear stress estimated from stream-wise velocity in the flow separation line was 2.54 times that of the bed shear stress in the approach

flow. However, an amplification of about 16 times is noticed in shear stress estimated using Reynolds stresses at $\theta = 45^{\circ}$.

4. As the highest amplification of shear stress occurs in the region of $\theta = 45^{\circ}$, the observations that scour around piers initiate in the region is thus explained. The scour protection measures should be designed for stability, against such enhancement in the shear stress.

Scouring around pier with and without collar

5. A collar having diameter equal to 2.5 *b* placed at or below the bed level reduces the depth of scour on an average by 63% under live-bed condition. Its effectiveness in scour reduction in clear-water condition is already established. Hence, the collar placed at channel bed level or below it can be considered to be an effective scour control device.

6. A collar of size 2.5*b* proves to be more effective in scour protection for live-bed conditions when compared to live-bed degradation conditions.

7. The experiments revealed that the deepest scour occurred in the front or wake of the pier depending upon the flow conditions for a single collar of size 2.5*b*.

8. For the live-bed conditions the deepest scour occurred below the collar near the pier nose.

9. Scour in the wake starts right from the beginning in the presence of collar. This result is in good conformity to Kumar (1996) and Melville (1975). The scour on the sides and in the front of the pier is delayed in the presence of a collar.

10. The temporal variation of scour for collar placed under the live-bed shows a periodic variation.

11. The sediment inflows occur from the upstream and the sediment fronts of are formed on the upstream bed. These fronts move up to the pier and on attaining a certain height the front collapses under its self weight, thereby increasing the diameter of scour hole and providing more periodicity temporal variation of scour depth.

Scouring around compound piers

Compound piers (piers resting on large dia footing with top of footing near general bedlevel of river) are invariably used as foundations of large bridges in Indian subcontinent. Therefore scouring around compound piers was studied herein in detail. Following conclusions are made based on this.

12. The method of Kothyari *et al*., (1992 a) for computation of temporal variation of scour depth around circular uniform pier has been updated based on new data collected from literature and present study.
13. The value of parameter *c* of Eq. (4.14) is found to vary as per the roughness characteristics of the channel bed.
14. The updated method for temporal variation of scour depth around circular uniform piers has produced satisfactory results for the data of present study which pertained to transient (developing) scour. Also this method produced good results for long term data of several investigators around the world.
15. A method has also been proposed based on mathematical modelling for computation of temporal variation of scour depth around the circular compound bridge piers while top of the footing was positioned at bed level, above the bed level and below the bed level.
16. The concept of effective diameter (Melville and Raudkivi, 1996) was utilized in model computations for temporal variation of scour depth around compound piers.
17. The differences in scour process around uniform piers and compound piers are quantified. Reasonably good agreement between the corresponding observed and computed values of scour depth around compound piers has been also noticed for the data of present study, Melville and Raudkivi, (1996) and Lu *et al*., (2011).
18. The proposed model has potential of application for computation of temporal variation scour depth around prototype circular compound piers during passage of the flood hydrographs.

5.2 SCOPE FOR FUTURE STUDY

Recommendations regarding possible future work in relation to the present work are as follows:

1. Since rivers usually carry debris, particularly during flood conditions, a study of the effect of debris on the performance of a collar and on the temporal development of scour in the presense of collar could be investigated in order to gain more knowledge or insight as to the use of a collar.

2. All previous studies on the use of a collar as a countermeasure for local scour at a bridge pier are based on experiments carried out using physical hydraulic models. It would be useful to investigate the practicality of using a collar through study at prototype bridge.

3. All previous studies on the use of a collar as a countermeasure for local scour at a bridge pier have been confined to cohesionless material. It could be useful to study bridge pier scour reduction under cohesive material since a bridge pier can be located on a soil other than cohesionless soil.

4. Commonly in the literature the study of flow mechanism causing local scour at a pier without collar has been studied. The flow behaviour around the collar has not yet been studied which may also be made.

APPENDIX-I: EXPERIMENTS WITH PROTOTYPE SIZE PIERS

1.0 INTRODUCTION

The main cause of concern in stability of the bridges founded in river beds is the scouring of river bed level caused by the flow around the bridge elements. The scour mechanism has the potential to threaten the structural integrity of bridges and hydraulic structures, ultimately causing failure when the foundation of the structures is undermined. A series of relatively recent bridge failures due to pier scour, as reported in the literature, has rekindled interest in furthering the understanding of the pier scour process and for developing improved ways of protecting bridges against the ravages of scour. The scour prediction methods developed in the laboratories and the scour equations based on laboratory data did not always produce reasonable results for field conditions. Scale effect becomes evident when one considers the similitude requirements for hydraulic modeling of pier scour. So it was proposed to test the validity of the present scour predicting equations for scour due to flows having high value of pier Reynolds number as is the case in field conditions where the pier Reynolds number is larger than 10^5.

2.0 EXPERIMENTAL SET-UP

Experiments were conducted in a masonry flume of length = 33.0 m, width = 9.6 m and depth = 0.6 m with a bed slope of 0.0015. The flume receives water supply from a constant head overhead tank. The supply of flow to the flume was regulated with the help of a valve provided at the inlet of the flume. Honeycomb masonry grid wall built of small size bricks were provided at the upstream end of the flume to minimize the disturbance in the flow entering the flume. Boulders were placed on flume bed, from flume entrance to 2.0 m length towards downstream to dissipate the excess energy in the flow entering the flume. An adjustable wooden tail gate was provided at the downstream end of the flume to enable adjustment of the depth of flow in the flume. A working section 3.0 m long, 9.0 m wide and 0.6 m deep was located at 12.0 m downstream of the flume entrance for conducting the

experiments. The mean flow in the working section was thus in a fully developed state. Figure A1 to A6 show the photographic views of the flume and Figs. A7 to A9 illustrates the photographic view of the flume after live-bed scour measurement.

Circular piers with three different diameters 1.2 m, 0.6m and 0.3m were constructed to perform live-bed local sediment scour tests. The pier protruded well above the water surface and is placed in the middle of the working section. Figure A9 shows the photographic view of pier.

3.0 EXPERIMENTS IN PROTOTYPE SIZE FLUME

A few numbers of experimental runs were performed in the prototype scale facility. These experiments revealed that process of scour in large size piers is greatly different than that at model size piers. Scour activity also beguns at sides of the prototype piers but it takes much longer time (than in case of model piers) to extend to upstream nose of the pier. However due to limitations of the laboratory facilities it was not possible to generate flows having b/h (b = pier dia, h= approach flow depth) values in experiments that are similar to those in field conditions. Therefore experiments were only done at much larger values of b/h (than those normally exist in field conditions). These flow conditions did not produce siginificant depth of scour in present experiments.

FIG. A1 Prototype Size Flume in which Test is conducted

FIG. A2 Working Section in which Test is conducted

FIG. A3 Adjustable Wooden Tail Gate Provided at the Downstream End of the Flume

FIG. A4 Flow Measurements using Pitot tube

FIG. A5 (A) Pier Exposed to Different Flow Conditions

FIG. A5 (b) Pier Exposed to Different Flow Conditions

FIG. A6 (a) Piers of Different Sizes Exposed to Different Flow Conditions

FIG. A6 (b) Piers of Different Sizes Exposed to Different Flow Conditions

FIG. A7 Scouring around Pier Exposed to Different Flow Conditions

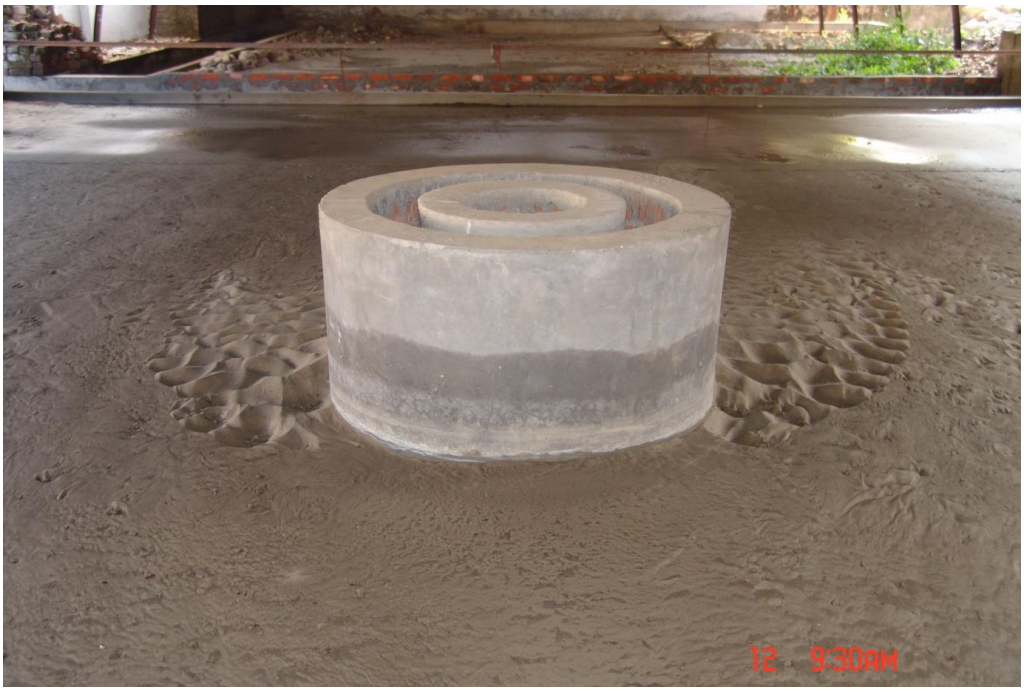

FIG.A8 Scouring around Pier Exposed to Different Flow Conditions

FIG. A9 Piers of Different Sizes Tested for Scouring Under Same Flow Conditions

4.0 CONCLUSIONS

The scour prediction methods developed in the laboratories and the scour equations based on laboratory data does not always produce reasonable results for field conditions. Scale effect also becomes evident when one considers the similitude requirements for hydraulic modeling of pier scour. Therefore a detailed experimentation on prototype were planned to understand the controlling parameters which influence the scouring around pier. In present project however it was proposed that the field studies (proto type pier) would be carried out by Railway Design Standards Organisation (RDSO) - Ministry of Railways, Lucknow. An abandoned railway bridge located in Moradabad-Ambala route on river Ganga at Balawali in U.P. was selected by the railways earlier for this purpose. However after the approval of present project by ministry of water resources, the investigations on proto type pier by RDSO were not made. Also the facility developed in IIT Roorkee to study the scour around bridge piers on proto type scale did not yield any decisive results. Whereas the flow discharge upto 0.5 m^3/s could be generated in laboratory flows under available facilities a rate of flow more than 3 m^3/s however would be required to minimise the scale effects in the scour experiments.

REFERENCES

1. Abdel, R.M., Abdel, M.M. and Bayoumy, M. (2003), "Scour reduction around bridge piers using internal openings through the pier", Proc., XXX IAHR Congress, Thessaloniki, Greece, August 24-29.
2. Agrawal A.K., Khan M.A., Yi Z. (2005), "Handbook of scour countermeasures design", University transportation Res. centre and New Jersey Department of transportation.
3. Ahmed, F. and Rajaratnam, N. (1998), "Flow around bridge piers", J. of Hydraulic Eng.., ASCE, 124(3), 288-300.
4. Ahmed, F., and Rajaratnam, N. (2000). "Observations on flow around bridge abutments." J. of Eng. Mechanics, ASCE 126 (1), 51-59.
5. Alabi, P.D. (2006), "Time development of local scour at a bridge pier fitted with collar." MS thesis, University of Saskatchewan, Saskatoon, Saskatchewan, Canada.
6. Ali, K. H. M., and Karim, O. (2006). Simulation of flow around piers. J. Hydraulic. Res. 40 (2), 510, 161-174.
7. Ansari, S.A. and Qadar, A. (1994). "Ultimate depth of Scour around bridge piers", Proc. A.S.C.E. National Hydraulics Conf., Buffalo, New York, U.S.A., 51-55.
8. Ansari, S.A., Kothyari, U.C. and Ranga Raju, K.G. (2002). "Influence of cohesion on scour around bridge piers", J. of Hydraulic Res., IAHR, 40(6), 717-729.
9. Ataie-Ashtiani, B., Baratian-Ghorghi, Z., and Beheshti, A. A. (2010). "Experimental Investigation of Clear-Water Local Scour of Compound Piers." J. of Hydr. Eng.., ASCE, 136(6), 343-351.
10. Baker, R. A. (1986) "Local scour at bridge piers in non-uniform sediment." Thesis presented to the University of Auckland, New Zealand, in partial fulfilment of the requirements for the degree of Master of Philosophy.
11. Balachandar, R. and Patel, V. (2002) "Rough wall boundary layer on plates in open channels." J. Hydraul. Eng., 128, 947–951.
12. Ballio, F., and Orsi, E. (2000). "Time evolution of scour around bridge abutments", Proc. of the 4th International Conf. on Hydroscience and Eng. ICHE2000, 26-29 Sept., Seoul, Korea.
13. Ballio, F., Radice, A., and Dey, S. (2010). "Temporal scales for live-bed scour at abutments". J. of Hydr. Eng.., ASCE, 136(7), 395-402.
14. Barbhuiya, A. K., Dey, S. (2004) "Measurement of turbulent flow field at a vertical semicircular cylinder attached to the sidewall of a rectangular channel", Flow Meas. and Inst., 15, 87–96.
15. Barkdoll, B.B. (2000). "Time scale for local scour at bridge piers", J. of Hydraulic Eng., ASCE, 126(10), 793-794.
16. Bateman, A., Fernandez, M., and Parker, G. (2005). "Morphodynamic model to predict temporal evolution of local scour in bridge piers." 4th IAHR Symp. on River,

Coastal and Estuarine Morphodynamics (RCEM 2005), Taylor & Francis/Balkema, 911-920.

17. Bergstrom, D., Tachie, M. and Balachandar, R. (2001) "Application of power laws to low Reynolds number boundary layers on smooth and rough surfaces." Phys. Fluids, 13, 3277–3284.
18. Bigillon, F., Nino, Y. and Garcia, M. H. (2006) "Measurements of turbulence characteristics in an open-channel flow over a transitionally-rough bed using particle image velocimetry" Exp. Fluids 41, 857–867.
19. Bozkus, Z. and Osman, Y. (2004), "Effects of inclination of bridge piers on scouring depth", J. of Hydraulic Eng., ASCE, 130(8), 827-832.
20. Breusers, H. N. C., Nicollet, G., and Shen, H. W. (1977). "Local scour around cylindrical piers." J. of Hydr. Res., IAHR, 15(3), 211-252.
21. Breusers, H.N.C. and Raudkivi, A.J. (1991). "Scouring - Hydraulic structures design manual." IAHR, A.A. Balkema, Rotterdam, 143.
22. Breusers, H.N.C., Nicollet, G. and Shen, H.W. (1977). "Local scour around cylindrical piers", J. of Hydraulic Res., IAHR 15(3), 211-252.
23. Briaud, J.L., Ting, F.C.K., Chen, H.C., Cao, Y., Han, S.W., and Kwak, K.W. (1999b), "Erosion function apparatus for scour rate predictions", J. of Geotechnical and Geoenvironmental Eng., ASCE, 127(2), 105-113.
24. Cardoso, A. H., and Bettess, R. (1999). "Effect of time and channel geometry on scour at bridge abutment." J. of Hydr. Eng.., ASCE, 125(4), 388-399.
25. Chabert, J. and Engeldinger, P. (1956), "Etude des affouillements autour des piles de points" (Study of scour at bridge piers). Bureau Central d.Etudes les Equipment d.Outre-Mer, Laboratoire National d.Hydraulique, France.
26. Chabert, J., and Engeldinger, P. (1956). "Etude des affouillements autour des piles des points." Laboratorie National d'Hydraulique, Chatou, France.
27. Chang, H.H. (1988), "Fluvial processes in river eng.", John Wiley & Sons, 432.
28. Chang, W. Y., Lai, J. S., and Yen, C. L. (2004). "Evolution of scour depth at circular bridge piers." J. of Hydr. Eng., ASCE, 130(9), 905-913.
29. Cheremisinoff, P.N., Cheremisinoff, N.P. and Cheng, S.L. (1987), "Hydraulic mechanics 2. Civil Eng. Practice", Technomic Publishing Company, Inc., Lancaster, Pennsylvania, U.S.A. 780 p.
30. Chiew Y.M. (1995), "Mechanics of riprap failure at bridge piers", J. of Hydraulic Eng., ASCE, 121(9), 635-643.
31. Chiew, Y. and Lim, S. (2003), "Protection of bridge piers using a sacrificial sill", Water & Maritime Eng. J., Proc.s of the Institution of Civil Engineers, Thomas Telford J.s, London, 156(1), 53-62.
32. Chiew, Y. M. (1984). "Local scour at bridge piers." Report No. 355, School of Eng.., Univ. of Auckland, Auckland, New Zealand.
33. Chiew, Y.M. (1992). "Scour protection at bridge piers.", J. of Hydraulic Eng., ASCE, 118(9), 1260-1269.

34. Chiew, Y.M. (2004), "Local scour and riprap stability at bridge piers in a degrading channel", J. of Hydraulic Eng., ASCE, 130(3), 218-226.

35. Chiew, Y.M. and Lim, F.H. (2000). "Failure behaviour of riprap layers at bridge piers under live-bed conditions", J. of Hydraulic Eng., ASCE, 126(1), 43-55.

36. Chiew, Y.M. and Melville, B.M. (1987). "Local scour around bridge piers", J. of Hydraulic Res., IAHR, 25(1), 15-26.

37. Chreties, C., Simarro, G., and Teixeir, L. (2008). "New Experimental Method to Find Equilibrium Scour at Bridge Piers." J. of Hydr. Eng.., ASCE, 134(10), 1491-1495.

38. Coleman, S. E. (2005). "Clearwater local scour at complex piers." J. of Hydr. Eng.., ASCE, 131(4), 330-334.

39. Cunha, L.V. (1975), "Time evolution of local scour", Proc.s, 16th IAHR Congress, Sao Paulo, Brazil, 285-299.

40. Dargahi, B. (1989). "The turbulent flow field around a circular cylinder." Exp. Fluids, 8, 1– 12.

41. Dargahi, B. (1990), "Controlling mechanism of local scouring", J. of Hydraulic Eng., ASCE, 116(10), 1197-1214.

42. Dey, S. (1997), "Local scour at piers, part 1: A review of development of Research.", International J. of Sediment Res., IJSH, 12(2), 23-46.

43. Dey, S. (1999), "Time-variation of scour in the vicinity of circular piers", Water & Maritime Eng. J., Proc.s of the Institution of Civil Engineers, Thomas Telford J.s, London, 136(2), 67-75.

44. Dey, S. and Barbhuiya, A.K. (2004), "Clear-water scour at abutments in thinly armoured beds", J. of Hydraulic Eng., ASCE, 130(7), 622-634.

45. Dey, S., and Raikar, R. V. (2007 a). "Characteristics of horseshoe vortex in developing scour holes at piers." J. of Hydr. Eng.., ASCE, 133(4), 399-413.

46. Dey, S., and Raikar, R. V. (2007 b). "Clear water scour at piers in sand beds with an armor layer of gravel." J. of Hydr. Eng.., ASCE, 133(6), 703-711

47. Ettema, R. (1980), "Scour at bridge piers", PhD Thesis, Auckland University, Auckland, New Zealand.

48. Ettema, R., Arndt, R., Robert, P. and Wahl, T. (2000), "Hydraulic modelling concepts and practice", ASCE Manuals and Reports on Eng. Practice No. 97, Sponsored by the Environmental and Water Res. Institute of the ASCE, ASCE, 390 p.

49. Fanzetti, S., Larcan, E. and Mignosa, P. (1982), "Influence of tests duration on the evaluation of ultimate scour around circular piers", International Conf. on the Hydraulic Modelling of Civil Eng. Structures, Organised and Sponsored by BHRA Fluid Eng., University of Warwick, Coventry, England, September 22- 24, 16 p.

50. Federico, F., Silvagni, G. and Volpi, F. (2003). "Scour vulnerability of river bridge piers", J. of Geotechnical and Geoenvironmental Eng., ASCE, 129(10), 890- 899.

51. Fotherby, L. M., and Jones, J. S. (1993). "The influence of exposed footings on pier scour depths." Proc., Hydr. Conf., ASCE, New York, 922-927.

52. Fotherby, L.M. and Jones, J.S. (1993), "The influence of exposed footings on pier scour depths", Proc. of Hydraulics Conf., ASCE, and New York, 922-927.

53. Froehlich, D.C. (1989) “Local Scour at Bridge Abutments”, Proc., A.S.C.E. National Hydraulics Conf., Colorado Spring, Colorado, U.S.A., 13-18.
54. Gao, D., G.L. and Nordin, C.F.(1993) “Pier scour equations used in the people’s Republic of China – Review and Summary”, Proc., A.S.C.E. National Hydraulics Conf., San Francisco, CA, U.S.A., 1031-1036.
55. Garde, R. J., and Ranga Raju, K. G. (2006). “Mechanics of sediment transportation and alluvial stream problem.” New Age International, New Delhi.
56. Garde, R.J. and Ranga-Raju, K.G. (1985). “Mechanics of sediment transportation and alluvial stream problems”, John Wiley & Sons, 618 p.
57. Goring, D. and Nikora, V., (2002). “Despiking acoustic doppler velocimeter data.” J. of Hydraul. Eng., 128(1), 117–126.
58. Gosselin, M.S. and Sheppard, M. (1995). “Time rate of local scour”, Proc.s, 1st International Conf. on Water Res. Eng., San Antonio, Texas, 1: 775-779.
59. Graf, W. H. & Yulistiyantou, B. (1998) “Experiments on flow around a cylinder; the velocity and vorticity fields”. J. Hydraul. Res. 36, 637–653.
60. Graf, W. H., and Istiarto, I. (2002). “Flow pattern in the scour hole around a cylinder.” J. of Hydr. Res., IAHR, 40(1), 13-20.
61. Graf, W. H., and Yulistiyanto, B. (1998). “Experiments on flow around a cylinder, the velocity and vorticity fields.” J. Hydraul. Res., 36(4), 637–653.
62. Graf, W.H, and Istiarto, I, (2001) "Flow Pattern in the Scour Hole around a Cylinder." J. of Hydraulic Res., 40(1), 13-20.
63. Hager, W.H. and Unger J.(2010). “Bridge pier scour under flood waves”. J. of Hydr. Eng., ASCE, 136(10), 842-847.
64. Haghighat, M. (1993), “Scour around bridge pier group,” ME thesis, Dept. of Civil Eng., Indian Institute of Technology, Roorkee, India.
65. Heidarpour, M., Khodarahmi, Z. and Mousavi, S.F. (2003), “Control and reduction of local scour at bridge pier groups using slot”, Proc., XXX IAHR Congress, Thessaloniki, Greece, August 24 - 29, 7 p.
66. Hjorth, P. (1975) Studies on the nature of local scour. Bull. Ser. A, no. 46, viii 191 pp., Department of Water Res. Eng., Lund Institute of Technology/University of Lund, Lund, Sweden.
67. Hjorth, P. (1975). “Studies on the nature of local scour.” Dept. of Water Res. Eng.., Univ. of Lund, Bulletin No. 46.
68. Hoffmans, G.J.C.M. and Verheij, H.J. (1997) Scour manual, A.A. Balkema, Rotterdam, Netherlands, 205 p.
69. Imamoto, H., and Ohtoshi, K. (1987). “Local scour around a non-uniform pier.” Proc., IAHR Congr., 304-309.
70. Jain, S. C., and Fischer, E. E. (1979). “Scour around bridge piers at high velocity.” J. of Hydr. Eng.., ASCE, 106(11), 1827-1841.
71. Jia, Y., Xu, Y. and Wang, S.Y. (2002), “Numerical simulation of local scouring around a cylindrical pier”, Proc. of First International Conf. on Scour of Foundations, Texas A & M University, College Station, Texas, USA, November 17- 20, 1181-1187.

72. Johnson, P.A., Hey, R.D., Tessier, M. and Rosgen, D.L. (2001), "Use of vanes for control of scour at vertical wall abutments", J. of Hydraulic Eng., ASCE, 127(9), 772-778.

73. Johnson, P.G. and Niezgoda, S.L. (2004), "Risk-based method for selecting bridge scour countermeasures", J. of Hydraulic Eng., ASCE, 130(2), 121-128.

74. Jones, J. S., Kilgore, R. T., and Mistichelli, M. P. (1992). "Effects of footing location on bridge pier scour." J. of Hydr. Eng.., ASCE, 118(2), 280-290.

75. Jones, J.S. (1984). "Comparison of Prediction Equations for Bridge Pier and Abutment Scour", Trans. Res. Rec. 1950, Transportation Research Board, Washington.

76. Jones, J.S. and Sheppard, D.M. (2000), "Scour at wide bridge piers", Joint Conf. on Water Res. Eng. and Water Res. Planning and Management, ASCE, July 30. August 2, 2000, Minneapolis, Minnesota, U.S., 10p.

77. Kayaturk, S.Y., Kokpinar, M.A. and Gogus, M. (2004), "Effect of collar on temporal development of scour around bridge abutments", 2nd International Conf. on scour and erosion, IAHR, Singapore, 14-17 November, 7 p.

78. Khullar, A. (2007). "Wake scour around bridge piers," MTech thesis, Dept. of Civil Eng., Indian Institute of Technology, Roorkee, India.

79. Kirkgoz, M. S. and Ardiclioglu, M. (1997). "Velocity profiles of developing and developed open-channel flow." J. Hydraul. Eng., 123(12), 1099–1105.

80. Kobus, H. (1980), "Hydraulic modelling", German Association for Water Res. and Land Management, Bulletin 7, Issued in cooperation with IAHR, 323 p.

81. Kothyari, U. C. (1989). "Scour around bridge piers." Ph.D. Thesis, Indian Institute of Tech. Roorkee (Formerly: Univ. of Roorkee, Roorkee), India.

82. Kothyari, U. C., and Ranga Raju, K.G. (2001). "Scour around spur dikes and bridge abutments." J. of Hydr. Res., 39(4), 367-374.

83. Kothyari, U. C., Garde, R. J., and Ranga Raju, K. G. (1992 a). "Temporal variation of scour around circular bridge piers." J. of Hydr. Eng.., ASCE, 118(8), 1091-1106.

84. Kothyari, U. C., Garde, R. J., and Ranga Raju, K. G. (1992 b). "Live-bed scour around cylindrical bridge piers." J. of Hydr. Res., IAHR, 30(5), 701-715.

85. Kothyari, U. C., Hager, W. H., and Oliveto, G. (2007). "Generalized Approach for Clear-Water Scour at Bridge Foundation Elements." J. of Hydr. Eng.., ASCE, 133, (11), 1229-1239.

86. Kothyari, U.C, Garde, R. J. and Ranga Raju, K.G. (1992a), "Temporal variation of scour around circular bridge piers", J. of Hydraulic Eng., ASCE, 118(8), 1091-1106.

87. Kothyari, U.C, Garde, R. J. and Ranga Raju, K.G. (1992b), "Live bed scour around circular bridge piers", J. of Hydraulic Res., IAHR, 30(5), 701-715.

88. Kothyari, U.C, Hager, W.H. and Oliveto, G. (2007), "Generalized approach for clear-water scour at bridge foundations", J. of Hydraulic Eng., ASCE, 133(11), 1229-1240.

89. Kothyari, U.C. (2006), "An Assessment on Indian Practice for Estimation of Scour around Bridge Piers and Abutments", Adv. in Bridge Eng.

90. Kraus, N.C., Lohrmann, A. and Cabrea, R. (1994) "New acoustic meter for measuring 3D laboratory flows" J. Hydraul. Eng., 120, 406-412

91. Kumar, A. (2007). "Scour around circular compound bridge piers." Ph.D. Thesis, Indian Institute of Tech. Roorkee (Formerly: Univ. of Roorkee, Roorkee), India.

92. Kumar, A., Kothyari, U. C., and Ranga Raju, K. G. (2003). "Scour around compound bridge." Proc. 30th Congress, IAHR, Thessaloniki, Greece, 309-316.

93. Kumar, V. (1996), "Reduction of scour around bridge piers using protective devices", Ph.D. thesis, Dept. of Civil Eng., Indian Institute of Technology, Roorkee, India.

94. Kumar, V., Ranga Raju, K.G. and Vittal, N. (1999), "Reduction of local scour around bridge piers using slots and collars", J. of Hydraulic Eng., ASCE, 125(12), 1302-1305.

95. Kuti, E.O. and Yen, C. (1976), "Scouring of cohesive soils", J. of Hydraulic Res., IAHR, 14(3), 195-206.

96. L. Cea, J. Puertas, and L. Pena. (2007) "Velocity measurements on highly turbulent free surface flow using adv", Experiments in Fluids, (42), 333–348.

97. Lagasse, P.F. and Richardson, E.V. (2001), "ASCE compendium of stream stability and bridge scour papers", J. of Hydraulic Eng., ASCE, 127(7), 531-533.

98. Lagasse, P.F., Zevenbergen, L.W., Schall, J.D. and Clopper, P.E. (2001), "Bridge scour and stream instability countermeasures: Experience, selection, and design guidelines", FHWA NHI 01-003: Federal Highway Administration, Hydraulic Eng. Circular No. 23, 2nd ed., U.S. Department of Transportation, Washington, D.C.

99. Lai, Jihn-sung., Chang, Wen-Yi., and Yen, Chin-Lien. (2009). "Maximum local scour depth at bridge piers under unsteady flow." J. of Hydr. Eng.., ASCE, 135(7), 609-614.

100. Landers, M.N., and Mueller, D.S., (1996) "Channel scour at bridges in the United States", Federal Highway Administration Research Report FHWA-RD-95-184.

101. Lauchlan, C.S. (1999), "Pier scour countermeasures", PhD Thesis, Department of Civil and Res. Eng., University of Auckland, Auckland, New Zealand.

102. Lauchlan, C.S. and Melville, B.W. (2001), "Riprap protection at bridge piers", J. of Hydraulic Eng., ASCE, 121(9), 635-643.

103. Laursen, E. M., and Toch, A. (1956). "Scour around bridge piers and abutments." Bull. No. 4, Iowa Highway Res. Board, U.S.A., May.

104. Le Roux, J. P. (2004). "An integrated law of the wall for hydrodynamically transitional flow over plane beds." Sedimentary Geology, 163, 311–321.

105. Le Roux, J. P. and Brodalkab, M. (2004). "An Excel™-VBA programme for the analysis of current velocity profiles." Computers & Geosciences, 30, 867–879.

106. Lee, S. O., and Sturm, T. W. (2009). "Effect of Sediment Size Scaling on Physical Modeling of Bridge Pier Scour." J. of Hydr. Eng.., ASCE, 135(10), 793-802.

107. Lim, F.H. and Chiew, Y.M. (2001). "Parametric study of riprap failure around bridge piers", J. of Hydraulic Res., IAHR, 39(1), 61-189.

108. Link, O. and Zanke, U. (2004). “On the time-dependent scour-hole volume evolution at a circular pier in uniform coarse sand”, 2nd International Conf. on scour and erosion, IAHR, Singapore, 14-17 November, 8 p.

109. Lohrmann, A., Cabrera, R. and N. C. Kraus. (1994) “Acoustic doppler velocimeter (adv) for laboratory use”. In Symp. on Fundamentals and Advancements in Hydraulic Measurements and Experimentation, ASCE, New York.

110. Lu, Jau-Yau., Shi, Zhong-Zhi., Hong, Jian-Hao., Lee, jun-ji., and Raikar, V. K. (2011). “Temporal variation of scour depth at non-unifrom cylindrical piers.” J. of Hydr. Eng.., ASCE, 137(1), 45-56.

111. Martin, V., Fisher, T. S. R, Millar, R. G. (2002) “Quick. Adv data analysis for turbulent flows: low correlation problem”, ASCE/EWRI and IAHR International Conf. on Hydraulic Measurements and experimental methods.

112. Mashair, M.B. and Zarrati, A.R. (2002), “Effect of collar on time development of scouring around rectangular bridge piers”, 5th International Conf. on Hydroscience and Eng., Warsaw, Poland, 9 p.

113. Mashair, M.B., Zarrati, A.R. and Rezayi, A.R. (2004), “Time development of scouring around a bridge pier protected by collar”, 2nd International Conf. on Scour and Erosion, ICSE-2, Singapore, 8 p.

114. McIntosh, J.L., (1989) “Use of scour prediction formulae”, Proc.s of the Bridge Scour Symp.: McLean, Va., Federal Highway Administration Research Report FHWA-RD-90-035.

115. Melville B. W., and Raudkivi, A. J. (1996). “Effects of foundation geometry on bridge pier scour.” J. of Hydr. Eng.., ASCE, 122(4), 203-209.

116. Melville, B. W. (1975). “Local scour at bridge sites.” Report No. 117, Univ. of Auckland, Auckland, New Zealand.

117. Melville, B. W. (1997). “Pier and abutment scour: Integrated approach.” J. of Hydr. Eng.., ASCE, 123(1), 125-136.

118. Melville, B. W. and Coleman, S. E. (2000). “Bridge scour” Water Res. Publications, Highlands Ranch, Colo.

119. Melville, B. W., and Sutherland, A. J. (1988). “Design method for local scour at bridge piers.” J. of Hydr. Eng.., ASCE, 114(10), 1210-1226.

120. Melville, B. W., and Sutherland, A. J. (1988). “Design method for local scour at bridge piers.” J. Hydraul. Eng., 114(10), 1210–1226.

121. Melville, B.W. (1984), “Live bed scour at bridge piers”, J. of Hydraulic Eng., ASCE, 110(9), 1234-1247.

122. Melville, B.W. and Chiew, Y.M. (1999), “Time scale for local scour at bridge piers”, J. of Hydraulic Eng., ASCE, 125(1), 59-65.

123. Melville, B.W. and Coleman, S.E. (2000), “Bridge scour”, Water Res. Publications, LLC, Colorado, U.S.A., 550 p.

124. Melville, B.W. and Hadfield, A.C. (1999), “Use of sacrificial piles as pier scour countermeasures”, J. of Hydraulic Eng., ASCE, 125(11), 1221-1224.

125. Melville, B.W. and Raudkivi, A.J. (1977), “Flow characteristics in local scour at bridge piers”, J. of Hydraulic Res.., IAHR, 15(1), 373-380.

126. Melville, B.W. and Raudkivi, A.J. (1996), "Effect of foundation geometry on bridge pier scour", J. of Hydraulic Eng., ASCE, 114(10), 203-209.

127. Mia, M. F., and Nago, H. (2003). "Design method of time-dependent local scour at circular bridge pier." J. of Hydr. Eng.., ASCE, 129(6), 420-427.

128. Middleton, G.V. and Southard, J.B., (1984). "Mechanics of sediment movement", Society of Economic Paleontologists Mineralogists, Eastern Section, Lecture Notes for Short Course,3, 400.

129. Mueller, D. and Chad R. Wagner (2002). "Analysis of Pier Scour Predictions and Real-Time Field Measurements", Proc.s of ICSF-1 First International Conf. on Scour of Foundations, Texas A&M University, College Station, Texas, USA

130. Muzzammil, M., Gangadharaiah, T. and Gupta, A. K. (2004), "An experimental investigation of a horseshoe vortex induced by a bridge pier", Water Management J., Proc.s of the Institution of Civil Engineers, Thomas Telford J.s, and London.157 (2): 109-119. Paper 13904, June 2004.

131. Neill, C.R. (1973), "Guide to bridge hydraulics", Project Committee on Bridge Hydraulics, Roads and Transportation Association of Canada. University of Toronto Press, Toronto and Buffalo, 191 p.

132. Nezu, I. and Nakagawa, H. (1993). "Turbulence in open-channel flow." IAHR Monograph series, Balkema, Rotterdam, The Netherlands.

133. Nezu, I. and Rodi, W. (1986). "Open-channel flow measurements with a laser Doppler anemometer." J. Hydraul. Eng., 112(5), 335–355.

134. Oliveto, G. and Hager, W.H. (2002), "Temporal evolution of clear-water pier and abutment scour", J. of Hydraulic Eng., ASCE. 128(9), 811-820.

135. Oliveto, G. and Hager, W.H. (2005), "Further results to time-dependent local scour at bridge elements", J. of Hydraulic Eng., ASCE. 131(2), 97-105.

136. Paintal, A. S. (1971). "A stochastic model of bed load transport." J.of Hydr. Res., IAHR, 9(4), 91-109.

137. Parola, A. C., Mahavadi, S. K., Brown, B. M., and El-Khoury, A. (1996). "Effects of rectangular foundation geometry on local pier scour." J. of Hydr. Eng., ASCE, 118(8), 1091-1106.

138. Perry, A. E., and Joubert, P. N., (1963). "Rough-wall boundary layers in adverse pressure gradients", J. Fluid Mech., 17, 193–211.

139. Posey, C.J. (1974), "Tests of scour protection for bridge piers", J. of Hydraulics Division, ASCE, 100(12), 1773-1783.

140. Prandtl, L. (1932). Zur turbulenten Strömung in Röhren und längs Platten. Ergebn. Aerodyn. Versuchsanstalt Göttingen 4, 18-29 [in German].

141. Raudkivi, A.J. (1998), "Loose boundary hydraulics", 4th Edition, Rotterdam, Brookfield, VT: Balkema. 496 p.

142. Raudkivi, A.J. and Ettema, R. (1977a), "Effect of sediment gradation on clear-water scour and measurement of scour depth", Proc. 17th Congress IAHR, Baden-Baden 4, 521- 527.

143. Raudkivi, A.J. and Ettema, R. (1977b), "Effect of sediment gradation on clear-water scour and measurement of scour depth", J. of the Hydraulics Division, ASCE, 103, 1209-1213.

144. Raudkivi, A.J. and Ettema, R. (1983), "Clear-water scour at cylindrical piers", J. of Hydraulic Eng., ASCE, 109(3), 339-350.

145. Richardson, E. V., and Davis, S. R. (2001). "Evaluating scour at bridges." Hydraulic Eng. Circular No. 18 (HEC-18), 4th Ed., Report No. FHWA NHI 01-001, Federal Highway Administration, Washington, D.C.

146. Richardson, E.V. and Davies, S.R. (1995), "Evaluating scour at bridges. Rep. No. FHWAIP- 90-017 (HEC 18).", Federal Administration, U.S. Department of Transportation, Washington, D.C.

147. Roulund, A., Sumer, B. M., Fredsoe, J., and Michelsen, J. (2005). "Numerical and experimental investigation of flow and scour around a circular pile." J. Fluid Mech., 534, 351–401.

148. Sadeque, M. A. F., Rajaratnam, N. and Loewen, M. R. (2008). " Flow around cylinders in open channels." J. Hydraul. Eng., 134(1), 60-71.

149. Schappman, B. (1975). "The mechanics of flow and transport of a progressive scour", Proc.s of the 16th congress, IAHR, 40(1), 13-20.

150. Schlichting, H. (1979). "Boundary-layer theory." 6th edn. McGraw-Hill, New York

151. Schneibe, D.E. (1951), "An investigation on the effect of bridge pier shape on the relative depth of scour", MSc. Thesis, State University of Iowa.

152. Schultz, M. P. and Flack, K. A. (2003) "Turbulent boundary layers over surfaces smoothed by sanding". ASME, J. Fluids Eng., 125, 863–870.

153. Shen, H. W., Schneider, V. R., and Karaki, S. (1969). "Mechanics of Local scour." J. of Hydr. Eng.., ASCE, 95(6), 1919-1940.

154. Shen, H.W. and Schneider, V.R. (1969), "Local scour around bridge piers", J. of the Hydraulics Division, Proc.s of the American Society of Civil Engineers, 95(6), 1919-1941.

155. Shen, H.W., Schneider, V.R. and Karaki, S.S., (1966) "Mechanics of Local Scour", Colorado State University, Civil Eng. Dept., Fort Collins, Colorado, Pub. No. CER66-HWS22.

156. Sheppard, D. M., Odeh, M., and Glasser, T. (2004). "Large Scale clear-water local pier scour experiments." J. of Hydr. Eng., ASCE, 130(10), 957-963.

157. Sheppard, D. M., Ontowirjo, B., and Zhao, G. (1995). "Local scour near single piles in steady currents." Proc., 1st Hydraulics Eng. Conf., San Antonio.

158. Simarro-Grande, G. and Martin-Vide, J.P. (2005), "Exponential expression for time evolution in local scour", J. of Hydraulic Res., IAHR, 42(6), 663-65.

159. Singh, C.P., Setia, B. and Verma, D.V.S. (2001), "Collar-sleeve combination as a scour protection device around a circular pier", Proc.s of Theme D, 29th Congress on Hydraulics of Rivers, Water Works and Machinery, Chinese Hydraulic Eng. Society, Beijing, China, September 16-21, 202-209.

160. Strom, K. and Papanicolaou, A.N. (2007). "ADV Measurements Around a Cluster Microform in a Shallow Mountain Stream." J. of Hydraul. Eng., 133(12), 1379.

161. Sumer, B.M., Christiansen, N. and Fredsoe, J. (1993), "Influence of cross-section on wave scour around piles", J. of Waterway, Port, Coastal, and Ocean Eng.. ASCE, 119(5), 477-495.

162. Tanaka, S. and Yano, M. (1967), "Local scour around a circular cylinder", Proc.s, 12th IAHR Congress, Colorado State University, Colorado, U.S.A., Published by IAHR, Delft, The Netherlands, 3, September 11-14.

163. Thomas, Z. (1967), "An interesting hydraulic effect occurring at local scour", Proc.s, 12th IAHR Congress, Colorado State University, Colorado, U.S.A., Published by IAHR, Delft, The Netherlands, 3, September 11-14.

164. Ting, F.C.K., Briaud, J.L., Chen, H.C., Gudavalli, R. and Perugu, S. (2001), "Flume tests for scour in clay at circular piers", J. of Hydraulic Eng., ASCE, 127(11), 969-978.

165. Tsujimoto, T., Murakami, S., Fukushima, T., and Shibata, R. (1987). "Local scour around bridge piers and its' protection works." Memoirs of the Faculty of Technology, Kanazawa Univ., Kanazawa, Japan, 20(1), 11-21.

166. Vittal, N., Kothyari, U.C. and Haghighat, M. (1993), "Clear-water scour around bridge pier group", J. of Hydraulic Eng., ASCE, 120(11), 1309-1318.

167. von Karman, T. (1930) Mechanische Ähnlichkeit und Turbulenz. Nachrichten Ges. Wiss. Göttingen Math.-Phys. Klasse, 58-76 [in German].

168. Voulgaris, G. and Trowbridge, J.H. (1998). "Evaluation of the acoustic Doppler Velocimeter (ADV) for Turbulence measurements" J. of Atmosp. and Ocean. Tech., 15, 272-289

169. Wahl, T.L. (2000). "Analyzing ADV data using WinADV." Proc., ASCE Joint Conf. on Water Res. Eng. and water res. Planning & Management, Minneapolis, Minn.

170. Wardhana, K. and Hadipriono, F.C. (2003), "Analysis of recent bridge failures in the United States", J. of Performance of Constructed Facilities, ASCE, 17(3), 144-150.

171. Whitebread, J. E., Benn, J. R. and Hailes, J. M. (2000), "Cost-effective management of scour-prone bridges", Transport J., Proc.s of the Institution of Civil Engineers, London. 141(2), 79-86. Paper 10752, May 2000.

172. Whitehouse, R.J.S. (1998), "Scour at marine structures: A manual for practical applications", Thomas Telford publications, Thomas Telford Ltd, 1 Heron Quay, London, United Kingdom, 198 p.

173. Wilczak, J. M., Oncley, S. P., and Stage, S. A. (2001). "Sonic anemometer tilt correction algorithms." Boundary-Layer Meteorol., 99, 127–150.

174. Wu, S. and Rajaratnam, N. (2000), "A simple method for measuring shear stress on rough boundaries." J. of Hydr. Res., IAHR, 38(5), 399-400.

175. WU, S. and Rajaratnam, N. (2000). "A simple method for measuring shear stress on rough boundaries", JHR, 38, 399-400.

176. Yalin, M. S. (1977). "Mechanics of sediment transport." 2nd Ed., Pergamon, Oxford, England.

177. Yang, Q. (2005). "Numerical investigations of scale effects on local scour around a bridge pier", MS thesis, Famu-Fsu college of Eng., the Florida state university.

178. Yanmaz, A. M., (2006). "Temporal variation of clear-water scour at cylindrical bridge piers." Can. J. of Civil. Eng., ASCE, 33, 1098-1102.

179. Yanmaz, A. M., and Altinbilek, H. D. (1991). "Study of time-dependent local scour around bridge piers." J. of Hydr. Eng.., ASCE, 117(10), 1247-1268.

180. Zarrati, A. M., Nazariha, M. and Mashahir, M.B. (2006). "Reduction of local scour in the vicinity of bridge pier groups using collars and riprap", J. of Hydraulic Eng., ASCE, 132(2), 154-162.

181. Zarrati, A.M., Gholami, H. and Mashahir, M.B. (2004). "Application of collar to control scouring around rectangular bridge piers", J. of Hydraulic Res., IAHR, 42(1), 97-103.